Investigating the role of *pal-1*, the *C. elegans caudal* homologue, in the development of the stem-like seam cells

THESIS SUBMITTED FOR THE DEGREE OF DOCTOR OF PHILOSOPHY

Sophie Patricia Rose Gilbert
Exeter College

DEPARTMENT OF BIOCHEMISTRY
UNIVERSITY OF OXFORD

TRINITY TERM 2015

Investigating the role of *pal-1*, the *C. elegans caudal* homologue, in the development of the stem-like seam cells

Sophie Patricia Rose Gilbert
Exeter College

Submitted for the degree of D. Phil.
Trinity Term 2015

Abstract

An organism's epithelium provides essential protection against mechanical stress and pathogenic infection, as well as specialised secretory and sensory functions. Intriguingly, at the end of the first larval moult in *C. elegans*, epidermal P cells, which until now have comprised the majority of the ventral epidermis, migrate and remodel, relinquishing their epidermal role before taking on neuroectoblast fate. This leaves a ventral 'hole' in the architecture of the *C. elegans* epidermis. This work describes how this hole is filled by a hitherto-overlooked ventral intercalation event that mirrors the well-described dorsal epidermal intercalation that takes place during embryogenesis and forms the dorsal hyp7 epidermal syncytium. Ventral intercalation involves polarised PAK-dependent cytoskeletal remodelling of anterior daughters of asymmetric (seam) stem cell divisions, prior to P cell migration, between the P cells. Conversely, the posterior seam-fated (self-renewing) daughters retain their lateral positions. This ensures the anterior daughters move ventrally to replace the P cells as they migrate into the ventral midline; thus, for the first time, the major syncytial epidermal organ, hyp7, on the ventral side of the animal is completed. Using this novel system, I have shown that patterning of adjacent epidermal tissues by *pal-1*/*caudal*, through expression driven by a putative Wnt-dependent intronic enhancer, determines the polarity of apical junction remodelling and thus polarity of migration during intercalation. Furthermore, the change of gene expression, structure and function of the P cells during this major epidermal remodelling event appears indicative of a transdifferentiation event.

An enhancer/suppressor screen for *pal-1* epidermal phenotypes during this newly described ventral intercalation has identified a novel role for netrin during posterior embryonic patterning. I have shown that this phenotype is dependent on an interaction with *pal-1* of both netrin receptors, UNC-40 and UNC-5, as well as having identified an *unc-40*-independent role for *unc-5* and *pal-1* earlier in development. Conversely, I have also discovered a role for *pal-1* in post-embryonic netrin-dependent motor neurone axon guidance. Given the high levels of conservation between members of the netrin signalling pathway in many organisms, as well as between *pal-1* and *caudal* genes, both at the sequence and functional levels, these new roles for *pal-1* and netrin may find resonance in other systems.

Finally, this work has characterised the expression of a member of the *C. elegans* Hedgehog-related family of genes, *wrt-2*, in the epidermis and has provided insight into the possible functions of this gene *in vivo*.

Thesis supervisor: Prof. Alison Woollard

Acknowledgements

I have been very fortunate to work with and be supervised by Alison Woollard during my D. Phil. Alison is not only an inspiring scientist, but someone who takes a keen interest in all aspects of her students' development, both scientifically and personally. The scientific trust and respect that Alison has given me throughout my time in her lab has gifted me with invaluable confidence and enthusiasm as a scientist, and I am enormously grateful for her supervision.

I have been lucky enough to work on Biochemistry's 'first floor', within a community of scientists who have provided constant encouragement and guidance throughout my four years. In particular, I would like to thank the people in both Alison's lab and Jonathan Hodgkin's lab, past and present, for the endless amount of advice, expertise and friendship they have shared with me throughout my D. Phil.

Finally, I would like to thank my parents, who have always prioritised my happiness and education, and without whose support I wouldn't have been in a position to undertake a D. Phil.

Table of contents

Abstract I
Acknowledgements II
Table of Contents III
Figures VII
Tables VIII
Abbreviations IX

Chapter 1 1
General Introduction 1
1.1 Developmental Biology 1
Transcription factors in developmental biology 2
Cell-cell communication: a common theme in developmental biology 3
Model organisms in developmental biology 3
1.2 An introduction to *Caenorhabditis elegans* 5
The *C. elegans* life cycle 6
C. elegans genetics and genome 7
Comparative genomics using *C. elegans* 8
C. elegans anatomy 10
Male anatomy 11
1.3 Embryonic development 13
Axis specification in the early *C. elegans* embryo 15
Morphogenesis 18
Dorsal intercalation 18
Ventral enclosure 20
Elongation 23
Cell fusions in the hypodermis during embryogenesis 26
1.4 *C. elegans* post-embryonic hypodermal development 30
C. elegans post-embryonic development 30
General structure of the *C. elegans* hypodermis 31
Ventral hypodermal development 33
Seam cell development 33
1.5 Control of seam cell development 36
Wnt signalling controls cell fate polarity during asymmetrical seam divisions 38
Hox genes in seam cell development 44
The Runx pathway promotes proliferative seam cell divisions 45
Heterochronic mutants and the role of miRNAs in the seam 47
The L1 division is genetically robust 48
1.6 *C. elegans* as a model for cellular migration 50
Axon migration 50
Distal tip cell (DTC) migration 52
Q neuroblast migration 54
P cell migration during L1 55
1.7 The role of *pal-1*, homologue of *Drosophila caudal*, during *C. elegans* development 57
The role of Cdx genes in vertebrate development 58
Cdx genes contribute to fate homeostasis in the posterior gut 59
pal-1 is the *C. elegans* homologue of *caudal* 60
pal-1 expression pattern 62
1.8 Summary 65
1.9 Aims of this work 66

Chapter 2 67
Materials and Methods **67**
2.1 Worm methods 67
C. elegans strains and maintenance 67
Single worm lysis 67
Genotyping *C. elegans* alleles 68
Individual genotyping details 70
Additional genetic methods used to generate strains 71
RNAi 73
Generation of transgenic worms 73

2.2 Bacterial methods 73
Bacterial strains used 73
Preparation of electro-competent *E. coli* 74
Electro-transformation of *E. coli* 74
2.3 Plasmid construction for bacterial or worm expression 75
Primer phosphorylation 75
PCR reactions for cloning 75
T/A cloning using TOPO XL PCR kit (Invitrogen) 76
pal-1(A2110G)::gfp 76
Triple tandem repeat of the *pal-1* A2110G intronic enhancer 76
Yeast plasmids pHisi-1 and pLacZi with triple tandem array *pal-1* intronic inserts 77
Cloning of the KanR cassette for yeast expression 77
Cloning the KanR cassette into pHisi-1 containing the *pal-1* inserts 77
wrt-2 promoter in pPD107.94 77
mCherry::wrt-2::gfp 77
wrt-2 RNAi clone 78
BiFC constructs 78
Mutagenesis of *rnt-1* to get *e1241* for BiFC 78
2.4 Construction of yeast strains 79
2.5 Microscopy 82
2.6 Laser ablation and live cell analysis 82
2.7 Bioinformatics 83
Acknowledgements 84

CHAPTER 3 85
Wnt signalling may control pal-1 expression to regulate epidermal patterning 85
3.1 Introduction 85
3.2 Results 89
pal-1(e2091) mutants hatch with a mid-body bulge and seam cell overlap 89
Mid-body phenotypes of *e2091* animals are not suppressed by *sop-1* 89
The 5' mutation in the 5th intron is responsible for the *e2091* phenotypes 90
pop-1 is predicted to bind to the A2110G locus of the *pal-1* 5th intron 95
A *wrm-1* temperature sensitive (ts) mutant causes seam cell overlap 95
Design of a yeast one-hybrid screen to identify transcription factors that bind to the *pal-1* 5th intron 98
The Hox gene *lin-39* alone is not responsible for the mid-body positioning of the *pal-1(e2091)* defects 99
3.3 Discussion 101
Wnt control of *pal-1* expression 102
pal-1(e2091) mid-body phenotypes are not suppressed by *sop-1* 105
The role of Hox genes in *pal-1(e2091)* phenotypes 105
pal-1(e2091) patterning phenotypes 106

CHAPTER 4 108
***pal-1* regulates the polarity of dorsoventral cell movement during the asymmetric L1 seam cell division 108**
4.1 Introduction 108
4.2 Results 110
pal-1(e2091) adults exhibit branched alae corresponding to the underlying position of the fused seam 110
Ventral projections of the seam originate at L1 112
The *e2091* aberrant seam cell movement is rescued by *pal-1::gfp* 114
The *e2091* L1 asymmetric seam division: L1 is unique within wild-type divisions 115
Seam cells in the newly hatched worm have anteriorly-polarised attachments to the ventral midline not present at any other stage of seam cell development 115
Projections of L1 seam cells to the ventral midline express the apical junction marker *ajm-1::gfp* 118
Projections are only present on posterior L1 seam cells and meet at the ventral midline 118
Ventral projections of the mid-body L1 seam cells are posterior in *pal-1(e2091)* animals 121
Seam cells begin to develop projections after ventral enclosure 123
Seam cell overlap in *pal-1(e2091)* perturbs relative positions of P cells and seam cells

in the embryo 123
Laser ablation of the seam cells has no effect on P cell remodelling and migration 126
Seam daughters of the symmetrical 'L1' seam division in *lin-14* loss-of-function mutants move ventrally 127
4.3 Discussion 130
Polarised projections on L1 dividing seam cells make this division unique 130
The L1 seam cell division completes the hyp7 sheath, partially formed during embryogenesis 130
P cells migrate independently of the L1 seam cell division 133
P cell apical boundaries determine the final position of the seam daughter cells 134
L1 epidermal remodelling is fast, requiring a rapid switch in the role of the P cells 135
L1 seam lineages should not be considered entirely independent from one another 137
The unique nature of the L1 ventral hypodermis has been observed once before 138
Addendum 139

CHAPTER 5 141
Ventral hypodermal migration in L1: *pal-1* works with netrin to regulate posterior patterning 141
5.1 Introduction 141
5.2 Results 143
RNAi suppressor/enhancer screen for *pal-1(e2091)* L1 ventral seam movement 143
Post-embryonic RNAi screen of embryonically lethal candidates 145
Summary of results from the RNAi suppressor/enhancer screen 146
A null mutant of *unc-6* enhances *pal-1* seam cell ventral movement during L1 147
unc-6 is synthetically lethal with *pal-1(e2091)*, both during larval and post-embryonic development 147
unc-6 has a role in regulating posterior embryonic development 150
unc-6(ev400); pal-1(e2091) adults show a synthetic increase in 'bagging' 151
Abnormal gonad migration in *unc-6(ev400)* is not exacerbated by *pal-1(e2091)* 152
Severity of male tail defects are synthetically increased in *unc-6(ev400); pal-1(e2091)* animals 154
An *unc-6* allele which affects ventral but not dorsal migration shows synthetic lethality and Nob phenotypes with *pal-1(e2091)* 156
unc-5 and *unc-40* display a synthetic interaction with *pal-1* 158
Axon migration defects in weak netrin mutants are increased by *pal-1(e2091)* 160
A mutant of the p21-activated kinase *max-2* suppresses the *pal-1(e2091)* seam branching phenotypes but not the seam cell overlap or mid-body bulge 164
pak-1, another p21-activated kinase known to regulate P cell migration, is not able to suppress *pal-1(e2091)* seam movement after knockdown with RNAi 166
max-2(nv162) is able to suppress the *unc-6(ev400); pal-1(e2091)* synthetic increase in seam cell migration 167
5.3 Discussion 169
The relationship between Wnt and *pal-1* is likely to be complex 169
A new role for netrin in posterior body patterning during embryogenesis 170
Dissecting the contributions of the netrin receptors *unc-5* and *unc-40* in posterior body patterning and embryonic development 172
The role of *pal-1* in neuronal development: a post-embryonic effect? 173
pal-1 works with netrin to specify the development of the male tail 175
max-2, a suppressor of *pal-1*, is a p21-activated kinase (PAK) 175

CHAPTER 6 177
A *C. elegans* Hedgehog? The role of *wrt-2* in the hypodermis 177
6.1 Introduction 177
Hedgehog (Hh) signalling in development 178
Hedgehog processing and secretion 179
The Hedgehog signalling pathway 181
Hedgehog signalling in *C. elegans* 181
wrt-2: a *C. elegans* Warthog 184
6.2 Results 187
heIs63, containing *wrt-2p::gfp::PH* and *wrt-2::gfp::H2B*, is expressed in the seam and remodelling P cells 187
Expression analysis of the upstream intergenic region of *wrt-2* 188

Bioinformatic analysis of the *wrt-2* promotor region reveals three highly conserved TF target sequences 191
Full-length WRT-2 localisation in vivo 193
WRT-2 is cleaved before export of the amino-terminal fragment into the hypodermis 195
An in-frame *wrt-2* deletion mutant removes a large section of the carboxyl domain 197
wrt-2(ok2810) does not cause abnormal hermaphrodite seam cell development 199
wrt-2(ok2810) mutants do not display embryonic lethality at 15ºC or 25ºC 199
wrt-2(ok2810) animals exhibit a low penetrant Muv phenotype 201
The *wrt-2(ok2810)* mutant has defects in gonad arm left-right positioning 203
wrt-2 over-expressing strain displays abnormal body morphologies 205
6.3 Discussion 206
Possible function of *wrt-2* expression in the P cells 206
Bioinformatics on the *wrt-2* promoter has highlighted potential regulatory interactions 207
Expression of the translational reporter indicates *wrt-2* encodes a divergent Hog 208
The hyp7 syncytium is not uniform 210
Analysis of the previously uncharacterised *wrt-2(ok2810)* deletion mutant 211

CHAPTER 7 213
General Discussion **213**
7.1 Development as an integration of signalling pathways 213
7.2 Expression driven from an intron 214
7.3 Migration is a theme of *pal-1* expression 215
7.4 When is the end of embryogenesis? 217
7.5 An edit of Wormbook and WormAtlas 219

APPENDIX I 221
Interaction of PAL-1 with RNT-1 **221**
I.i Introduction 221
I.ii Results 224
rnt-1; pal-1 double mutants exhibit a synthetic decrease in seam cell number 224
Using BiFC to visualise the RNT-1/BRO-1 interaction *in vivo* 226
BiFC analysis supports a RNT-1 and PAL-1 interaction 228
I.III Discussion 230

APPENDIX II 232
Strain List **233**
Plasmid List **236**
Primer List **238**

SUPPLEMENTARY FIGURES 240
REFERENCES 243

Figures

Fig. 1.2.1 – The *C. elegans* life cycle at 22ºC (Wormaltas). 6
Fig. 1.2.2 – Phylogenetic relationship between members of the *Caenorhabditis* genus (adapted from Kiontke, Felix et al. 2011). 9
Fig. 1.2.3 – Overview of *C. elegans* anatomy, adapted from Wormatlas. 12
Fig. 1.3.1 – *C. elegans* embryonic development at 22ºC (Wormatlas). 14
Fig. 1.3.2 – Early divisions of the *C. elegans* embryo (Sulston, Schierenberg et al. 1983, figure from Rose and Gonczy 2014). 17
Fig. 1.3.3 – Dorsal intercalation of hypodermal cells (adapted from Chisholm and Hardin 2005). 19
Fig. 1.3.4 – Ventral enclosure of the *C. elegans* embryo (Chisholm and Hardin 2005). 22
Fig 1.3.5 – Embryonic elongation (Chisholm and Hardin 2005). 25
Fig. 1.3.6 – Cell fusion in the epidermis during embryogenesis (Smurova and Podbilewicz 2016). 29
Fig. 1.4.1 – The *C. elegans* hypodermis. 32
Fig. 1.4.2 – Post-embryonic P cell lineage in the hermaphrodite and male (Sulston and Horvitz 1977). 34
Fig. 1.4.3 – Post-embryonic seam cell lineages in the hermaphrodite and male (Sulston and Horvitz 1977). 35
Fig. 1.5.1 – Wild-type post-embryonic epidermal development. 37
Fig. 1.5.2 – Localisation and relationship of the Wnt/ß-catenin asymmetry pathway components during an asymmetrical seam cell division (Baldwin and Phillips 2014). 41
Fig. 1.5.3 – Temporal regulation of the miRNAs *lin-4* and *let-7* and their target genes. 49
Fig. 1.6.1 – Netrin-mediated circumferential axon guidance (Wadsworth 2002). 51
Fig. 1.6.2 – *C. elegans* hermaphrodite gonad (adapted from Zarkower 2006). 54
Fig. 1.6.3 – P cell migration to the ventral midline during L1. 56
Fig. 1.7.1 – Terminal *pal-1* null mutant phenotypes (reproduced from Edgar, Carr et al. 2001). 61
Fig. 1.7.2 – Expression of *pal-1* in the *C. elegans* embryo (Edgar, Carr et al. 2001). 63
Fig. 1.7.3 – Expression and rescue constructs of *pal-1* used to study *pal-1* embryonic function (Edgar, Carr et al. 2001). 64
Fig. 2.1.1 – Schematic for genotyping by tetra-primer ARMS-PCR (figure taken from Ye, Dhillon et al. 2001). 69
Fig. 3.1.1 – *pal-1* gene structure showing the two point mutations (asterisks) in the last intron of the *e2091* allele (adapted from C. Brabin, D. Phil. thesis, 2011). 87
Fig. 3.1.2 – Expression of *pal-1* constructs (C. Brabin, D. Phil thesis, 2011). 88
Fig. 3.2.1 – *pal-1(e2091)* animals hatch with a seam cell overlap and mid-body bulge that are evident in the 3-fold embryo. 91
Fig. 3.2.2 – *sop-1* RNAi is able to suppress the male tail phenotypes of *pal-1(e2091)* mutants, but not the mid-body bulge and overlapping seam defects. 92
Fig. 3.2.3 – Sequence alignment of the fifth *pal-1* intron between *C. elegans*, *C. briggsae* and *C. remanei*. 93
Fig. 3.2.4 – Rescue of the bulge and seam cell overlap phenotypes by *pal-1::gfp* constructs. 94
Fig. 3.2.5 – *wrm-1(ne1982)ts* superficially phenocopies the *pal-1(e2091)* seam cell overlap. 97
Fig. 3.2.6 – *lin-39(n1880)* does not effect the incidence nor identity of seam cells involved in the *pal-1(e2091)* overlap defect. 100
Fig. 4.2.1 – *pal-1(e2091)* adult hermaphrodites have T-shaped alae corresponding to the shape of the underlying seam syncytium. 111
Fig. 4.2.2 – The *pal-1(e2091)* branching phenotype originates at the L1 seam cell division. 113
Fig. 4.2.3 – *pal-1::gfp* rescues the *e2091* branched seam phenotype. 114
Fig. 4.2.4 – Wild-type L1 seam cell division visualised with *heIs63*. 117
Fig. 4.2.5 – L1 protrusions from seam cells express *ajm-1::gfp*. 119
Fig. 4.2.6 – Seam cells in an L1 animal before the L1 seam cell division visualised with *ajm-1::gfp*. 120
Fig. 4.2.7 – *pal-1(e2091)* L1 seam cell division visualised with *heIs63*. 122
Fig. 4.2.8 – Projections on seam cells can be seen in the wild-type embryo after ventral intercalation. 124
Fig. 4.2.9 – Seam cell overlap in *pal-1(e2091)* mutants causes abnormally-positioned posterior formation of projections. 125
Fig. 4.2.10 – Laser ablation experiments on wild-type seam and P cells. 126
Fig. 4.2.11 – Seam cells in *lin-14* loss-of-function mutants move to the ventral midline after the symmetrical 'L1' division. 128
Fig. 4.2.12 – Seam cell daughters and P cells do not migrate ventrally until the second asymmetric *lin-14(lf)* division. 129
Fig. 4.3.1 – Three-dimentional schematic of the ventral epidermis during the L1 seam cell division and P cell migration. 131
Fig. 4.3.2 – Summary of the newly-described ventral intercalation of the seam anterior daughter cells with the P cells during L1. 132
Fig. 4.3.3 – Illustration of the cross-section through a newly hatched worm showing the muscle attachments

through the epidermis (adapted from Hresko, Schriefer et al. 1999). 136
Fig. 4.3.4 – Accurate anatomical drawing of the ventral hypodermis by John White and colleagues, published in the Worm Breeder's Gazette 5(2): 43. 138
Fig. 4.3.5 – Lineaged wild-type and *pal-1(e2091)* embryos showing the failure of V3 to successfully intercalate into the lateral seam cell line during embryogenesis. 140
Fig. 5.2.1 – RNAi screen to identify suppressors and enhancers of the *pal-1(e2091)* branched seam. 144
Fig. 5.2.2 – Post-embryonic RNAi screen for genes lethal when knocked out during embryogenesis. 145
Fig. 5.2.3 – unc-6 is an enhancer of the *pal-1(e2091)* ventral seam migration at L1. 148
Fig. 5.2.4 – Synthetic lethality between *pal-1* and *unc-6* at 20ºC. 149
Fig. 5.2.5 – DIC images and quantification of the *unc-6(ev400); pal-1(e2091)* synthetic Nob phenotype. 150
Fig. 5.2.6 – *unc-6(ev400); pal-1(e2091)* double mutants show a synthetic increase in bagging but no significant brood size reduction. 151
Fig. 5.2.7 – Gonad migration defects in *unc-6(ev400)* and *pal-1(e2091)* single and double mutants. 153
Fig. 5.2.8 – Male tail defects synergise in *unc-6(ev400);pal-1(e2091)* animals. 155
Fig. 5.2.9 – Embryonic and larval lethality data with the incidence of Nob L1s for *pal-1(e2091); unc-6(e78)* and *pal-1(e2091); unc-6(ju152)* double mutants. 157
Fig. 5.2.10 – Both *unc-5(e53)* and *unc-40(e271)* mutants display synthetic lethality and Nob phenotypes with *pal-1(e2091)*. 159
Fig. 5.2.11 – Axon migration defects in the weak *unc-6(ju152)* allele are increased by *pal-1(e2091)*. 162
Fig. 5.2.12 – Quantification of ventral nerve cord defects in weak netrin alleles with and without *pal-1(e2091)*. 163
Fig. 5.2.13 – *max-2(nv162)* suppresses the *pal-1(e2091)* aberrant seam movement defect but not the seam cell overlap defect or mid-body bulge. 165
Fig. 5.2.14 – *pak-1* RNAi is unable to suppress aberrant *pal-1(e2091)* seam migration. 166
Fig. 5.2.15 – Suppression of the *unc-6(ev400); pal-1(e2091)* enhancement of seam cell ventral movement by *max-2(nv162)*. 168
Fig. 6.1.1 – A summary of Hedgehog processing and secretion (figure from Briscoe and Therond 2013). 180
Fig. 6.1.2 – A comparison of Hedgehog signalling in *Drosophila* and *C. elegans* (from Kolotuev, Apaydin et al. 2009). 183
Fig. 6.1.3 – Hedgehog related genes in *C. elegans*. 185
Fig. 6.2.1 – Dynamic expression of *heIs63* in the P cells during the first two seam cell divisions. 189
Fig. 6.2.2 – Expression of a transcriptional reporter for the *wrt-2* upstream intergenic region during L1. 190
Fig. 6.2.3 – Bioinformatic analysis of the intergenic region upstream of *wrt-2* reveals *blmp-1*, *ets-4* and *egl-13* as potential activators of *wrt-2* transcription. 192
Fig. 6.2.4 – Scaled schematic of the *mCherry::wrt-2::gfp* transgenic reporter. 194
Fig. 6.2.5 – Transgenic reporter line expressing *mCherry::wrt-2::gfp*. 196
Fig. 6.2.6 – *ok2810*, an in-frame deletion allele of *wrt-2*, removes much of the 'Hog' domain of WRT-2 but is downstream of the predicted protein cleavage site. 198
Fig. 6.2.7 – *wrt-2(ok2810)* seam cell phenotypes. 200
Fig. 6.2.8 – *wrt-2(ok2810)* mutants display a low penetrant Muv phenotype. 202
Fig. 6.2.9 – *wrt-2(ok2810)* mutants exhibit left-right anomalies in gonad positioning. 204
Fig. 6.2.10 – DIC image of abnormal body morphology in the *mCherry::wrt-2::gfp* over-expressing strain. 205
Fig. 7.1 – Diagrams of the L1 epidermis in WormAtlas and Wormbook with inaccurate epidermal patterning. 220
Fig. i.i.i – Synthetic lethality between *rnt-1* and *pal-1* (adapted from C. Brabin, D. Phil. thesis, 2011). 223
Fig. i.ii.i – *pal-1(e2091); rnt-1* double mutants do not show synthetic lethality but do display a small synthetic decrease in terminal seam cell number. 225
Fig. i.ii.ii – Schematic representation of the BiFC technique (adapted from Shyu, Hiatt et al. 2008). 226
Fig. i.ii.iii – BiFC visualisation of the RNT-1/BRO-1 interaction in vivo. 227
Fig. i.ii.iv – BiFC analysis of the interaction between PAL-1 and members of the Runx complex. 229
Fig. S1 – Alignment of the *wrt-2* upstream intergenic region between different *Caenorhabditis* species. 241
Fig. S2 – Alignment of *C. elegans* WRT-2 with predicted 'Hog'-containing Warthogs. 242

Tables

Table 1.5.1 – *C. elegans* homologues of the Wnt signalling pathway. 39
Table 5.2.1 – Genes identified as either suppressors or enhancers of the *pal-1(e2091)* branched seam phenotype. 146

Abbreviations

3' UTR	3' Untranslated Region	DNC	Dorsal Nerve Cord
5' UTR	5' Untranslated Region	dNTP	Deoxynucleotide triphosphate
ADAMTS	A disintegrin and metalloprotease with thrombospondin type-1-like repeats	*Drosophila*	*Drosophila melanogaster*
aff	*a*nchor cell *f*usion *f*ailure	Dsh	Dishevelled
ajm	*a*pical *j*unction *m*olecule	DTC	distal tip cell
AML	acute myeloid leukaemia	*E. coli*	*Escherichia coli*
APC	Adenomatous polyposis coli	ECM	Extracellular Matrix
apx	*a*nterior *p*harynx in e*x*cess	*eff*	*e*pithelial *f*usion *f*ailure
ATP	Adenosine triphosphate	*egl*	*egg l*aying defective
B. malayi	*Brugia malayi*	*elt*	*e*rythroid-*l*ike *t*ranscription factor family
BiFC	Bimolecular Fluorescence Complementation	EMSA	electrophoretic mobility shift assay
bp	base pair	EMT	Epithelial-to-mesenchymal transition
bro	Homologue of *bro*ther	ER	endoplasmic reticulum
C. brenneri	*Caenorhabditis brenneri*	FITC	Fluorescein
C. briggsae	*Caenorhabditis briggsae*	Fz	Frizzled
C. elegans	*Caenorhabditis elegans*	g	grams
C. japonica	*Caenorhabditis japonica*	*gf*	gain-of-function
C. remanei	*Caenorhabditis remanei*	GFP	Green Fluorescent Protein
cad	*caudal*	*glp*	abnormal *g*erm *l*ine *p*roliferation
CBFß	Core Binding Factor ß	*gon*	abnormal *gon*ad development
cDNA	complementary DNA	GSK3ß	Glycogen synthase kinase-3ß
Cdx	*caudal*-related homeobox	H2B	Histone 2B
ceh	C. e*legans h*omoeobox	Hh	Hedgehog
CGC	*Caenorhabditis* Genetics Centre	KanR	Kanamycin resistance
CK1	Casein kinase 1	kb	kilobase
cM	centimorgans	L	litre
dATP	Deoxyadenosine triphosphate	*let*	*let*hal
DIC	Differential Interference Contrast	*lf*	loss-of-function
dlg	*Drosophila d*iscs large homologue	LG	Linkage Group
DMSO	Dimethyl sulphoxide	LiAc	Lithium Acetate
DNA	Deoxyribonucleic Acid	*lin*	*lin*eage abnormal
LPR6	lipoprotein receptor-related protein 6	Ras	Rat sarcoma
M	molar	Rb	Retinoblastoma
mab	*m*ale *ab*normal	*ref*	*re*gulator of *f*usion
Mb	Megabase	RNAi	Ribonucleic Acid (RNA) interference
MBV	Multi-vesicular body	*rnt*	Homologue of Runt-related transcription factor

MCS	multiple cloning site	*unc*	*unc*oodinated
Meis	myeloid ecotropic viral integration site homologue	TF	transcription factor
mig	abnormal cell migration	TGFß	Transforming growth factor ß
mm	millimeter	ts	temperature sensitive
mRNA	messenger Ribonucleic Acid (RNA)	*unc*	*unc*oodinated
Muv	Multivulva	VNC	Ventral Nerve Cord
NaCl	Sodium Chloride	WIF	Wnt inhibitory factor
ncRNA	non-coding RNA	Wnt	Wingless
NGM	Nematode Growth Media	*wrt*	Warthog
NLK	Nemo-like kinase	WT	wild-type
NLS	nuclear localisation signal	YPD	yeast extract peptone dextrose
nm	nanometer	µl	microlitre
nob	*no b*ack end	µm	micrometer
NuRD	Nucleosome Remodeling Deacetylase		
ORF	open reading frame		
PAK	p21-activated kinase		
pal	*p*osterior *al*ae		
PAR	PARtitioning defective		
Pbx	Pre-B-cell leukaemia transcription factor		
PCP	planar cell polarity		
PCR	Polymerase Chain Reaction		
PEBP2	polyomavirus enhancer binding protein 2		
PEG	Polyethylene glycol		
PH	Pleckstrin Homology		
PNK	polynucleotide kinase		
Rac	Ras-related C3 botulinum toxin substrate		
rpm	revolutions per minute		
Runx	Runt-related transcription factor		
S.E.M.	Standard Error of the Mean		
SNP	single nucleotide polymorphism		
sop	*s*uppressor *o*f *pal-1*		
Tcf	T-cell factor		
TE	Tris and EDTA		
TF	transcription factor		
TGFß	Transforming growth factor ß		
ts	temperature sensitive		

CHAPTER 1

General Introduction

1.1 Developmental Biology

Developmental biology is the study of how a single fertilised egg, the zygote, develops into a fully-functional multi-cellular organism with all the various specialised tissues and organs associated with that individual. However, the study of development does not stop at adulthood: during a single lifetime, many multicellular organisms are able to repair, grow or even regenerate lost or injured tissues, as well as beginning immediately to age. Furthermore, a vast number of the genes involved in multicellular life have been preserved throughout evolution, allowing, along with recent advances in whole-genome sequencing, the dissection of phylogenetic relationships and the investigation of evolutionary processes at high resolution. The study of developmental biology is therefore far-reaching, encompassing many varied fields including

embryology, post-embryonic development, differentiation, cell communication, morphogenesis, cell death, stem cell biology, genetics, epigenetics, ageing and evolution.

The usefulness of this knowledge is immediately apparent: if a cell in the embryo has the potential to generate different organs, can a human cell be induced back to this potential state before being re-differentiated into different cell types for therapeutic purposes? Or can cells simply be switched from one fate to another, at will? If we can understand how a newt can re-generate a lost tail, can we replicate this to treat humans with lost limbs? Developmental biology is used to investigate the causes of congenital diseases, cancers and pathologies related to the process of ageing, because all of these diseases are ultimately united by a loss of cellular identity. This understanding can lead in turn to the detection of effective drug targets, development of stem cell or gene therapy, generation of transgenic bacteria or animals capable of producing critical substances such as insulin, and a healthier ageing population. Moreover, applications of developmental biology are not restricted to therapeutic advancements: the study of plant development is critical to the optimisation of crop fertilisation and yield in adverse conditions.

Finally, a thorough understanding of the development of an organism means that distinctions between environmental influences versus genetic input can be dissected, allowing for example the study of behavioural characteristics, which until now have remained elusive due to an incomplete understanding of neuronal development.

Transcription factors in developmental biology

After the discovery that DNA encodes all of the proteins required by an organism to give it life, one of the greatest challenges to developmental biologists was understanding how, if every organism has an entire genome in every cell, this could result in one cell of an organism being so

different from another. An example of this is a mammalian muscle cell that expresses high levels of actin and myosin, compared to a skin cell that expresses keratin. The expression of each gene in each cell is therefore critical to the differentiation of cells into specific cell types. In turn, gene expression is controlled by a complex network of transcription factors (TFs). These are proteins which bind to specific DNA motifs to temporally and spatially activate or repress a particular gene or gene set. Investigating the regulatory networks that control gene expression and thus the protein content of each cell has become essential to our understanding of how organisms and tissues develop.

Cell-cell communication: a common theme in developmental biology

Communication between individual cells is important in the life-cycle of many organisms, but is particularly vital during the development of multi-cellular organisms, in which many different cell types must act co-operatively to generate a functional individual. Throughout development, the identity of any given cell is linked to its position in the body plan of that organism, requiring each cell to receive and impart contextual information about its environment. Both cell-cell contacts and longer-ranging morphogenic communication through means of chemical gradients have been shown to play a role in establishing the position, and ultimately fate, of a cell at any given time.

Model organisms in developmental biology

There are many reasons why humans cannot be used to study developmental biology, the most important of which are ethical. Practically, humans are expensive, have long lifespans, small brood sizes and are large complex mammals with extensive processes and systems of development. Alternative, ‘model’ organisms have therefore been used to study the fundamental

mechanisms of development in a simpler and more malleable context. One of the first models for development was the *Xenopus laevis* egg: it is large and therefore easily viewed thorough the light microscope, and can be physically manipulated via microinjection. Other classic model organisms include the fruit fly *Drosophila melanogaster*, with which many of the first genetic experiments were conducted, the nematode worm *Caenorhabditis elegans* (*C. elegans*), the sea urchin *Strongylocentrotus purpuratus*, and vertebrate systems including the chicken *Gallus gallus*, zebrafish *Danio rerio*, and mouse *Mus musculus*. The thale cress *Arabidopsis thaliana* is the most widely used plant model organism. Each organism presents its own unique advantages and disadvantages, with differing levels of complexity suitable for investigations into different aspects of development. Before choosing any organism, the generation time, brood size, ease of manipulation and cost of maintenance must be weighed against the suitability of that organism to answer the question proposed: to model blood cell development, only an organism with a vascular system will suffice, whereas for large genetic screens *C. elegans* and *Drosophila* are ideal.

The conservation of genes and processes throughout evolution continuously validates the use of model organisms to investigate human diseases. One classic example is the understanding of apoptosis, a safeguarding mechanism of cell death bypassed by cancer cells, the genetics of which was first characterised in *C. elegans*; both the molecular mechanisms and cellular processes were found to be conserved in humans (Driscoll 1992, Miura, Zhu et al. 1993, Hengartner and Horvitz 1994, Hengartner and Horvitz 1994, Sugimoto, Friesen et al. 1994, Chinnaiyan, O'Rourke et al. 1997, Xue and Horvitz 1997).

1.2 An introduction to *Caenorhabditis elegans*

In 1974 Sydney Brenner published his experiments on the genetics of *Caenorhabditis elegans* (Brenner 1974) which described the ease of genetic manipulation and analysis of this 1mm long nematode. Since then, the worm has risen to become one of the most widely used model organisms in developmental biology: not only is *C. elegans* ideal for genetic analysis, being able to both self-fertilise (hermaphrodites) or cross-fertilise (involving males), it is also small, easy to maintain in the laboratory, has a short generation time and produces large numbers of offspring. Despite its small size (just under 1000 somatic cells in an adult hermaphrodite), *C. elegans* has many of the differentiated cell types found in higher organisms, making it suitable for investigating a wide range of developmental questions. Together with the ease of mutagenesis of the worm which continues to generate large numbers of informative alleles, *C. elegans* may be recovered from freezing in dilute glycerol and storage in liquid nitrogen for an indeterminate length of time (Brenner 1974), allowing large libraries of mutants to be maintained indefinitely. Following the discovery of GFP (Shimomura, Johnson et al. 1962), *C. elegans* has proven to be an ideal candidate for visualising gene expression (Chalfie, Tu et al. 1994) due to its transparency and amenability to producing transgenic strains (Mello, Kramer et al. 1991, Mello and Fire 1995).

Significantly, development in *C. elegans* can be analysed at single cell resolution due to the mapping of the invariant cell lineage from fertilisation though to the end of post-embryonic development by John Sulston and colleagues (Sulston and Horvitz 1977, Sulston, Schierenberg et al. 1983). The information provided by this work allows the subtlest effects of mutations to be identified and investigated, as well as providing insight into fate changes, amongst the many other applications.

The *C. elegans* life cycle

The *C. elegans* life cycle at 22ºC is shown in figure 1.2.1. The timings of the worm life cycle are highly dependent on temperature; it may take up to 6 days egg to egg at 15ºC or as little as 3 days at 25ºC.

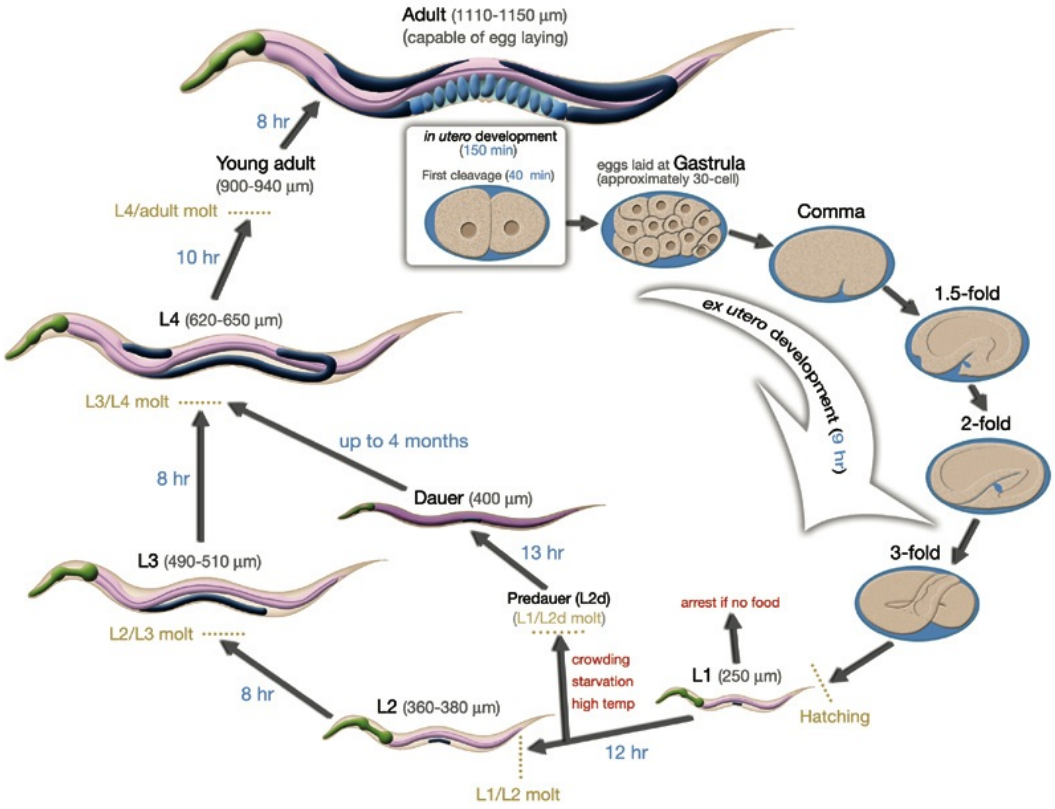

FIG. 1.2.1 – THE *C. ELEGANS* LIFE CYCLE AT 22ºC (WORMALTAS).
Fertilisation occurs at 0 minutes as the oocyte passes through the spermatheca in the gonad of the hermaphroditic parent. The egg is laid at approximately 150 minutes post-fertilisation and the embryo develops through distinct morphologies before hatching as an L1 larva. If conditions are appropriate, the worm progresses through four larval moults (L1-L4) until it reaches adulthood. If the worm hatches with insufficient food available the worm will enter L1 diapause, where post-embryonic development is paused, from which the worm may re-enter the life cycle at the same point on provision of food. Alternatively, in suboptimal conditions the larva may enter a dauer state, during which the morphological changes in the larva allow it to live for several months without food. Approximate timings are given in blue.

In hermaphrodites, oocytes are self-fertilised in the gonad as they pass through the spermatheca. After fertilisation, the zygote undergoes a series of rapid cell divisions until the embryo progresses through gastrulation (the rearrangement of cells into germ layers). Post-gastrulation,

morphogenesis ensues: the embryo becomes enclosed by the epidermis, completed at the comma stage, and subsequently elongates through 2-fold into a distinctive 3-fold moving embryo encased by the egg (see later figure 1.3.1). After hatching and in the presence of food, post-embryonic development will commence. This involves the progression through four larval moults, L1 - L4, between which the cuticle is shed and the worm grows in size. After a fourth and final moult the worm produces its adult cuticle and the germ line is fully mature. During the first few days of a 2-3 week long adulthood, a single hermaphrodite worm will lay its entire brood of between 200 and 300 eggs (Byerly, Cassada et al. 1976).

Two points exist during post-embryonic development when the worm may exit the life cycle in order to halt development in the face of adverse conditions. The first point of exit is during L1. If the worm hatches without food, it will enter a diapause state, during which post-embryonic development is stopped until food is encountered. On re-entry into the life cycle, the L1 larva will complete L1 development and progress to L2 as normal after the diapause. If the worm has already progressed through much of L1 and post-embryonic development has commenced before the animal runs out of food, then the animal may enter an alternative dauer phase in place of the L2 and L3 moults (Cassada and Russell 1975). This is the second point of exit. Many morphological changes take place as the animal enters dauer - the worm becomes slimmer, faster and its mouth and anus seal - to maximise chances of surviving to re-encounter food. It may remain in this state for several months.

C. elegans genetics and genome

C. elegans is a diploid organism with five paired autosomes, often referred to as linkage groups (LGs) I-V, and one sex chromosome, X. The majority of the wild-type population is hermaphroditic (genotype XX). Occasionally (approximately 1 in 1000 animals), a spontaneous

loss of one X chromosome via non-disjunction in gamete production leads to the presence of a morphologically distinct male, of genotype X0. The presence of both self-fertile hermaphrodites and inducible males in its population makes *C. elegans* a powerful genetically tractable organism. The first genetic map of *C. elegans* was published in 1974 (Brenner 1974), showing each chromosome to be approximately 50cM long due to a single crossover event per chromosome per meiosis.

C. elegans, with a genome of around 100Mb, was the first multicellular organism to have its genome completely sequenced (C. elegans Sequencing Consortium 1998), owing this completeness to its holocentric chromosomes and consequent absence of centromeric heterochromatin (Albertson and Thomson 1982). Since then, the genome has been extensively annotated and found to contain many protein-coding genes (27,943, including alternatively spliced forms, Wormbase release WS252), non-coding RNA genes, and relatively rare pseudogenes (Harrison, Echols et al. 2001). Protein coding genes are on average 3kb long, containing introns, exons and promoter sequences. Additionally, about 15% of *C. elegans* genes are organised into operons, with associated promoter sequences driving the transcription of more than one gene as a polycistronic unit (Blumenthal, Evans et al. 2002).

Comparative genomics using *C. elegans*

Due to the relatively early evolution of genes involved in common developmental processes, together with the full genomic sequences being available for many closely related nematode species, it is possible to use alignments of orthologous genomic sequences from different members of the *Caenorhabditis* genus to identify key elements of conserved genetic control. The phylogenetic relationship between nematode species most closely related to *C. elegans* is shown in figure 1.2.2. Using both the nBLAST tool of NCBI (http://blast.ncbi.nlm.nih.gov/Blast.cgi)

and the vast amount of data available in Wormbase (www.wormbase.org), it is possible to identify with great accuracy any orthologues of a gene of interest present in these species. Alignments between resulting sequences are a powerful tool for detecting conserved gene expression motifs both within and around *C. elegans* genes.

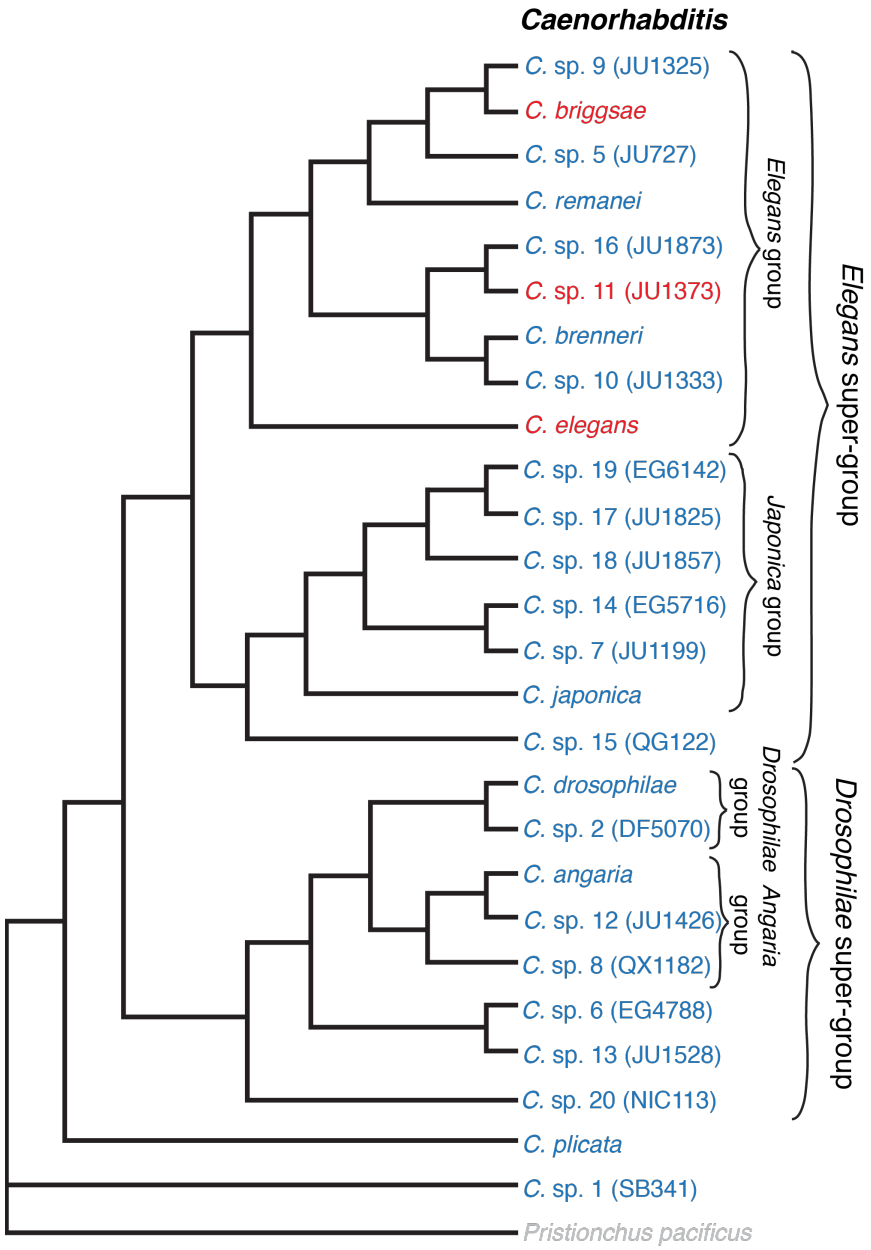

FIG. 1.2.2 – PHYLOGENETIC RELATIONSHIP BETWEEN MEMBERS OF THE *CAENORHABDITIS* GENUS (ADAPTED FROM KIONTKE, FELIX ET AL. 2011).
Three species (red) exist as predominantly hermaphrodite populations with a low incidence of males, whereas all other species (blue) exist as populations of approximately equal numbers of males and females.

C. elegans anatomy

C. elegans anatomy has been studied at single cell resolution through both reconstruction of the entire animal using electron microscopy (Brenner 1973) and mapping of its complete, invariant cell lineage (Sulston and Horvitz 1977, Sulston, Schierenberg et al. 1983). Both of these data sets have been made available at wormatlas.org, an invaluable resource for *C. elegans* anatomical information.

An adult *C. elegans* hermaphrodite has 959 somatic cell nuclei plus around 2000 germ cell nuclei; the male has 1033 somatic cell nuclei, the additional cells due mostly to specialised organs in the tail to facilitate mating (see below), and neuronal differences, including a pair of newly discovered neurones in the head (Sammut, Cook et al. 2015). The *C. elegans* body plan follows that of all other nematodes, being comprised of two concentric cylinders separated by a fluid-filled cavity, known as the pseudocoelom (Fig. 1.2.3 D). This cavity confers internal hydrostatic pressure and provides the worm with structure. The whole animal is covered with an extracellular collagenous cuticle that is secreted by the hypodermis and is specific to, and replaced during, each larval moult.

The ‘inner tube’ of the worm contains the alimentary system - including the muscular pharynx at the anterior end together with its associated nervous system - and the gonad, made up of both somatic and germ line cells. The ‘outer tube’ consists of the hypodermis, the two major nerve cords, dorsal (DNC) and ventral (VNC), the seam cells which lie above the major hypodermis, and four quadrants of body wall muscles. The muscles are attached through the hypodermis to the cuticle, and are thus able to confer, through opposing waves of contraction and relaxation, a sinusoidal movement along the dorsoventral plane with which the wild-type animal can move

both forwards and backwards. Among other roles, the bilateral seam secretes three parallel ridges into the mature cuticle, known as alae (Fig. 1.2.3 D).

Male anatomy

Males differ from hermaphrodites not only in their germ line, which does not contain oocytes, but also to a large extent in the tail (see figure 1.2.3 C). Whilst hermaphrodites possess a vulva in their ventral mid-body region, through which eggs can be laid and though which sperm may enter from male animals, males develop a tail that is not tapered like that of the hermaphrodite, but instead forms a cuticular fan within which are embedded 18 sensory rays (9 on each side). This creates a sensory organ surrounding the spicules, used for sperm transfer, with which the male can mate. The rays of the male tail are derived from the posterior seam cell lineages during larval development.

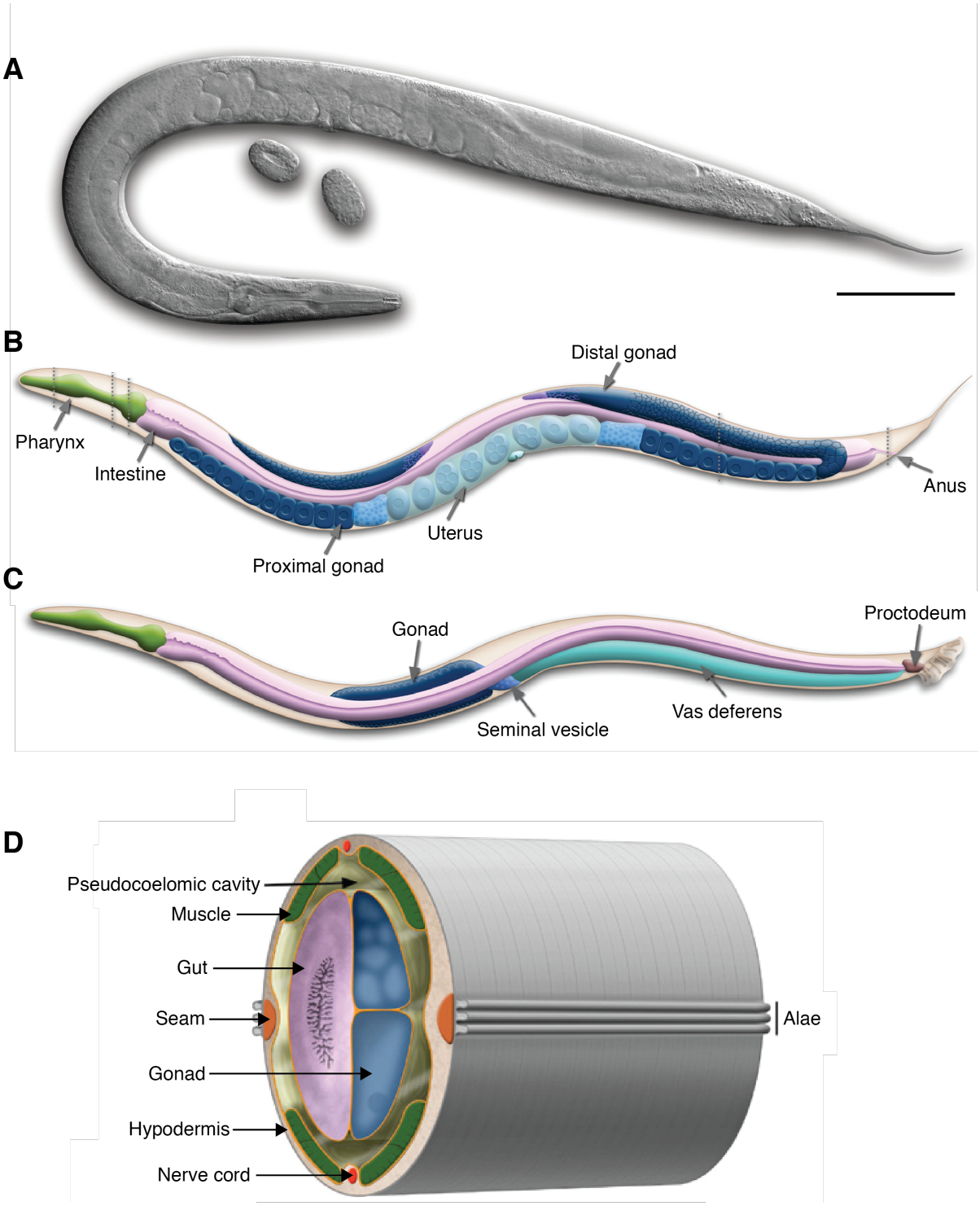

FIG. 1.2.3 – OVERVIEW OF *C. ELEGANS* ANATOMY, ADAPTED FROM WORMATLAS.
A. DIC image of an adult hermaphrodite. Scale bar = 0.1nm. **B.** Schematic diagram of the adult hermaphrodite, showing the internal structures and tissues. **C.** A corresponding diagram of an adult male animal: the tail develops a fan structure to facilitate mating. **D.** Cross-section through an adult hermaphrodite. The nematode comprises of two concentric tubes separated by a fluid-filled cavity, the pseudocoelom. The inner tube contains the alimentary system, associated nervous system and gonad, whereas the outer tube contains the body wall muscles, nervous system and epithelium, including the seam cells and hypodermis. Surrounding the whole is the collagenous cuticle, with its three lateral ridges, called alae, secreted by the seam cells.

1.3 Embryonic development

Embryonic development of *C. elegans* at 22ºC occurs over 14 hours, at the end of which the worm hatches as an L1 larva. During the first stages of embryonic development, the zygote undergoes many cycles of rapid division to generate a large number of cells which subsequently organise themselves into the three germ layers: the endoderm, mesoderm and ectoderm. Separation into layers occurs during gastrulation, by the end of which the gastrulation cleft is enclosed as short-range cell movements move the endoderm to the centre of the embryo. Following gastrulation, the embryo undergoes morphogenesis. The hypodermis moves to fully enclose the embryo and subsequent elongation of the embryo takes place. The morphology of the embryo in the egg at different stages under DIC optics are often referred to successively as: 'bean', the newly enclosed embryo; 'comma', the tail is beginning to elongate; '1.5-fold', the embryo is now long enough to fold back on itself halfway; '2-fold', the embryo can fold fully in half; '3-fold' or 'pretzel', the embryo is nearing hatching and elongation is complete. These stages of development are summarised in figure 1.3.1.

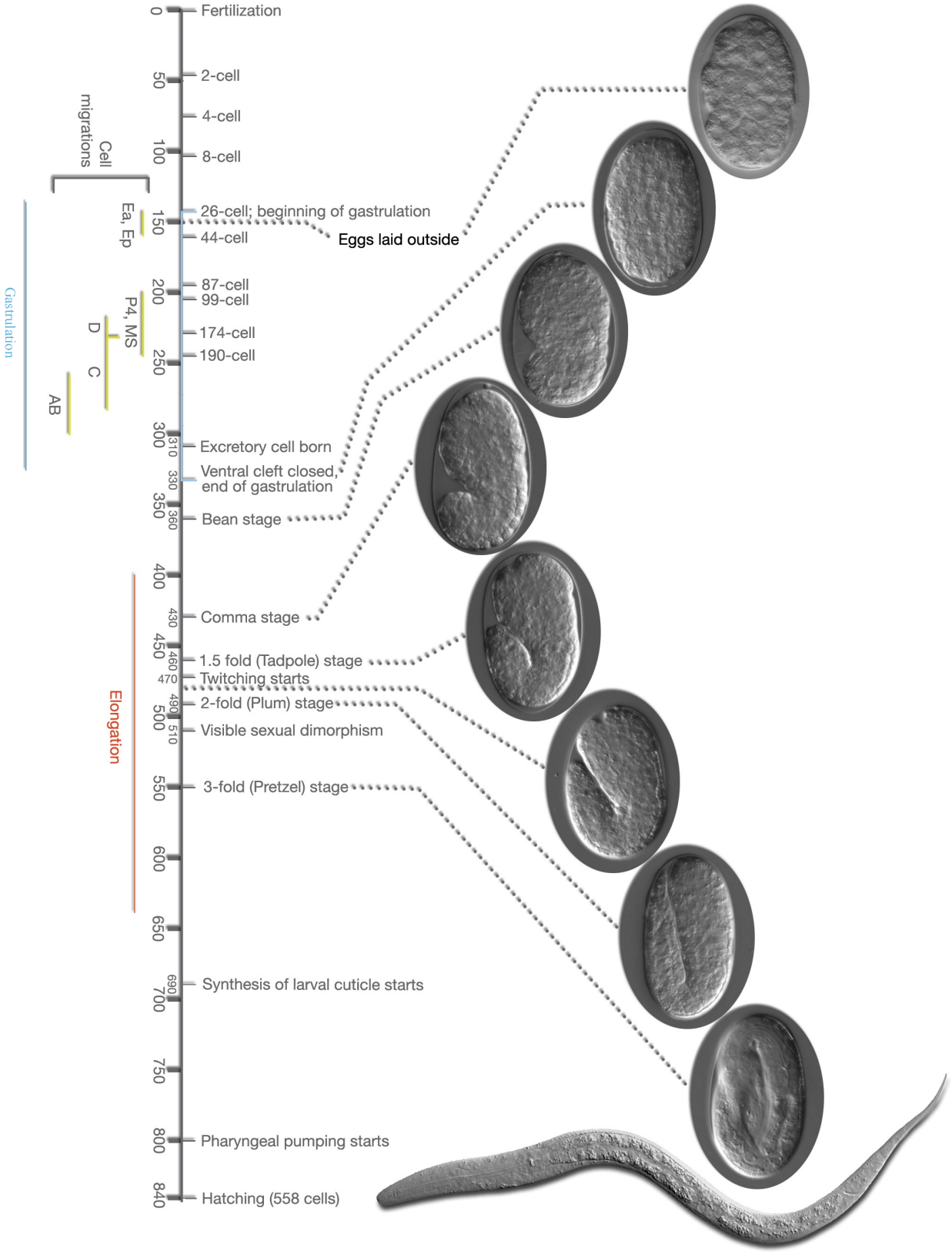

FIG. 1.3.1 – *C. ELEGANS* EMBRYONIC DEVELOPMENT AT 22ºC (WORMATLAS).
Numbers on the left-hand axis refer to minutes after fertilisation. The green bars indicate when cells from a particular lineage migrate inwards during gastrulation, at the end of which the ventral cleft is closed and gastrulation is complete (blue bar). Elongation (red bar) takes place during morphogenesis. DIC images show characteristic morphology for each stage of embryogenesis (in this orientation, the eggs are ventral left and posterior downwards).

Axis specification in the early *C. elegans* embryo

As well as creating diversity during development, asymmetrical divisions (divisions in which each daughter cell differs in fate) in the early embryo contribute to the definition of the three axes of the developing animal: the anteroposterior axis, the dorsoventral axis and the left-right axis. At fertilisation, sperm entry (specifically the sperm-derived centrosome) defines the posterior end of the embryo (Goldstein and Hird 1996, O'Connell, Maxwell et al. 2000, Sadler and Shakes 2000, Wallenfang and Seydoux 2000, Hamill, Severson et al. 2002, Cuenca, Schetter et al. 2003, Cowan and Hyman 2004, Bienkowska and Cowan 2012). Subsequent movements in the cortical actomyosin network result in the polarised separation of PAR proteins (PARtitioning defective) (Kemphues, Priess et al. 1988, Morton, Roos et al. 1992, Watts, Etemad-Moghadam et al. 1996, Munro, Nance et al. 2004) which in turn cause an asymmetric distribution of fate determinants (Kirby, Kusch et al. 1990, Hird and White 1993, Hird, Paulsen et al. 1996, Cheeks, Canman et al. 2004). Thus the embryo divides asymmetrically along the newly established anteroposterior axis to produce, through asymmetric spindle positioning (Grill, Gonczy et al. 2001, Grill, Howard et al. 2003, Labbe, McCarthy et al. 2004), the large anterior AB and smaller posterior P_1 blastomeres (Fig. 1.3.2).

The dorsoventral axis is set up as the embryo reaches the four-cell stage. After the asymmetric first division, the centrosomes of both daughter cells migrate around each nucleus to sit on a lateral axis. The centrosomes of AB do not move from this position, ensuring AB divides perpendicular to the first division. The division of AB gives rise to ABa (anterior daughter) and ABp (posterior daughter), named for their final positions at the four cell stage rather than for the division plane of their division. Although this is the first division perpendicular to the anteroposterior plane in the embryo, ABa and ABp have previously been shown to be functionally equivalent (Priess and Thomson 1987) and therefore do not break the dorsoventral

symmetry of the embryo, and both cells express GLP-1, the Notch receptor (Evans, Crittenden et al. 1994). In contrast, the P_1 nucleus-centrosome complex rotates 90º via an interaction with the mid-body remnant from the first embryonic division (Keating and White 1998, Singh and Pohl 2014). The resulting division of P_1 now starts in parallel to the first division, dividing to give rise to two daughter cells, EMS and P_2, where only P_2 expresses the Notch ligand APX-1 (Mickey, Mello et al. 1996). During late prophase of the P_1 division, the spindle rotates again 90ºC and EMS is pushed ventrally to sit beneath ABp, which moves to the dorsal side of the embryo (Fig. 1.3.2 B). This brings ABp into contact with the ligand-expressing P_2 cell, activating GLP-1 in this cell only, hence breaking the functional symmetry of the dorsoventral axis. EMS now defines the ventral side.

The first symmetry-breaking division along the final axis of development, the left-right axis, occurs at the division of ABa and ABp. These cells divide to give rise to left and right daughters, whereby ABal (left-hand daughter of ABa) and ABpl (left-hand daughter of ABp) are positioned slightly more anteriorly than their right-hand counterparts (Deppe, Schierenberg et al. 1978). The bilateral pairs of cells on the left and right side of the embryo are functionally equivalent until induction by MS (see lineage in Fig. 1.3.2 A) at the 12- and 24-cell stages creates asymmetry between the two sets of lineages (Sulston, Schierenberg et al. 1983, Wood 1991, Hutter and Schnabel 1994, Hutter and Schnabel 1995). All three major axes of the embryo have now been established.

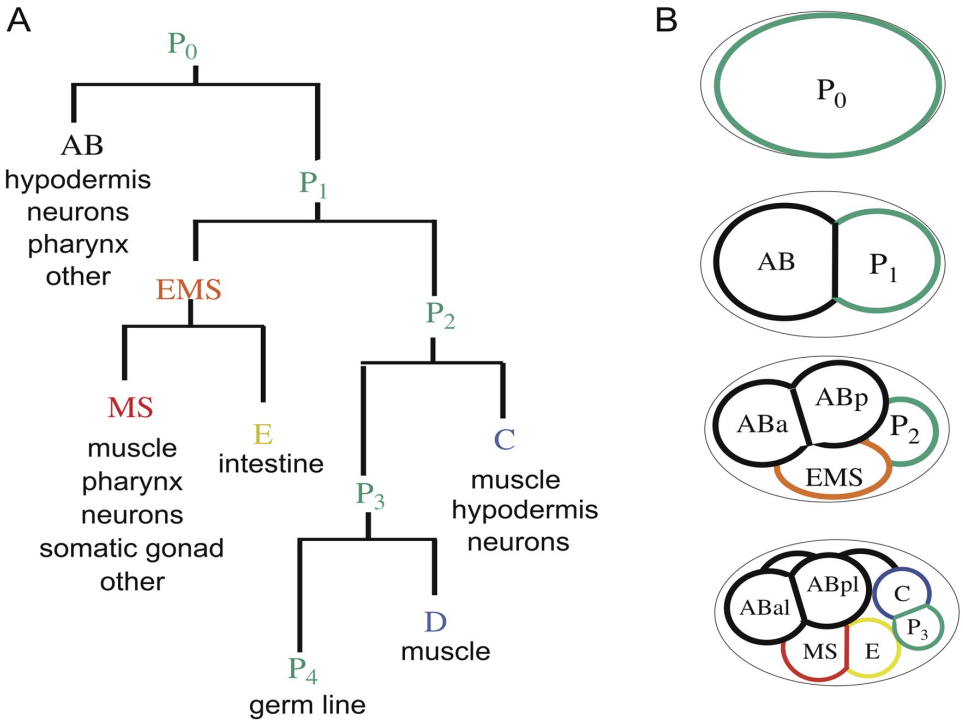

FIG. 1.3.2 – EARLY DIVISIONS OF THE *C. ELEGANS* EMBRYO (SULSTON, SCHIERENBERG ET AL. 1983, FIGURE FROM ROSE AND GONCZY 2014).
A. Early embryonic lineage diagram. P_0, the zygote, divides along the anteroposterior axis to generate the anterior AB and posterior P_1 blastomeres. Subsequent division into the four-cell embryo establishes the dorsoventral axis as EMS defines the ventral side, and the left-right axis is set up by descendants of the AB blastomere, ABal and ABpl (not shown). Fates of the descendants of the six major blastomeres AB, MS, E, P_4, D and C are indicated. The immortal germ line lineage (P_{1-4}) is coloured green at each stage. **B.** Relative positions of the blastomeres in the early embryo within the egg shell (thin black oval). In **A** and **B** (and all subsequent diagrams) anterior is to the left and ventral is down.

Morphogenesis

After gastrulation, during which the cells of the developing embryo arrange themselves into germ layers, embryonic morphogenesis occurs. In the late embryo this process of cell movement is largely driven by the outermost layer of cells called the hypodermis (or epidermis). Morphogenesis is an essential process to shape the animal, and to also form the shape of tissues and organs within it. Although many tissues rely on the hypodermis to drive morphogenesis though cell-cell interactions, the hypodermis displays a level of interdependency with body wall muscle development in order to complete the process. Embryonic morphogenesis can be split into three discrete processes that take place roughly one after the other: dorsal intercalation, ventral enclosure and elongation (described below). The final shape of the organism is maintained by the collagenous cuticle, secreted by the hypodermis (Priess and Hirsh 1986, Roberts, Clucas et al. 2003, Novelli, Ahmed et al. 2004).

Dorsal intercalation

Dorsal intercalation in the *C. elegans* embryo is a process whereby two rows of dorsal epidermal cells rearrange by moving between each other to form a single line of cells down the dorsal midline. This process occurs when the embryo is still arranged in sheets, with the dorsal layer comprised of hypodermal cells and the ventral layer a group of substrate neuroblasts. During dorsal intercalation, the two rows of hypodermal cells become wedge shaped, extending basolateral projections between the cells in the row opposite, each row moving in the direction of the dorsal midline. Two lines of seam epidermal cells flank these dorsal rows of hypodermal cells, and the interdigitating cells continue to extend until they reach the seam cells on the opposite side of the animal (Fig. 1.3.3, Sulston, Schierenberg et al. 1983, Williams-Masson, Heid et al. 1998, Heid, Raich et al. 2001).

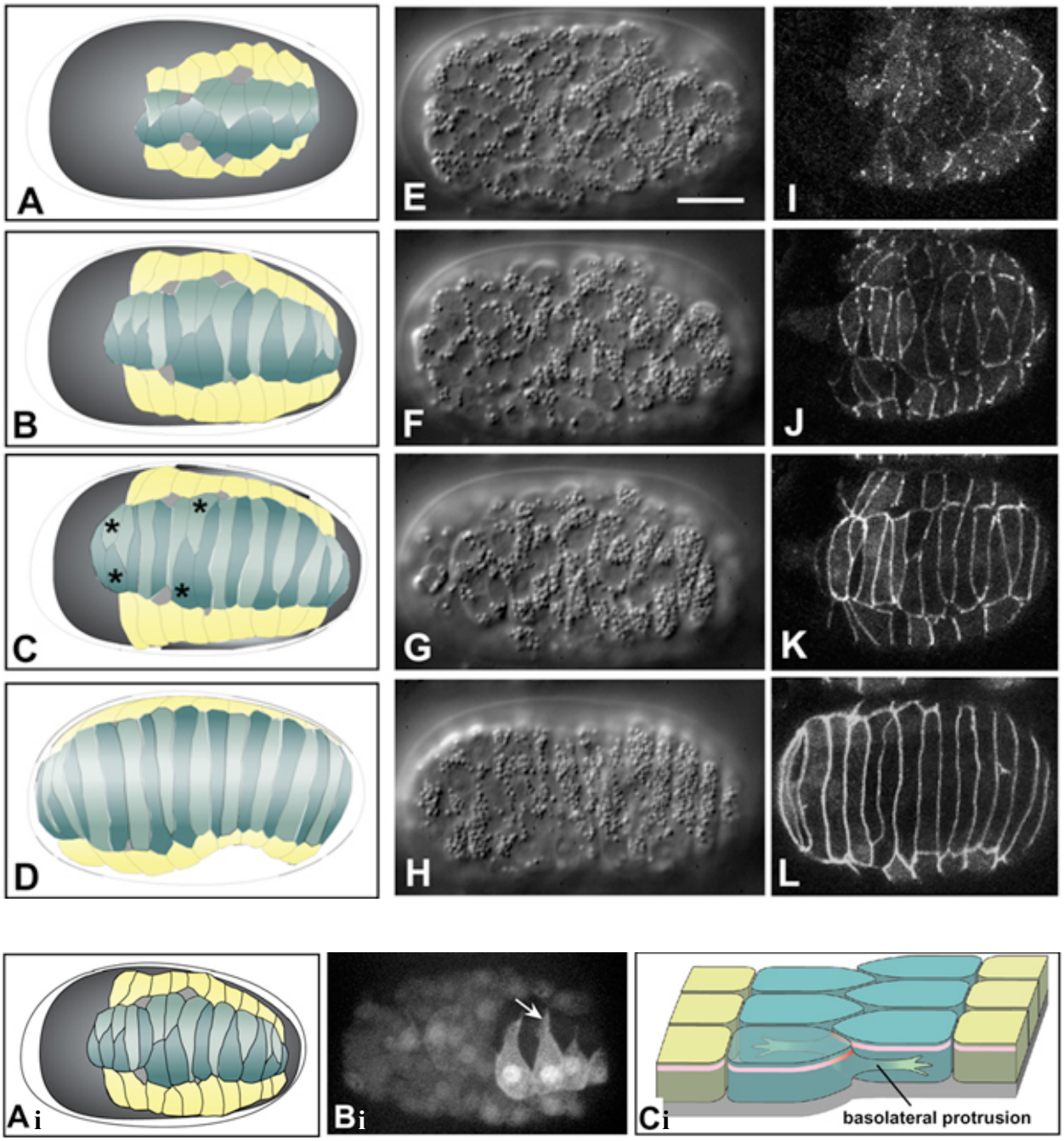

FIG. 1.3.3 – DORSAL INTERCALATION OF HYPODERMAL CELLS (ADAPTED FROM CHISHOLM AND HARDIN 2005).
A-D. Schematics of the dorsal intercalation process over time, shown from the dorsal view. The two rows of intercalating hypodermal cells are shown in teal, and the flanking rows of epidermis, the seam cells, are shown in yellow. Other hypodermal cells are not shown. Asterisks indicate the last two pairs of cells to intercalate, used for marking the progression of dorsal intercalation in wild-type embryos. **E-H.** DIC images of live embryos undergoing the stages of dorsal intercalation shown in the schematics. Scale bar = 5μm. **I-L.** Fluorescent images of the apical junction marker *dlg-1::gfp* in wild-type embryos undergoing dorsal intercalation. Cell boundaries can be visualised as the cells change shape. **Ai.** A schematic of the protrusive activity of intercalating dorsal hypodermal cells. **Bi.** A live embryo expressing a mosaic epidermal cell marker (*lbp-1::gfp*), at the same stage as the schematic. The arrow corresponds to the long basolateral protrusions extended by migrating cells. **Ci.** A schematic showing the position of the protrusions (blue) compared to the adherens junctions between cells (pink). The basolateral protrusion must cause a subsequent remodelling of adherens junctions as the cells move past one another.

Although both actin microfilaments and microtubules are necessary for the process of dorsal intercalation, little is known about the mechanism by which the cells move past one another (Williams-Masson, Heid et al. 1998). However, laser ablation experiments in which either the seam cells, underlying muscle or the posterior dorsal epidermal cells are removed suggest that each cell may autonomously adopt the cell shape required, as none of these experiments disrupted intercalation in any cells that remained (Williams-Masson, Heid et al. 1998, Heid, Raich et al. 2001).

Mosaic loss of the transcription factor DIE-1 has shown that it is required cell autonomously for dorsal intercalation, although initial polarisation of cells towards the dorsal midline is not perturbed (Heid, Raich et al. 2001). Other than DIE-1, other genes known to perturb dorsal intercalation are involved in dorsal hypodermal patterning, such as the redundant genes *tbx-8* and *tbx-9*. Double mutants display a severe disruption in the patterning of the dorsal hypodermis and also in morphogenesis (Andachi 2004, Pocock, Ahringer et al. 2004). However, mispositioned cells are able to complete dorsal intercalation (Pocock, Ahringer et al. 2004) suggesting *tbx-8* and *tbx-9* actively regulate morphogenesis separately to the process regulated by *die-1* in which cells are positioned correctly but do not migrate.

Ventral enclosure

Shortly after dorsal intercalation begins, a second morphological event takes place on the other side of the embryo. This is when ventral epidermal cells migrate towards each other, moving around underling cells to meet and thus enclose the embryo into a tube (Fig. 1.3.4). In a process essential to initiate ventral enclosure, two pairs of epidermal P cells at the anterior end of the embryo (leader cells) extend protrusions towards the ventral midline (Williams-Masson, Malik et al. 1997). Posterior ventral hypodermal cells then elongate towards the ventral midline, until they

reach and establish apical junctions with the corresponding cell on the other side of the embryo. This encloses the embryo via a 'purse-string' mechanism. Laser ablation experiments in which a substantial number of these posterior cells were rendered stationary also perturbed ventral enclosure; this experiment also highlighted the mechanical tension these cells experience, as cells recoiled from the ventral midline after failure to enclose the embryo (Williams-Masson, Malik et al. 1997). The wedge shape of the posterior ventral cells means that the leading edge of each cell is shorter in width than the rest of the cell. This results in an ingression on the ventral side and leads to the bean-shaped embryo, prior to active elongation of the embryo. Finally, hypodermal cells in the head complete the process of ventral enclosure by the epidermis.

As with dorsal intercalation, both actin and microtubules are required for ventral enclosure (Williams-Masson, Malik et al. 1997, Antoshechkin and Han 2002). Initial migration by the leading cells has been shown to be Rac-dependent, thought to be operating through the Arp2/3 complex, since embryos homozygous for mutations in this pathway are unable to initiate ventral enclosure (Chen, Chen et al. 1996, Lundquist, Reddien et al. 2001, Severson, Baillie et al. 2002, Soto, Qadota et al. 2002, Sawa, Suetsugu et al. 2003). The leading protrusive edge is continually regulated by *wsp-1* and *unc-34* (Sawa, Suetsugu et al. 2003, Withee, Galligan et al. 2004). The WSP-1 family of proteins is known to regulate the Arp2/3 complex, whereas the UNC-34 family regulates the dynamics of the plus end of actin filaments, therefore these proteins presumably act by regulating actin polymerisation at leading edges. Signalling though the sole *C. elegans* IP_3 receptor, *itr-1*, is also required for leading edge migration, as a mutant of this gene exhibits reduced protrusion activity and ventral enclosure defects (Thomas-Virnig, Sims et al. 2004).

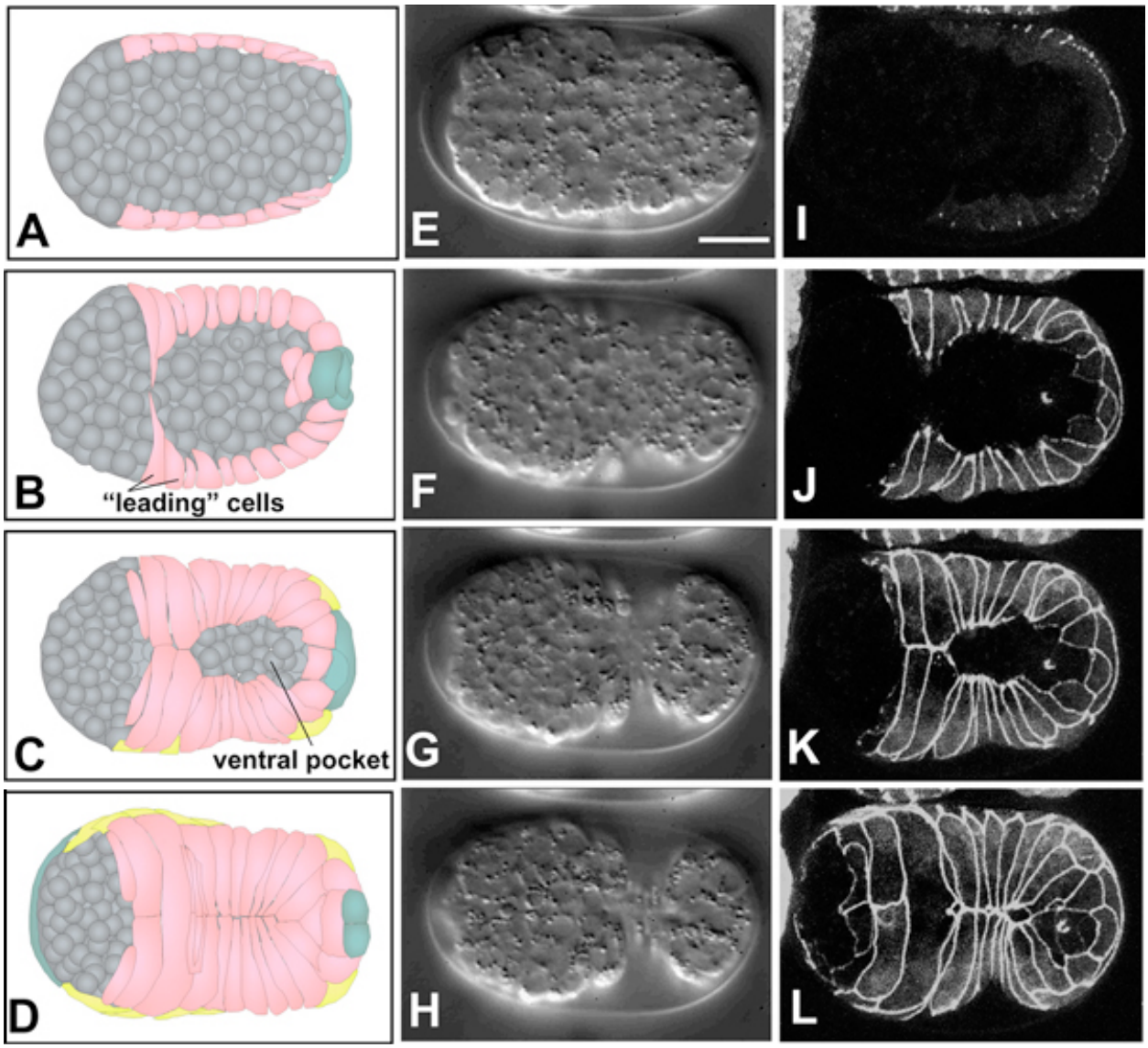

FIG. 1.3.4 – VENTRAL ENCLOSURE OF THE *C. ELEGANS* EMBRYO (CHISHOLM AND HARDIN 2005). **A-D.** Schematics showing the process of ventral enclosure over time, from a ventral viewpoint. Ventral epidermal cells are shown in pink; dorsal epidermal cells are in teal and the lateral seam cells are shown in yellow. Internal cells are shown in grey. The leading cells that initiate ventral enclosure are indicated in **B**, and the ventral pocket is shown in **C**. Over time, the leading cells move ventrally around the embryo until they meet at the ventral midline. Following the leading cells, the posterior ventral epidermal cells enclose the ventral pocket to seal the ventral epidermis. Finally, ventral enclosure is completed by enclosure of the head hypodermis (not shown). **E-H.** DIC images corresponding to the stages of ventral enclosure shown in the schematics. Scale bar = 5μm. **I-L.** Fluorescent images showing the cell junctions with *dlg-1::gfp* during the stages of ventral enclosure.

The cadherin/catenin junctional complex is required for the establishment and maintenance of stable cell junctions at the ventral midline. Animals lacking any of the components of the cadherin/catenin complex are able to extend protrusions but regress after failure to stably contact cells on the opposite side of the embryo (Raich, Agbunag et al. 1999).

Two mechanisms are thought to play a part in the final stage of ventral enclosure, involving the closure of the ventral 'pocket' (see Fig. 1.3.4) by the posterior epidermal cells. Firstly, the ventral tips of cells are known to be very actin rich, consistent with a purse-string mechanism of enclosure (Williams-Masson, Malik et al. 1997), but secondly, the posterior cells can be seen extending short filopodial protrusions towards the ventral midline (Thomas-Virnig, Sims et al. 2004). Both mechanisms may play a role in ventral pocket enclosure in a process similar to that of *Drosophila* dorsal enclosure, during which the actin remodelling provides the forces required for enclosure and the filopodia ensure correct bilateral cell-cell matching.

Elongation

Elongation describes the process following on immediately from ventral enclosure that turns the comma-shaped embryo into a long worm (Fig. 1.3.5). Two processes actively induce elongation. Firstly, epidermal tension provided by actomyosin allows the reshaping of the epidermis, driven by remodelling of the lateral seam cells. Secondly, rapid twitching of the underlying developing body wall muscles is necessary to complete elongation past the two-fold stage.

During early elongation, the actin microfilaments and microtubules of the dorsal and ventral epidermal cells become arranged circumferentially (known as circumferential filament bundles) that persist only until the end of elongation (Priess and Hirsh 1986, Costa, Draper et al. 1997, Williams-Masson, Malik et al. 1997, Costa, Raich et al. 1998). Actomyosin-mediated contraction

of epidermal cells has been shown to be essential for elongation. In addition, LET-502, homologue of the Rho-binding kinase, and the myosin phosphatase MEL-11 have been shown to act antagonistically during elongation to regulate cell shape and tension in the epidermis (Piekny, Johnson et al. 2003). Expression patterns of these genes show that they are largely active in the seam cells, and it is thought that the linkage of the circumferential filament bundles to the adherens junctions of the seam cells is critical for the uniform propagation of tension across the epidermis. Mutants for the cadherin/catenin complex all result in elongation failure and abnormalities due to detachment of the circumferential filament bundles (Costa, Raich et al. 1998).

By the time the embryo reaches the two-fold stage, the mechanism described above is no longer sufficient to drive elongation. It had been observed that mutants effecting muscle development were unable to progress the two-fold stage of elongation, suggesting that later stages of elongation were muscle-dependent (Williams and Waterston 1994). The muscles are connected though the hypodermis to the cuticle via *C. elegans* hemidesmosome structures, which act to transmit force from the muscle to the cuticle. Loss of any of the hemidesmosome components results in a failure in elongation, suggesting that it is this connection that allows the muscles to shape the epidermis (Hresko, Schriefer et al. 1999, Bosher, Hahn et al. 2003, Ding, Goncharov et al. 2003, Woo, Goncharov et al. 2004). Subsequently, hemidesmosomes have been shown to actively sense tension and induce a mechanotransduction signalling pathway during elongation. Tension from the contracting muscles (or externally applied pressure) maintains the adaptor protein GIT-1 at hemidesmosomes, and in turn GIT-1, with its partner PIX-1, activates the p21-activated kinase PAK-1 through a Rac GTPase. This results in the maturation of hemidesmosomes to allow them to resist stress during elongation (Zhang, Landmann et al. 2011).

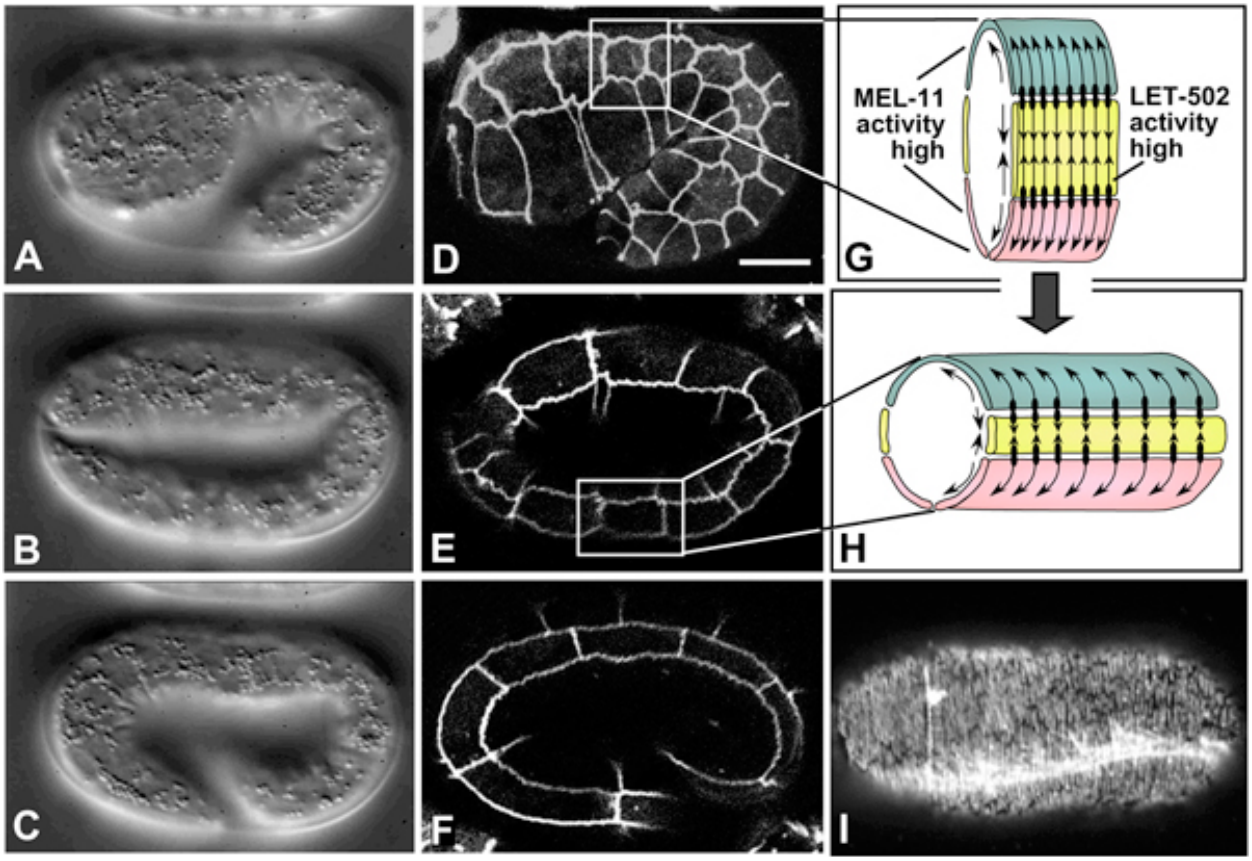

FIG 1.3.5 – EMBRYONIC ELONGATION (CHISHOLM AND HARDIN 2005).
A-C. DIC images showing the stages of elongation over time. D-F. Fluorescent images of *dlg-1::gfp* animals during elongation. Scale bar = 5μm. G-H. Schematics indicating the tension experienced during elongation (arrows). Seam cells are shown in yellow, the dorsal epidermis in teal and the ventral epidermis in pink. Initially, contractile forces from the seam cells drive elongation through the adherens junctions (black ovals) and circumferential actin filament bundles (arrows in the dorsal and ventral hypodermis). LET-502 activity is high in seam cells inducing myosin-dependent contraction, whereas MEL-11, the myosin phosphatase, is presumed high in the dorsal and ventral hypodermis. I. Dorsal view of phalloidin staining at the two-fold stage of elongation, showing the circumferential actin filament bundles. The brighter straining indicates one of the four muscle quadrants.

Cell fusions in the hypodermis during embryogenesis

As the processes of dorsal intercalation and ventral enclosure complete, fusion of dorsal hypodermal cells and some ventral hypodermal cells occurs (Fig. 1.3.6). Amongst other hypodermal tissues, this forms the beginning of the multinucleate hyp7 syncytium that will, by adulthood, form the majority of the *C. elegans* epidermis (Sulston and Horvitz 1977, Sulston, Schierenberg et al. 1983, Podbilewicz and White 1994).

Syncytia occur in many organisms and tissues, including the lens of the eye, muscles, placenta, bones and stem cells, although it is interesting to note that most do not form until development of the tissue is complete (Jee and Nolan 1963, Kuszak, Macsai et al. 1985, Cross, Werb et al. 1994, Hickey, Jacobson et al. 2002, Terada, Hamazaki et al. 2002, Xiang, Rasmussen et al. 2002, Ying, Nichols et al. 2002, Baroux, Fransz et al. 2004, Chen and Olson 2004). In *C. elegans* 300 of the 1090 somatic cells born during development fuse (Sulston and Horvitz 1977, Sulston, Schierenberg et al. 1983, Hedgecock and White 1985, Podbilewicz and White 1994). Prevention of fusion in these cells, though not affecting cell fate or behaviour, affects the morphology, behaviour of the animal and fertility (Mohler, Shemer et al. 2002, Shemer and Podbilewicz 2002, Shemer, Suissa et al. 2004, Cassata, Shemer et al. 2005).

Two membrane fusion effector proteins (fusogens) have been identified in *C. elegans*: *eff-1*, required for cell fusion in the epidermis, vulva and pharyngeal muscle (Mohler, Shemer et al. 2002, Shemer and Podbilewicz 2002, Shemer, Suissa et al. 2004, del Campo, Opoku-Serebuoh et al. 2005, Podbilewicz, Leikina et al. 2006, Gattegno, Mittal et al. 2007); and *aff-1*, required for cell fusion in the uterus, terminally differentiated epidermal seam cells and certain vulval cells (Sapir, Choi et al. 2007). *aff-1* mediated cell fusions all occur late in post-embryonic development at the L4 stage, suggesting that this fusogen takes over the control of cell fusion at this stage. *eff-1* has been shown to localise to the site of cell fusion in fusing cells (del Campo, Opoku-Serebuoh et al. 2005, Smurova and Podbilewicz 2016)

and experiments using a heat shock promoter show that ectopic cell autonomous expression of either *eff-1* or *aff-1* in neighbouring cells is sufficient to promote cell fusion in cell types that do no usually fuse (Shemer, Suissa et al. 2004, Sapir, Choi et al. 2007). It has recently been shown that expression of EFF-1 in the epidermis is vesicular and dynamic, with EFF-1 accumulating in the early endosomes of epidermal cells (Fig. 1.3.6, Smurova and Podbilewicz 2016). Endocytosis of EFF-1 has been shown to be dynamin- and RAB-5-dependent: if either one is down-regulated, EFF-1 accumulates on the membranes of cells and precocious cell fusion occurs, suggesting that the endocytosis of EFF-1 is a mechanism with which cells prevent cell fusion (Smurova and Podbilewicz 2016).

It is thought that nearly all cells have the potential to fuse in *C. elegans*, but cells which remain unfused during development are known to contain additional Hox, Ras, Wnt, Rb and NuRD mediated pathways to suppress *eff-1* activity (Kenyon 1986, Clark, Chisholm et al. 1993, Eisenmann, Maloof et al. 1998, Brunschwig, Wittmann et al. 1999, Ch'ng and Kenyon 1999, Shemer, Kishore et al. 2000, Alper and Kenyon 2001, Chen and Han 2001, Koh and Rothman 2001, Alper and Kenyon 2002, Koh, Peyrot et al. 2002, Shemer and Podbilewicz 2002, Chen, Eastburn et al. 2004, Cassata, Shemer et al. 2005). Two GATA-type transcription factors ELT5/ EGL-18 and ELT-6 act in the lateral seam cells to prevent fusion to the hyp7 syncytium, and *elt-5* expression has been shown to be regulated by the homeobox transcription factor *ceh-16* (Koh and Rothman 2001, Cassata, Shemer et al. 2005). How this inhibition of cell fusion is overcome in the hypodermally-fated daughters of the seam cell divisions is not yet clear.

In the posterior ventral epidermis, where the P cells remain unfused even when most other epidermal cells fuse to form the hyp7 syncytium during embryogenesis, the zinc finger transcription factor *ref-2* acts to repress cell fusion (Alper and Kenyon 2002). RNA interference

(RNAi) against *ref-2* resulted in ectopic fusion of the Pn.p cells (posterior daughters of the P cells after their division at the ventral midline, see later figures 1.4.4 and 1.6.3) and also of the un-migrated P cells with the hyp7 syncytium, whereas a dominant gain-of-function mutant acted to inhibit cell fusion of Pn.p cells (Alper and Kenyon 2002). Two Hox genes control the pattern of Pn.p cell fusion along the anteroposterior body axis, *lin-39* (mid-body fates, P3-8.p) and *mab-5* (posterior fates, P7-11.p) (Clark, Chisholm et al. 1993, Salser, Loer et al. 1993, Wang, Muller-Immergluck et al. 1993). *lin-39* has been shown in hermaphrodites to prevent cell fusion by promoting *ref-2* expression in the mid-body Pn.p cells (Salser, Loer et al. 1993, Alper and Kenyon 2002), important for later formation of the hermaphrodite vulva. *lin-39* also regulates transcription of the *eff-1* fusogen (Shemer and Podbilewicz 2002), and the complex interactions between *lin-39*, *ref-2* and *eff-1* act to protect the P cells and their descendants from premature fusion during L1. *elt-5* and *elt-6*, active in the seam cell lineage, have been shown to act redundantly to regulate Pn.p fusion during later vulval formation (L2-L4); expression of these genes in the Pn.p cells are also regulated by LIN-39, together with the homeobox cofactor CEH-20 (Koh, Peyrot et al. 2002, Koh, Bernstein et al. 2004).

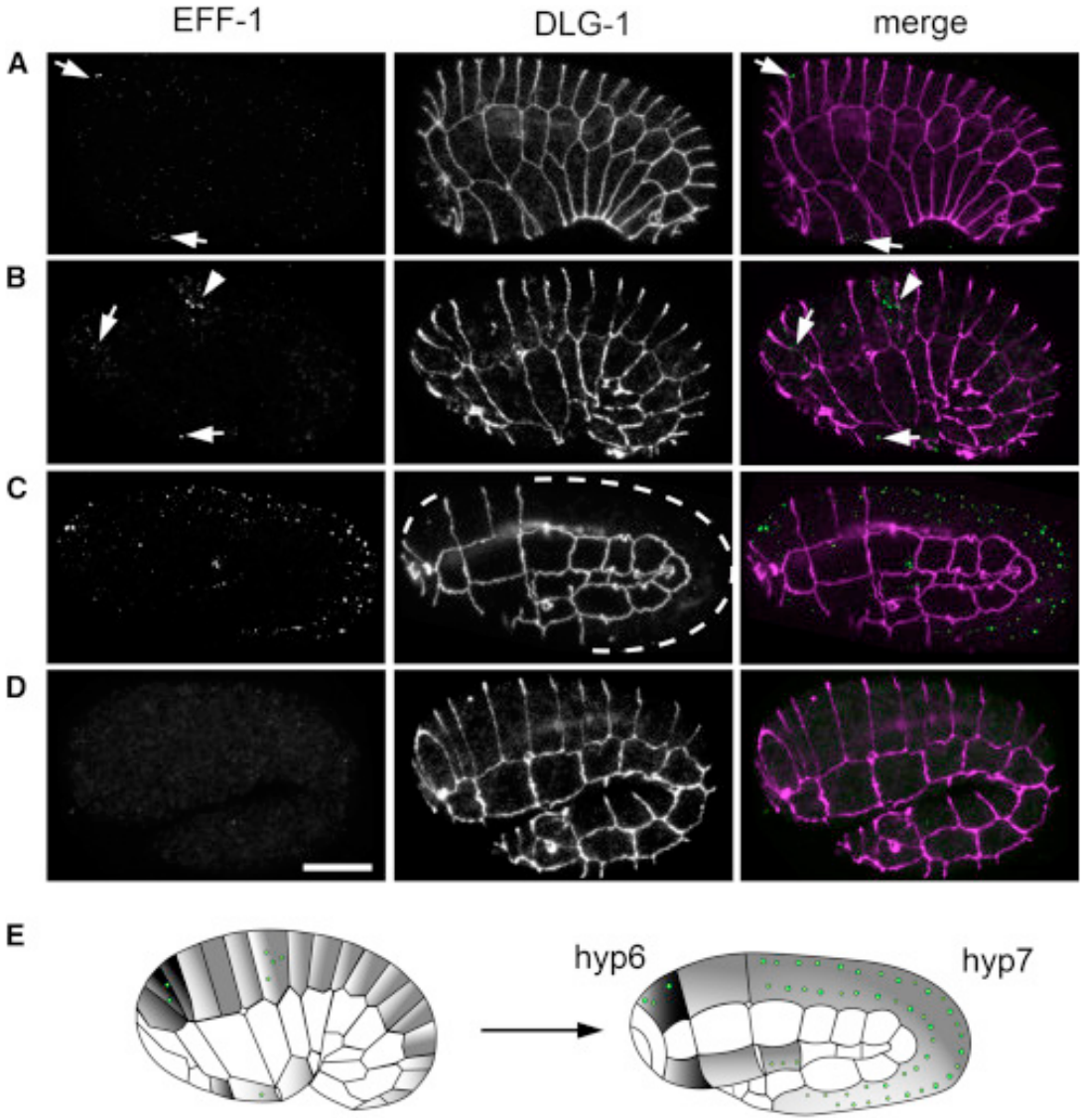

FIG. 1.3.6 – CELL FUSION IN THE EPIDERMIS DURING EMBRYOGENESIS (SMUROVA AND PODBILEWICZ 2016).
A-C. The wild-type embryo during epidermal cell fusion. The expression of EFF-1 is immunostained with anti-EFF-1 monoclonal antibody (green) and anti-DLG-1 antibody stains the apical junctions between cells (magenta). The arrows highlight the vesicular localisation of EFF-1 prior to and during cell fusion. Co-localisation of the apical junction and EFF-1 is indicated in **B** with an arrowhead. The white dashed line in **C** highlights fused epidermal cells. **D.** A null *eff-1* embryo showing no EFF-1 staining and no cell fusion. Scale bar = 10μm. **E.** Schematics of embryonic cell fusions during early elongation in *C. elegans*, with the EFF-1 expression pattern shown in green. The hyp6 and hyp7 syncytia are shown in dark and light grey respectively. Cell borders are shown as black lines.

1.4 *C. elegans* post-embryonic hypodermal development

C. elegans post-embryonic development

Although the main body plan remains unaltered during post-embryonic development, during this time the worm increases from 558 cells to approximately 1000 cells at adulthood (Sulston, Schierenberg et al. 1983). Of the 558 cells in the newly hatched larva, approximately 10% are blast cells that continue to divide during the 4 larval moults, L1-L4 (Sulston and Horvitz 1977). Post-embryonic development is triggered by the presence of food; in conditions of starvation, the L1 worm will arrest development until food is encountered and cells re-enter a normal life cycle. It can remain in this diapaused state for 6-10 days (Johnson, Mitchell et al. 1984).

Cells which are born during post-embryonic development contribute to the nervous system, the reproductive system, the coelomocyte system, the epidermis and sex-specific muscles (Sulston and Horvitz 1977). It is important to note that post-embryonic development involves, as does embryonic development, stereotypical programmed cell deaths (Sulston and Horvitz 1977, Sulston, Schierenberg et al. 1983, Driscoll 1995). In the case of hermaphrodite animals, this occurs in 131 of the total 1090 cells that are born by adulthood (Sulston and Horvitz 1977, Sulston, Schierenberg et al. 1983).

General structure of the *C. elegans* hypodermis

The majority of the adult *C. elegans* hypodermis is comprised of the hyp7 syncytium, a single multinucleate cell that surrounds the animal. This is created from 23 mononucleate cells that are born and fuse during embryogenesis (see previous section about cell fusion, Sulston, Schierenberg et al. 1983, Podbilewicz and White 1994). A further 110 cells are contributed throughout post-embryonic development by the ectoblast lineages of the lateral seam cells and ventral P cells (Figs. 1.4.2 and 1.4.3). At least in the case of the seam-derived cells, these later nuclei to join the syncytium are, in contrast to diploid embryonic hyp7 nuclei, tetraploid (Hedgecock and White 1985). The hypodermis of the head and tail is not covered by the hyp7 syncytium; instead, additional hypodermal cells and syncytia formed during embryogenesis cover these regions (Fig. 1.4.1). Of these, only the hyp7 is added to during post-embryonic development.

A

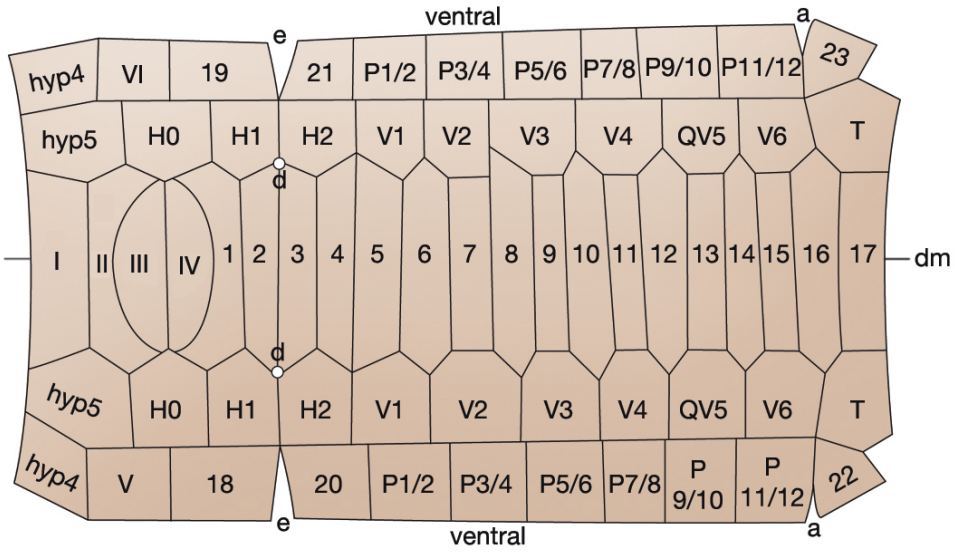
ventral
e
a
hyp4
VI
19
21
P1/2
P3/4
P5/6
P7/8
P9/10
P11/12
23
hyp5
H0
H1
H2
V1
V2
V3
V4
QV5
V6
T
d
I
II
III
IV
1
2
3
4
5
6
7
8
9
10
11
12
13
14
15
16
17
dm
d
hyp5
H0
H1
H2
V1
V2
V3
V4
QV5
V6
T
hyp4
V
18
20
P1/2
P3/4
P5/6
P7/8
P 9/10
P 11/12
22
e
a
ventral

B

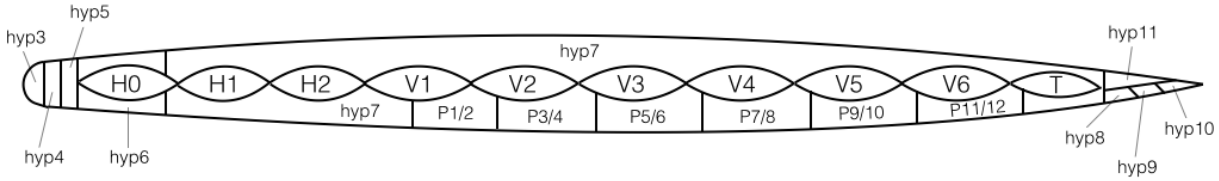
hyp3
hyp5
hyp7
hyp11
H0
H1
H2
V1
V2
V3
V4
V5
V6
T
hyp7
P1/2
P3/4
P5/6
P7/8
P9/10
P11/12
hyp4
hyp6
hyp8
hyp9
hyp10

C

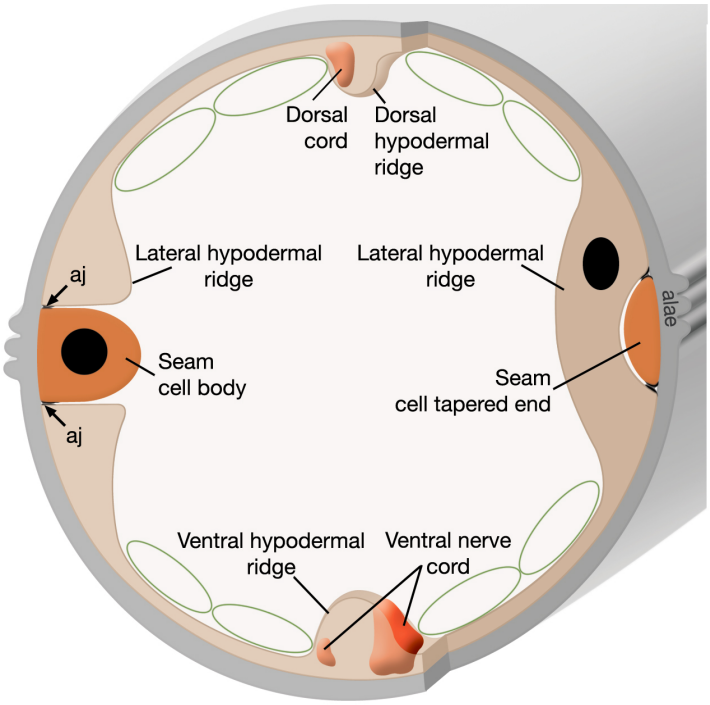
Dorsal cord
Dorsal hypodermal ridge
Lateral hypodermal ridge
Lateral hypodermal ridge
aj
alae
Seam cell body
Seam cell tapered end
aj
Ventral hypodermal ridge
Ventral nerve cord

Ventral hypodermal development

At hatching, P cells rather than the hyp7 form the main ventral hypodermis (Fig. 1.4.1 B) but later in L1 these migrate to the ventral midline where they divide to contribute cells to the ventral nerve cord, hyp7, the developing vulva in hermaphrodites and the hook mating structure of the tail in males (P10 and P11, Fig. 1.4.2, Sulston and Horvitz 1977, also see Section 1.6 of this chapter).

Seam cell development

At hatching, seam cells run in lines of 10 unfused cells along both lateral sides of the animal (H0-2, V1-6 and T, shown in figure 1.4.1 B). During the four larval moults, the seam cells (excepting H0) divide symmetrically and asymmetrically, both increasing the number of seam cells on each side of the worm and contributing cells to the growing hyp7 syncytium and neuronal development (Sulston and Horvitz 1977). In males, the seam cell lineage also contributes to the sensory rays in the cuticular fan of the male tail. The post-embryonic lineage of the seam cells in both hermaphrodites and males is shown in figure 1.4.3.

At adulthood, the seam cells are thought to reach terminal differentiation and the two seam lines of individual cells fuse to form two lateral seam syncytia (Podbilewicz and White 1994). For the majority of the hypodermis, the hyp7 is basal to the seam cells, and the ventral hyp7 is continuously connected to the dorsal hyp7. However, at regions of the seam syncytium in which a nucleus is present, the seam syncytium penetrates the hyp7 through its basal side (Fig. 1.4.1 C). Terminally differentiated seam cells secrete three lines of cuticular ridges on the adult cuticle known as alae (Fig. 1.4.1 C, Cox, Staprans et al. 1981, George, Simokat et al. 1998, Petalcorin, Oka et al. 1999, Koh and Rothman 2001, Frand, Russel et al. 2005).

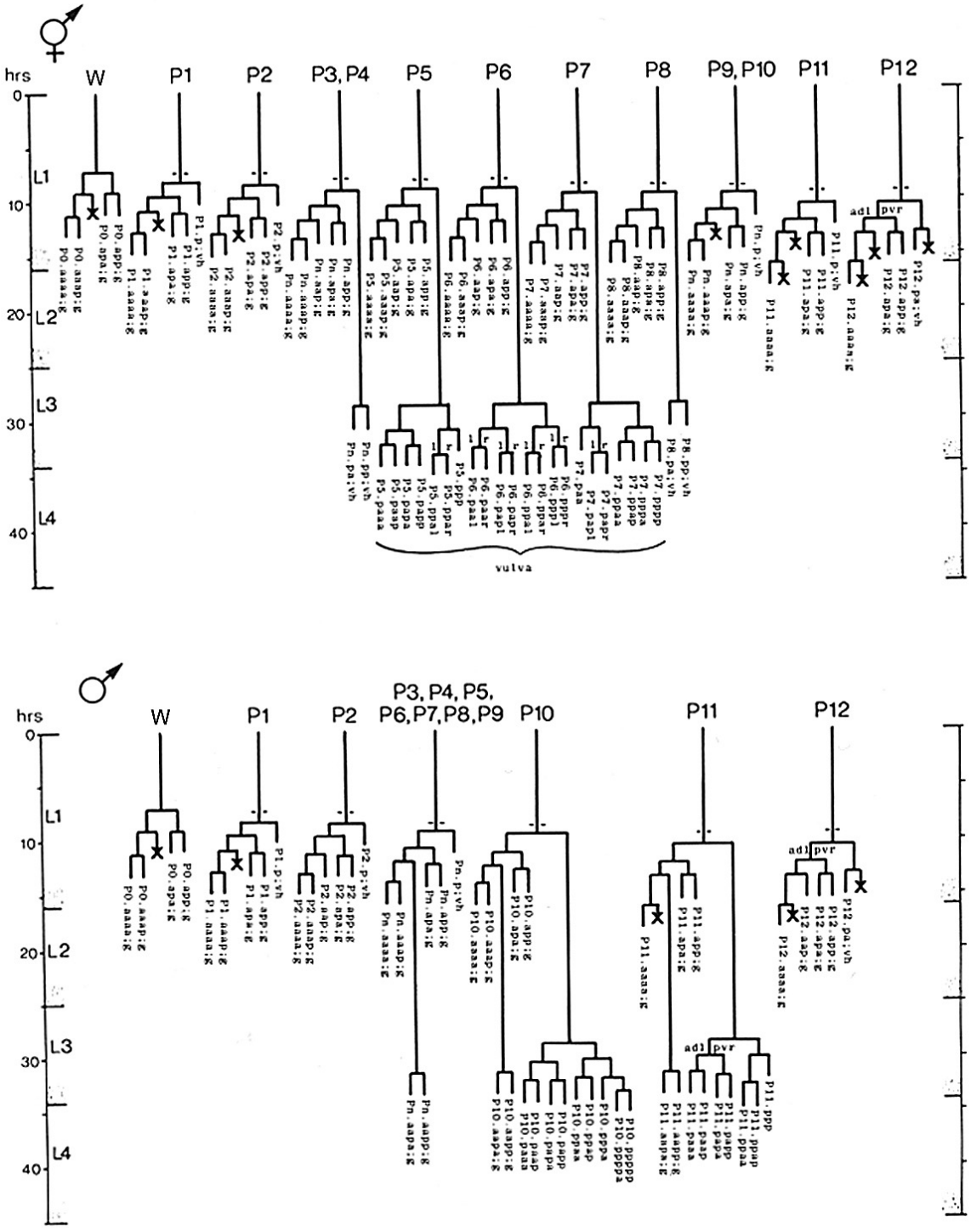

FIG. 1.4.2 – POST-EMBRYONIC P CELL LINEAGE IN THE HERMAPHRODITE AND MALE (SULSTON AND HORVITZ 1977).

Hours from hatching are indicated down the left hand side, along with the timing of the larval moults. Anterior is on the left; posterior is on the right. The first P cell division occurs after the P cells have migrated to the ventral midline (indicated by dots next to the cell lineage). Crosses indicate programmed cell death. P cell descendants contribute to the ventral nerve cord (g), the hyp7 syncytium (vh) and in hermaphrodites the developing vulva. In males P cells contribute male-specific neurones.

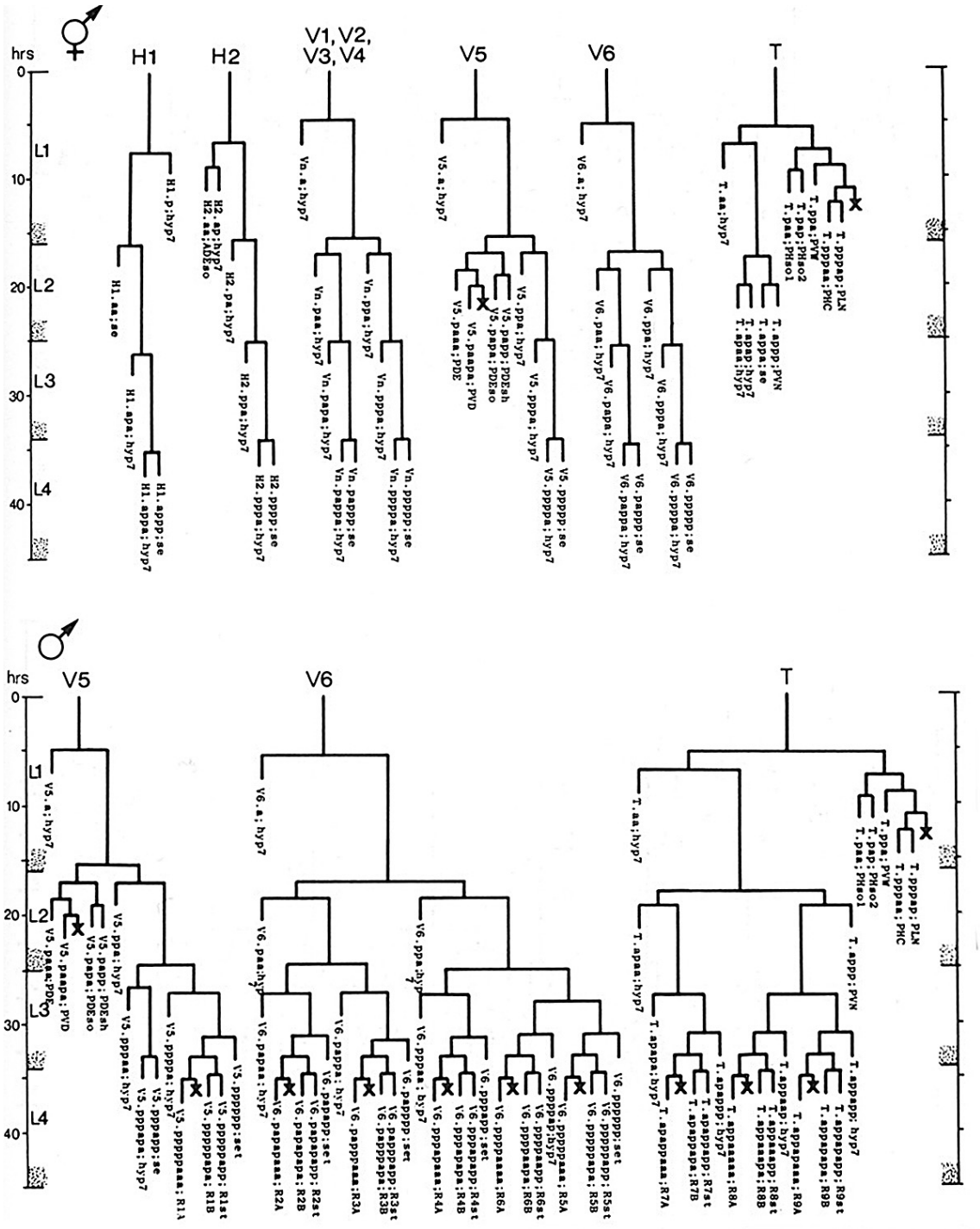

FIG. 1.4.3 – POST-EMBRYONIC SEAM CELL LINEAGES IN THE HERMAPHRODITE AND MALE (SULSTON AND HORVITZ 1977).

The seam cells, with the exception of H0, divide during each larval moult (hours post-hatching are shown down the side with larval moults indicated; anterior is left). V1-4 and V6 in the hermaphrodite divide in a typical manner that provides a model for asymmetrical *versus* symmetrical division. These lineages undergo one asymmetric division during each larval stage until adulthood, with the exception of L2, during which the seam cells also divide symmetrically. An asymmetrical division of the seam is one in which one daughter cell retains the seam cell fate (se) and can continue to divide, whereas the other (anterior) daughter differentiates (hyp7 or neuronal cell fate in the case of V5). Symmetrical seam divisions after which both daughters retain the seam fate increase the total number of seam cells from 10 at hatching to 16 by the end of post-embryonic development. Other seam cells undergo variations upon this typical lineage, and in the male, V6, V5 and T contribute to the rays of the sensory tail (R). Crosses indicate programmed cell death.

1.5 Control of seam cell development

Epidermal post-embryonic development consists of both seam and P cell divisions. Seam cell divisions have been the focus of considerable interest, however, because they divide in a pattern that is reminiscent of stem cell divisions in other organisms. This is because they divide both to self-renew and also to donate cells to other tissues. The ability of a cell to divide and replicate itself must be highly regulated, with loss of this regulation being associated with cancer formation in other organisms. Furthermore, the asymmetrical divisions to produce one seam daughter that continues to divide and another daughter that differentiates must also be tightly controlled: if both daughter cells differentiate (i.e. undergo a symmetrical division to the differentiated fate) then the dividing cell pool will be depleted. Seam cells divide in a robust stereotypical pattern. Together with the fact that seam cell divisions have been found to be controlled by genes which are conserved in stem cell development, this makes seam cells an attractive model of the stem cell mode of division. Because of this paradigm, genes regulating seam cell divisions have been the subject of investigation.

A summary of the post-embryonic epidermal development of the seam and ventral P cells is shown in figure 1.5.1, together with a schematic of a typical wild-type asymmetrical seam cell division. During the L2 symmetrical seam cell division, the only difference is that both daughters remain in the lateral seam line and both continue to divide (i.e. the division is symmetrised to the seam cell fate). Genes found to be important in the regulation of seam cell divisions include members of the Wnt pathway, the Runx pathway, the heterochronic pathway and the Hox family of transcription factors. Given the complexity of development and yet the seemingly small number of regulatory pathways that control it, it is perhaps unsurprising that each of these pathways interact with each other to provide more intricate levels of regulation during seam cell development. I have attempted to highlight these interactions whenever possible in this section.

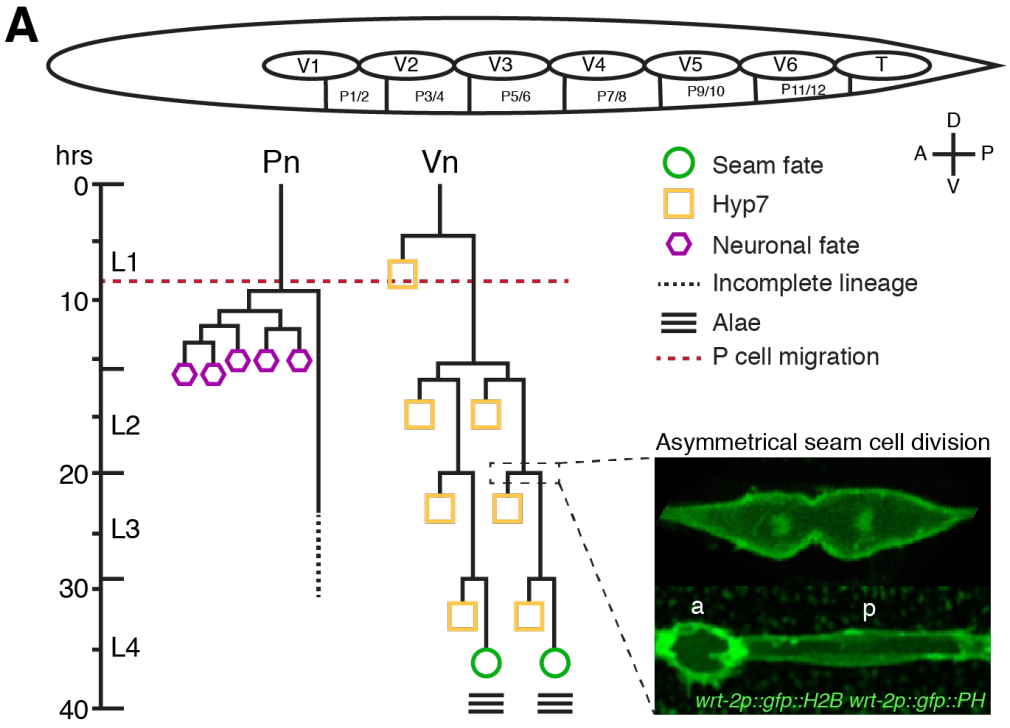
A
V1
V2
V3
V4
V5
V6
T
P1/2
P3/4
P5/6
P7/8
P9/10
P11/12
D
A
P
V
hrs
Pn
Vn
0
10
20
30
40
L1
L2
L3
L4
Seam fate
Hyp7
Neuronal fate
Incomplete lineage
Alae
P cell migration
Asymmetrical seam cell division
a
p
wrt-2p::gfp::H2B wrt-2p::gfp::PH

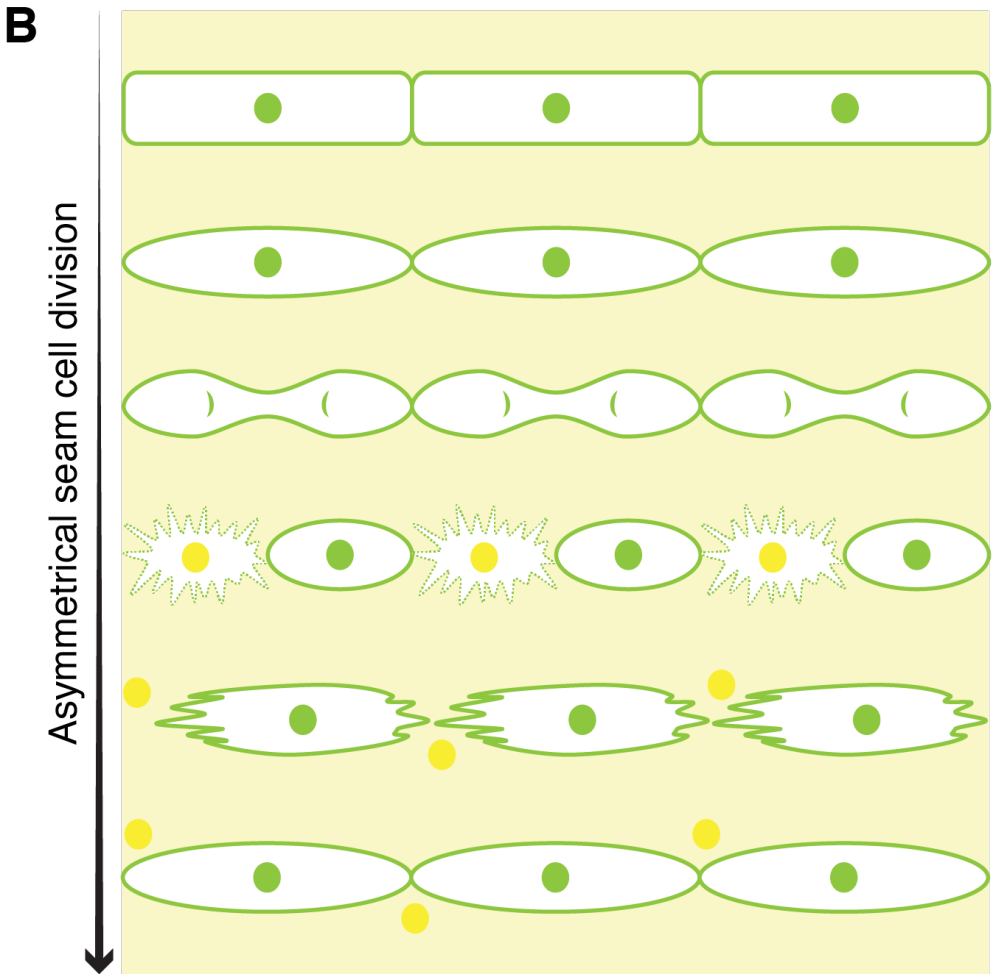
B
Asymmetrical seam cell division

Wnt signalling controls cell fate polarity during asymmetrical seam divisions

Wnts are secreted lipid-modified glycoproteins that can act both as short-range signalling molecules and as morphogens to control processes such as cell fate specification, asymmetrical division and cell migration in a diverse range of multicellular metazoans, including mammals (Zecca, Basler et al. 1996, Cadigan and Nusse 1997, Angers and Moon 2009, Clevers and Nusse 2012). Deregulation of the Wnt signalling pathway is frequently associated with cancer (Clevers and Nusse 2012), and Wnt is required for both stem cell maintenance and tissue regeneration in developed animals.

The most studied pathway of Wnt signalling is the 'canonical' Wnt pathway. This controls the transcription of target genes through an effector protein, ß-catenin (Angers and Moon 2009, Clevers and Nusse 2012). An unactivated cell will constitutively proteasomally degrade ß-catenin, through the action of a degradation complex comprising of Axin, APC and two kinases, CK1 and GSK3ß. Upon Wnt binding to the receptors Frizzled and LRP6, the degradation pathway is inhibited, a process requiring the cytoplasmic protein Dishevelled. The stabilised ß-catenin is now translocated to the nucleus where it co-activates target gene transcription with its interacting partner, a member of the Tcf family of transcription factors.

Other Wnt signalling pathways which do not require ß-catenin exist, such as the planar cell polarity (PCP) pathway and the Ror and Ryk dependent pathways (Lawrence, Struhl et al. 2007, Green, Inoue et al. 2008, Angers and Moon 2009, Wallingford 2012). These are commonly known as the 'non-canonical' Wnt pathways. The PCP pathway involves the asymmetric localisation of Frizzled, Dishevelled and two PCP-specific components Prickle and Van Gogh (Lawrence, Struhl et al. 2007, Wallingford 2012). Ror is an alternative Wnt receptor related to Frizzled (Xu and Nusse 1998) which can, amongst other responses, inhibit canonical Wnt

signalling (Green, Inoue et al. 2008). Ryk, or Derailed in *Drosophila*, is yet another alternative receptor, this time related to the Wnt inhibitor WIF (Yoshikawa, McKinnon et al. 2003, Lu, Yamamoto et al. 2004).

C. elegans has five Wnt genes, four Frizzled receptors but no LRP6, three Dishevelleds, four ß-catenins and one Tcf. All other components of the canonical signalling pathway are also conserved. In addition, the genome contains homologues of the non-canonical Wnt pathways, including Van Gogh and Prickle of the PCP pathway (Wu and Herman 2006), and Ror (Forrester, Dell et al. 1999) and Ryk (Inoue, Oz et al. 2004). These *C. elegans* homologues are summarised in Table 1.5.1

Wnt component	***C. elegans* homologues**
Wnt ligand	*mom-2*, *lin-44*, *egl-20*, *cwn-1*, *cwn-2*
Frizzled	*mom-5*, *lin-17*, *mig-1*, *cfz-2*
Ror	*cam-1*
Ryk/Derailed	*lin-18*
CK1	*kin-19*
Dishevelled	*mig-5*, *dsh-1*, *dsh-2*
GSK3ß	*gsk-3*
Axin	*pry-1*, *axl-1*
APC	*apr-1*
ß-catenin	*bar-1*, *sys-1*, *wrm-1*, *hmp-2*
Tcf	*pop-1*
Van Gogh	*vang-1*
Prickle	*prkl-1*
NLK (asymmetrical pathway only)	*lit-1*

TABLE 1.5.1 – *C. ELEGANS* HOMOLOGUES OF THE WNT SIGNALLING PATHWAY.
The components of the Wnt signalling pathways, both canonical and non-canonical, are shown in the left-hand column. The *C. elegans* orthologues that have been shown to function in the Wnt pathway are shown on the right.

The four ß-catenins in *C. elegans* are each responsible for a different aspect of the canonical ß-catenin function characterised in *Drosophila* and vertebrates (Korswagen, Herman et al. 2000). Canonical Wnt signalling is mediated by BAR-1, whereas SYS-1 and WRM-1 are part of a divergent Wnt pathway called the Wnt/ß-catenin asymmetry pathway. HMR-1 appears to assume the role of Wnt at adherens junctions and does not interact with POP-1 (Costa, Raich et al. 1998, Korswagen, Herman et al. 2000, Natarajan, Witwer et al. 2001).

The divergent canonical Wnt/ß-catenin asymmetry pathway is involved in controlling asymmetrical divisions along the anteroposterior axis and is known to be active in the seam cells (Mizumoto and Sawa 2007). This pathway is considered a divergent canonical pathway because, although it involves two ß-catenins (WRM-1 and SYS-1), it has a unique regulatory mechanism. Rather than stabilising ß-catenin, this pathway relies on the asymmetrical localisation of signalling components in the dividing cell. During an asymmetrical seam cell division, the Frizzled and Dishevelled homologues, LIN-17 and DSH-1 respectively, localise to the posterior cortex of the dividing cell (Goldstein, Takeshita et al. 2006, Mizumoto and Sawa 2007). At the same time, WRM-1/ß-catenin, ARP-1/APC, PRY-1/Axin and LIT-1/NLK localise to the anterior cortex of the cell (Takeshita and Sawa 2005). As the cell reaches telophase, the two ß-catenins (WRM-1 and SYS-1) as well as LIT-1 start to localise to the posterior nucleus where they act to export POP-1 from the nucleus (Lo, Gay et al. 2004, Takeshita and Sawa 2005, Phillips, Kidd et al. 2007), leaving POP-1 predominantly localised in the anterior nucleus (Lin, Thompson et al. 1995, Sugioka, Mizumoto et al. 2011, Yamamoto, Takeshita et al. 2011). This localisation is summarised in figure 1.5.2.

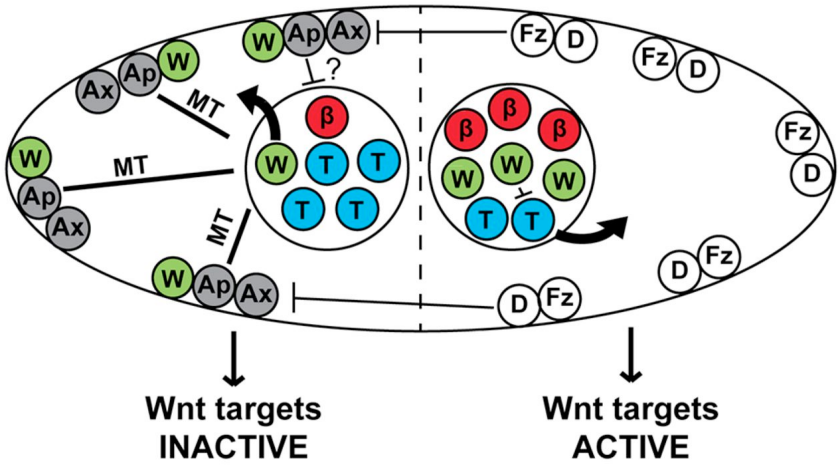

FIG. 1.5.2 – LOCALISATION AND RELATIONSHIP OF THE WNT/ß-CATENIN ASYMMETRY PATHWAY COMPONENTS DURING AN ASYMMETRICAL SEAM CELL DIVISION (BALDWIN AND PHILLIPS 2014).
The dividing seam cell is represented as the black outline of an oval, and its two daughter nuclei as black outlines of circles. The localisation of Wnt pathway components are indicated, showing the asymmetric distribution of WRM-1/ß-catenin, APC/APR-1 and Axin/PRY-1 to the anterior cortex and Frizzled/LIN-17 and Disheveled/DSH-1 to the posterior cortex. APR-1/APC stabilises microtubules (MT) in the anterior daughter to increase WRM-1/β-catenin nuclear export and cortical localisation. As the seam cell reaches the end of telophase during an asymmetrical division, the ß-catenins WRM-1 and SYS-1 localise to the posterior nucleus and cause the phosphorylation of POP-1 by activation of the LIT-1/NLK kinase (not shown). This promotes export of POP-1 from the nucleus, resulting in all remaining nuclear POP-1 to be bound by SYS-1/ß-catenin and thus Wnt transcriptional targets to be active. In contrast, the lack of ß-catenin in the anterior cell causes unbound POP-1 to be retained in the nucleus, leading to transcriptional repression. This asymmetry of expression results in two daughter cells with differing cell fates. β = SYS-1/β-catenin (red), W = WRM-1/β-catenin (green), T = POP-1/TCF (blue), Fz = Frizzled (white), D = Disheveled (white), Ax = PRY-1/Axin (gray), Ap = APR-1/APC (gray).

Wnts act redundantly to control the polarity of asymmetric divisions of the seam cells V1-V5 and V6, since compound mutants of Wnts exhibit random polarity reversals (Yamamoto, Takeshita et al. 2011). However, the polarity of the V5 and T divisions are frequently reversed in *egl-20* and *lin-44* single mutants respectively (Herman, Vassilieva et al. 1995, Whangbo, Harris et al. 2000), indicating that for these seam lineages, specific Wnts are required for the correct polarity of division. Wnt receptors, but not Wnt ligands, have been shown to be essential for establishing polarity itself during the asymmetrical seam division, as the triple mutant *lin-17 mom-5; cam-1* shows no polarity in seam cell divisions (Yamamoto, Takeshita et al. 2011). The quintuple knockout of all five Wnts does not have this effect, suggesting the receptors may have a Wnt-independent role in establishing polarity (Yamamoto, Takeshita et al. 2011).

Wnts are required in T and V5 to establish the correct cortical asymmetry of Wnt pathway components (Takeshita and Sawa 2005, Mizumoto and Sawa 2007, Sugioka, Mizumoto et al. 2011). In other organisms, Dishevelled is known to interact with the Frizzled receptor (Wong, Bourdelas et al. 2003), so it is likely that, given the co-localisation of the two proteins in worms (Mizumoto and Sawa 2007), DSH-1/Dishevelled is recruited to the posterior cortex along with activated Frizzled/LIN-17. This initial polarisation is speculated to regulate the distribution of anteriorly localised components, although, possibly due to redundancy between the three *C. elegans* Dishevelleds, it has not been shown in the seam cells that correct cortical localisation is dependent on Dishevelled.

Experiments tethering WRM-1 to the cortex have been shown to correspondingly regulate nuclear WRM-1 levels (Mizumoto and Sawa 2007), possibly through recruitment of APR-1 (Mizumoto and Sawa 2007, Sugioka, Mizumoto et al. 2011), which binds to and stabilises microtubules. The number of astral microtubules therefore becomes asymmetric; perturbing this

asymmetry perturbs the asymmetry of WRM-1 and POP-1 in the daughter nuclei (Sugioka, Mizumoto et al. 2011). In the posterior nucleus, the high levels of WRM-1 bind to and activate the co-localised kinase LIT-1 (Lo, Gay et al. 2004). This phosphorylates POP-1, which is then exported, via PAR-5/14-3-3, from the posterior nucleus, resulting in the asymmetrical distribution of nuclear POP-1 (Yang, Huang et al. 2011).

A second ß-catenin, SYS-1, is also known to be localised asymmetrically during asymmetrical divisions (Huang, Shetty et al. 2007, Phillips, Kidd et al. 2007). WRM-1 and LIT-1 are not required for this asymmetry, but rather there is evidence that SYS-1 is regulated at the level of protein stability, as with ß-catenins in other organisms (Huang, Shetty et al. 2007, Phillips, Kidd et al. 2007). In the canonical Wnt pathway, POP-1 is bound to and activated by a ß-catenin. WRM-1 does not appear to play this role in *C. elegans*, since it does not act as a cofactor of POP-1 (Natarajan, Witwer et al. 2001, Korswagen, Coudreuse et al. 2002), whereas SYS-1 is able to bind to and activate POP-1 in mammalian cells (Kidd, Miskowski et al. 2005). In most cases, the ratio of POP-1 to SYS-1 in the nucleus determines the activity of POP-1; whereas POP-1 bound to SYS-1 acts as a transcriptional activator, unbound POP-1 acts as a repressor (Kidd, Miskowski et al. 2005). Therefore, a nucleus with high levels of POP-1 but low levels of SYS-1 will experience the repression of transcription by the unbound POP-1 (the anterior daughter cell), whereas a nucleus with low levels of POP-1 and higher levels of SYS-1 will have all POP-1 present bound to SYS-1 in an active form (the posterior daughter cell). This binary output ultimately determines the asymmetric fates of the daughter cells (Phillips, Kidd et al. 2007). There are exceptions to this binary mode of Wnt activation, however, such as the control of *ttx-3* expression, activated by Wnt in the anterior daughter cell but not the posterior daughter. In this case, unbound POP-1 is able to recruit a Zic transcription factor in order to activate *ttx-3*

transcription in the anterior cell, whereas SYS-1 acts as a repressor of *ttx-3* transcription (Murgan, Kari et al. 2015).

Hox genes in seam cell development

Hox transcription factors, developmental patterning genes which contain the homeobox DNA-binding domain, confer positional information along the longitudinal axis during *C. elegans* development (Clark, Chisholm et al. 1993, Salser, Loer et al. 1993, Wang, Muller-Immergluck et al. 1993, Brunschwig, Wittmann et al. 1999, Ferreira, Zhang et al. 1999, Liu and Fire 2000, Van Auken, Weaver et al. 2000). Activation by Hox genes in a spatial and temporal manner results in the regulation of fate-determining transcriptional targets. First discovered in *Drosophila* as a cluster of genes that controlled the arrangement and identity of specific segments of the body (Lewis 1978), Hox genes have been found to be conserved from cnidarians to vertebrates, although the homeobox domain is much older and present in both fungi and plants (Ruddle, Bartels et al. 1994, Larroux, Fahey et al. 2007, Holland 2013). In *C. elegans*, Hox factors can act both singly and combinatorially to confer cell identity (Clark, Chisholm et al. 1993, Salser, Loer et al. 1993, Wang, Muller-Immergluck et al. 1993, Brunschwig, Wittmann et al. 1999, Ferreira, Zhang et al. 1999, Liu and Fire 2000, Van Auken, Weaver et al. 2000).

The *C. elegans* genome contains six Hox genes, *ceh-13*, *lin-39*, *mab-5*, *egl-5*, *nob-1* and *php-3*. As well as being required for general body patterning during embryogenesis, three of the Hox genes, two posterior (*mab-5*, *egl-5*) and one medial (*lin-39*) have roles in post-embryonic development. Specifically in the context of seam cell development, in males, the Hox gene *mab-5* is required for V5 and V6 to generate the lineages that lead to formation of the male tail, and in the case of the V6 lineage acts though a second Hox gene *egl-5* (Kenyon 1986, Chisholm 1991, Salser and Kenyon 1996, Ferreira, Zhang et al. 1999, Hunter, Harris et al. 1999). Hox

control of hermaphrodite post-embryonic development is confined mainly to the role of *lin-39* in specifying the mid-body during vulval development, and does not play a large role in the seam (Maloof and Kenyon 1998).

Hox gene expression in *C. elegans*, unlike in *Drosophila* or vertebrates, is mainly cell-lineage specific (Cowing and Kenyon 1996). However, the Wnt pathway has been shown to play a role in the regulation of Hox gene expression (Eisenmann, Maloof et al. 1998, Maloof, Whangbo et al. 1999, Zhang and Emmons 2001, Streit, Kohler et al. 2002) and due to the ability of Wnt to replace Hox genes in certain cases (Hunter, Harris et al. 1999, Zhang and Emmons 2000), it seems likely that Hox genes have evolved to replace Wnts in specifying regional identity (Li, Kulkarni et al. 2009).

The Runx pathway promotes proliferative seam cell divisions

Runx genes are defined by a the presence of a 'Runt-box' DNA binding domain. The first member of this gene family described was *Drosophila runt* (Gergen and Butler 1988), which plays a role in embryonic patterning, sex determination and neuronal development. Subsequently, three additional *Drosophila* Runx genes have been identified, and homologues found in even very basic metazoans such as sponges (Sullivan, Sher et al. 2008). The importance of Runx genes in the control of proliferation was highlighted by the independent discoveries of their mis-regulation in the t(8;21) chromosome translocation of acute myeloid leukaemia (AML) and also as a subunit of the polyomavirus enhancer-binding protein 2 (PEBP2) (Kamachi, Ogawa et al. 1990, Miyoshi, Shimizu et al. 1991, Erickson, Gao et al. 1992, Meyers, Lenny et al. 1995). It has been found that the human genome contains three Runx factors: *Runx1* is required for haematopoiesis (Okuda, van Deursen et al. 1996, Wang, Stacy et al. 1996, Chen, Yokomizo et al. 2009), *Runx2* is required for bone formation (Komori, Yagi et al. 1997, Otto, Thornell et al.

1997, Hassan, Gordon et al. 2010) and *Runx3* is necessary for neurogenesis, thymogenesis and gut development (Inoue, Ozaki et al. 2002, Levanon, Bettoun et al. 2002, Li, Ito et al. 2002, Taniuchi, Osato et al. 2002).

rnt-1, the sole *C. elegans* homologue of the Runx family of transcription factors, together with its cofactor *bro-1*, the CBFß homologue (CBFß is a known binding partner of Runx), is known to promote proliferative (symmetrical to the seam fate) seam cell divisions (Nimmo, Antebi et al. 2005, Kagoshima, Nimmo et al. 2007). First identified in screens for mab (*m*ale *ab*normal) phenotypes (Hodgkin 1983), the loss of rays in the male tail of *rnt-1* mutants was found to stem from loss of divisions in the V and T seam cell lineages, a phenotype also found to be the case for mutants of *bro-1* (Kagoshima, Nimmo et al. 2007). The Runx-CBFß interaction was known to occur in mammals and *Drosophila*, but it was only after the discovery of *bro-1* that this was found to be conserved in *C. elegans* (Lee, Ahnn et al. 2004, Kagoshima, Nimmo et al. 2007). Although RNT-1 alone is able to bind DNA, the specificity and affinity of this binding was found to be vastly improved by the presence of BRO-1 (Kagoshima, Nimmo et al. 2007), a role conserved in mammals and drosophila (Adya, Castilla et al. 2000).

Expression studies of *rnt-1* have shown it to act downstream of the Hox cofactors CEH-20/Pbx and UNC-62/Meis (Hughes, Brabin et al. 2013). In addition, Wnt target genes are known to be co-regulated by *rnt-1* during T cell division (Hajduskova, Jindra et al. 2009), whilst there is evidence for a co-operative model of regulation between Wnt and Runx during stem cell divisions in both mammals and sea urchins (Robertson, Coluccio et al. 2008, Fiedler, Graeb et al. 2015). It is therefore likely that Runx operates downstream of Hox and co-operatively with Wnt to regulate seam cell divisions. Interestingly, given the role of Runx in AML, mis-regulation of Hox and Meis expression also leads to AML (Thorsteinsdottir, Kroon et al. 2001). Furthermore,

inappropriate over-expression of Wnt components, particularly of ß-catenin, has been found to be both necessary and specific to AML formation (Muller-Tidow, Steffen et al. 2004, Serinsoz, Neusch et al. 2004, Simon, Grandage et al. 2005, Wang, Krivtsov et al. 2010) and also to leads to poor prognosis in patients (Ysebaert, Chicanne et al. 2006).

Heterochronic mutants and the role of miRNAs in the seam

The Wnt, Hox and Runx pathways of seam cell regulation are all required for the specification of cell fates and spatial positioning of cells. However, in a wild-type animal, the re-iterative seam cell divisions can be up to ten hours apart, and yet the division will robustly occur within minutes of its predicted timing. Furthermore, the cells will only undergo one asymmetrical division per larval moult, with an additional symmetrical division only after the L2 transition (see previous figures 1.4.3 and 1.4.4). This tight temporal regulation of the seam cell divisions has been shown to be regulated by the *C. elegans* heterochronic pathway (Ambros and Horvitz 1984), a temporal regulatory pathway shown to be conserved in other animals and plants (Pasquinelli, Reinhart et al. 2000, Reinhart, Weinstein et al. 2002). Notably, this regulatory pathway has been shown to link environmental cues to developmental timing in the worm (Hammell, Karp et al. 2009).

The heterochronic pathway relies on the action of two main microRNAs (miRNAs), *lin-4* and *let-7*, together with a family of *let-7* miRNA genes (Ambros and Horvitz 1984, Lee, Feinbaum et al. 1993, Reinhart, Slack et al. 2000). miRNAs down-regulate target genes by binding to the 3'-UTRs of mRNAs and either inducing an mRNA degradation pathway or repressing translation of the mRNA (Olsen and Ambros 1999, Hutvagner and Zamore 2002, Zeng, Wagner et al. 2002, Doench, Petersen et al. 2003, Zeng, Yi et al. 2003). The two major targets of *lin-4* and *let-7* are LIN-14 and LIN-41, respectively (Fig. 1.5.3, Ambros and Horvitz 1987, Lee, Feinbaum et al.

1993, Wightman, Ha et al. 1993, Slack, Basson et al. 2000). *lin-4* and LIN-14 primarily regulate the L1 division: *lin-14* gain-of-function (*gf*) mutants reiterate the division whereas *lin-14* loss-of-function (*lf*) mutants skip the division all together and undergo the L2 symmetrical division prior to the L2 moult (Ambros and Horvitz 1984). Other heterochronic genes control the later larval stages (see Fig. 1.5.3).

The L1 division is genetically robust

Despite the many seam lineage abnormalities found in mutants of the Wnt, Hox and Runx signalling pathways, to date there has been no mutant or combination of mutants found that is able to disrupt the fate of the L1 asymmetrical division under normal growth conditions. The L1 division appears superficially to be no different from the asymmetric divisions that occur during later larval stages, yet in mutants that disrupt later divisions, the L1 division remains normal. The only mutants isolated that can perturb the L1 division are the heterochronic mutants, but even then they are able either to eliminate or to reiterate the division, but not the fate choice during the division itself. The asymmetrical L1 division, therefore, appears unique within seam cell divisions as being robust to genetic manipulation of known seam regulatory pathways, indicative of a different mechanism of control that is active during this stage in development.

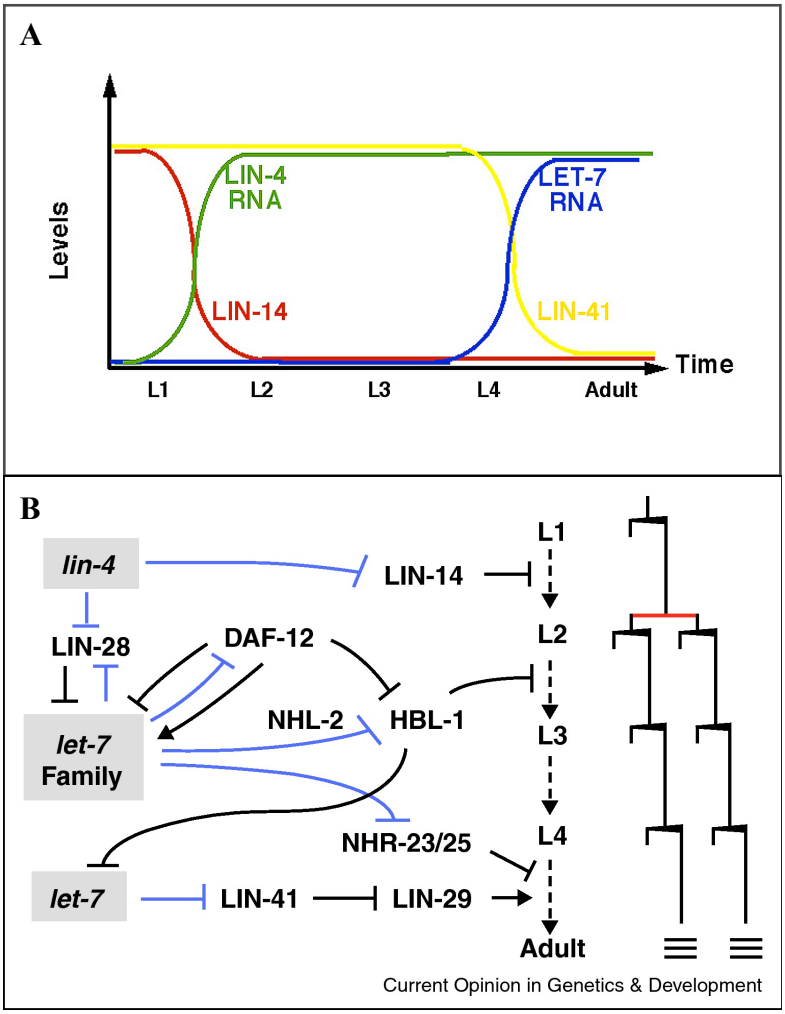

FIG. 1.5.3 – TEMPORAL REGULATION OF THE MIRNAS *LIN-4* AND *LET-7* AND THEIR TARGET GENES.
A. Relative levels of *lin-4* and *let-7* miRNAs and expression of their target genes *lin-14* and *lin-41* over the four larval moults until adulthood (Vella and Slack 2005). **B.** A schematic showing the network of temporal regulation in the seam by the heterochronic pathway (Ambros 2011). The wild-type seam cell lineage is shown on the right, with the three parallel lines at the end representing the alae secreted at terminal differentiation. miRNAs (shaded grey boxes) post-transcriptionally down-regulate target mRNAs by direct interactions with their 3'-UTR sequences (blue lines).

1.6 *C. elegans* as a model for cellular migration

Migration of cells and processes emanating from cells during development have been widely studied in *C. elegans*. How cells and tissues receive directional cues, become competent to respond to these cues and the mechanism of cell movement itself are all processes of particular interest when investigating both organ development and cancer metastasis. In *C. elegans,* models for migration include the migration of the distal tips cells (DTCs) of the gonad during larval development, migration of the Q neuroblasts during late embryogenesis and early larval development, post-embryonic axon migration and migration of the ventral epidermal P cells at L1. Through study of these processes, pioneering work in *C. elegans* has discovered many novel mechanisms for cell migration, including the highly conserved netrin signalling pathway with which mammalian neuronal networks are formed.

Axon migration

Circumferential navigation of axon tracts from cells that make up the ventral nerve cord to the dorsal midline is required for normal motor-neurone connectivity and thus normal movement of the animal. The pathway that mediates this migration is the netrin pathway. Netrin/UNC-6 was first discovered in *C. elegans* (Ishii, Wadsworth et al. 1992) and has since been shown to be part of a conserved pathway of axon migration in many organisms including *Drosophila* and vertebrates (Kennedy, Serafini et al. 1994, Serafini, Kennedy et al. 1994, Harris, Sabatelli et al. 1996, Lauderdale, Davis et al. 1997). In *C. elegans*, mutations in *unc-6* or either of its receptors *unc-5* or *unc-40* result in defects in axon migration and an 'unc' (*unc*oordinated) phenotype (Hedgecock, Culotti et al. 1990).

UNC-6 is secreted from ventral cells and is thought to form a gradient along which the migrating neurones can move (Kennedy, Serafini et al. 1994, Wadsworth, Bhatt et al. 1996, Asakura, Waga

et al. 2010). Cells which express both UNC-5 and UNC-40 move away from UNC-6 dorsally (Hedgecock, Culotti et al. 1990, Leung-Hagesteijn, Spence et al. 1992, Chan, Zheng et al. 1996, Ackerman, Kozak et al. 1997, Leonardo, Hinck et al. 1997) whereas cells expressing UNC-40 alone move towards UNC-6 ventrally (Hedgecock, Culotti et al. 1990, Chan, Zheng et al. 1996, Keino-Masu, Masu et al. 1996, Kolodziej, Timpe et al. 1996). Once neuronal commissures reach the dorsal side of the animal they are thought to be directed into the dorsal nerve cord by the putative chemoattractant UNC-129, a TGFß homologue (Yu and Bargmann 2001). Astoundingly, the preference for a ventral source of the netrin ligand has been conserved along with the netrin pathway itself (Kennedy, Serafini et al. 1994, Harris, Sabatelli et al. 1996, Mitchell, Doyle et al. 1996, Wadsworth, Bhatt et al. 1996, de la Torre, Hopker et al. 1997, Lauderdale, Davis et al. 1997, Strahle, Fischer et al. 1997).

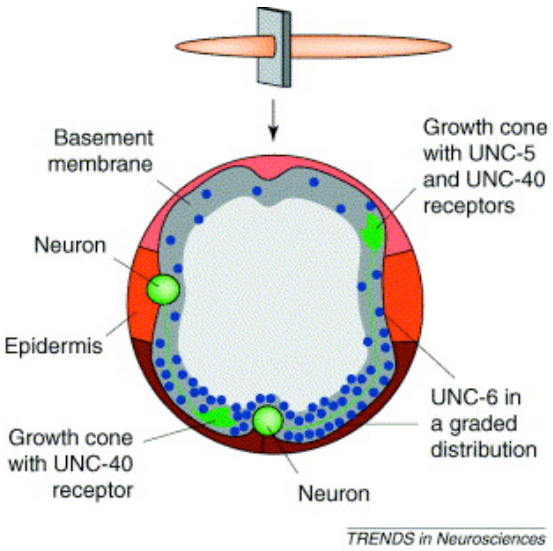

FIG. 1.6.1 – NETRIN-MEDIATED CIRCUMFERENTIAL AXON GUIDANCE (WADSWORTH 2002).
A cross-section through the worm showing the epidermis at L1, with the lateral seam cells (red), ventral P cells (brown) and dorsal hyp7 (pink). Ventral epidermal cells (as well as other ventral cells, not shown) secrete UNC-6 (blue) to form a gradient that is most concentrated at the ventral midline. Neurones (green) express either UNC-5 and UNC-40 or just UNC-40, allowing them to be either repelled or attracted to higher levels of UNC-6 respectively. Axons then move along the basement membrane (grey).

It is known that UNC-5 signalling is mediated through MAX-2, a p21-activated kinase (PAK) (Lucanic, Kiley et al. 2006). In migrating vertebrate cells, PAKs function upstream of actin polymerisation and microtubule disassembly (Kiosses, Daniels et al. 1999, Cau and Hall 2005, Vadlamudi, Barnes et al. 2005) and therefore MAX-2 potentially links UNC-5 signalling to cytoskeletal regulators, allowing for cell shape remodelling.

Distal tip cell (DTC) migration

The *C. elegans* gonad starts off in L1 as four cells in a ventrally-placed primordium, comprising of two distal somatic precursors and two germline precursors between them (Hirsh, Oppenheim et al. 1976, Kimble and Hirsh 1979, Kimble and White 1981). Beginning at L2, the gonad grows to fill much of the volume of the worm by adulthood, and forms two 'U-shapes' in the anterior and posterior of the animal (Fig. 1.6.2, Hirsh, Oppenheim et al. 1976, Kimble and Hirsh 1979). To guide formation of the correct shape of the gonad arms, two somatic cells known as distal tip cells (DTCs), located at the tip of each arm, respond to migratory signals along the worm (Kimble and Hirsh 1979, Kimble and White 1981, Hall, Winfrey et al. 1999). The DTCs first migrate outwards along the ventral epidermal basement membrane, then turn once perpendicularly to the dorsal side to cross the lateral hypodermal basement membrane (first turn) before finally turning again to face in the opposite direction to the original pathway (second turn). Here the DTCs travel along the dorsal epidermal membrane back towards each other until they meet at the middle (Fig. 1.6.2). By adulthood, the gonad is fully formed and does not migrate further, a cessation mediated by MIG-39 and Rac GTPases (Kikuchi, Shibata et al. 2015). The gonad has its own basement membrane (Huang, Hall et al. 2003) that contacts the basement membrane of the muscles and hypodermis, the constituents of which are either produced by the gonadal cells or by nearby external tissues (Graham, Johnson et al. 1997, Kubota, Kuroki et al. 2004).

Genes required for DTC migration have been studied with both forward and reverse genetics (Nishiwaki 1999, Cram, Shang et al. 2006). This has revealed a large number of gene functions involved in DTC migration, including those for cell fate specification, cell signalling, cell adhesion, extracellular matrix (ECM) components as well as enzymes that re-model the ECM. Indeed, in order for DTCs to migrate at all, two genes must be functional, *gon-1* and *mig-6* (Blelloch and Kimble 1999, Kawano, Zheng et al. 2009). Both encode members of the ADAMTS or ADAMTS-like families of proteins that remodel the ECM in many different systems (Blelloch and Kimble 1999, Kramerova, Kawaguchi et al. 2000, Porter, Clark et al. 2005, Kawano, Zheng et al. 2009), so it is likely that basement membrane remodelling is an integral migratory mechanism for gonad morphogenesis.

The first turn of the gonad is probably the most well-studied migratory event in the DTC pathway, involving a move away from muscle-covering basement membrane and onto the lateral basement membrane. For this turn, the netrin pathway, well characterised in *C. elegans* for its role in neuronal development and axon migration (see previous section), plays a vital role (Hedgecock, Culotti et al. 1990, Levy-Strumpf and Culotti 2014). The DTCs display *unc-40* expression from the L2 stage onwards (Chan, Zheng et al. 1996), whereas the *unc-5* receptor is only expressed at the time of the first turn (Su, Merz et al. 2000), apparently acting as a switch to turn the DTC from being attracted to the ventral UNC-6 gradient to being repulsed by it. This critical switch in expression is regulated by the heterochronic pathway (Su, Merz et al. 2000, Motola, Cummins et al. 2006). The turn dorsally has also been found to involve UNC-129, a TGFß homologue expressed in dorsal body wall muscles, which acts to promote the UNC-40/ UNC-5 mediated repulsive pathway in favour of the UNC-40 pathway alone (Colavita and Culotti 1998, Colavita, Krishna et al. 1998, Nash, Colavita et al. 2000, MacNeil, Hardy et al. 2009).

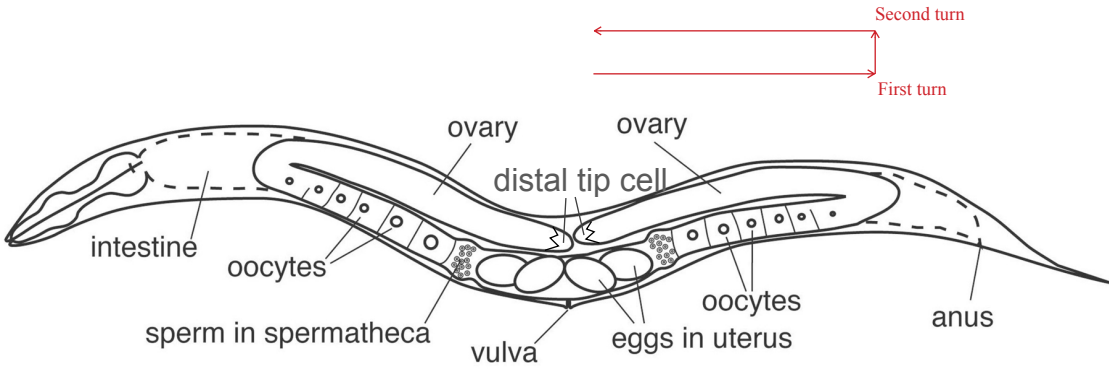

FIG. 1.6.2 – *C. ELEGANS* HERMAPHRODITE GONAD (ADAPTED FROM ZARKOWER 2006).
Schematic of the hermaphrodite gonad showing the final position of the two gonad arms within the body of the worm. Distal tip cells drive migration of the gonad arms from the ventral midpoint out along the ventral sides of the worm, before turning first to the dorsal side of the animal and then again, back along the dorsal anteroposterior axis until they meet again, this time at the dorsal midpoint. The migration pathway of the posterior distal tip cell is shown in red; the pathway of the anterior cell is the mirror-image. In addition, the anterior gonad is located on the right-hand lateral side of the animal (bottom plane in this view) whereas the posterior branch follows the left-hand lateral side (top plane). This is not shown in this diagram.

Q neuroblast migration

At hatching, two Q neuroblast cells, one on the left side of the animal and the other on the right, are located between the seam cells V4 and V5 in the seam line (Sulston and Horvitz 1977). Throughout larval development, these cells move out of the seam line before dividing and migrating further (Sulston and Horvitz 1977). Unusually, the neuroblast lineage on the left lateral side migrates posteriorly, whereas the neuroblast lineage on the right lateral side migrates anteriorly. Both lineages migrate a substantial distance down the length of the animal.

This migration initially requires the netrin receptor UNC-40, a Wnt modulator MIG-21 and an enzyme that mannosylates both UNC-40 and MIG-21, DPY-19 (Honigberg and Kenyon 2000, Middelkoop, Williams et al. 2012, Sundararajan and Lundquist 2012). Migration later relies on Wnt signalling and Hox genes (Harris, Honigberg et al. 1996, Maloof, Whangbo et al. 1999, Whangbo and Kenyon 1999, Honigberg and Kenyon 2000, Zinovyeva, Yamamoto et al. 2008).

P cell migration during L1

During mid-L1, the two lines of six bilaterally symmetrical P cells (P1/2, P3/4, P5/6, P7/8, P9/10, P11/12), which until now have formed a substantial area of the ventral hypodermis, migrate ventrally to intercalate in a single line of 12 cells at the ventral midline (shown in Fig. 1.6.3, Sulston and Horvitz 1977). It is in this ventral position that the P cells undergo post-embryonic divisions which result in a large number of cells contributing to the development of the ventral nerve cord, and others forming hypodermal tissues, either by fusing to the *hyp7* syncytium or forming sex-specific blast cells during the formation of the vulva (Sulston and Horvitz 1977). Migration of the P cells firstly involves the migration of the nucleus to the ventral midline (Sulston and Horvitz 1977) via the nuclear membrane proteins UNC-84 and UNC-83 as well as other members of the SUN/KASH pathway (Malone, Fixsen et al. 1999, Starr, Hermann et al. 2001, McGee, Rillo et al. 2006, Meyerzon, Fridolfsson et al. 2009, Fridolfsson, Ly et al. 2010, Bone, Tapley et al. 2014). Secondly, successful P cell migration requires the substantial remodelling of the cell shape and cytoplasm to follow the nucleus (Sulston and Horvitz 1977). RHO GTPase-mediated pathways involving *rho-1*, *let-502*, *mig-2* and *unc-73* have been implicated in P cell migration (Zipkin, Kindt et al. 1997, Spencer, Orita et al. 2001).

If nuclear migration fails, but part of the cell migrates ventrally, resulting in a segmented cell in which the nucleus remains in the lateral non-migrated section, the stranded cell will die, as in the case of *unc-83* or *unc-84* nuclear migration defective mutants (Malone, Fixsen et al. 1999, Starr, Hermann et al. 2001). However, it the cell completely fails to migrate, as in the case of a *rho-1* mutant, it will follow a normal cell lineage in an abnormal lateral position, resulting in neurones produced in lateral positions along the worm (Spencer, Orita et al. 2001).

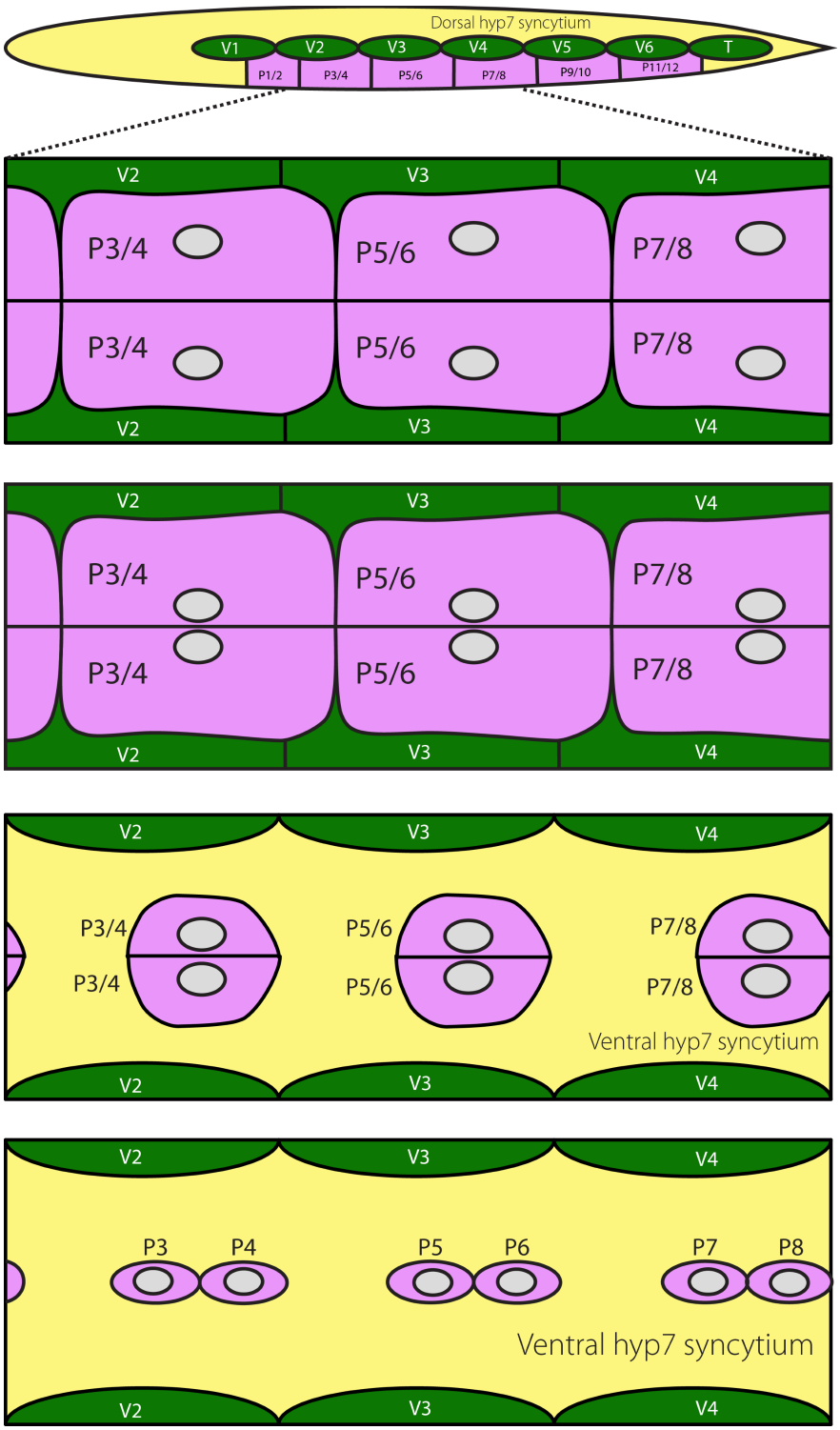

FIG. 1.6.3 – P CELL MIGRATION TO THE VENTRAL MIDLINE DURING L1.
A lateral schematic of a newly hatched L1 larva (top) shows the posterior seam cells V1-T in green, P cells in pink and the single multinucleate cell of the hyp7 syncytium in yellow. Below, ventral views over time show the migration of the P cells to the ventral midline during L1 (all P cells behave in the same way, although only P3-P8 are shown here). When the worms hatch, the P cells sit ventrally to the seam cells and form the majority of the ventral hypodermis (there is no hyp7 syncytium present). During L1, the nuclei of the P cells (grey) migrate ventrally, in a process that involves the SUN/KASH pathway proteins UNC-84 and UNC-83 (second panel), before the rest of the cell follows to remodel down to the ventral midline (panel 3). Here, the P cells move past each other to intercalate in a single line, and it is in this position that they divide to contribute cells to the ventral nerve cord and hypodermis. The behaviour of the seam cells during this process has not been investigated prior to this thesis, nor has the cellular process of how the ventral hyp7 is formed.

1.7 The role of *pal-1*, homologue of *Drosophila caudal*, during *C. elegans* development

The *caudal* (*cad*) transcription factor was first identified in *Drosophila* during screens for genomic sequences encoding a homeobox (Mlodzik, Fjose et al. 1985). Homeobox domains bind with specificity to DNA and the domain is one of the defining features of Hox genes (Fainsod, Bogarad et al. 1986, Hall and Johnson 1987, Laughon, Howell et al. 1988). Since its discovery, homologues of *caudal* have been found in many organisms, from the cnidarians through to insects, nematodes, amphibians and mammals (Duprey, Chowdhury et al. 1988, Hunter and Kenyon 1996, Marom, Shapira et al. 1997, Isaacs, Pownall et al. 1998, Katsuyama, Sato et al. 1999, Ehrman and Yutzey 2001, Reece-Hoyes, Keenan et al. 2002, Copf, Schroder et al. 2004, Hui, Holland et al. 2008).

Despite having a homeobox domain, *caudal* is not a true Hox gene due to its evolutionary origin and subsequent position on the genome. Hox genes in most organisms are found in one or more genomic clusters, arranged in an order that corresponds directly to the spatial organisation of the regions of the body that they specify. Some time before cnidarian branching from the phylogenetic tree, an original Hox cluster is thought to have been duplicated, followed by a subsequent functional divergence of genes contained therein (Brooke, Garcia-Fernandez et al. 1998, Chourrout, Delsuc et al. 2006, Hui, Holland et al. 2008, Holland 2013). *caudal* belongs to this second cluster of homeobox genes, known as the ParaHox cluster (Brooke, Garcia-Fernandez et al. 1998).

Although not a member of the Hox cluster, *caudal* was identified as the homeotic gene required for patterning of the most posterior segment of *Drosophila* (Mlodzik, Fjose et al. 1985, Macdonald and Struhl 1986, Moreno and Morata 1999). In contrast, mammalian homologues of

caudal, although also required for posterior specification, work at least partially by regulation of Hox gene expression (Subramanian, Meyer et al. 1995, Charite, de Graaff et al. 1998, van den Akker, Forlani et al. 2002, Tabaries, Lapointe et al. 2005). This Hox-dependent mechanism of posterior patterning by *caudal* is also evident in other vertebrates including *Xenopus laevis* (Isaacs, Pownall et al. 1998) and chickens (Ehrman and Yutzey 2001, Bel-Vialar, Itasaki et al. 2002).

The role of *Cdx* genes in vertebrate development

In the mouse and humans, there are three *Cdx* genes, *Cdx1*, *Cdx2* and *Cdx4* (Gamer and Wright 1993, Hu, Kazenwadel et al. 1993, Suh and Traber 1996). In mice, all are expressed in the posterior of the developing embryo. In addition, *Cdx2* is expressed from embryogenesis in the lining of the intestinal epithelium, posterior to the stomach, and this expression continues throughout the life of the animal. *Cdx1* is also expressed in the endoderm for the same duration; however, unlike *Cdx2*, which is expressed primarily in the villous region of the epithelium, *Cdx1* is expressed primarily in the crypts of the intestine (Subramanian, Meyer et al. 1998, Silberg, Swain et al. 2000).

After knocking out *Cdx1*, it was found that both the gut and posterior of the animal developed normally (Subramanian, Meyer et al. 1995). However, Hox gene expression was shifted posteriorly. In contrast, knocking out *Cdx2* resulted in embryonic lethality due to blastocyst abnormalities and subsequent implantation defects; heterozygotes that survived to birth displayed growth defects and varying degrees of posterior truncation (Chawengsaksophak, James et al. 1997, Strumpf, Mao et al. 2005). *Cdx2* heterozygotes which were also null for *Cdx1* displayed a synthetic increase in posterior truncation, showing that to some degree these genes are redundant in posterior development (van den Akker, Forlani et al. 2002). By overcoming the

implantation defects, it was later shown that homozygous *Cdx2* null animals displayed severe defects in all development posterior to the forelimb bud (Chawengsaksophak, de Graaff et al. 2004). Again, loss of *Cdx2* was accompanied by a shift in Hox expression. *Cdx4* knockout had a similar effect as *Cdx1*, with severe posterior developmental effects apparent only after combination with a heterozygote *Cdx2* null allele (van Nes, de Graaff et al. 2006). *Cdx4* has also been shown to induce ectopic Hox gene expression when mis-expressed (Charite, de Graaff et al. 1998). Interestingly, by using knock-in experiments, *Cdx1* and *Cdx2* have been shown to be functionally equivalent in the mouse (Savory, Pilon et al. 2009).

Cdx genes contribute to fate homeostasis in the posterior gut

Cdx2 mutants frequently develop abnormal polyps formed of foregut tissue in the midgut and colon (Chawengsaksophak, James et al. 1997, Beck, Chawengsaksophak et al. 1999). Using conditional knockouts, loss of gut expression of *Cdx2* resulted in the entire colon turing to foregut tissue (Gao, White et al. 2009), partial gastric identity (Grainger, Savory et al. 2010), and defects in epithelial polarity (Gao and Kaestner 2010), all suggesting the role of *Cdx2* in the gut is to promote a posterior gastrointestinal fate. Consistently, ectopic *Cdx2* expression is sufficient to confer a posterior intestinal fate (Mutoh, Hakamata et al. 2002, Silberg, Sullivan et al. 2002, Mutoh, Sashikawa et al. 2011). Synthetic effects between *Cdx1* and *Cdx2* in the colon but not intestine suggest that *Cdx1* contributes to the specification of the colon but that *Cdx2* alone specifies the small intestine (Hryniuk, Grainger et al. 2012). Given their role in gastrointestinal differentiation, it is perhaps unsurprising that *Cdx1* and *Cdx2* have been implicated in colorectal cancer (Mallo, Soubeyran et al. 1998, Lorentz, Cadoret et al. 1999, Aoki, Tamai et al. 2003, Bonhomme, Duluc et al. 2003, Hinoi, Loda et al. 2003, Dang, Chen et al. 2006, Salari, Spulak et al. 2012, Hryniuk, Grainger et al. 2014).

pal-1 is the *C. elegans* homologue of *caudal*

pal-1 (*p*osterior *al*ae), the sole *C. elegans* homologue of the *caudal* homeobox transcription factor, has an essential role in posterior embryonic patterning (Waring and Kenyon 1990, Waring and Kenyon 1991, Hunter and Kenyon 1996, Ahringer 1997, Edgar, Carr et al. 2001, Baugh, Hill et al. 2005, Maduro, Kasmir et al. 2005, Maurer, Chiorazzi et al. 2007, Lei, Liu et al. 2009). Mutants null for *pal-1* die during embryogenesis or hatch with severe morphological defects (Fig.1.7.1); evidence has been shown for both maternal and zygotic transcripts being essential for proper fate specification and patterning in the early and late embryo (Hunter and Kenyon 1996, Ahringer 1997, Edgar, Carr et al. 2001). In particular, *pal-1* has been shown to specify the C and D lineages, with translation of maternal transcripts being firstly restricted to the posterior blastomere P1, followed by the limitation of PAL-1 activity to the somatic descendants of P2 (Draper, Mello et al. 1996, Hunter and Kenyon 1996). Both the posterior C and D lineages give rise to muscle tissue, with the addition of hypodermal cells, two neurones and a cell death from the C lineage (Sulston, Schierenberg et al. 1983). Ectopic expression of *pal-1* has been shown to be sufficient to induce a C lineage-like fate in other blastomeres (Draper, Mello et al. 1996, Hunter and Kenyon 1996).

As is the case for vertebrate *caudal* homologues, there is evidence that *pal-1* specifies posterior patterning by control of Hox gene expression. It has been shown that direct regulation of *mab-5* expression by *pal-1* in the seam cell V6 is required for the development of the male tail (Waring and Kenyon 1990, Austin and Kenyon 1994, Salser and Kenyon 1996, Hunter, Harris et al. 1999), and it has also been suggested that *mab-5* expression in the sex myoblasts (descended from the M lineage) may require *pal-1* (Hunter, Harris et al. 1999). It would also appear likely that *pal-1* is required for expression of a second posterior Hox gene, *egl-5*, in the late embryo, although there is no evidence for a direct interaction (Cowing and Kenyon 1992, Ferreira, Zhang

et al. 1999). Finally, expression of the third posterior Hox gene, *nob-1*, in the C lineage has been shown to be dependent on *pal-1* (Baugh, Hill et al. 2005). Other than the Hox genes, targets of *pal-1* include the homologue of the *Drosophila* pair-rule *even-skipped* gene, *vab-7*, mutants of which display defects in the C lineage (Ahringer 1996, Ahringer 1997), and the muscle-specific transcription factor *hlh-1* (Lei, Liu et al. 2009). A regulatory interaction between *caudal* and *even-skipped* has also been observed in *Drosophila* (Moreno and Morata 1999).

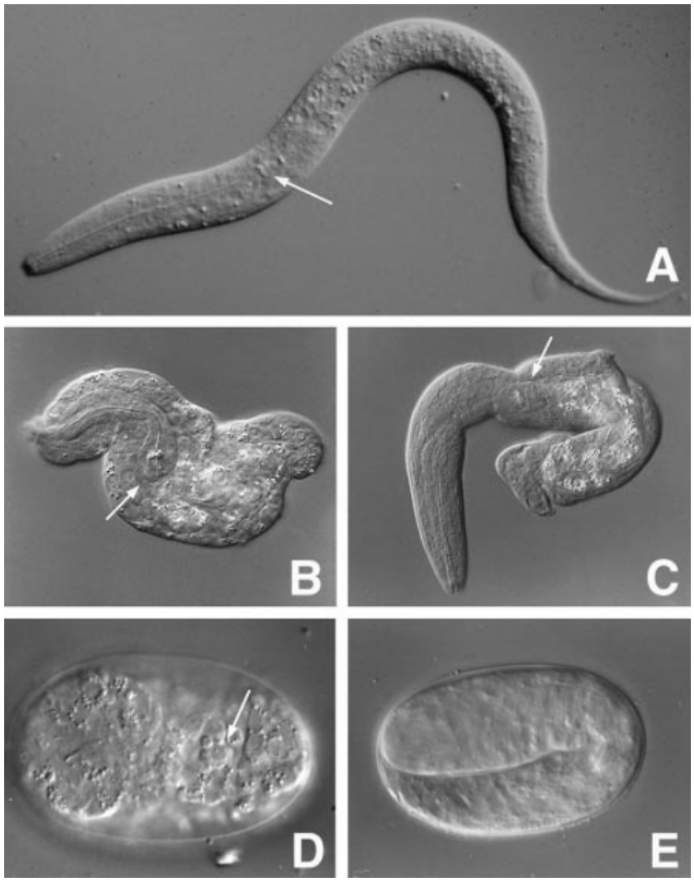

FIG. 1.7.1 – TERMINAL *PAL-1* NULL MUTANT PHENOTYPES (REPRODUCED FROM EDGAR, CARR ET AL. 2001).
A. Wild-type L1 at hatching. **B and C.** *pal-1* null animals at the same stage as **A** displaying Nob phenotypes. Arrows indicate the posterior bulb of the pharynx. **D.** Approximately 20% of *pal-1* null progeny do not make it to hatching due to failures in ventral enclosure. The arrow indicates the exposed gut cells. An equivalent stage wild-type animal is shown in **E**.

pal-1 expression pattern

The expression pattern of *pal-1* in the *C. elegans* embryo has been studied using both GFP reporter constructs and antibody staining (Edgar, Carr et al. 2001). A summary of this expression pattern is shown in figure 1.7.2. During this study, mosaic analyses indicated that *pal-1* acts for the most part cell autonomously, although some exceptions were noted, including the lineage of the seam cell precursor ABarpp, in which no *pal-1* expression was observed, and yet descendants were found to exhibit abnormal positioning in a *pal-1* mutant. Since *pal-1* has not been shown to act non-cell autonomously elsewhere, Lois Edgar and colleagues proposed the likelihood that they had not included all of the regulatory features of *pal-1* in their constructs. The constructs used during this investigation are shown in figure 1.7.3, and it is notable that the last intron of *pal-1* is missing in both a rescue construct and the construct used to analyse *pal-1* expression. This is particularly relevant in light of the cloning of a viable *pal-1* allele, *e2091*, which exhibits defects in epidermal patterning and the male tail ray lineages, and was found to contain two point mutations in the last intron of *pal-1* but no change in the coding sequence. This would suggest that important regulatory information is contained within the last intron of *pal-1* (Zhang and Emmons 2000), missing from the investigation into *pal-1* expression by Lois Edgar and colleagues.

Age (min) Cell #	Pattern	Cell identification and cell fate
80 min 26 cells	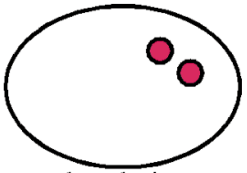 lateral view	2C: hypodermis, muscle
140 min ~50 cells	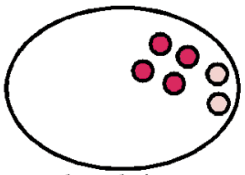 lateral view	4C: hypodermis, muscle 2D: muscle
195 min ~200 cells	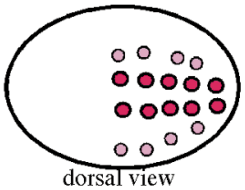 dorsal view	16 C 8 D
230-260 min ~250 cells	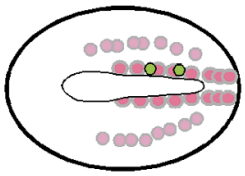 ventral view	16 C 16 D (faint) ABplpappp ABplpppppp
260-290 min ~300 cells	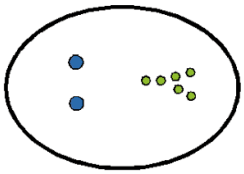 ventral view	MSapaapp: mesoblast M, death MSppaapp: int mu R, death ABplpapppa/p: rectal epithelium, neuron, K, K' ABplpppppa/p: anal depressor, int mu L, hyp 10, tail spike ABprpppppa/p: sphincter, body muscle, hyp 10, tail spike
310-370 min 350-500 cells	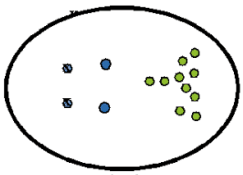 ventral view	MSapaappa/p MSppaappa/p ABplpapppa/p ABplpppppa/p ABprpppppa/p ABplpppapap: hyp 8/9 ABprpppapap: hyp 8/9
lima 370 min 550 cells	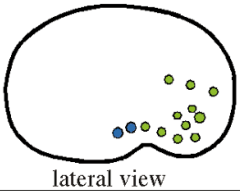 lateral view	MSapaappp MSppaappp ABpl/rappapp:P7/8 ABplpppppaa/p ABpl/rapapap:P9/10 ABplpppppppa/p ABpl/rapappa:P11/12 ABprpppppaa/p ABprpppapap:hyp 8/9 ABprpppppppa/p ABplpppapap:hyp 8/9
1 1/2-fold 430 min 550 cells	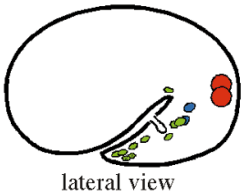 lateral view	MSapaappp ABprpppapap:hyp 8/9 MSppaappp ABplpppapap:hyp 8/9 ABplpppppaa/p ABplpppppppa/p Ealpp:int ring 5 ABprpppppaa/p Earpp:int ring 5 ABprpppppppa/p

FIG. 1.7.2 – EXPRESSION OF *PAL-1* IN THE *C. ELEGANS* EMBRYO (EDGAR, CARR ET AL. 2001). Diagrams of the *pal-1* embryonic expression patterns reported in Edgar, Carr et al. 2001, with the cell identities listed. The constructs that were used for this study are shown in figure 1.7.3.

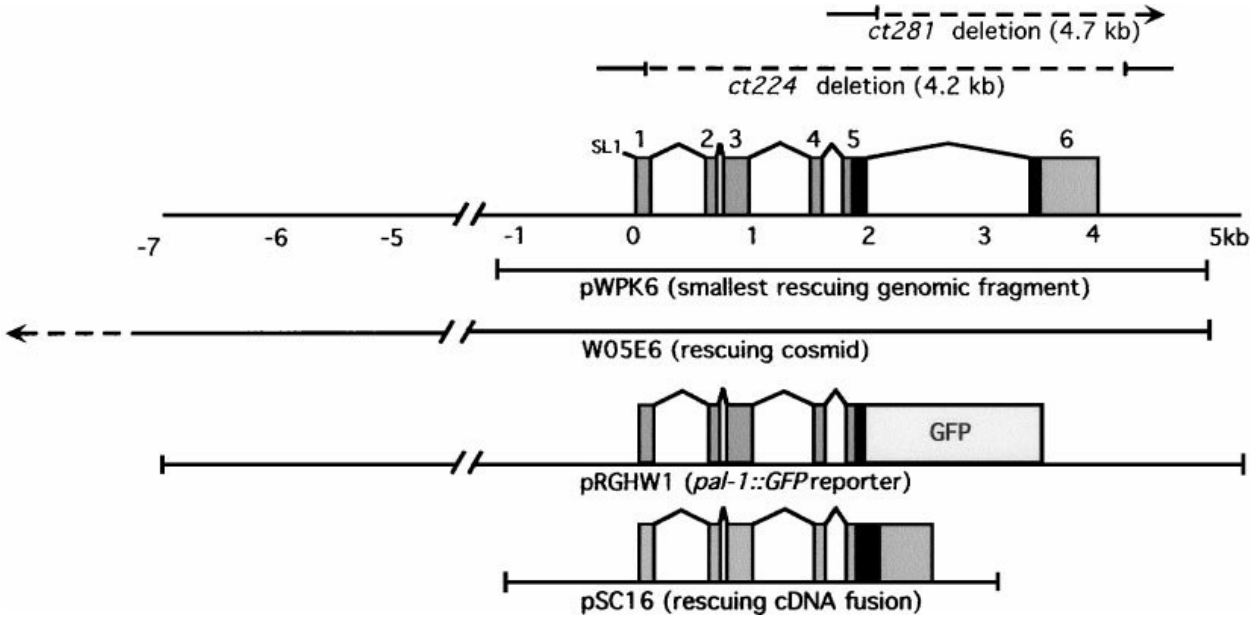

FIG. 1.7.3 – EXPRESSION AND RESCUE CONSTRUCTS OF *PAL-1* USED TO STUDY *PAL-1* EMBRYONIC FUNCTION (EDGAR, CARR ET AL. 2001).
The genomic structure of *pal-1*, with two null *pal-1* alleles indicated, *ct281* and *ct224*, is shown in the first schematic. pRGHW1 was used to study the expression pattern of *pal-1*, but is missing the last (5th) intron and 6th exon of the *pal-1* genomic sequence. In addition, the rescuing construct pSC16 is also missing the 5th intronic sequence of *pal-1*, although expression of this construct has been shown to be sufficient to rescue the *pal-1* null ventral enclosure defects and Nob phenotypes.

1.8 Summary

C. elegans is a valuable system in developmental biology with which to study conserved processes required for the development of tissues, organs and disease. However, much is still unknown about fate specification, tissue remodelling and the interaction of regulatory pathways in both *C. elegans* and other organisms. In this study, I hope to shed light on a mechanism of gene regulation involving the integration of different developmental signalling pathways, as well as to explore mechanisms that govern the correct patterning of cells in *C. elegans*, particularly with respect to the homeobox gene *pal-1* and its role in patterning the ventral epidermis.

Previous work in the laboratory identified *pal-1* as a potential interactor with the Runx factor *rnt-1* (C. Brabin, D. Phil. thesis, 2011). I started work on *pal-1* in order to further characterise this interaction, but in the event, the RNT-1/PAL-1 interaction proved difficult to follow biologically. However, a viable mutant of *pal-1* results in seam cell patterning defects and so I decided instead to turn my attention to the seam-specific roles of *pal-1* in epidermal patterning. The *rnt-1*/*pal-1* work is presented in the appendix (Appendix I).

1.9 Aims of this work

Overall, this project has attempted to characterise the role of *pal-1* in the development of the stem-like seam cells, particularly with respect to the seam developmental defects of a *pal-1(e2091)* allele.

Firstly, this has involved dissection and analysis of a putative Wnt-activated seam-specific enhancer element of *pal-1*, perturbed in *pal-1(e2091)* mutant animals, outlined in Chapter 3. This chapter also includes analysis of how a point mutation in the relevant enhancer changes the expression pattern of *pal-1* in the organism, and in turn how this leads to the seam phenotypes of the *e2091* mutant.

In the second results chapter, Chapter 4, I describe a novel seam phenotype of *pal-1(e2091)* mutants with respect to the first asymmetric division of the seam during L1. I also describe how this phenotype has shed light on the cell biology of the L1 seam cell division and how this division contributes to vital re-modelling of the epidermis during this larval stage.

The third results chapter describes an investigation into the molecular basis for this novel phenotype, and reveals the netrin pathway as having a role in posterior patterning of the *C. elegans* embryo in the absence of *pal-1*, among other synthetic interactions.

Finally, I have analysed the expression pattern and functioning of the Warthog gene *wrt-2*, the promoter of which has been used throughout this study to visualise seam cell development due to the high level of expression in the seam. This has involved analysis of a previously uncharacterised allele of *wrt-2*, *ok2810*, uncovering a role in *C. elegans* development for this Hedgehog-related gene.

CHAPTER 2

Materials and Methods

2.1 Worm methods

C. elegans strains and maintenance

All *C. elegans* strains described were derived from the N2 Bristol wild-type strain. Worms were maintained at room temperature, unless otherwise indicated. All manipulations and maintenance of strains were performed as previously described (Wood 1988). Strains used in this study are listed in Appendix II.

Single worm lysis

Genomic *C. elegans* DNA templates for PCR, either for genotyping alleles (see next section), for generating the *mCherry::wrt-2::gfp* reporter construct, or for generating the promoter constructs

for *wrt-2*, was obtained by single worm lysis (Williams, Schrank et al. 1992). A single worm was picked into a PCR tube containing 2.5µl of worm lysis buffer (50µM KCl, 2.5µM $MgCl_2$, 10µM Tris-HCl pH 8.3, 0.45% NP40, 0.45% Tween 20, 0.01% gelatine and 10mg/ml Proteinase K) and snap frozen at -80ºC for > 20mins. The tubes were then transferred to a PCR machine where they were incubated for 1 hour at 60ºC and then the Proteinase K was inactivated by 15 mins at 95ºC. The tube contents could now be used directly in a PCR reaction.

Genotyping *C. elegans* alleles

Although many alleles could be followed by phenotype of the mutation directly or by exclusion of a linked phenotype on either the same chromosome (for generation of linked double mutants) or the opposing chromosome, for ease some alleles were followed by PCR genotyping. For the smaller deletion alleles, primers were designed to anneal either side of (but not adjacent to) the deletion. In worms carrying the wild-type copy of the allele, a full-sized PCR product will be generated, whereas a copy of the mutant allele would result in a shorter PCR product containing the deletion. In this way, homozygous worms can also be distinguished from heterozygous worms, depending on the number of bands on the gel.

Due to the nature of PCR, larger deletions are harder to detect by this method due to the large discrepancy between the sizes of the mutant and wild-type bands. This means that one programme of specific extension times and annealing temperatures is unlikely to be optimal for the generation of both fragments. In these cases, a cocktail of three PCR primers was used; one either side of the deletion, and one within the deletion itself. If the deletion is present (mutant allele), the short band will be generated by the primers either side of the deletion. If a wild-type allele is present, a PCR fragment will be generated between one of the flanking primers and the primer contained in the deletion (although is is possible that the long fragment between the two

outer deletion-flaking primers is generated, the conditions of the PCR reaction make this product unfavourable and it is not detected). As long as this wild-type fragment is of a different size to that generated by the two flanking primers in the case of the deletion, the genotype can be determined.

The third method of genotyping by PCR used in this project was by tetra-primer ARMS-PCR (Ye, Dhillon et al. 2001). This powerful method can detect the presence of a single nucleotide polymorphism (SNP) within an allele, and is summarised in figure 2.1.1.

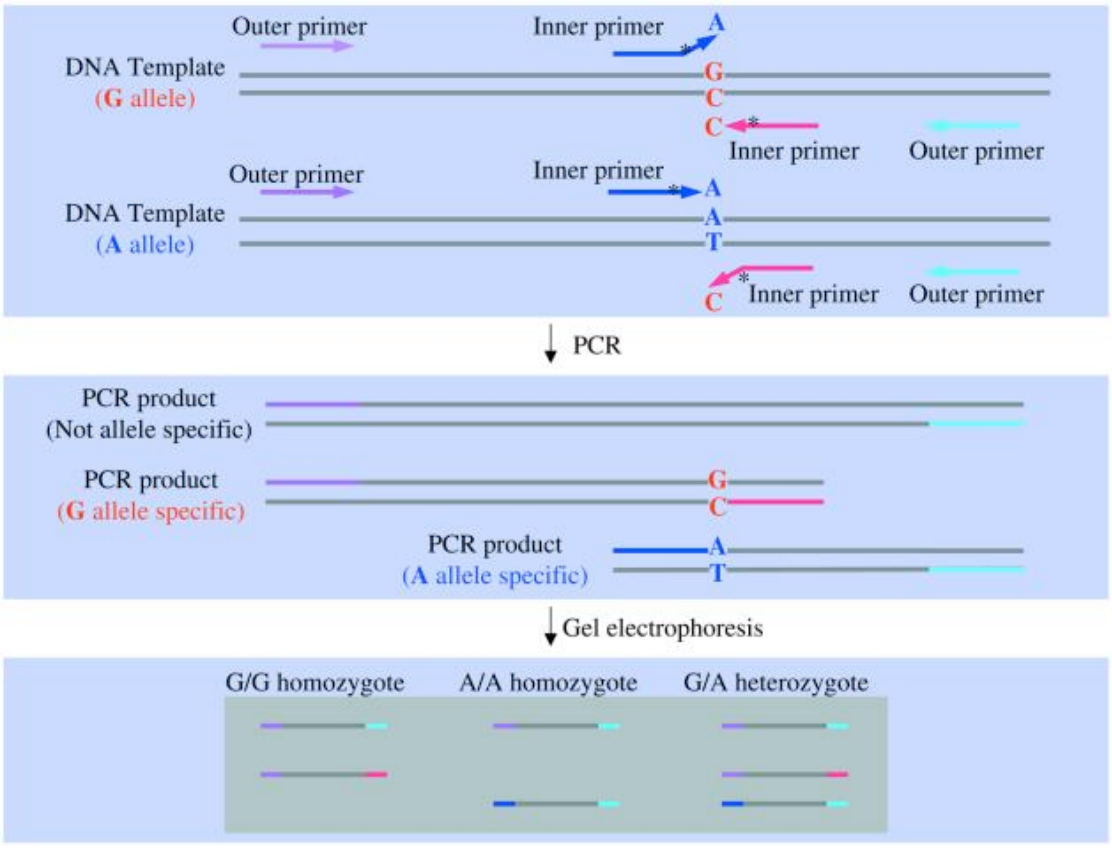

FIG. 2.1.1 – SCHEMATIC FOR GENOTYPING BY TETRA-PRIMER ARMS-PCR (FIGURE TAKEN FROM YE, DHILLON ET AL. 2001).
Four primers are used in this method of detecting SNPs in alleles. Two outer primers bind in all instances, whereas carefully optimised PCR conditions mean that the two inner primers depend on their individual affinities with the SNP as to which one will bind more favourably and generate a product. The two alternative products are designed to be different sizes.

Individual genotyping details

For primer sequences, see Appendix II for details.

rnt-1(tm388) (small deletion):

DNA sample	2.5µl	94ºC	2 mins	
Primer 1 oSG84 (4µM)	2.5µl	94ºC	30 sec	
Primer 2 oSG85 (4µM)	2.5µl	56ºC	30 sec	
dNTPs (2.5mM)	4µl	72ºC	2 mins	Cycle to step 2 x30
ThermoTaq Buffer (x10)	2.5µl	72ºC	10 mins	
H20	10µl	4ºC	Pause	
Taq DNA Polymerase	1µl			**Run on 1% agarose gel**

rnt-1(e1241) (SNP):

DNA sample	2.5µl	95ºC	2 mins	
Primer 1 oSG107 (4µM)	2.5µl	95ºC	30 sec	
Primer 2 oSG108 (4µM)	2.5µl	58ºC	30 sec	
Primer 3 oSG109 (4µM)	2.5µl	72ºC	25 sec	Cycle to step 2 x30
Primer 4 oSG110 (4µM)	2.5µl	72ºC	10 mins	
dNTPs (2.5mM)	4µl	4ºC	Pause	
ThermoTaq Buffer (x10)	2.5µl			WT band = 335bp
H20	8.5µl			*e1241* band = 257bp
Taq DNA Polymerase	0.5µl			**Run on 2% agarose gel**

max-2(nv162) (large deletion):

DNA sample	2.5µl	94ºC	2 mins	
Primer 1 oSG185 (4µM)	2.5µl	94ºC	30 sec	
Primer 2 oSG186 (4µM)	2.5µl	60ºC	30 sec	
Primer 3 oSG187 (4µM)	2.5µl	72ºC	50 sec	Cycle to step 2 x30
dNTPs (2.5mM)	4µl	72ºC	10 mins	
ThermoTaq Buffer (x10)	2.5µl	4ºC	Pause	
H20	3µl			WT band = 1092bp
Q Solution (Qiagen)	5µl			*nv162* band = 674bp
Taq DNA Polymerase	0.5µl			**Run on 1% agarose gel**

wrt-2(ok2810) (small deletion):

DNA sample	2.5µl	94ºC	2 mins	
Primer 1 oSG181 (4µM)	2.5µl	94ºC	30 sec	
Primer 2 oSG167 (4µM)	2.5µl	58ºC	30 sec	
dNTPs (2.5mM)	4µl	72ºC	1 min 30 sec	Cycle to step 2 x30
ThermoTaq Buffer (x10)	2.5µl	72ºC	10 mins	
H20	10.5µl	4ºC	Pause	WT band = 1287bp
Taq DNA Polymerase	0.5µl			*ok2810* band = 735bp
				Run on 1% agarose gel

Additional genetic methods used to generate strains

Although many alleles were visible and either on separate chromosomes or far enough apart from each other on the same chromosome that recombination occurred frequently between them (as was the case for *unc-119(ed3)* and *pal-1(e2091)*, both on LGIII), some alleles were close enough to each other on the genome to be considered linked, or very hard to score for. Some strains were also difficult to build due to low mating efficiencies. For these crosses, and for

alleles not described above, which were genotyped by PCR, I used various genetic approaches to build the desired strains. These are described below:

- ***pal-1(e2091) lin-39(n1880)III; him-5(e1490) heIs63 V*:** The linked double mutant *pal-1(e2091) lin-39(n1880)III* was created by first crossing *pal-1(e2091) III; him-5(e1490) V* males into *dpy-17(e164) unc-32(e189)III* to select for worms wild-type for *dpy-17* and carrying *unc-32(e189)*. The resulting strain was of the genotype *pal-1(e2091) unc-32(e189)III; him-5(e1490)V*. I then crossed the seam cell marker *heIs63* into both this strain and *lin-39(n1880)III; him-5(e1490)V*, as the final desired strain would be both vulvaless from the *lin-39* mutation and would have an extremely low male mating efficiency. *lin-39(n1880)III; him-5(e1490)V* was created by heatshocking *lin-39(n1880)* hermaphrodites to generate males and crossing these into *him-5(e1490)V* hermaphrodites. Finally, *pal-1(e2091) unc-32(e189)III; him-5(e1490) heIs63 V* hermaphrodites were crossed with *lin-39(n1880)III; him-5(e1490) heIs63 V* males and worms which displayed the *pal* mid-body bulge were selected that were wild-type for *unc-32*. The final strain is of the genotype *pal-1(e2091) lin-39(n1880) III; him-5(e1490) heIs63 V*.

- ***unc-6(ju152)X* and *unc-5(ju181)IV*:** To follow the weak (and largely wild-type in terms of mating efficiency) *unc-6* and *unc-5*, alleles *ju152* and *ju181* respectively, I first crossed in the stronger, much more visible alleles *unc-6(ev400)* and *unc-5(e53)* into any strain before subsequently excluding them in the next cross to ensure I obtained the weak alleles in the resulting strain.

- **Heat-shocking for males:** L4 hermaphrodites (6 per plate, 6 plates) were placed at 30ºC for 6 hours before recovery at 20ºC, and their progeny examined for males.

RNAi

RNA interference (RNAi), was provided by feeding (Timmons, Court et al. 2001). Clones were either generated using the L4440 RNAi feeding vector (see Section 2.3) or obtained from the Source-bioscience Ahringer whole-genome library (Kamath and Ahringer 2003) where available and correct upon sequencing.

Generation of transgenic worms

Transgenic worm lines were generated as previously described (Mello, Kramer et al. 1991, Mello and Fire 1995). All constructs were injected (at a concentration of 10-20ng/µl) into an *unc-119(ed3)* background, unless indicated otherwise, using a rescuing *unc-119*$^{+}$ plasmid (pDP#MM016ß) as a co-injection marker (Maduro and Pilgrim 1995). Lines were likewise maintained by selection for the wild-type *unc-119* phenotype.

2.2 Bacterial methods

Bacterial strains used

NGM plates were seeded with the *OP50* strain of *E. coli* to prevent lawn overgrowth as described previously (Brenner 1974). Electro-competent XL1-Blue cells (Stratagene) were used to transform all plasmids except cloning using the pCR®-XL-TOPO® plasmid, for which the ccdb cassette-sensitive Top 10 strain of cells was used to ensure selection (Invitrogen). RNAi by feeding was performed using the *HT115* strain of *E. coli*, an RNAse III mutant that tolerates the presence of double stranded RNA. All bacterial stocks are kept in a 20-25% glycerol solution at -80ºC.

Preparation of electro-competent *E. coli*

Electro-competent cells were created by first streaking out the cell strain from a glycerol stock onto a 2YT agar plate with no antibiotics added. A single colony was then used to seed two 50ml falcon tubes of 2YT broth, grown overnight at 37ºC. These falcons were then used to seed two 500ml flasks of 2YT broth, then incubated for approximately 6 hours at 37ºC. These flasks were then placed on ice to cool and arrest further growth of the bacteria during their logarithmic growth stage, and the cells were subsequently separated from the broth using a cooled centrifuge and new sterile Falcon tubes. Cells were washed 6 times in ice-cold deionised water before resuspension in ice-cold 10% glycerol. This suspension was then aliquotted and stored at -80ºC.

Electro-transformation of *E. coli*

A 40µl aliquot of XL1-Blue electro-competent bacteria was thawed on ice and gently mixed with 0.5-1µl of plasmid or ligation reaction. The mixture was then transferred to a chilled 2mm electroporation cuvette (Geneflow Ltd) and pulsed with a micropulser (Biorad) on the setting EC2 for approximately 5ms. Immediately after pulsing, 250µl of 2YT broth (for 1 litre: tryptone 16g, yeast extract 10g, NaCl 5g, distilled water 1L) without antibiotics was added to the cuvette, followed by an hour incubation at 37ºC. The culture was then spread onto a 2YT agar plate (for 1 litre: tryptone 16g, yeast extract 10g, NaCl 5g, agar 20g, distilled water 1L) containing the appropriate antibiotic and left at 37ºC to grow overnight.

2.3 Plasmid construction for bacterial or worm expression

For plasmid names, see Appendix II. Where genomic DNA templates were used during PCRs, single worm lysis of appropriate worms was performed and the whole mixture used as a template for the reaction.

Primer phosphorylation

Primers were phosphorylated using the New England Biolabs T4 polynucleotide kinase (PNK). 2.5µl of a 40mM primer stock was added to 9.5µl H_2O, 5µl 10mM ATP and 1µl of the enzyme PNK, and incubated for 30 minutes at 37ºC.

PCR reactions for cloning

All PCR reactions used for cloning were carried out using Phusion® High-Fidelity DNA Polymerase from New England Biolabs. For products that were to be T/A cloned ('TOPO cloned', see below), A-overhangs were added to the product after purification by incubation at 72ºC for 10 minutes in a mixture of 7µl purified DNA, 1µl Taq buffer (x10), 1µl dATPs (10µM) and 1µl Taq polymerase. The product was then used directly.

T/A cloning using TOPO XL PCR kit (Invitrogen)

The TOPO XL PCR kit was used to clone PCR products with 3' A-overhangs by using the topoisomerase I (from the Vaccinia virus) that nicks one strand of DNA after 5'-CCCTT. The 3' phosphate of the nicked strand forms a covalent bond with a tyrosyl residue of topoisomerase I, whilst the 5' hydroxyl group of the nicked strand then reverses the reaction by attacking the reaction by attacking the phospho-tyrosyl bond and releasing the topoisomerase. The pCR®-XL-TOPO® plasmid contains two convergent CCCTT sites that overlap by one base, therefore

ensuring the topoisomerase I nicks the plasmid on both strands and thus linearises the plasmid in a manner that leaves 3' T-overhangs. This allows annealing of the 3' A-overhangs of the PCR product. The 5' hydroxyl group of the PCR product then attacks the phospho-tyrosyl bond between the 3' thymidine and the topoisomerase and thus ligates the PCR product into the plasmid.

pal-1(A2110G)::gfp

A construct comprising the TOPO XL backbone with an insert of the 5th and 6th exons of *pal-1*, with the *e2091* version of the 5th intron between them, had already been made by C. Brabin. This plasmid was subjected to site-directed mutagenesis of the Δ3' mutation in the intron back to wild-type using overlapping mismatched primers oSG3 and oSG4. The *pal-1* 5th intron containing only A2110G was then sub-cloned into the TOPO XL backbone using oSG101 and oSG102 in order to re-introduce a naturally occurring *SalI* site in the *pal-1* genomic sequence. This was then cloned back into a full-length *pal-1::gfp* reporter construct made previously by C. Brabin.

Triple tandem repeat of the *pal-1* A2110G intronic enhancer

The 3x tandem repeat of the *pal-1* A2110G intronic enhancer region of the last intron was generated by using a PCR approach. This required primers that had homology not only to the region of the intron that was to be amplified, but also to the primer at the other side of the sequence (oSG132 and oSG133). This generated a 'ladder' of PCR products after amplification due to the annealed products of the primers. The 'rung' that corresponded to a triple repeat of the enhancer region was gel purified and TOPO cloned.

Yeast plasmids pHisi-1 and pLacZi with triple tandem array *pal-1* intronic inserts

The TOPO XL plasmid containing the triple tandem repeat of the *e2091* A2110G version of the *pal-1* intron was cloned into the Clontech yeast vectors pHisi-1 and pLacZi using *EcoRI* (non-directional cloning). The wild-type version of the array in TOPO XL was cloned into pHisi-1 using *MluI* and *XbaI*, and into pLacZi using *KpnI* and *XhoI*. The pHisi-1 backbone was cloned without any purification after digest.

Cloning of the KanR cassette for yeast expression

The KanR cassette was PCR amplified from the plasmid PFA6a-kanMX6 using primers oSG198 and oSG199. This fragment was then TOPO cloned.

Cloning the KanR cassette into pHisi-1 containing the *pal-1* inserts

The yeast KanR cassette was inserted into the pHisi-1 backbone in a site with no functional consequence, using *BamHI*.

wrt-2 promoter in pPD107.94

The *wrt-2* promoter was amplified from single worm lysis preparations using oSG165 and oSG166, and TOPO cloned. This insert was then cloned into pPD107.94 using *XbaI* and *HindIII*.

mCherry::wrt-2::gfp

Genomic *wrt-2* plus the 5' intergenic region was amplified using oSG165 and oSG167, with oSG167 containing a GFP-compatible overhang. A second PCR reaction was performed on the template pPD95.75 to amplify GFP using oSG168 and oSG170. Both PCR products were gel purified and then 1µl of each were pooled to use as the template for a third PCR reaction, using

primers oSG169 and oSG165, in order to fuse the GFP to the carboxyl terminus of *wrt-2*. This final product was TOPO cloned. The mCherry ORF was amplified from pcFJ104 using oSG195 and oSG196 to remove the stop codon and to add flanking splice sites. This construct was TOPO cloned, and then digested out and inserted into the *wrt-2::gfp* plasmid using *PacI*, in a naturally occurring site in the third intron of *wrt-2*. For this last ligation, neither digest was gel purified.

wrt-2 RNAi clone

Primers oSG191 and oSG192 were used to amplify a region of *wrt-2* which did not correspond to any other part of the genome. The resulting fragment was TOPO cloned and then cut using *SacI*-HF and *SalI*-HF to clone into L4440.

BiFC constructs

All cDNAs for cloning into BiFC expression vectors were first amplified using primers with *BglII* and *KpnI* sites and primers included a frame shift of two bases at the start in order to be in frame with the BiFC ATG site included in the plasmid. No cDNA construct contained a stop codon. These PCR products were sub-cloned into TOPO XL vectors and sequenced before subsequent cloning into BiFC vectors using *BglII* and *KpnI*. *rnt-1* cDNA was amplified using oSG9 and oSG10, *bro-1* cDNA was amplified using oSG11 and oSG12, and *pal-1* cDNA was amplified using oSG26 and oSG27.

Mutagenesis of *rnt-1* to get *e1241* for BiFC

The wild-type *rnt-1* cDNA construct in TOPO XL for cloning into the BiFC vectors was mutagenised using two phosphorylated primers, oSG76 and oSG77, one of which was mismatched to the basepair that was to be changed. The plasmid was amplified, *DpnI* digested to

get rid of the template plasmid and then transformed. This sequenced plasmid was then used for BiFC cloning.

2.4 Construction of yeast strains

Plasmids for yeast expression were linearised and gel purified (pHisi-1 constructs linearised with *AflII*, pLacZi constructs linearised with *NcoI*-HF). Three different integration protocols were used on the host strain YM4271 (the Clontech integration method described in the manual, a recommended 'conventional' protocol outlined below, and a 'quick' protocol, also outlined below), with the best results from the 'quick' protocol.

'Conventional' protocol

Day 1:

- Set up overnight culture in YPD (for 1 litre: peptone 10g, yeast extract 10g, glucose 20g, distilled water 1L) of host yeast strain at 30ºC.

Day 2:

- Dilute yeast (250µl in 25ml YPD) and grow for 6 hours at 30ºC in a 50ml Falcon tube.

- Harvest (3,000 rpm, 5 minutes).

- Transfer cells to 1.5 ml Eppendorf and wash with sterile water.

- Re-suspend in 450µl 0.1M LiAc/TE (sterile). Leave overnight at 4ºC, or move to day 3 straight away.

Day 3:

- Mix (vortex briefly): 100µl competent yeast cells (from steps above), 10µl calf thymus DNA (10mg/ml), 10µl DNA (200ng/µl), 700µl 0.1M LiAc/40% PEG.

- Incubate for 30 minutes at 30ºC.

- Optional: add 50µl DMSO to improve transformation efficiency.

- Heat shock for 20 minutes at 42ºC.

- Spin at 7000rpm for 5 minutes at room temperature.

- Re-suspend in 100µl YPD and plate onto appropriate selection plates.

'Quick' protocol

- Pick a ~20µl patch of yeast from a YPD plate (for 1 litre: peptone 10g, yeast extract 10g, glucose 20g, agar 20g, distilled water 1L).

- Wash with 1ml of 1M LiAc in a 2ml Eppendorf.

- Spin down gently at about 1-3000rpm for 10s.

- Re-suspend in 1M LiAc which is equal in volume to the pellet.
- Into another tube (1.5ml Eppendorf) put 12µl of cut vector (~50ng/µl).
- Add 8µl of boiled salmon sperm carrier DNA (10mg/ml) into the same tube.
- Add 24µl of the cell suspension.
- Add 90µl of 50% PEG 3350 solution.
- Gently mix (flick the tube, don't pipette up and down).
- Leave for 0.5-1hr at room temperature.
- Add 12µl of 60% glycerol and mix gently.
- Leave for 0.5-1hr at room temperature.
- Heat shock at 42ºC for 20mins.
- Dilute to 400µl and spread on at least 2 plates.

2.5 Microscopy

An epifluorescent Zeiss microscope fitted with Nomarski (DIC), GFP, FITC and mCherry filters and a 63x oil immersion objective and Axiovision software was used to capture fluorescent and DIC images. Worms were mounted on 2% agarose pads containing 0.5% phenoxypropanol (anaesthetic) in order to immobilise them.

A Leica SP5 laser scanning confocal fitted with a 488nm argon laser was used to capture all fluorescent confocal images of larval seam cells and motor neurone commissures.

An Ultra-VIEW VoX PerkinElmer spinning disk confocal mounted on a IX81 Olympus microscope fitted with a 60x 1.3 NA silicon immersion objective, a 488nm laser line and Volocity software was used to capture images of live *ajm-1::gfp* embryos. Very high laser power (80%) was used to minimise the time needed to create a z stack through the twitching embryo in order to obtain static images. This microscope is owned by the lab of Kim Nasmyth and managed though Micron (University of Oxford).

2.6 Laser ablation and live cell analysis

Laser ablation of seam and P cells at L1 was performed using a Micropoint pulsed Nitrogen dye laser mounted on a Zeiss Axioplan 2 scope (on loan to Richard Poole, University College London). Identification of cells was aided by the integrated markers *heIs63* (containing a *wrt-2* promoter driving GFP construct to mark the seam cells) and *stIs10166* (containing a *dpy-7* promoter driving mCherry, to mark the hyp7 and P cells).

After ablation and several hours recovery on an NGM plate, individual worms were placed between a water-based 2% agarose pad and a circular coverslip upon which 3µl of an M9/*OP50* concentrated suspension was placed as a food source. Worms were transferred into this bacteria-rich drop with an eyelash pick before careful inversion of the coverslip onto the agarose pad, keeping the worm central and the slide with minimal bubbles. The L1 division of seam cells and P cell migration was then analysed using Nomarski (DIC) optics and a 100x oil immersion objective (Zeiss). When needed, a very short exposure to UV allowed the fluorescent markers to be observed using appropriate filters. Worms were periodically transferred back onto NGM plates to recover if they arrested development, and re-mounted.

2.7 Bioinformatics

All *Caenorhabditis* sequences were obtained from wormbase.com. BLAST searches were performed using the databases available at http://blast.ncbi.nlm.nih.gov, and in wormbase.com. Sequences were handled and annotated using Ape (http://biologylabs.utah.edu/jorgensen/wayned/ape/), and alignments between *Caenorhabditis* genomic and protein sequences were performed using CLC Sequence Viewer 7 (http://www.clcbio.com). Transcription factor binding analysis was performed using the JASPAR vertebrate 2014 database (Mathelier, Zhao et al. 2014).

Acknowledgements

I would like to thank Charles Brabin for the many *pal-1* strains and constructs created during his D. Phil. in the Woollard lab, and Marjolein Wildwater, Yishi Jin and Jonathan Hodgkin for their gifts of various strains, as well as the CGC, from whom some strains were obtained. I would also like to thank Richard Poole and Arantza Barrios for the use of and invaluable help training me on their laser ablation apparatus, as well as Ian Dobbie for sharing his expertise in imaging moving samples using the spinning disk confocal microscope. Finally I would like to thank members of Jane Mellor's lab who shared their equipment and protocols for yeast methods with me.

CHAPTER 3

Wnt signalling may control *pal-1* expression to regulate epidermal patterning

3.1 Introduction

Null alleles of *pal-1* are embryonically lethal, resulting in a failure of ventral enclosure or strong *nob* (*no* *b*ackend) phenotypes (Hunter and Kenyon 1996, Edgar, Carr et al. 2001). However, a viable allele, *e2091*, has been shown to have a seam cell positioning defect (consisting of overlapped seam cells) upon hatching (Edgar, Carr et al. 2001) and a fate transition of V6 in males which results in the loss of the V6-derived rays in the male tail (Zhang and Emmons 2000). Despite the viable phenotype of *e2091*, heterozygote animals of genotype *e2091*/*rhDf1*, where *rhDf1* is a small deficiency that knocks out *pal-1* as well as its two flanking genes, have the same phenotype as *e2091* homozygote animals, indicating that *e2091* is a strong loss-of-function allele rather than a hypomorph (Edgar, Carr et al. 2001). Analysis of this mutant

identified two point mutations in the last (5th) intron of the *pal-1* gene, a 5' mutation A2110G and a 3' mutation G3004A (mutations defined by their distance from the start codon of the *pal-1* genomic sequence, Fig. 3.1.1); a subsequent suppressor screen for the male tail phenotype isolated a reversion of the 5' mutated site (A2110G) back to wild-type whilst leaving the 3' mutation (G3004A) in place, therefore identifying A2110G as necessary and sufficient to confer the *e2091* male tail phenotype (Zhang and Emmons 2000). Analysis of this point mutation shows that it is too far away from the exon/intron boundary to be likely to interfere with the splice site (see Fig. 3.1.1).

Previous work in the laboratory has demonstrated that the 5th intron of *pal-1* is able to drive expression in the posterior seam cells V2-T, whereas an *e2091* mutant version cannot (Fig. 3.1.2, C. Brabin, D. Phil. thesis, 2011). All other expression driven from this intron appears unperturbed by the *e2091* point mutations (C. Brabin, D. Phil. thesis, 2011). Until this work, *pal-1* expression in the seam was only reported in V6, as the translational reporter used for analysis was missing this last enhancer-containing intron (Edgar, Carr et al. 2001). A full-length *pal-1* genomic translational C-terminal GFP fusion construct has now been shown to include this L1 seam cell expression driven by the 5th intron (Fig. 3.1.2, C. Brabin, D. Phil. thesis, 2011).

The last intron of *pal-1* therefore contains a seam-specific enhancer that drives expression of *pal-1* during L1, and a loss-of-function mutant of *pal-1(e2091)* lacking this enhancer displays seam defects. The work presented in this chapter is aimed at understanding the precise function of *pal-1* in the seam cells as well as investigating its molecular basis.

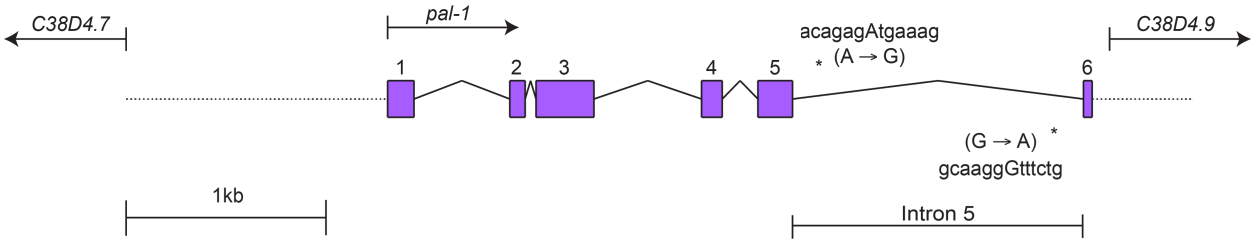

FIG. 3.1.1 – *PAL-1* GENE STRUCTURE SHOWING THE TWO POINT MUTATIONS (ASTERISKS) IN THE LAST INTRON OF THE *E2091* ALLELE (ADAPTED FROM C. BRABIN, D. PHIL. THESIS, 2011).
The loss-of-function *e2091* allele contains two point mutations in the last intron of *pal-1*, A2110G and G3004A. A2110G has been previously found necessary and sufficient to confer the *pal-1* male tail phenotype.

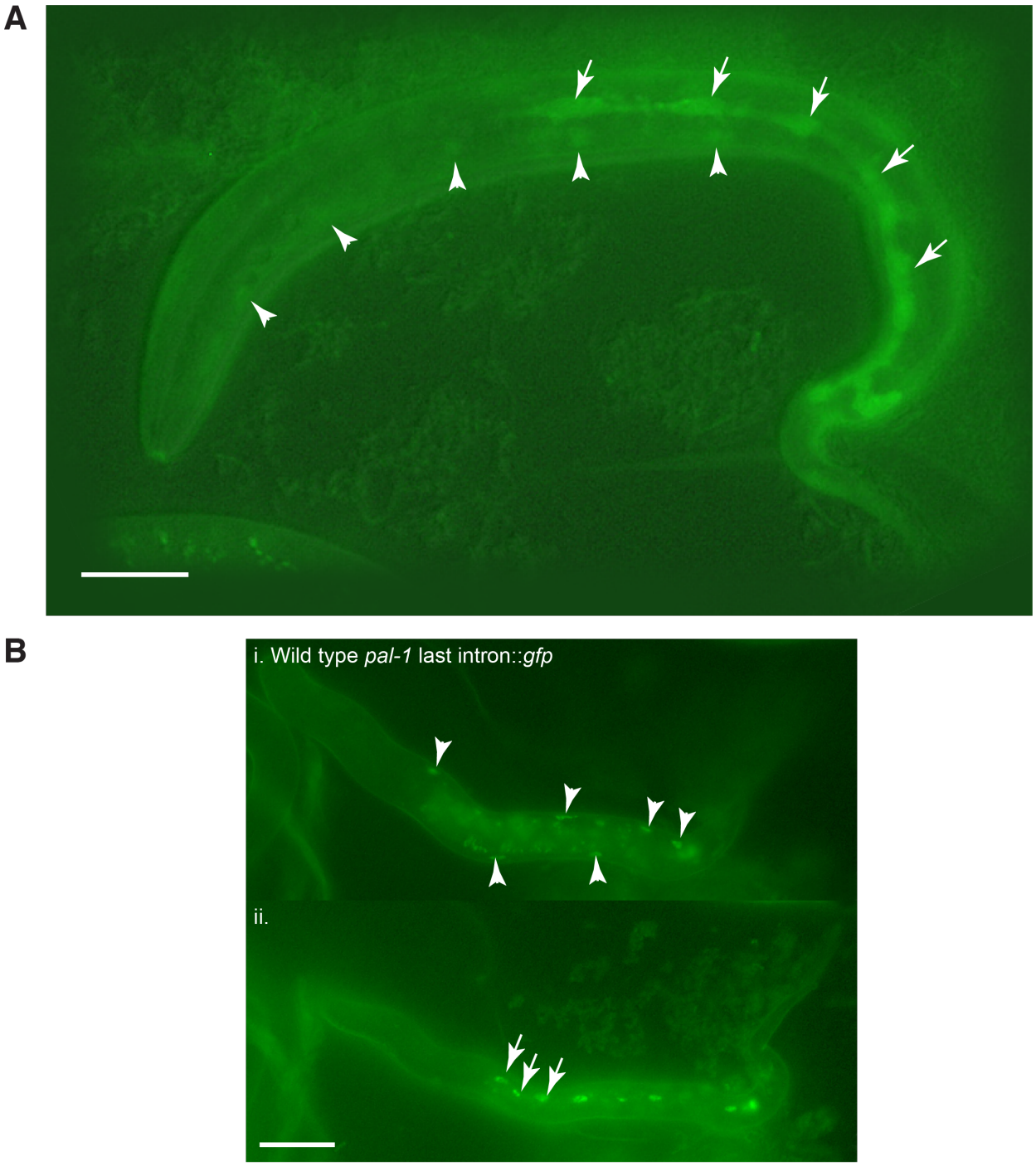
A
B
i. Wild type *pal-1* last intron::*gfp*
ii.
C
i. *e2091 pal-1* last intron::*gfp*
ii.
iii.

3.2 Results

pal-1(e2091) mutants hatch with a mid-body bulge and seam cell overlap

An overlapping seam cell phenotype and mid-body bulge of *pal-1(e2091)* hermaphrodites has previously been reported (Edgar, Carr et al. 2001), and is shown in figure 3.2.1. I found that both phenotypes are present at the 3-fold stage of embryonic development (Fig. 3.2.1, insets to A and B), suggesting that the defect in *pal-1* function in the *e2091* mutant that produces this phenotype must occur before this developmental stage. After hatching, the incidence within the population of the overlap of the seam cells decreases with post-embryonic stage, although the bulge persists in the population (Fig. 3.2.1), indicating some of the worms are either able to recover from the seam cell overlap between hatching and adulthood, or that the worms carrying the phenotype die during larval development. To address this, I counted the incidence of larval lethality in the *pal-1(e2091)* population. There was no detectable larval lethality over the total of six broods analysed, suggesting that animals are able to recover from the phenotypes shown at hatching.

Mid-body phenotypes of *e2091* animals are not suppressed by *sop-1*

In addition to the mid-body phenotypes described above, male *e2091* animals exhibit a male tail phenotype of an average of 3 rays per side compared to 9 in wild-type (data not shown). The male lineage of V6, which normally gives rise to rays of the male tail, instead adopts a 'hermaphrodite' V6 lineage due to lack of *mab-5* expression, causing a lack of tail rays by adulthood (Hunter, Harris et al. 1999, Zhang and Emmons 2000). This ray loss is suppressed by knocking out the *sop-1* mediator component either by using a mutant (Zhang and Emmons 2000), or by RNAi (Fig. 3.2.2 A). In contrast, I found that the seam cell overlap and the mid-body bulge phenotypes exhibited by both sexes are not effected by *sop-1* RNAi (Fig. 3.2.2 B),

suggesting that the mid-body phenotypes are caused by an alternative pathway of regulation by *pal-1*.

The 5' mutation in the 5th intron is responsible for the *e2091* phenotypes

pal-1(e2091) contains two point mutations within 1kb of each other in the fifth intron of *pal-1*. These mutations alone confer highly penetrant phenotypes of a mid-body bulge and overlapping seam cells in the V2-V4 region of the worm, as discussed above. Alignments of the entire intronic region with other members of the *Caenorhabditis* genus show a high level of sequence conservation over the entire intron, including 100% alignment around the 5'-most *e2091* point mutation (A2110G), but although the base at the 3'-most mutation site is conserved (G3004A), there is no distinguishable conservation surrounding this base, suggesting that it is not part of a critical expression motif in the *C. elegans* gene (Fig. 3.2.3). As further evidence for A2110G being in an important *pal-1* enhancer region, a suppressor screen for *pal-1(e2091)* isolated a strain for which A2110G but not G3004A had been reverted to wild-type (Zhang and Emmons 2000). In order to confirm that A2110G is responsible for the *pal-1(e2091)* mutant phenotypes, I generated a full-length *pal-1::gfp* reporter construct identical to the wild-type reporter but including A2110G in the 5th intron (Fig. 3.2.3 Biii). Although the wild-type reporter was able to fully rescue the mid-body bulge and seam cell overlap phenotypes of the *pal-1(e2091)* mutant, the 5'-mutated construct was not, proving not only that compromised *pal-1* function is indeed causative of these phenotypes in the *e2091* mutant, but also that A2110G must be responsible for these phenotypes (Fig. 3.2.4).

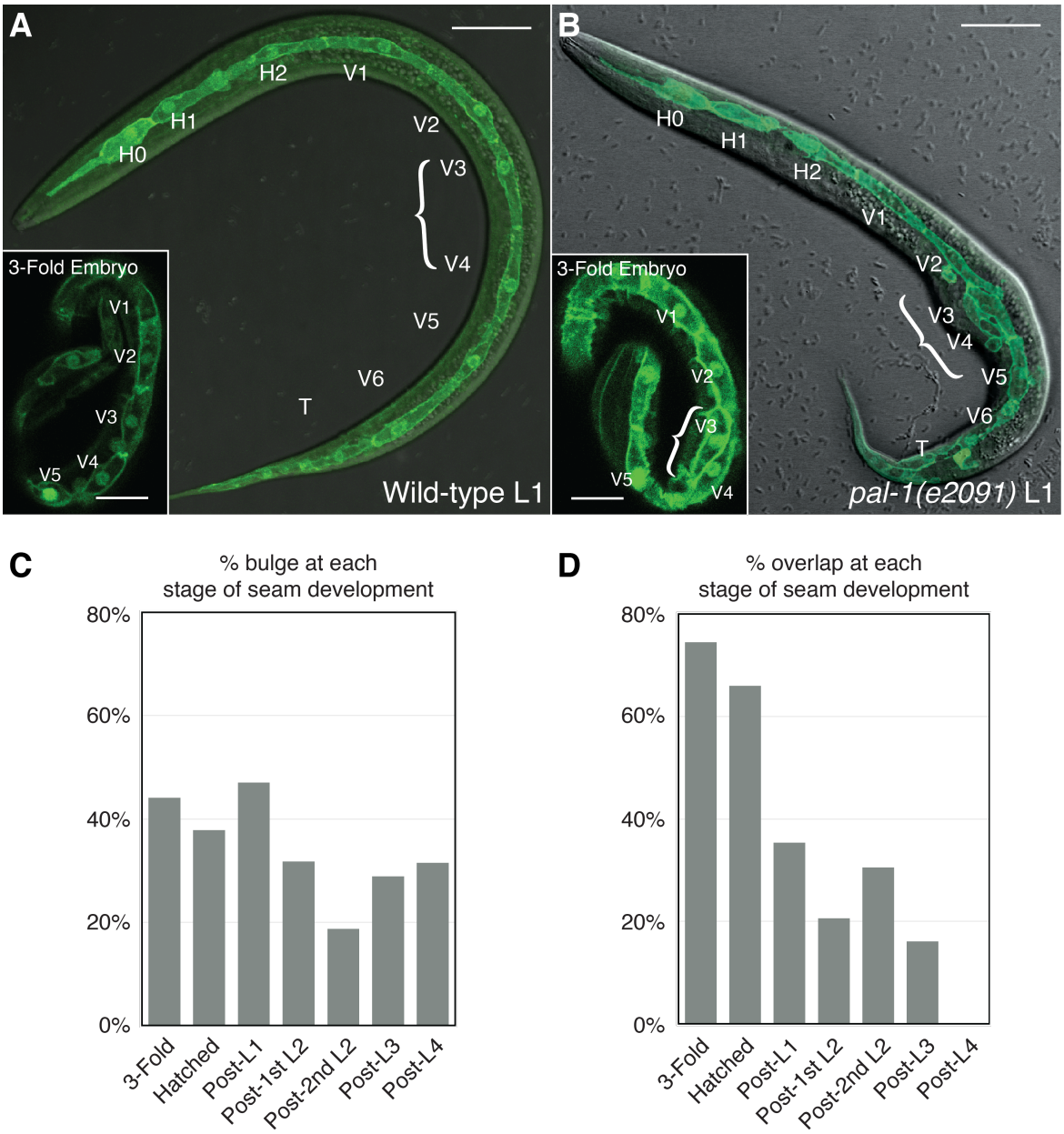

FIG. 3.2.1 – *PAL-1(e2091)* ANIMALS HATCH WITH A SEAM CELL OVERLAP AND MID-BODY BULGE THAT ARE EVIDENT IN THE 3-FOLD EMBRYO.

A. A wild-type L1 worm hatches with a line of 10 seam cells down each lateral side of the body (only one side shown). The inset shows a wild-type 3-fold embryo expressing the same seam cell marker. **B.** A *pal-1(e2091)* animal exhibits a mid-body bulge and although the worm hatches with 10 seam cells, they are not aligned end to end in the region of the central V cells, instead overlapping each other (bracketed region). The inset shows a *pal-1(e2091)* 3-fold embryo with the seam cell overlap already visible. Scale bars = 10 μm. **C.** Incidence of the mid-body bulge in *pal-1(e2091)* at different stages of seam cell development ('post-L1' refers to the L1 seam cell division). $52 \leq n \leq 68$ per time point. **D.** Incidence of seam cell overlap in *pal-1(e2091)* animals at each stage of seam cell development. $50 \leq n \leq 68$ per time point. In contrast to the bulge phenotype, the incidence of overlap decreases from nearly 80% in the late embryo though the larval stages until eventual fusion of the seam at the end of L4. Nevertheless, the average incidence of larval lethality over 6 broods is 0%, suggesting worms recover from this phenotype as they develop. At no developmental stage has either the bulge or overlap phenotype described here been observed in wild-type animals (n = 210 total over all developmental stages, except for after the first L2 division which was not recorded).

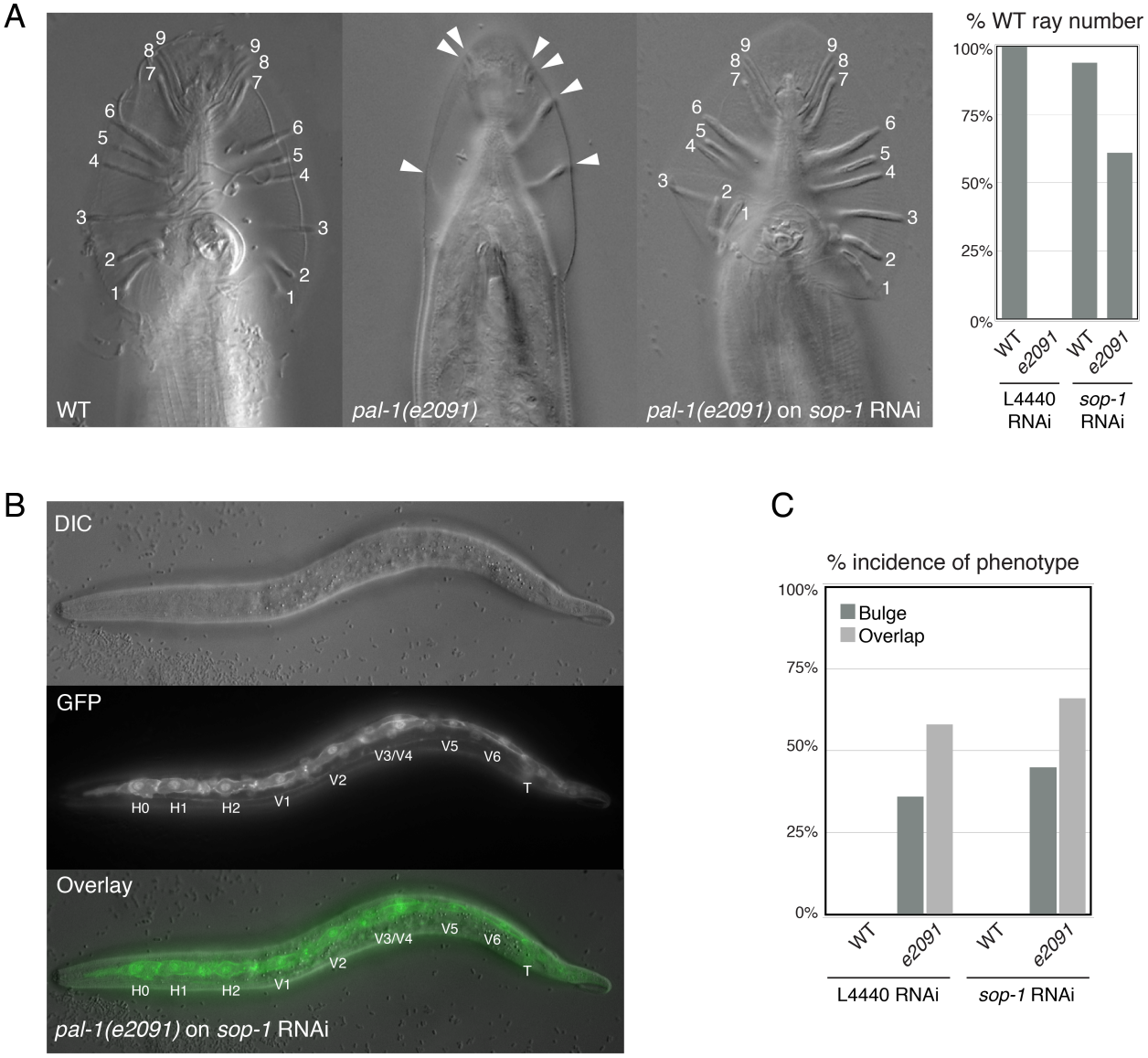

FIG. 3.2.2 – *SOP-1* RNAi IS ABLE TO SUPPRESS THE MALE TAIL PHENOTYPES OF *PAL-1(e2091)* MUTANTS, BUT NOT THE MID-BODY BULGE AND OVERLAPPING SEAM DEFECTS.

A. 100% of the population of *pal-1(e2091)* single mutants exhibit abnormal male tail structures, as ray lineages are compromised. This defect is suppressed by *sop-1* RNAi, as published by Zhang and Emmons, 2000. 40 ≤ n ≤ 57 individuals from 2 RNAi experiments. Scale bar = 50 μm. **B.** *pal-1(e2091)* animals exposed to *sop-1* RNAi exhibit the same mid-body bulge and overlapping seam defects as the *pal-1(e2091)* mutant alone. Scale bar = 10μm. **C.** Incidence of the bulge and seam overlap phenotypes in *pal-1(e2091)* animals subjected to *sop-1* RNAi. *sop-1* knockdown does not suppress these mid-body *pal-1(e2091)* phenotypes; *sop-1* RNAi has no effect on the seam cells in a wild-type background. Neither phenotype was observed in wild-type animals grown on either L4440 (empty vector) or *sop-1* RNAi-inducing bacteria. 53 ≤ n ≤ 55 individuals from two RNAi experiments.

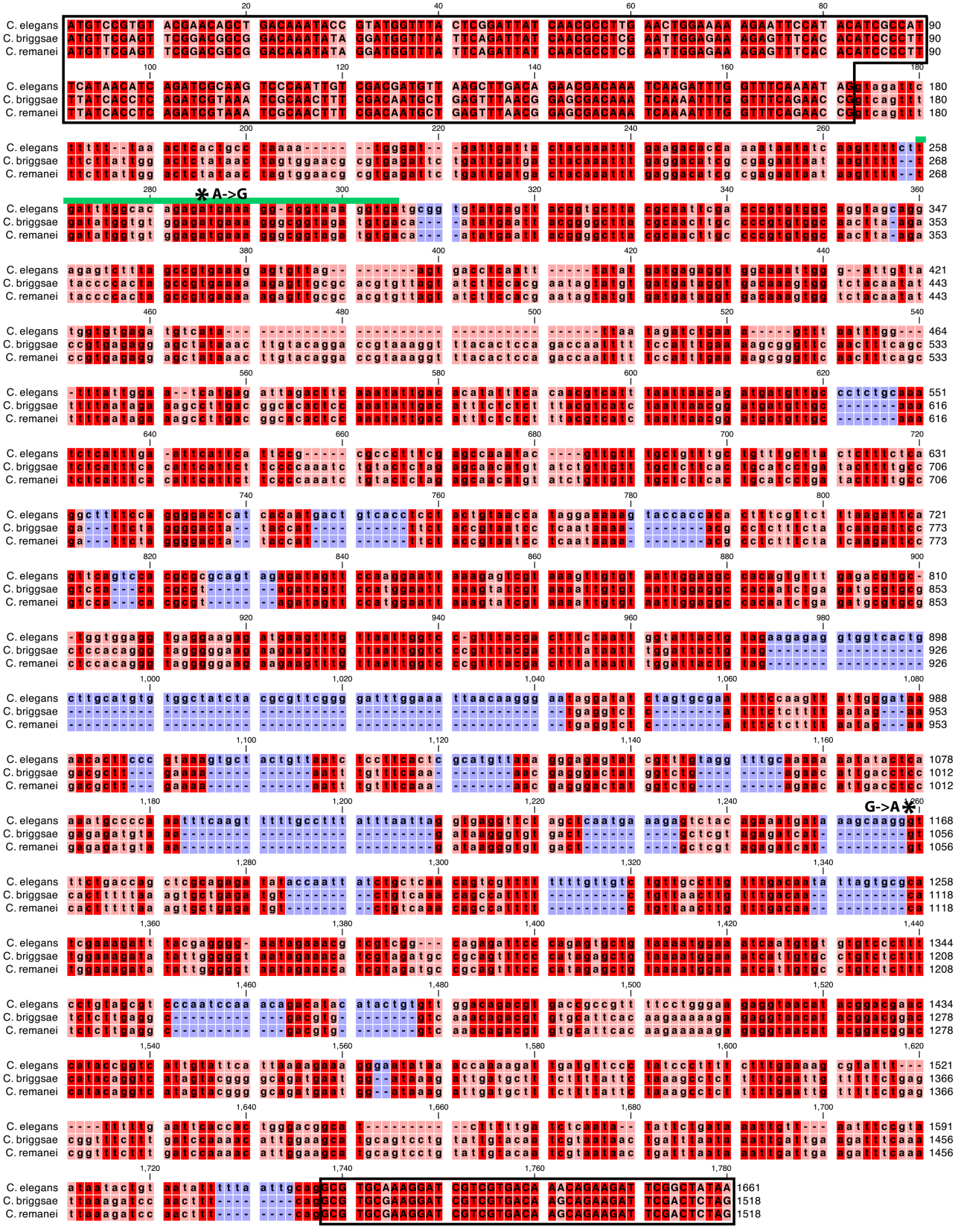

FIG. 3.2.3 – SEQUENCE ALIGNMENT OF THE FIFTH *PAL-1* INTRON BETWEEN *C. ELEGANS*, *C. BRIGGSAE* AND *C. REMANEI*.
Black boxed areas indicate the flanking exons. Regions of high conservation are indicated in red; low conservation is shown in blue. Both mutated bases of the *e2091* allele, indicated with asterisks, are conserved, but whereas the 5'-most base change (A2110G) is within a highly conserved sequence motif, the 3'-most base change (G3004A) is not. The green line indicates the sequence that was input into the JASPAR database.

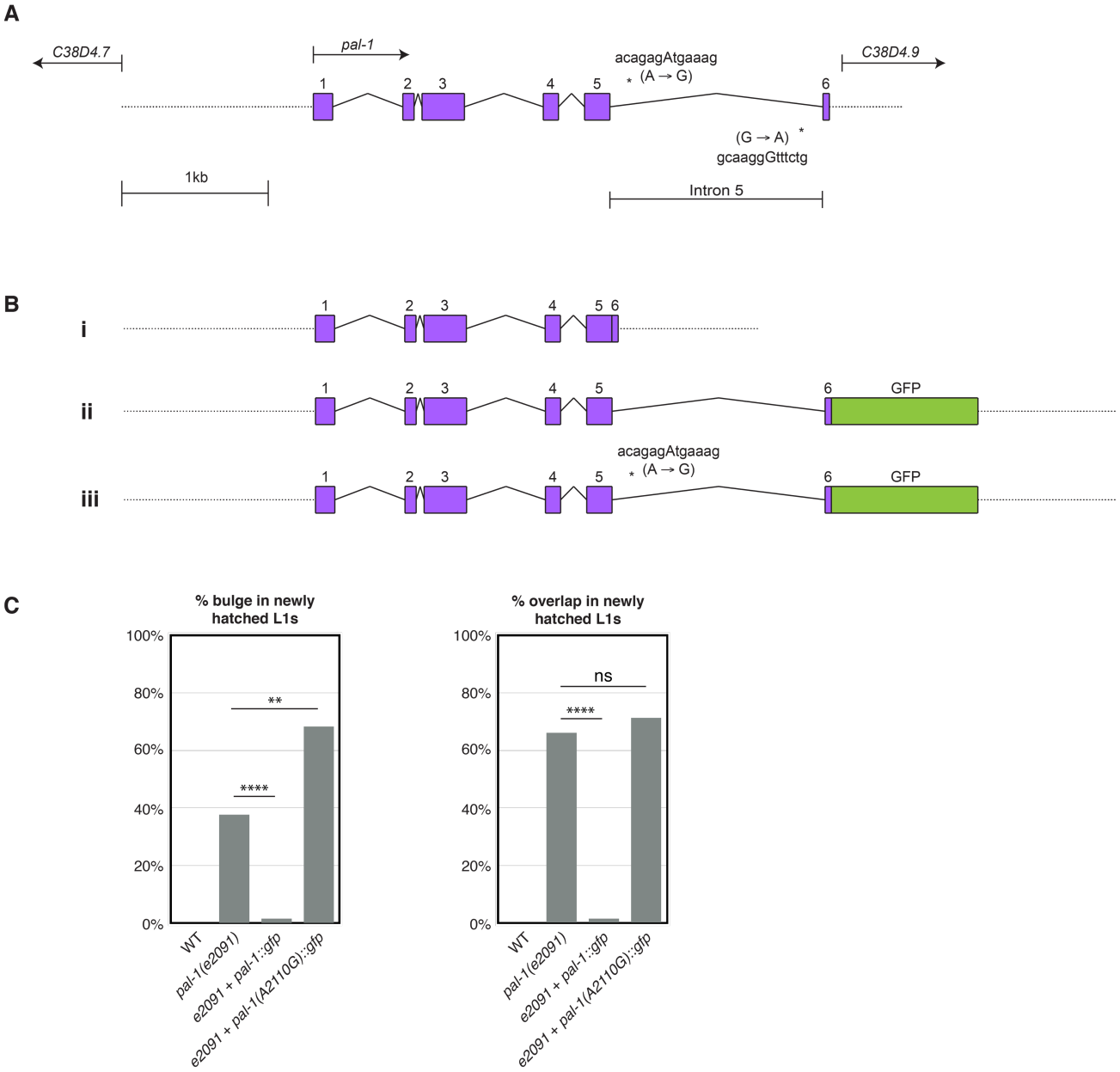

FIG. 3.2.4 – RESCUE OF THE BULGE AND SEAM CELL OVERLAP PHENOTYPES BY *PAL-1::GFP* CONSTRUCTS.

A. *pal-1* gene structure (to scale) including all introns, exons and the entire upstream intergenic region (adapted from C. Brabin, D. Phil. thesis, 2011). Both point mutations in the 5th intron of the *e2091* allele are marked with an asterisk, and the mutation illustrated. **B.** Rescue and expression constructs for *pal-1*. The first rescue construct shown (**i**) was able to rescue the *pal-1* null embryonic phenotype (Edgar, Carr et al. 2001). However, the construct was generated from a genomic-cDNA fusion PCR, resulting in a missing intron 5 and therefore missing part of the *pal-1* expression profile. The second construct (**ii**) which included the full wild-type 5th intron (generated by C. Brabin) was able to rescue both the bulge and the seam cell overlap phenotypes of *e2091* (rescue data shown in **C**). A construct identical to **ii** except containing the A2110G mutation (with a wild-type G3004 locus) from *e2091* (**iii**) was unable to rescue either *e2091* phenotype. $50 \leq n \leq 69$ per strain, Student's T-test P****< 0.00001, P**< 0.001. The increased incidence of the bulge phenotype with construct **iii** is surprising, and may be due to the abundance of the copies of the *pal-1* genomic sequence present in each cell causing a saturation of enhancer/promoter binding factors by sequences contained within the construct, thus producing paradoxically increased phenotypes.

pop-1 is predicted to bind to the A2110G locus of the *pal-1* 5th intron

It has been established previously (C. Brabin, D. Phil. thesis, 2011) that mutations in the 5th intron of *pal-1* in the *e2091* allele perturb L1 seam cell expression (the wild-type intron taken in isolation with the *pes10* minimal promoter is able to drive GFP expression in the L1 posterior seam, whereas the *e2091* version of the intron is not). Taken together with the evidence that it is the A2110G mutation and not the G3004A locus that is responsible for the *e2091* phenotypes, we could now put the A2110G and immediate highly conserved surrounding sequence (Fig. 3.2.3) into the transcription factor (TF) binding site prediction software JASPAR (Mathelier, Zhao et al. 2014). We used the vertebrate database in JASPAR rather than the nematode database due to a recommendation that this larger database was ultimately more accurate than the nematode version in predicting sites of real interaction (R. Pocock, pers. comm.). Using a 90% relative profile score threshold, we pulled out three TF-binding hits in this region. Only one of these overlapped with the site of the A2110G base change: mammalian Tcf4. The sole *C. elegans* Tcf homologue is *pop-1*, a transcription factor at the end of the Wnt pathway.

A *wrm-1* temperature sensitive (ts) mutant causes seam cell overlap

To test whether the Wnt pathway was indeed involved in the regulation of *pal-1*, we used the temperature sensitive (*ts*) allele of *wrm-1*, *(ne1982)ts*, a ß-catenin upstream of *pop-1* in the Wnt pathway. As *wrm-1* is essential for early embryonic cleavages, this *ts* allele allowed us to perturb *wrm-1* only after the completion of crucial embryonic divisions involving the Wnt pathway, therefore allowing any seam cell or later embryonic patterning defects to be observed in hatched animals. We found that we were able to bleach gravid hermaphrodites (grown at 15ºC) on the bench, leave the eggs for three hours at this temperature and then move them to higher restrictive temperatures. This resulted in a superficial phenocopy of the *pal-1(e2091)* seam cell overlap

phenotype in these single mutant animals, with a penetrance of over 30% at the highest restrictive temperature tested (Fig. 3.2.5). However, unlike *pal-1(e2091)* mutants, the seam overlap in the *wrm-1(ne1982)ts* animals upon hatching was not restricted to the mid-body of the animal but was able to involve any of the V lineage seam cells. Likewise, the overlap did not always occur once down the length of the animal, but rather could repeat in another region of the seam, as shown in figure 3.2.5 A.

By L4, *wrm-1(ne1982)ts* mutants grown at restrictive temperatures have reduced numbers of seam cells due to fate perturbations during later (L2 onwards) larval asymmetric seam cell divisions (Gleason and Eisenmann 2010). In order to determine whether *wrm-1(ne1982)ts* affects just seam cell positioning at L1, and not cell fate determination (which could have secondary effects on positioning), we used the integrated *wsIs51* (*scm::gfp*) marker to count seam cell nuclei after the temperature shift. We found that there was no loss of seam cell fate in the *wrm-1* temperature shifted mutants compared to wild-type (Fig. 3.2.5 C). According to the Student's T-Test there is a significant difference between the averages of 9.78 seam cell nuclei in wild-type animals compared to 10.16 in *wrm-1* animals at 25ºC, however this difference does not increase at 26.5ºC and is therefore unlikely to be a product of the seam cell overlap phenotype.

Animals were shifted to both 25ºC and 26.5ºC due to previous findings that in order to perturb fate during post-embryonic divisions, worms containing the *wrm-1(ne1982)ts* allele had to be grown at 26.5ºC, as 25ºC was unable to cause sufficient loss of *wrm-1* function (Gleason and Eisenmann 2010).

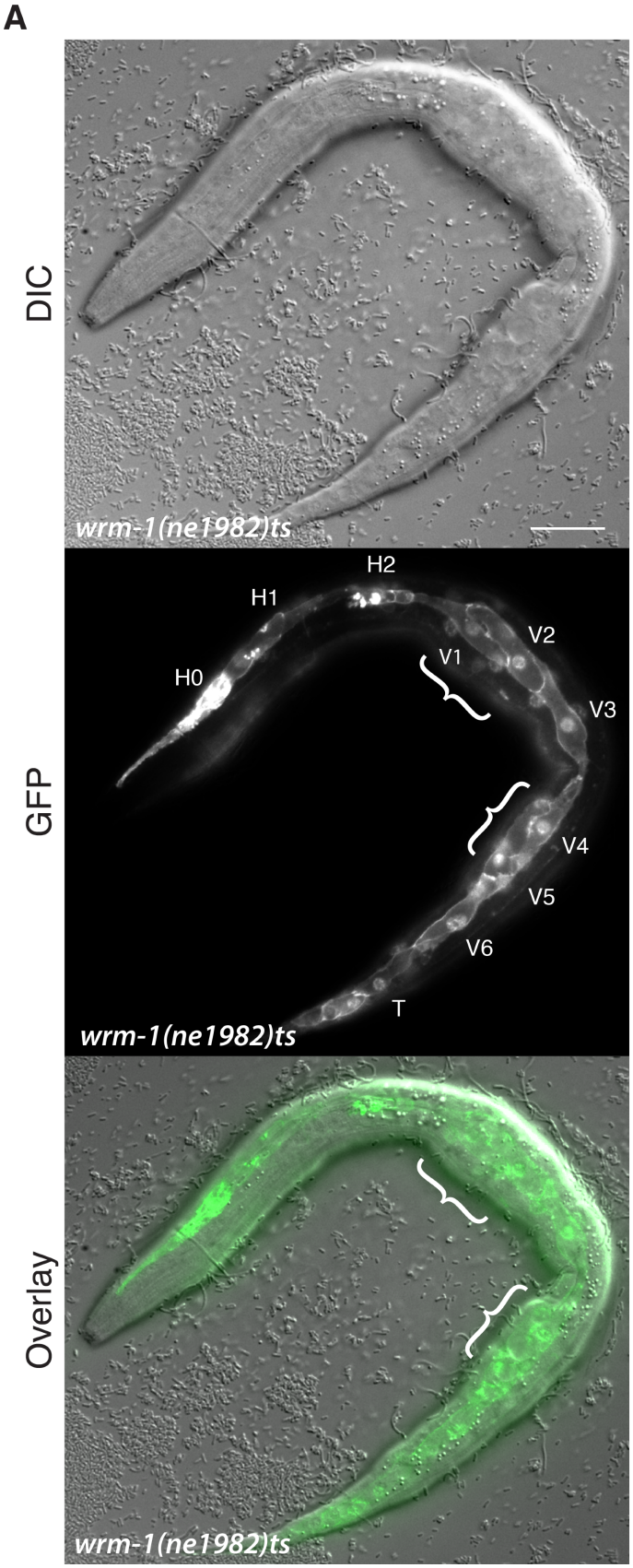
A
DIC
GFP
Overlay
wrm-1(ne1982)ts
wrm-1(ne1982)ts
wrm-1(ne1982)ts
H2
H1
H0
V1
V2
V3
V4
V5
V6
T

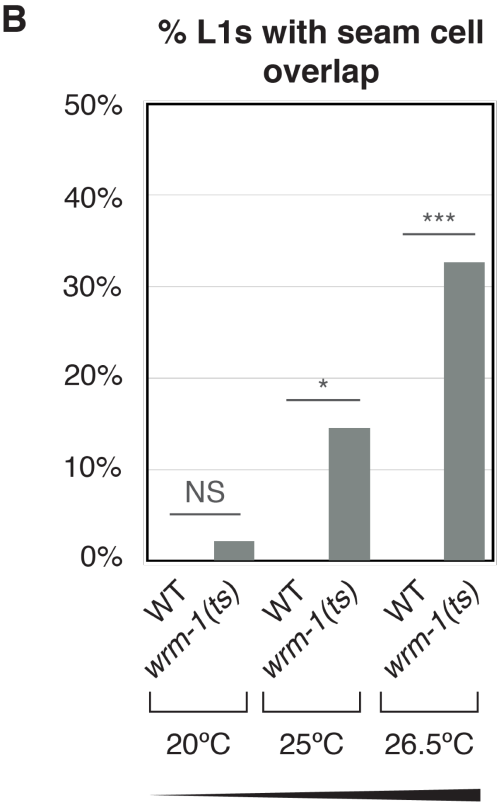
B
% L1s with seam cell overlap
50%
40%
30%
20%
10%
0%
NS
*
***
WT
wrm-1(ts)
20ºC
25ºC
26.5ºC

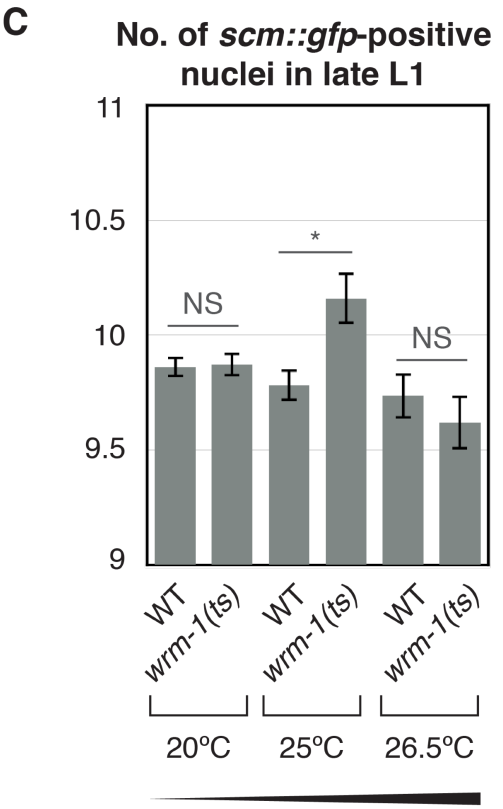
C
No. of scm::gfp-positive nuclei in late L1
11
10.5
10
9.5
9
NS
*
NS
WT
wrm-1(ts)
20ºC
25ºC
26.5ºC

Design of a yeast one-hybrid screen to identify transcription factors that bind to the *pal-1* 5th intron

Superficially, the Wnt mutant *wrm-1(ne1982)ts* appears to phenocopy *pal-1(e2091)*. However, without evidence of a direct regulatory interaction between POP-1 and *pal-1*, we cannot be sure that this phenotype is a result of *pal-1* mis-regulation. Although we have detected differences in seam cell expression between the mutant and wild-type forms of the *pal-1::gfp* construct during larval development, during embryogenesis we have not detected a difference in expression between transgenic lines containing *pal-1(A2110G)::gfp* and *pal-1::gfp*. Therefore studies of *pal-1* gene expression in a *wrm-1* mutant are not likely to be informative.

Yeast one-hybrid screens have previously been used successfully in the laboratory to detect regulatory transcription factor interactions without bias (Brabin, Appleford et al. 2011). After creating a triple tandem repeat of approximately 100bps surrounding the locus of A2110G in both the wild-type and *e2091* intron, I cloned both versions into the Clontech yeast expression vectors pLacZi and pHisi-1, for selection of positive interactions by a ß-galactosidase blue/white assay and by nutritional selection, respectively (see materials and methods). After successful integration of the LacZ reporter constructs into the provided yeast host strain YM4271, I attempted to integrate the nutritional selective marker plasmids (in the pHisi-1 backbone), which proved unsuccessful. Without this marker, any subsequent screening of the yeast strain would rely on the white/blue selection provided by the pLacZ marker, but not limit the growth of colonies on the plates, making accurate detection in the context of a screen difficult. Modification of the backbone of the pHisi-1 plasmid to add an additional yeast Kanamycin-resistant cassette to aid selection after integration allowed for successful integration of the pHisi-1 construct, however, transformation of the new yeast strain with control plasmids containing the nutritional selection marker of the transcription factor library (LEU) failed.

Unfortunately there has been precedent for the temperamentality of this screening method (C. Brabin, D. Phil. thesis, 2011) and it appears that some yeast clones may be incompatible with the system. I was therefore unable to complete this screen for transcription factors which interact with the *pal-1* enhancer element.

The Hox gene *lin-39* alone is not responsible for the mid-body positioning of the *pal-1(e2091)* defects

wrm-1(1982)ts mutants show a larger variability in the region of the seam line in which defects may occur compared to *pal-1(e2091)* mutants. We therefore wanted to ask whether the restriction of defects to the mid-body in *pal-1(e2091)* animals relied on an interaction with one of six *C. elegans* Hox factors, specifically that specifying the mid-region of the worm, *lin-39*. After constructing the double mutant *pal-1(e2091) lin-39(n1880)*, we found no significant difference in the variance or identity of seam cells involved in the overlap defect (Fig. 3.2.6), suggesting either that the strict mid-body positioning of the *e2091* defect is not due to interaction with the *lin-39* Hox gene, or that the overlapping nature of regions of Hox influence in the worm are such that more than one Hox gene must be mutated before an effect may be seen.

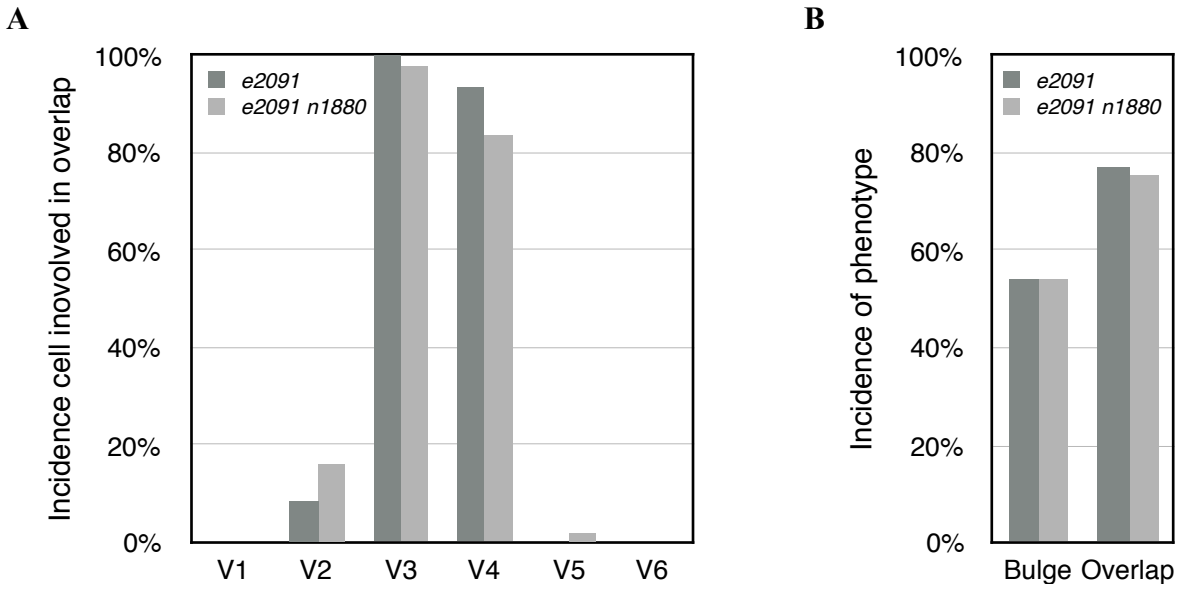

FIG. 3.2.6 – *LIN-39(N1880)* DOES NOT EFFECT THE INCIDENCE NOR IDENTITY OF SEAM CELLS INVOLVED IN THE *PAL-1(E2091)* OVERLAP DEFECT.

A. Graph showing the percentage involvement in the population of each V-lineage seam cell in the seam overlap phenotype of *pal-1(e2091)* in single and *pal-1(e2091) lin-39(n1880)* double mutants. There is no significant difference between the incidence of any cell involved in the overlap with the addition of *lin-39(n1880)* (Student's T-test, $46 \geq n \geq 49$ individual animals analysed per strain). *lin-39(n1880)* single mutants do not experience seam cell overlap (data not shown). **B.** Incidence of the mid-body bulge and seam cell overlap phenotypes in *pal-1(e2091)* and *pal-1(e2091) lin-39(n1880)* populations. There is no difference in the incidence of either phenotype between the two strains (Student's T-test, $54 \leq n \leq 105$ individuals per strain).

3.3 Discussion

pal-1 has an important and conserved role in specifying posterior body patterning and fate in *C. elegans*. Given that null alleles of *pal-1* are embryonic lethal due to a variety of failures of fate and patterning in the developing embryo (Edgar, Carr et al. 2001), a viable allele of *pal-1*, *e2091*, is likely to be useful in establishing and dissecting specific roles for *pal-1* during posterior development. The *pal-1(e2091)* mutant is striking in that its strong loss-of-function phenotype is a result of two single base changes in a non-coding region of the gene. Although it has been previously established in the field that the first introns of many *C. elegans* genes may contain regulatory information, the *e2091* mutant is even more noteworthy in that both of these point mutations are in the last (5th) intron of the gene. Alignments of this intronic sequence between different members of the *Caenorhabditis* genus show a remarkable degree of sequence conservation between species, which is likely to reflect the importance of the whole intron in regulating *pal-1* expression.

We have pin-pointed the cause of the *e2091* loss-of-function phenotypes to just one of the two *e2091* base pair changes, A2110G. Previous work in the laboratory has established that the *pal-1(e2091)* allele perturbs a seam-specific enhancer element, and that expression in the posterior seam cells from this enhancer is eliminated in the *e2091* mutant (C. Brabin, D. Phil. thesis, 2011). Taken together, we can assume that the A2110G locus of the *pal-1* gene encodes an enhancer element required for complete *pal-1* function.

Despite the observed change in expression at L1 caused by *e2091*, the majority of phenotypes observed in a *pal-1(e2091)* mutant animal are apparent by late embryogenesis. These include a mis-patterning of the epidermal seam cells, so that they no longer lie end to end down the lateral side of the animal but instead exhibit an overlapped, or bunched up, arrangement in the region of

the V3 seam cell. Interestingly, *pal-1* null animals experience seam cell migration defects during embryogenesis, resulting in bunching of cells around the V4 cell (Edgar, Carr et al. 2001). In the same region of the worm there is also a highly penetrant 'bulge' phenotype upon hatching. This would indicate that defects in epidermal and body patterning in the mid-body of the worm are due to defects in *pal-1* expression earlier than the mis-expression observed during L1. In an attempt to characterise changes in the embryonic expression of *pal-1(e2091)* compared to wild-type, I have separately integrated two extrachromosomal arrays of the wild-type and A2110G mutant *pal-1::gfp* expression vector using gamma irradiation. After outcrossing, this should allow for non-mosaic analysis of each reporter and allow the expression pattern of each reporter to be lineaged from early embryogenesis. Although extensive analysis of *pal-1* expression has been carried out previously (Edgar, Carr et al. 2001), the reporter used did not contain the last intron of *pal-1*; it was remarked even during this study that it was suspected that not all expression data was contained in their reporter. Comparing this expression to a lineage analysis of the *pal-1(e2091)* mutant is likely to provide considerable information on the exact requirement of *pal-1* expression from the A2110G enhancer element.

Wnt control of *pal-1* expression

We have identified the Wnt pathway as being a likely candidate for activation of *pal-1* through the intronic enhancer element. This is due to transcription factor target site prediction of a Tcf binding site at the A2110G locus. In order to investigate this further, we looked at an upstream temperature sensitive component of the Wnt pathway, *wrm-1,* for which we found a novel overlapping seam cell phenotype in hatched worms grown at restrictive temperatures. This *wrm-1* phenotype is very similar to the bulge and seam cell overlap seen in *pal-1* mutants, but involves different seam cell identities, and therefore may regulate seam cell morphology more generally than *pal-1* alone. However, this does not rule out that Wnt may control *pal-1*

expression in mid-body seam cells to specify the positions of these cells specifically, with a separate mechanism by which to regulate other seam cell positioning. By crossing the *wrm-1* mutation into the integrated *pal-1::gfp* marker strain after expression analysis during embryogenesis, we should be able to look for *pal-1::gfp* mis-expression to support this hypothesis. A double mutant of *pal-1(e2091)* and *wrm-1(ne1982)ts* would also be informative; unfortunately, they lie approximately 1cM apart from each other on LGIII. Although it is usually possible to select for homozygous *pal-1(e2091)* alleles using the L1 bulge phenotype, I have discovered that this phenotype disappears at 15ºC, the temperature at which the *wrm-1(ne1982)ts* allele must be maintained to produce viable homozygous offspring. However, additional appropriate genetic markers should make this cross feasible given more time.

pop-1 is the sole Tcf homologue in *C. elegans*. In this investigation we have used a temperature-sensitive *wrm-1* to explore the possibility of an interaction of the Wnt pathway with *pal-1* because knocking out *pop-1* completely results in total embryonic lethality, due to the essential role of *pop-1* in the early embryo (Lin, Hill et al. 1998). Although this is also the case for *wrm-1*, the temperature-sensitive nature of the available allele allowed for the temporal control of *wrm-1* knockdown during development, allowing later effects of *wrm-1* loss-of-function to be analysed. However, a viable allele of *pop-1* has been isolated, *hu9*, that encodes a missense mutation at the *pop-1*-β-catenin interface which is able to suppress constitutively active *bar-1* (Korswagen, Coudreuse et al. 2002). Although embryonic divisions are relatively normal in these mutant animals, *hu9* does result in abnormal migration of Q neuroblast progeny (Korswagen, Coudreuse et al. 2002) and is able to suppress *pry-1* knockdown effects (*pry-1* is a negative regulator of the Wnt pathway) (Gleason, Korswagen et al. 2002, Korswagen, Coudreuse et al. 2002). As the sole *pop-1* allele to be homozygous viable, it may be worthwhile to look for evidence of *pal-1(e2091)* phenotypes in this strain. However, given that *pop-1* activation has not been shown to require

bar-1-dependent Wnt signalling in the seam, a negative result may not necessarily mean that *pop-1* is not an activator of *pal-1* expression via the enhancer in the last intron.

Although genetic techniques can determine whether Wnt is indeed upstream of *pal-1*, evidence for a direct interaction between POP-1 and the A2110G locus of *pal-1* is still required. In order to address this, we wished to conduct a non-biased yeast one-hybrid interaction screen to detect factors that bound to this region of *pal-1*. However, for reasons described in the results section of this chapter, this proved unsuccessful. An alternative technique for assessing POP-1 binding to the *pal-1* enhancer would be to perform an electrophoretic mobility shift assay (EMSA). Given the short-term nature of GFP expression from the *pal-1* intron during L1, the expression of *pal-1* from the intronic enhancer may be equally as transient during embryogenesis. The binding of POP-1 to the enhancer may therefore be either too sensitive to detect in an EMSA or require additional co-factors.

The Wnt pathway has been shown to directly control *caudal* expression in other organisms, including insects (Oberhofer, Grossmann et al. 2014), mammals (Ikeya and Takada 2001, Prinos, Joseph et al. 2001, Nordstrom, Maier et al. 2006, Pilon, Oh et al. 2006, Lengerke, Schmitt et al. 2008, Sanchez-Ferras, Coutaud et al. 2012, Zhao, Gan et al. 2014), zebrafish (Shimizu, Bae et al. 2005, Ro and Dawid 2011), and *Xenopus laevis* (Haremaki, Tanaka et al. 2003). In the mouse and chick, it has also been shown that Cdx genes can act upstream of Wnt signalling (Ehrman and Yutzey 2001, van de Ven, Bialecka et al. 2011), and in the mouse it has been shown that Cdx and Wnt pathways may act in a regulatory loop, with evidence of direct protein-protein interactions between Tcf and Cdx on promoter sequences (Beland, Pilon et al. 2004). Although a direct regulatory interaction placing *caudal* upstream of Wnt has been proposed in *Drosophila* (Wu and Lengyel 1998), only hints of this interaction have been found since (Buchon, Osman et

al. 2013). In *C. elegans* it has been found that in some incidences of either Wnt or *pal-1*/*caudal* loss-of-function, the other pathway may act as a suppressor in the activation of transcriptional targets (Hunter, Harris et al. 1999, Maduro, Kasmir et al. 2005). However, there has been no evidence of a direct regulatory interaction between Wnt and *pal-1* in *C. elegans* prior to this investigation, although a suppressor screen for *e2091* did isolate a normally inhibited Wnt-dependent re-activation of *pal-1* expression in V6, whilst leaving the *e2091* point mutations in place (Zhang and Emmons 2000).

pal-1(e2091) mid-body phenotypes are not suppressed by *sop-1*

It has been found previously that post-embryonic expression of *pal-1* in V6, lost in the *e2091* mutant, is restored by a mutation in the suppressor *sop-1* which leads to the activation of a secondary Wnt-dependent pathway (Zhang and Emmons 2000). As this leaves the *e2091* point mutations in place, this secondary pathway of activation is independent of the wild-type regulatory mechanism, dependent on the enhancer present in the last intron of *pal-1*. We found that this re-activation of *pal-1* by the suppressor *sop-1* was insufficient to rescue the mid-body phenotypes of *pal-1(e2091)*, suggesting that this second, usually repressed, activation by Wnt is insufficient to recapitulate wild-type *pal-1* expression.

The role of Hox genes in *pal-1(e2091)* phenotypes

An initial hypothesis at the start of this investigation was that the mid-body patterning defect of the *pal-1(e2091)* mutant was dependent on the mid-body Hox gene, *lin-39*. However, there was no change in *pal-1(e2091)* phenotypes in the *pal-1(e2091) lin-39 (n1880)* double mutant. Although this alone does not rule out *pal-1* being upstream of *lin-39* in the regulation of body patterning, *pal-1(e2091)*-like phenotypes have never been observed in *lin-39* single mutants, and

developmental control by this Hox gene appears to commence only during larval development. It is therefore unlikely that embryonic phenotypes of *pal-1(e2091)* are due to mis-regulation of *lin-39*.

Nevertheless, control of Hox gene expression during embryogenesis by *caudal* homologues has previously been shown to be critical for *caudal*-dependent posterior patterning in vertebrates (Subramanian, Meyer et al. 1995, Charite, de Graaff et al. 1998, Isaacs, Pownall et al. 1998, Ehrman and Yutzey 2001, Bel-Vialar, Itasaki et al. 2002, van den Akker, Forlani et al. 2002, Tabaries, Lapointe et al. 2005). Control of Hox gene expression by *pal-1* has also been shown in *C. elegans*, with post-embryonic mis-expression of *mab-5* and *egl-5* previously having been observed in *pal-1(e2091)* mutants (Waring and Kenyon 1990, Cowing and Kenyon 1992, Austin and Kenyon 1994, Salser and Kenyon 1996, Ferreira, Zhang et al. 1999, Hunter, Harris et al. 1999). Intriguingly, evidence for direct protein-protein interactions between mammalian caudal homologues and specific Hox proteins has been shown, suggesting that the regulation of development by *caudal* and Hox genes may not be as linear as previously thought (Lafontaine, Grainger et al. 2012). It would be interesting to explore this potential regulatory protein-protein interaction between embryonically-expressed Hox gene products and PAL-1 in worms.

pal-1(e2091) patterning phenotypes

It is interesting to observe that the 100% penetrant disorganised Nob phenotype of *pal-1* null animals extends from the posterior end of the pharynx to the tail tip (Edgar, Carr et al. 2001), whereas the embryonic patterning defects of *pal-1(e2091)* are confined to the mid-region of the body, posterior to the pharynx but anterior of the tail region. Since this indicates full native expression of *pal-1* is necessary to specify correct posterior patterning of all tissues from the pharynx downwards, the *e2091* enhancer mutation may be sufficient to change only *pal-1*

expression in the mid-region of the embryo, leaving the more posterior expression intact and functional. This would cause this mid-region alone to be disorganised, as it is posterior to the pharynx and presumably requires *pal-1* for proper patterning. This may result in a 'truncated Nob' phenotype such that the very posterior is normal, due to normal *pal-1* function, but the mid-region of the worm displays patterning defects.

The bulge phenotype of *pal-1(e2091)* animals may arise independently of the seam cell patterning defect, or it may be a direct cause of the seam cell overlap. Tension induced by the remodelling of the seam cells into longitudinal brick-shaped cells lined up end-to-end along the lateral hypodermis is a key driver of embryonic elongation. By shortening the final length of the seam line with cells lying on top of one another rather than end-to-end, the *e2091* mutation may lead to a failure in complete morphogenesis during elongation in this region of the animal. It is interesting to note that *pal-1(e2091)* L1s are generally shorter than their wild-type counterparts (see Fig. 3.2.1 for an example), although this has not been quantified. Previous quantification of the number of nuclei in the hypodermis of the animal has concluded that the bulge is due to an abnormal distribution of tissue, rather than extra cell divisions (C. Brabin, D. Phil. thesis, 2011).

CHAPTER 4

pal-1 regulates the polarity of dorsoventral cell movement during the asymmetric L1 seam cell division

4.1 Introduction

pal-1 has been widely studied during embryogenesis for its role in posterior development (Hunter and Kenyon 1996, Ahringer 1997, Edgar, Carr et al. 2001, Baugh, Hill et al. 2005, Maduro, Kasmir et al. 2005, Maurer, Chiorazzi et al. 2007, Lei, Liu et al. 2009). It has also been noted that in males, post-embryonic *pal-1* expression in V6 is necessary for the specification of the correct ray lineage (Hunter, Harris et al. 1999, Zhang and Emmons 2000). Until now, however, larval expression in other cells has not been detected nor a phenotype ascribed other than those which originate in embryogenesis (the mid-body bulge and seam cell overlap). Given that we have shown the last intron of *pal-1* to contain enhancers which promote seam, muscle

and neuronal expression in the larval stages of both sexes (C. Brabin, D. Phil thesis, 2011), it is interesting to ask what the non-sex specific roles of *pal-1* might entail post-embryonically. Here I have characterised a novel aberrant seam cell movement phenotype of *pal-1(e2091)* mutants out of the lateral seam cell line during the L1 seam cell division. Perhaps the most interesting aspect of this particular *pal-1(e2091)* phenotype is the insight it has given into a mechanism of directed cell movement engaged during the L1 division and not in later, apparently equivalent, asymmetrical larval seam cell divisions. The L1 division is notoriously robust in circumstances in which all later asymmetrical seam cell divisions are subject to perturbation, such as in Wnt or Runx mutant backgrounds, suggesting that this division experiences different control mechanisms to later divisions. The results presented here suggest that aspects of the L1 division are indeed unique in the seam cell post-embryonic lineage.

4.2 Results

pal-1(e2091) adults exhibit branched alae corresponding to the underlying position of the fused seam

By adulthood in wild-type animals, the seam has reached terminal differentiation: the seam cells are fused to form a single syncytium which secretes a line of three cuticular ridges collectively known as alae. During my observations of *pal-1(e2091)* animals, however, I noticed that a small but significant number (4%, n = 188) of adult *pal-1(e2091)* animals have alae which branch abnormally from the expected lateral position along the dorsoventral axis (Fig. 4.2.1). These animals were predominantly those which had retained the mid-body bulge phenotype perturbed at hatching. Since the terminally differentiated seam secretes the alae, the abnormal shape in these animals suggested that perhaps the underlying seam was also correspondingly shaped. By crossing in *heIs63*, an integrated array of the seam cell markers *wrt-2p*::GFP::PH and *wrt-2p*::GFP::H2B, a gift of Marjolein Wildwater during her time in Sander van den Heuvel's laboratory, the membrane of the seam syncytium could be visualised. In *e2091* animals the seam syncytium was indeed branched, following the pattern of the abnormal alae in all animals observed (n = 9). It was also noted that the ectopic branch of the alae and seam in all cases extends from the mid-body region of the syncytium, and follows a ventral trajectory down to the ventral midline.

Given the embryonic nature of all other hermaphrodite *pal-1(e2091)* defects (the mid-body bulge and seam cell overlap), this branched alae and seam syncytium phenotype appeared unexpectedly late in the development of the worm. This indicates either that the defects in patterning during embryogenesis have unexpected consequences during later development, or that *pal-1* has a previously undiscovered role in post-embryonic development.

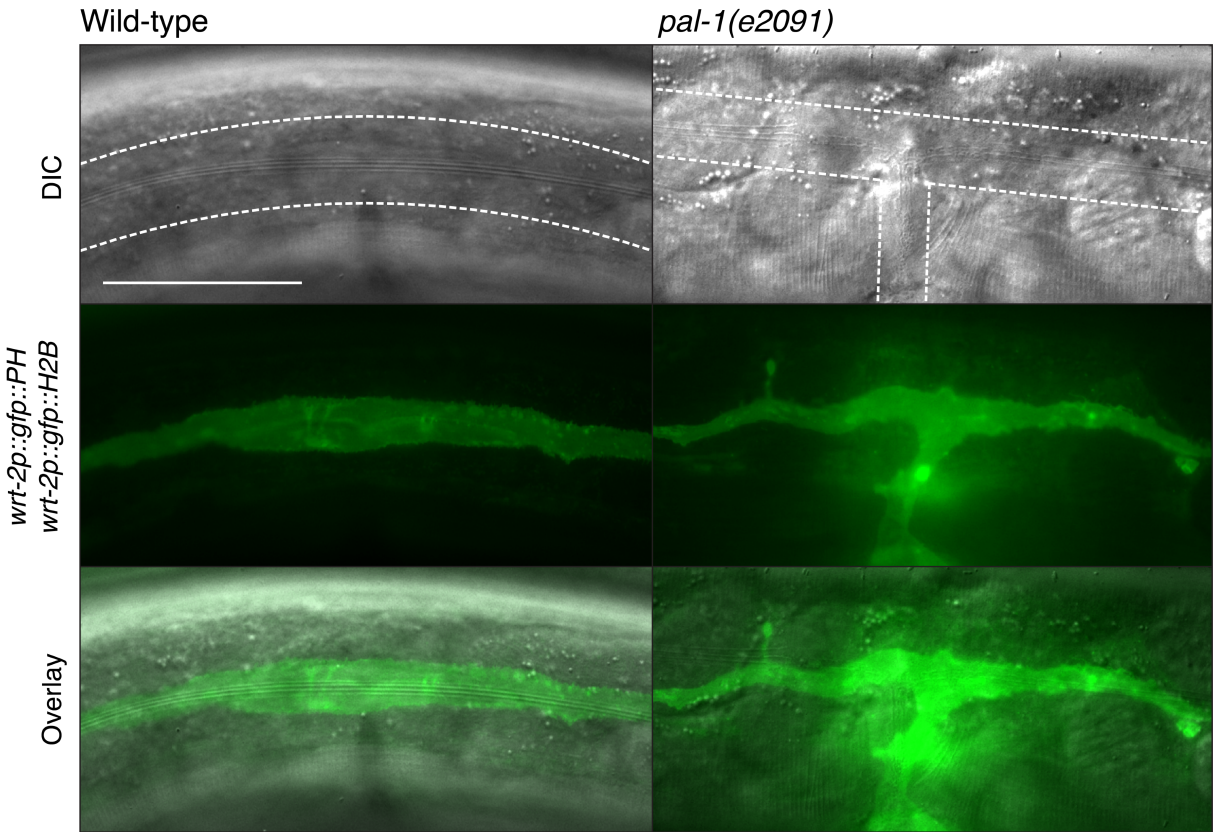

FIG. 4.2.1 – *PAL-1(E2091)* ADULT HERMAPHRODITES HAVE T-SHAPED ALAE CORRESPONDING TO THE SHAPE OF THE UNDERLYING SEAM SYNCYTIUM.
Wild-type alae run in a continuous straight line down the lateral side of the animal whereas *pal-1(e2091)* animals sometimes exhibit a branched alae patten, always to the ventral midline as shown here (DIC). The integrated GFP reporter *heIs63* shows that the underlying seam syncytium in the wild-type animal runs beneath the alae in a straight lateral anteroposterior line. *pal-1(e2091)* animals, in contrast, have a seam which is branched underneath the branched the alae. The dorsoventral extension of the seam is invariably in the mid-body region and extends from the main seam line ventrally. Scale bar = 50 μm.

Ventral projections of the seam originate at L1

Since by adulthood the dramatic morphological difference in seam shape could already be detected, I followed the phenotype backwards in development by looking at earlier stage larvae in an attempt to pinpoint the source of the branching, which is clearly not present in the 3-fold embryo (Fig. 3.2.1). In *e2091* animals, I found that as early as L1 a proportion of animals exhibit an extension of a mid-body seam cell (or occasionally two neighbouring cells) ventrally (Fig. 4.2.2 A). Quantifying the incidences of these misshapen seam cells at each stage of larval seam cell development reveals a striking observation: although upon hatching the seam cells in this respect look normal, after the first L1 division, almost 70% of *e2091* animals show some level of seam branching towards the ventral midline (Fig. 4.2.2 C). This percentage decreases as the animals progress through the larval stages, suggesting that the larvae containing the abnormality either die, or the seam cells are able to recover from their abnormal position. This could occur if the affected cell or daughter of the original posterior cell inherits both the abnormal positioning and a normal hypodermal cell fate and fuses to the hyp7 syncytium. It is interesting to note that no animals at any stage show branching of the seam cells in the dorsal direction. Branching is also confined to the mid-body region, as with the bulge and overlapping seam cell phenotypes already observed in *e2091* mutants.

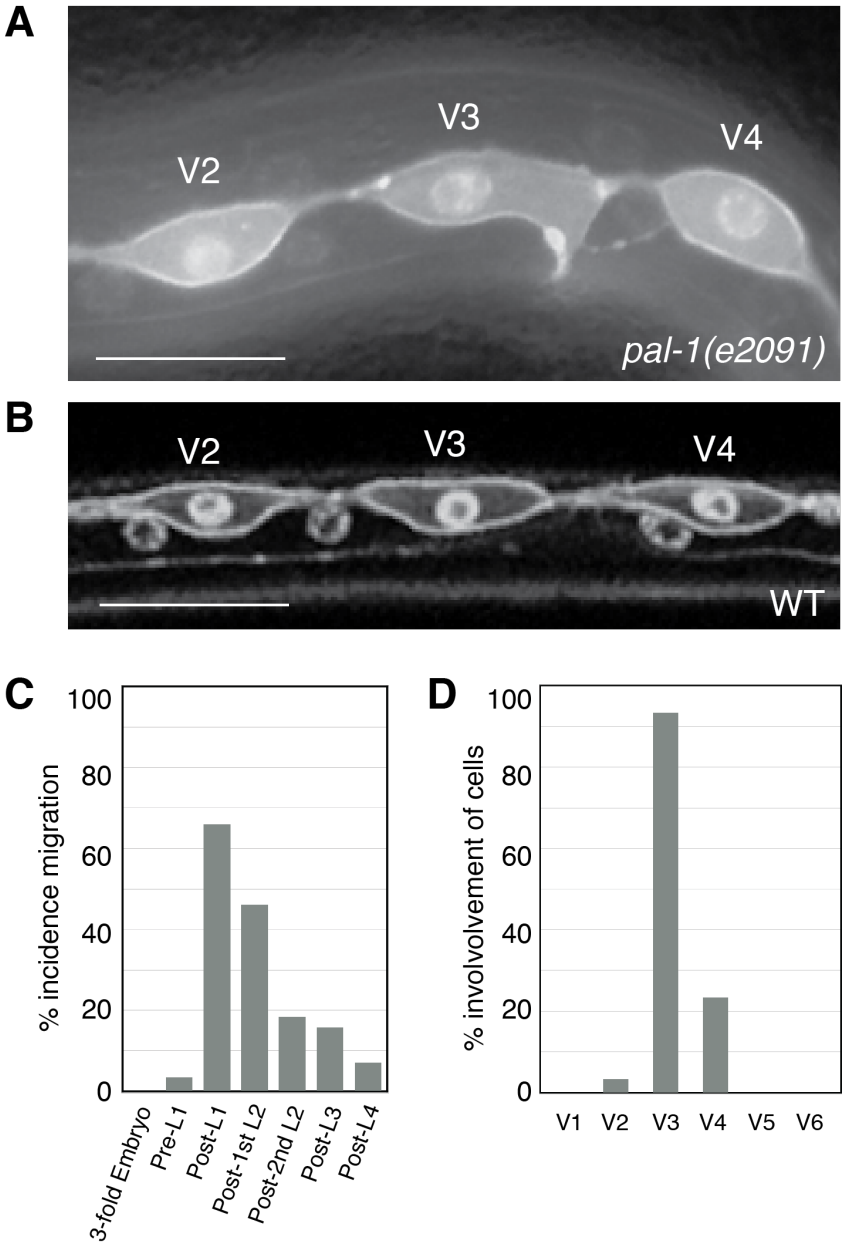

FIG. 4.2.2 – THE *PAL-1(E2091)* BRANCHING PHENOTYPE ORIGINATES AT THE L1 SEAM CELL DIVISION.

A. A late L1 *pal-1(e2091)* animal displaying the branched phenotype of the seam towards the ventral midline (*c.f.* wild-type animal at the same stage shown in **B**). Scale bars = 10 μm. **C.** Quantification of the seam cell branched phenotype at each stage of seam development (post-L1 refers to post the L1 seam cell division) reveals that the phenotype originates during the L1 seam cell division. For each stage, $59 \leq n \leq 239$. **D.** For the animals that displayed a seam movement down to the ventral midline, the identity of the seam cell involved was recorded. The results show the percentage involvement of each cell in the V lineages (no other seam cell lineage showed movement ventrally in these strains, data not shown). V3 was the most likely cell to move ventrally, occasionally with V4 or V2, or these other cells alone.

The *e2091* aberrant seam cell movement is rescued by *pal-1::gfp*

To ensure that the branching of the seam cells at L1 is due to the *e2091* allele of *pal-1* and not a background mutation, the *pal-1::gfp* construct, which is able to rescue the embryonic bulge and seam cell overlap phenotypes of *pal-1(e2091)*, was tested for rescue of this novel aberrant seam branching phenotype. Worms were spot bleached for synchronisation and inspected after the L1 seam cell division, as this stage has the highest proportion of animals exhibiting the *e2091* seam cell branching phenotype. The wild-type version of the *pal-1::gfp* construct was able to completely rescue the *pal-1(e2091)* branched seam phenotype, whereas the version carrying the 5' mutation of the *e2091* intron, *pal-1(A2110G)::gfp*, was not able to rescue (Fig. 4.2.3). This indicates that the phenotype is not due to a non *pal-1* mutation, or the second site mutation in the *pal-1* intron, but the same site which has been shown to cause the bulge and seam overlap phenotypes during embryogenesis.

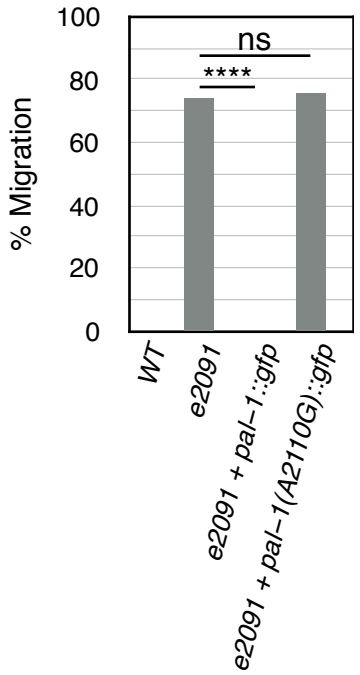

FIG. 4.2.3 – *PAL-1::GFP* RESCUES THE *e2091* BRANCHED SEAM PHENOTYPE.
The branched seam phenotype was scored after the L1 seam cell division in *pal-1(e2091)* and *pal-1(e2091)* worms carrying the reporters *pal-1::gfp* or *pal-1(A2110G)::gfp*. The wild-type genomic *pal-1::gfp* construct shows complete rescue of the L1 branched seam phenotype, whereas the reporter carrying the 5' mutation from *e2091* (A2110G) in the last intron of *pal-1* is unable to rescue. $50 \leq n \leq 171$ per strain, Student's T-test P**** < 0.00001.

The *e2091* L1 asymmetric seam division: L1 is unique within wild-type divisions

That the first larval seam cell division is perturbed in *pal-1(e2091)* mutants is intriguing: the L1 division is notoriously robust even in genetic conditions where any other division may be affected (Nimmo, Antebi et al. 2005, Hajduskova, Jindra et al. 2009, Huang, Tian et al. 2009, Gleason and Eisenmann 2010, Brabin, Appleford et al. 2011, Yamamoto, Takeshita et al. 2011, Hughes, Brabin et al. 2013). It has been a challenge, therefore, to find out what is so different about a division that in all other respects looks exactly like the later asymmetric L2, L3 and L4 divisions of the V lineage seam cells. Before investigating the L1 division of *pal-1(e2091)* animals for the origins of the abnormal seam cell branching, it was first necessary to look in wild-type animals carrying the seam cell marker for any mechanism of normal seam lineage movement that might be perturbed in *e2091* animals. Viewed in the light of the *pal-1(e2091)* data, the wild-type observations for this L1 asymmetric division described below are in themselves significant, because this division has not been properly studied before.

Seam cells in the newly hatched worm have anteriorly-polarised attachments to the ventral midline not present at any other stage of seam cell development

During the larval stages, seam cells are classically thought to be ‘eye-shaped’, with the anterior and posterior points of each cell contacting adjacent seam cells. Each seam cell divides and, in most cases, the anterior daughter cell rounds up - differentiating into a hypodermal cell - and moves out of the seam line before fusing to the underlying hyp7 syncytium. The remaining posterior daughter retains the seam fate and elongates along the anteroposterior axis until it makes contact with the neighbouring seam cells: a cycle of asymmetric division is complete (see Fig. 1.5.1).

Whilst imaging newly hatched wild-type worms with *heIs63*, a seam cell marker relatively recently introduced to the seam cell field that contains an integrated array of *wrt-2* promotor-driven histone (*gfp::H2B*) and membrane associated GFP (*gfp::PH*) (Wildwater, Sander et al. 2011), we were excited to observe something previously overlooked: the posterior (V2-T) L1 seam cells are not truly 'eye-shaped'. Instead they possess one anterior projection per cell down to the ventral midline, positioned between the ventrally positioned P cells (Fig. 3.2.4, first panel). These projections meet up with those from the opposing line of seam cells on the other side of the animal. As the seam cells start their L1 asymmetrical division, the projections widen (see Fig. 4.2.4). Due to their anterior position on the seam cells, these widening projections are inherited by the anterior seam cell daughter which will differentiate into the hypodermal fate. The projection, being tethered to the ventral midline, ensures that the hypodermal daughter moves ventrally rather than dorsally after the L1 division, as the underlying P cells migrate and collapse down to the ventral midline, thereby giving up their role as transient, but essential, constituents of the ventral hypodermis. The anterior daughters of the posterior seam cells take the place of the P cells to complete, for the first time in the development of the animal, the hyp7 syncytium. Later seam cells were never observed to display anterior protrusions, either ventrally or dorsally.

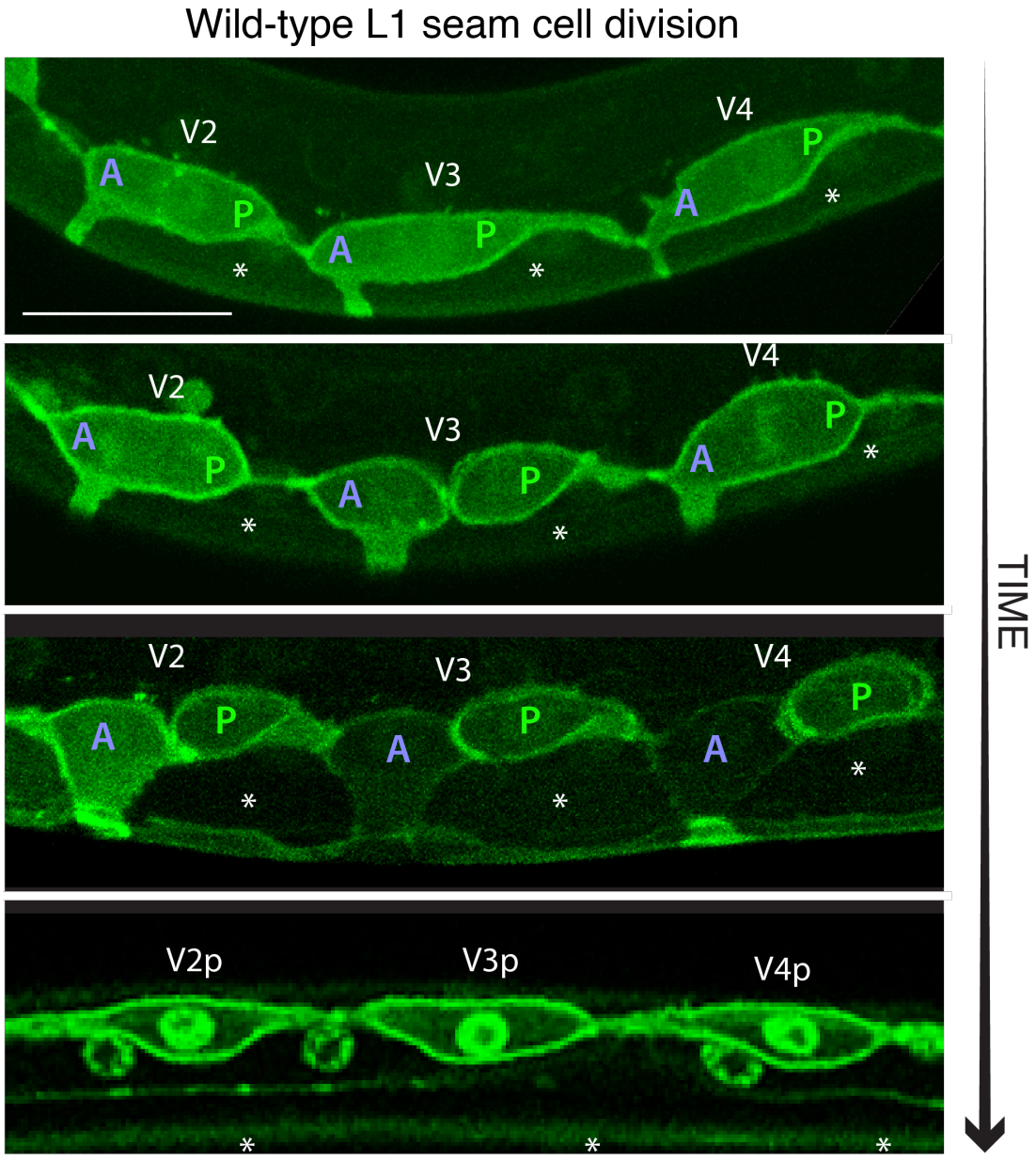

FIG. 4.2.4 – WILD-TYPE L1 SEAM CELL DIVISION VISUALISED WITH *helS63*.
The wild-type seam cell division is visualised here over time. In the newly hatched animal, seam cells V2-T possess projections down to the ventral midline, where they meet with projections from seam cells on the opposite side of the animal. Invariably, these projections extend from the anterior end of the seam cell. As the L1 seam cell divides the projection widens and is inherited by the anterior daughter of the division. Typically, the anterior daughter differentiates to a hypodermal fate, fusing to the hyp7 syncytium. This L1 projection, therefore, ensures that this anterior daughter cell invariably contributes to the ventral hypodermis, rather than interchangeably to either dorsal or ventral sides as observed after divisions later in the seam lineage. P cells are indicated with asterisks. Scale bar = 10μm.

Projections of L1 seam cells to the ventral midline express the apical junction marker *ajm-1::gfp*

The GFP reporter used in the previous figure (Fig. 4.2.4) is a relatively new seam cell marker, with limited previous characterisation of its expression. We therefore used the apical junction reporter, *ajm-1::gfp* to establish whether these protrusions from the seam cells observed at L1 contain members of the apical junction protein complex, that serves as a tight junction complex in *C. elegans*. We found this to be the case (Fig. 4.2.5).

Projections are only present on posterior L1 seam cells and meet at the ventral midline

It is only the posterior seam cells, V2-T, which exhibit an anterior projection to the ventral midline (Fig. 4.2.6). V1 possesses a posterior projection, and this does not appear to behave through the L1 division as the other, anterior projections do on the more posterior seam cells (not shown). Projections from the seam cells meet the ventral midline at the same point as the corresponding seam cell from the opposite side of the animal, therefore providing a point in post-embryonic development when these cells contact each other directly (inset, Fig. 4.2.6).

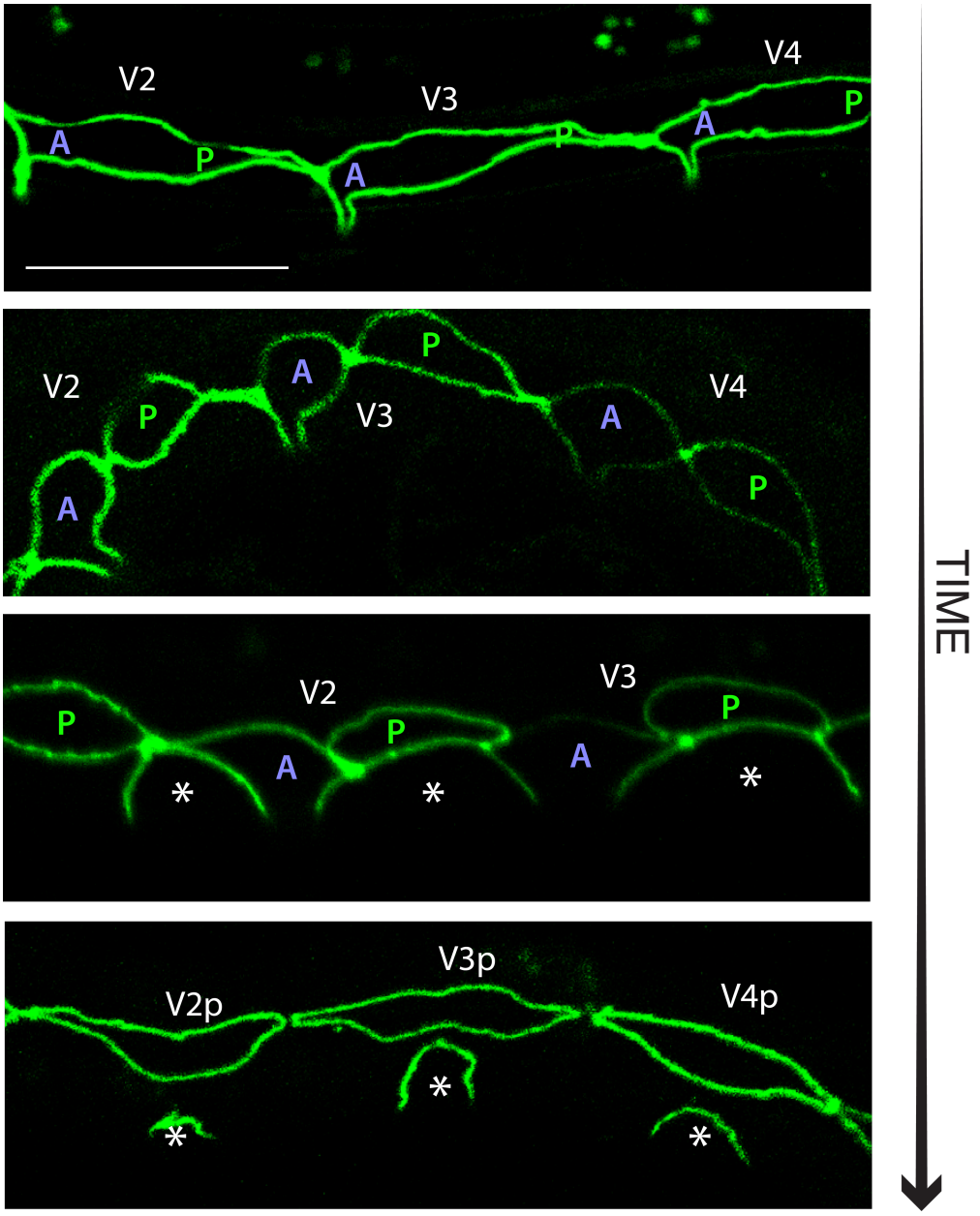

FIG. 4.2.5 – L1 PROTRUSIONS FROM SEAM CELLS EXPRESS *AJM-1::GFP*.
The apical junction marker *ajm-1::gfp* is expressed throughout the L1 seam cell division in seam cells and P cells (P cells marked with an asterisk). Importantly, the anteriorally-placed projections from the seam cells are *ajm-1::gfp*-positive, and this continues as they widen and remodel throughout the seam cell division. Scale bar = 10 μm.

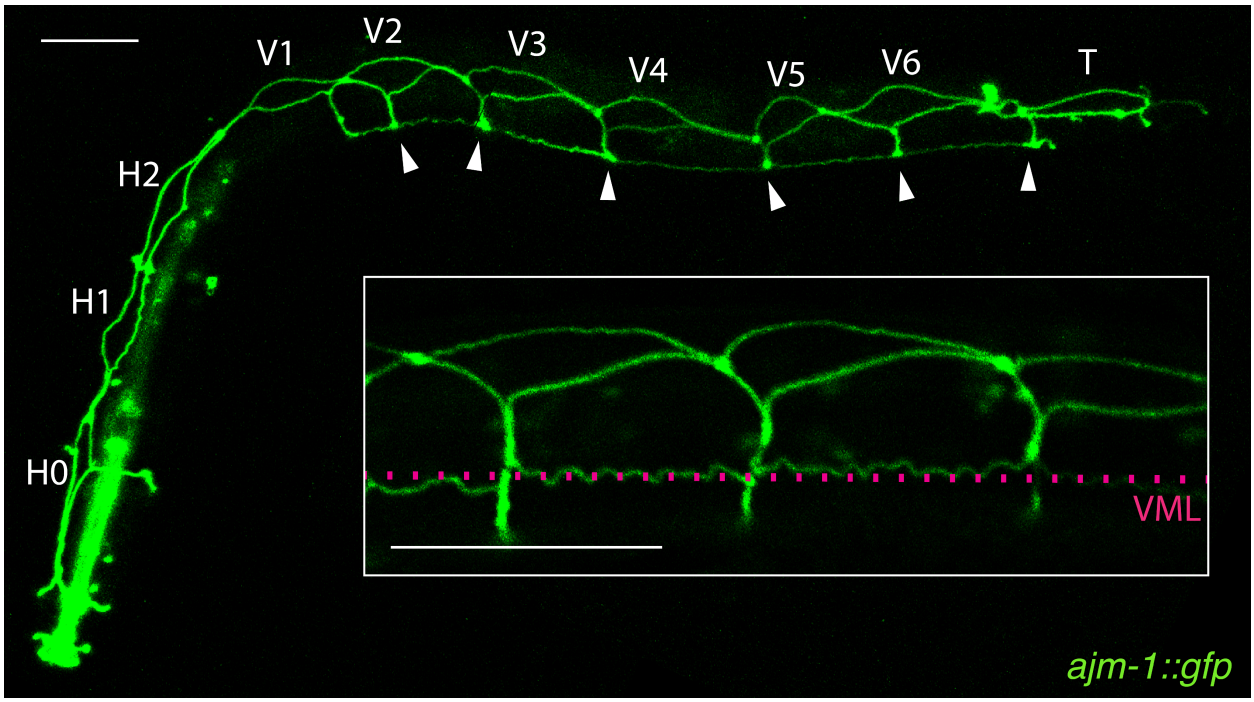

FIG. 4.2.6 – SEAM CELLS IN AN L1 ANIMAL BEFORE THE L1 SEAM CELL DIVISION VISUALISED WITH *AJM-1::GFP*.
Anterior projections from the early L1 seam cells are only present on the posterior seam cells, V2-T. These projections meet the ventral midline (arrowheads) where they meet the projection from the corresponding opposite seam line (inset shows a lateral-ventral view, with the ventral midline (VML) indicated with a dotted line). Scale bars = 10 μm.

Ventral projections of the mid-body L1 seam cells are posterior in *pal-1(e2091)* animals

After studying the wild-type L1 seam cell division, it became apparent that this process of anterior projection formation on each seam cell was perturbed in *pal-1(e2091)* mutants. By imaging the seam cells at hatching we could observe projections down to the ventral midline that were incorrectly positioned at the posterior, not anterior, of the seam cell (see Fig. 4.2.7, first panel). Following the consequence of this mis-positioning through the L1 seam division, we observed that the posteriorly-positioned projection behaved as in wild-type, widening throughout the division, but was inherited by the posterior, seam-fated daughter rather than the anterior, hypodermally-fated daughter. Although the anterior daughter fused to the hyp7 correctly and the posterior seam daughter retained the seam fate (these daughters went on to divide in later larval stages), the posterior daughter was now attached to the ventral midline through the presence of the initial projection. As the seam cell daughters extended to touch each other and reform the seam cell line, the seam cell remained attached to the ventral midline and caused a ventral branch in the final seam line. This, then, is the origin of the seam branching observed during later larval development.

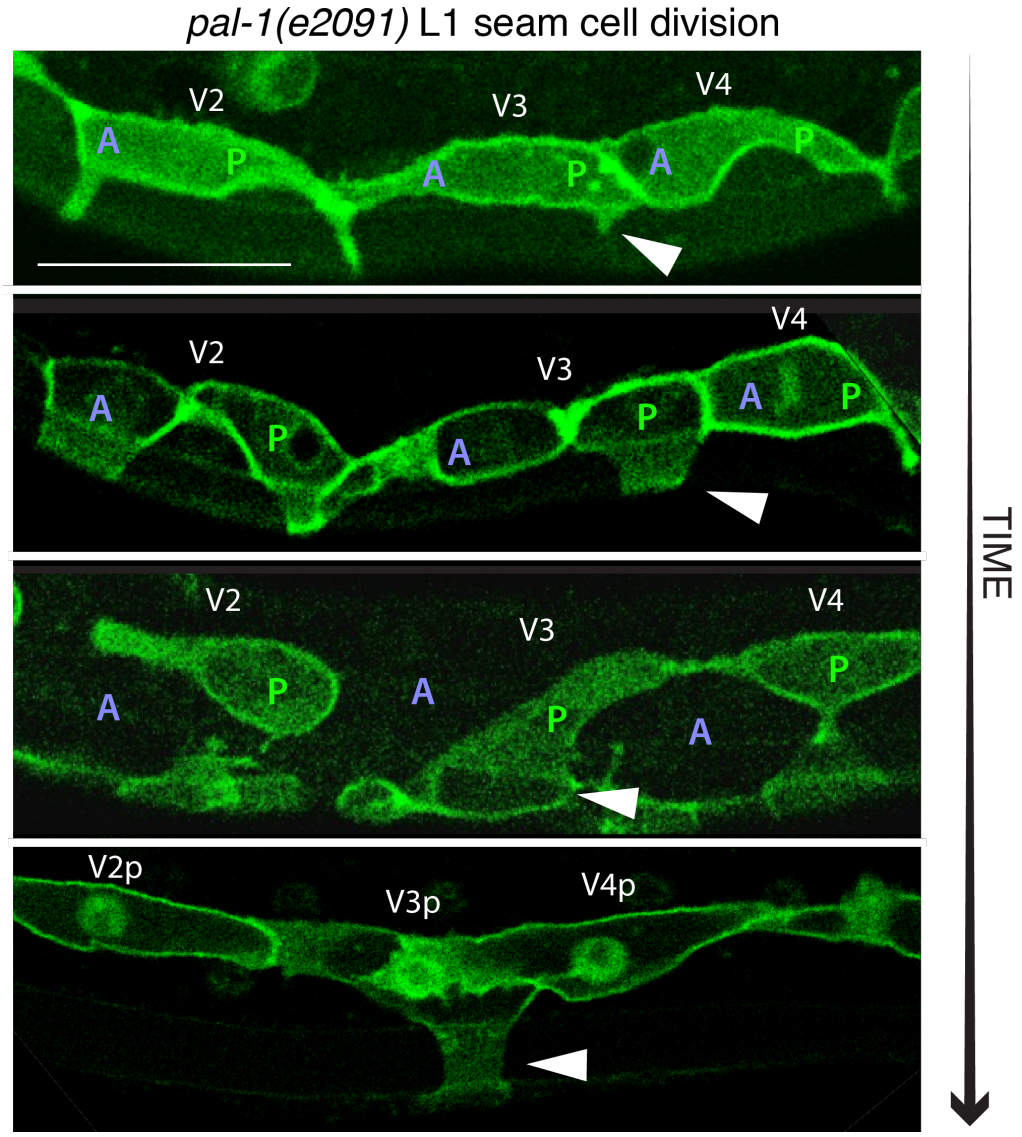

FIG. 4.2.7 – *PAL-1(E2091)* L1 SEAM CELL DIVISION VISUALISED WITH *HEIS63*.
At hatching, the L1 seam cell projections in *pal-1(e2091)* animals are incorrectly positioned at the posterior end of the cell (first panel, arrowhead). The projection is inherited by the posterior seam daughter of the L1 seam division, causing this daughter to move to the ventral midline (arrowheads). Although neither daughter cell fate is affected, the resulting seam line after the L1 division is branched in these animals. The second panel shows both daughter cells of V2 moving ventrally, indicating that this is not a binary switch where only one daughter cell may inherit the ventral projection. Scale bar = 10 μm.

Seam cells begin to develop projections after ventral enclosure

Using *ajm-1::gfp* to visualise the apical junctions in the *C. elegans* embryo, the shapes of the seam cells and the ventrally positioned P cells in the epidermis can be observed (Fig. 4.2.8). Even at this embryonic stage, evidence of an early projection on the posterior seam cells in wild-type embryos can be observed at the junctions between the ventrally lying P cells. This highlights a striking correlation between the positioning of apical junctions between neighbouring P cells relative to the position of the seam cells, which is always at the anterior end of the seam cells, and the position where an anterior projection on the seam cells will form and eventually widen as the adherens junctions presumably remodel, prior to anterior daughter movement.

Seam cell overlap in *pal-1(e2091)* perturbs relative positions of P cells and seam cells in the embryo

In the previous chapter, I described how seam cells are disorganised in the middle of the embryo, resulting in L1 hatchlings with an overlapping seam cell phenotype in the mid-body (Fig. 3.2.1). By imaging the 1.5-fold embryo with *ajm-1::gfp*, it is apparent that this seam disorganisation is evident even at this early stage (Fig. 4.2.9). As described in figure 4.2.8, in wild-type animals the P cells display a distinct organisation that results in the apical boundaries between the P cells being placed ventrally to, but at the anterior of, the seam cell above. However, the disorganisation of the seam in *pal-1(e2091)* animals means that this placement of P cell boundaries is now perturbed, and instead some seam cells are unable to form a ventral projection at the anterior of the cell. Instead, the cell finds another apical junction between the cells lying ventrally to itself and remodels itself through that pathway instead. This is often at the posterior of the seam cell, rather than the anterior, resulting in the phenotypes described in figure 4.2.7.

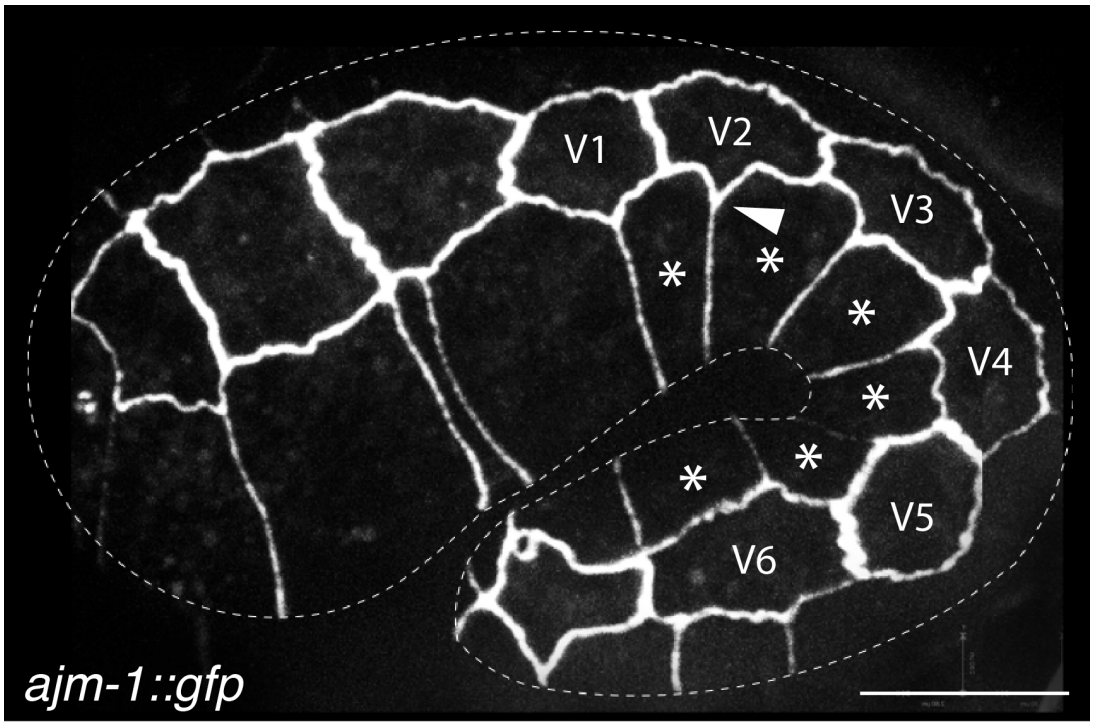

Fig. 4.2.8 – Projections on seam cells can be seen in the wild-type embryo after ventral intercalation.
1.5-fold wild-type embryo visualised using an integrated *ajm-1::gfp* marker for apical junction components in the epidermis. The dotted line shows the outline of the embryo. The posterior V-lineage seam cells are labelled and P cells are marked with asterisks. A seam cell projection forming at the junction between two P cells on V2 is indicated with an arrowhead, which is clearly polarised to the anterior of the seam cell. These anterior projections, always at the apical junction between the P cells, can also be observed for all seam cells posterior to V2, indicating that the position of the P cells relative to the seam cells in embryogenesis is integral to projection positioning on the seam cells. Scale bar = 10 μm.

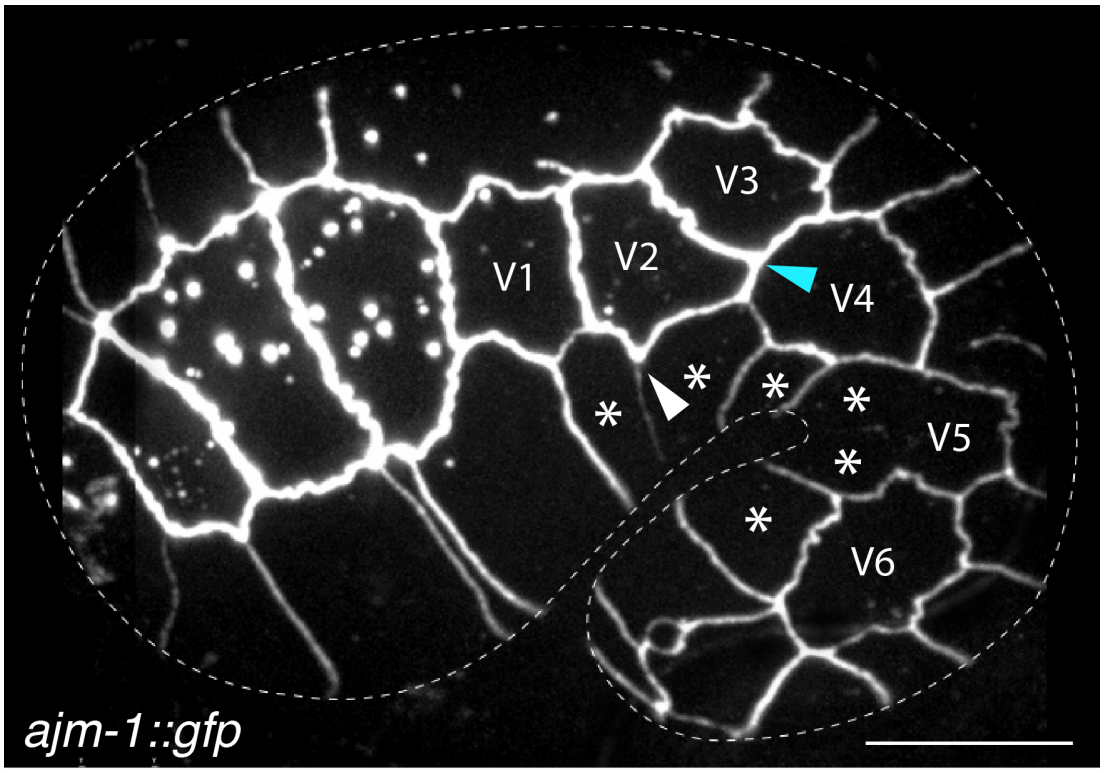

FIG. 4.2.9 – SEAM CELL OVERLAP IN *PAL-1(E2091)* MUTANTS CAUSES ABNORMALLY-POSITIONED POSTERIOR FORMATION OF PROJECTIONS.
pal-1(e2091) embryo at 1.5-fold imaged using *ajm-1::gfp*. V-lineage seam cells are labelled and P cells are marked with an asterisk. V2 exhibits a wild-type arrangement of P cells with respect to the seam cell, resulting a normal anteriorly-polarised ventral tab to form on V2 (white arrowhead). However, the abnormal arrangement of V3 with respect to the seam line means that the anterior of V3 can no longer make a projection through remodelling of an apical junction between P cells, as the P cells are no longer lying ventrally to V3. Instead evidence of a projection can be observed further to the posterior of V3 (blue arrowhead) and this is likely to account for the misplacement of projections at L1 to the posterior, rather than anterior, of the seam cell. Scale bar = 10 μm.

Laser ablation of the seam cells has no effect on P cell remodelling and migration

An interesting question raised by the abnormal effects of cell movement in *pal-1(e2091)* animals is whether the process of seam cell daughter movement is active, or a passive result of the simultaneous movement of the P cells to the ventral midline. To test this, we performed laser ablations on either the seam cells or P cells of a wild-type animal containing the *heIs63* reporter and a *dpy-7::mCherry* marker, before the L1 seam cell division (Fig. 4.2.10). Ablation of two adjacent seam cells had no effect on the migration of the underlying P cell (n=6 individuals) confirming that the process of P cell migration during L1 is an active process and does not rely on the seam cell division. However, ablation of two adjacent P cells resulted in the total displacement of the seam cell between them to the ventral midline, prior to division, although only one animal survived to be analysed.

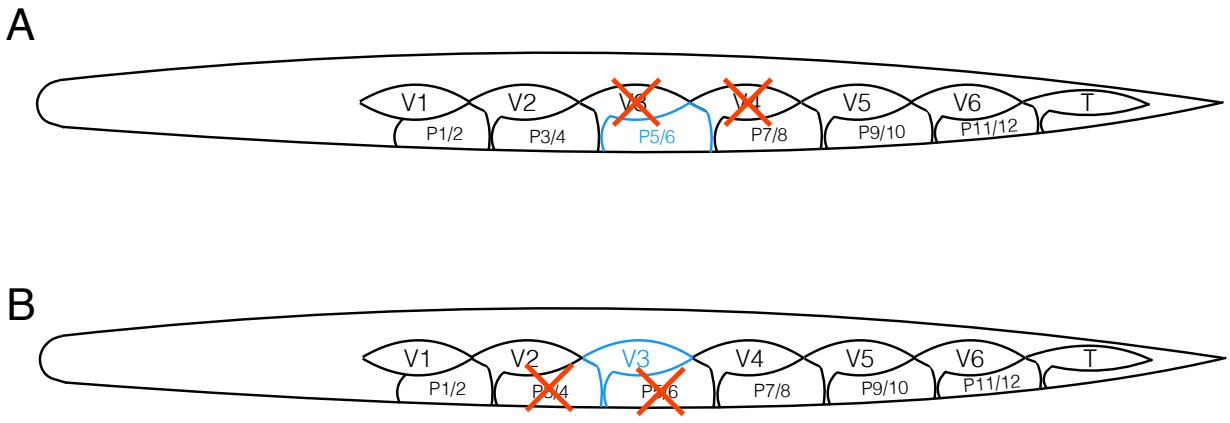

FIG. 4.2.10 – LASER ABLATION EXPERIMENTS ON WILD-TYPE SEAM AND P CELLS.
A. Adjacent seam cells V3 and V4 were ablated in the wild-type newly hatched animal bearing the *heIs63* seam cell marker. The P cells ventral to these cells (P5/6, shown in blue) was then observed for normal migratory behaviour down to the ventral midline. B. In a second experiment the adjacent P cells P3/4 and P5/6 were ablated and the seam cell between them (V3, shown in blue) observed for maintenance of correct seam cell positioning during L1.

Seam daughters of the symmetrical 'L1' seam division in *lin-14* loss-of-function mutants move ventrally

As stated previously, mutations affecting the L1 seam cell division are extremely rare. However, *lin-14* heterochronic mutants can either reiterate the L1 division (*lin-14* gain-of-function) or skip L1 entirely (*lin-14* loss-of-function): seam cells in the newly hatched animal immediately undergo the symmetrical L2 division, after which neither daughter would normally move to the ventral midline, followed by the asymmetric L2 division before the L1/L2 moult. It is this loss-of-function allele, *n179(ts)*, that I chose to investigate here; if all newly hatched seam cells possess a projection to the ventral midline, then by cultivating these worms at 25ºC, the restrictive temperature, and thus inducing a symmetrical seam-fated division at L1 (i.e. skipping the normal asymmetrical L1 division), one would expect some of these seam-fated anterior daughters to move ventrally to the midline. Of the 62 *lin-14(n179)ts* animals observed at the late L1 stage, 82% showed at least one seam branch to the ventral midline (Fig. 4.2.11 B). In some animals (not shown), so many cells moved to the ventral midline that the entire seam line was now ventral, and no longer lateral, in the posterior half of the worm.

Contrary to my expectations, I observed that in *lin-14(n179)ts* animals the seam cell daughters did not move ventrally immediately after the first symmetrical division and the P cells remained in place, comprising the ventral hypodermis (Fig. 4.2.12 A). It was only after the second, asymmetrical L1 division that the P cells migrated to the ventral midline and the seam cell projections widened to allow seam daughters to move ventrally (Fig. 4.2.12 B). In conclusion, therefore, the penetrant seam migration phenotype observed at the end of the L1 moult in *lin-14(n179)ts* animals must be due to the first seam cell division perturbing the original polarised position of the seam cell projections, causing the seam-fated daughters of the second, asymmetrical division to contribute to the abnormal phenotype.

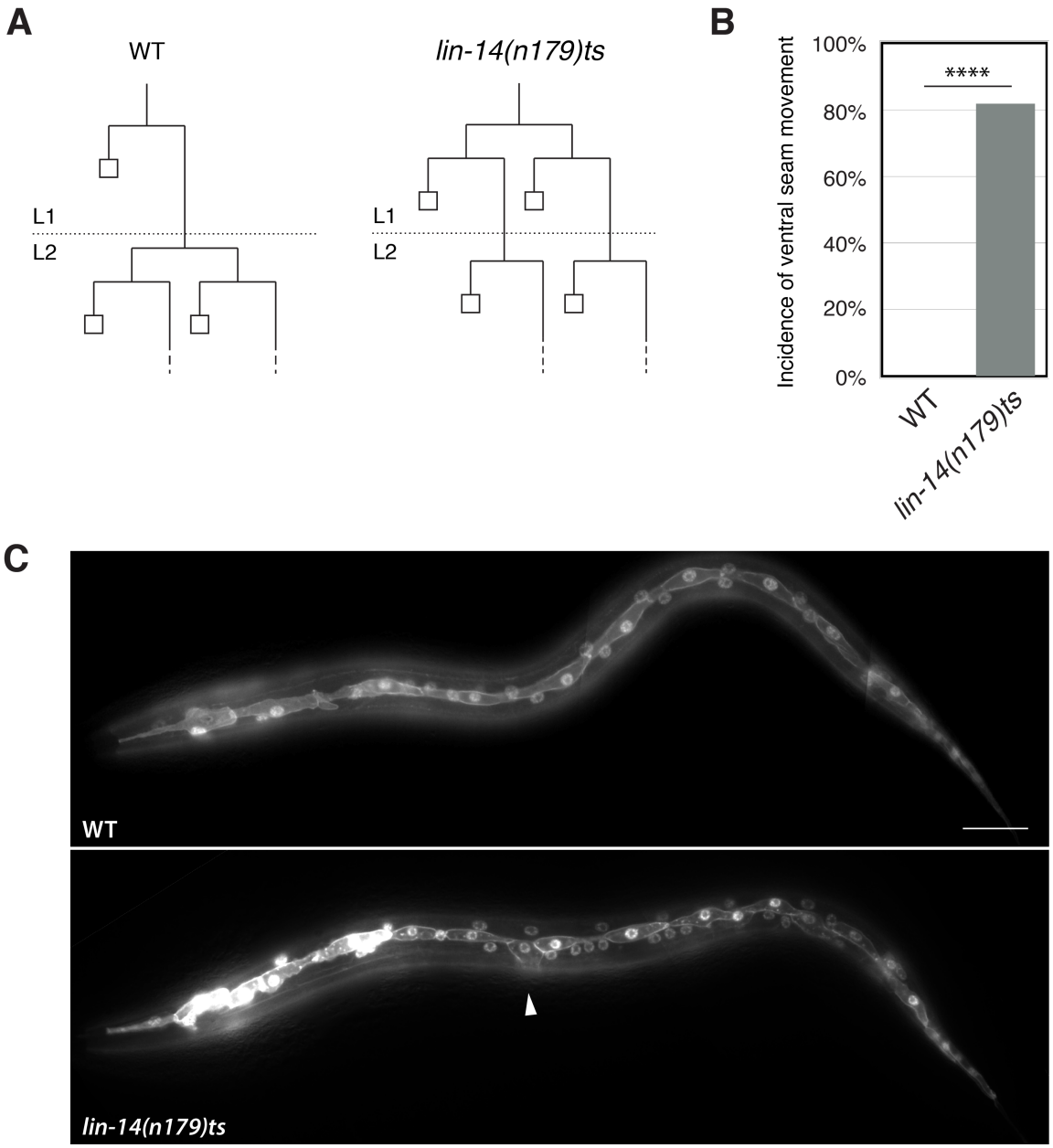

FIG. 4.2.11 – SEAM CELLS IN *LIN-14* LOSS-OF-FUNCTION MUTANTS MOVE TO THE VENTRAL MIDLINE AFTER THE SYMMETRICAL 'L1' DIVISION.

A. Seam cell lineage in *lin-14(n179)ts* loss-of-function mutants at 25ºC (reproduced from information in Ambros and Horvitz 1987). Dotted lines indicate incomplete lineages. *lin-14* loss-of-function alleles such as *n179* undergo the L2 seam cell lineage during the L1 moult, skipping out the wild-type L1 seam cell division all together. **B.** Incidence of migration in wild-type and *lin-14(n179)ts* animals grown at 25ºC (Student's T-test P**** < 0.00001, 61 ≤ n ≤ 81). **C.** Late L1 *lin-14(n179)ts* animals maintained at 25ºC show seam cells branching to the ventral midline, in contrast to WT animals maintained at 25ºC. 82% of the 62 *lin-14(n179)ts* animals observed show this seam branching to the midline at 25ºC. Note that although the phenotype of *lin-14(n179)ts* should double the number of V1-4 and V6 lineage seam cells at the end of L1, this phenotype does not affect every cell in every worm, and hence the worm imaged has 14 and not 16 seam cells. Scale bar = 10 μm.

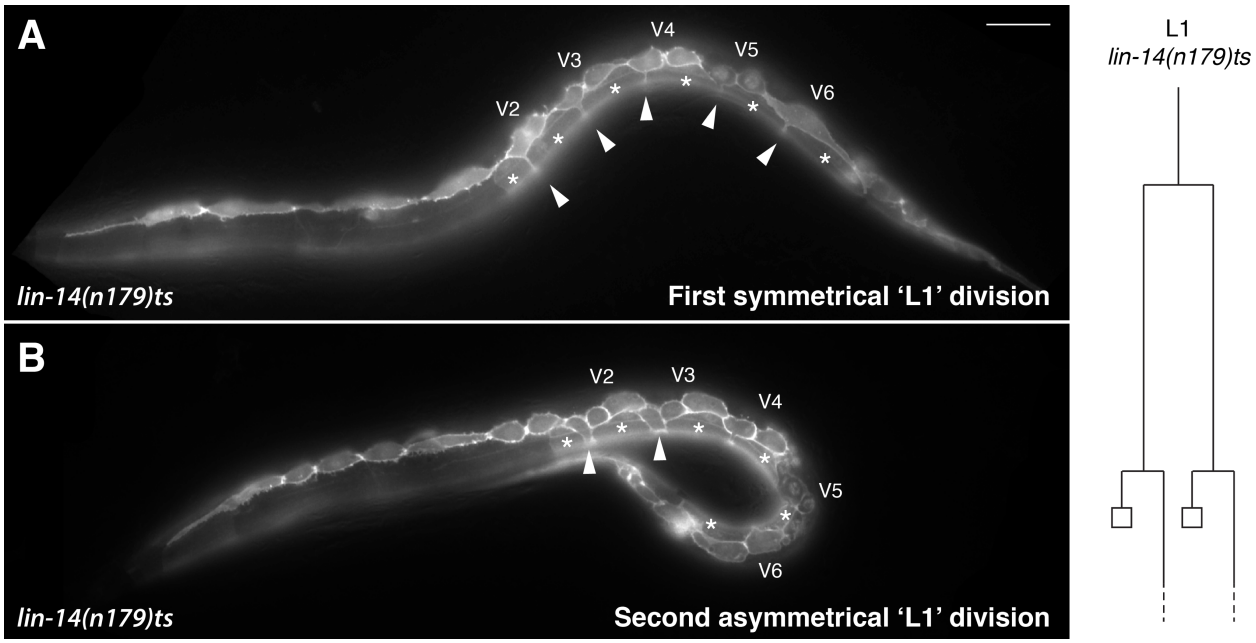

FIG. 4.2.12 – SEAM CELL DAUGHTERS AND P CELLS DO NOT MIGRATE VENTRALLY UNTIL THE SECOND ASYMMETRIC *LIN-14(LF)* DIVISION.
Dividing L1 seam cells in *lin-14(n179)ts* animals at 25ºC. The expected seam cell lineage in these animals is shown on the right (dotted line indicates incomplete lineage. **A.** During the first L1 symmetrical division the P cells (asterisks) do not migrate to the ventral midline and the seam cell projections remain very narrow (arrowheads). **B.** During the second, asymmetrical L1 seam cell division in these animals, the P cells migrate ventrally and the seam cell projections widen (arrowheads). In this respect the second division resembles the wild-type L1 division, whereas the first division does not (besides the fact that the division is symmetrical). Scale bar = 10 μm.

4.3 Discussion

To find a mutation that perturbs the L1 seam cell division is very unusual, as this division appears robust to many genetic manipulations of seam cell fate. This alone suggests that alternative, or additional, mechanisms govern the molecular and cellular aspects of this division. Although the asymmetric fates of the daughter cells remain normal in a *pal-1(e2091)* mutant, the defects in epidermal remodelling resulting from abnormal cell positioning in this mutant sheds light on the unique nature of the L1 seam cell division and its essential role in the development of the ventral hypodermis.

Polarised projections on L1 dividing seam cells make this division unique

One of the most striking aspects of the L1 seam cell division is that the cells create a singular polarised projection down to the ventral midline as an integral component of the seam cell division. This phenomenon has never been observed in later seam cell divisions and appears to be a unique feature of the L1 division. The projection is positive for apical junction markers, but how this forms between already-present apical junctions between the ventrally placed P cells remains an unanswered question. The re-modelling of apical junctions in many organisms is an essential process in the morphogenesis of many organs and tissues, as well as having a key role in invasive cancers. That protrusions formed from seam cells at L1 are able to invade adjacent P cell junctions before widening and changing shape would make them a tempting model through which to study apical junction re-modelling in *C. elegans*.

The L1 seam cell division completes the hyp7 sheath, partially formed during embryogenesis

Why the L1 division must make a ventral projection whereas other seam cell divisions do not is apparent only when looking at the arrangement of the epidermis in a newly hatched L1 animal.

At this time, hyp7 cells which have undergone dorsal intercalation during embryonic development before becoming fused to create a dorsal syncytium lie on the dorsal side of the animal. Other hypodermal tissues enclose the head and tail, and remain relatively unchanged during post-embryonic development. The two rows of ten lateral seam cells lie end-to-end down the side of the animal, and the posterior ventral hypodermis is made up of the unfused P blast cells. During late L1, these P cells move from their lateral-ventral position in the epidermis, becoming substantially smaller and migrating down to the ventral midline where they divide to give rise to cells of the ventral nerve cord and, in the case of the hermaphrodite, hypodermal precursor cells destined for vulval development. The L1 animal will therefore have lost its ventral acting hypodermis at this point. However, simultaneous asymmetrical division and ventral migration of hypodermally-fated seam cell daughters fills in the ventral hole in the hyp7 previously occupied by the P cells. The projections on the L1 seam cells ensure that all hypodermal daughters of these cells move ventrally to fill this gap in a newly described ventral intercalation with the P cells (Fig. 4.3.1). This is in stark contrast to later seam cell divisions, after which hypodermal daughters may move both dorsally and ventrally out of the seam line to contribute nuclei to either side of the hypodermis. A summary of the entire ventral intercalation of the seam cell daughters with the P cells is shown in figure 4.3.2.

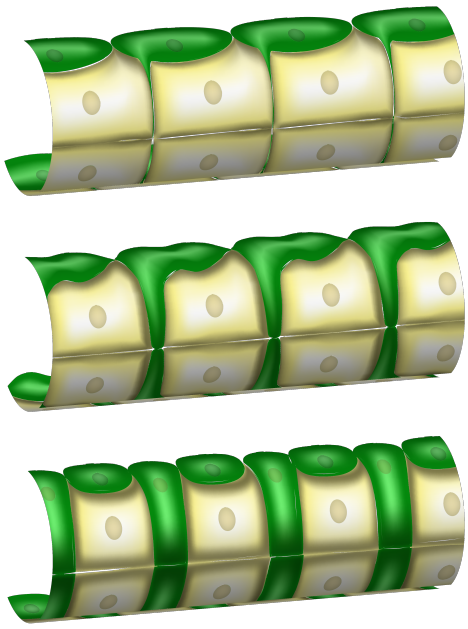

FIG. 4.3.1 – THREE-DIMENTIONAL SCHEMATIC OF THE VENTRAL EPIDERMIS DURING THE L1 SEAM CELL DIVISION AND P CELL MIGRATION.
The ventral hypodermis contains a 'hole' at hatching that is occupied by the P cells (yellow). As the seam cells (green) divide, their hypodermally-fated anterior daughters move ventrally along the seam cell projection to fill this ventral hole in the hyp7 syncytium. At the same time the P cells retreat to sit next to one another at the ventral midline where they later divide to give neuronal and hypodermal tissue.

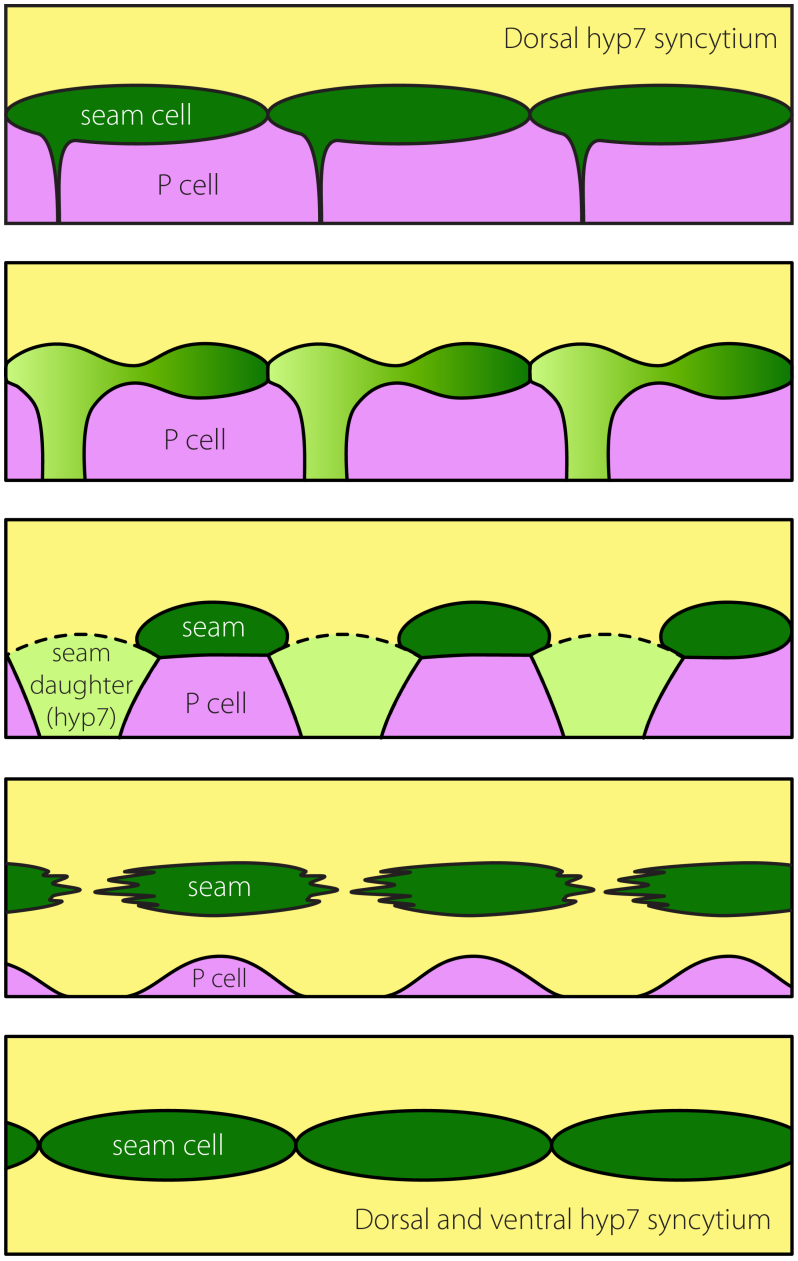

FIG. 4.3.2 – SUMMARY OF THE NEWLY-DESCRIBED VENTRAL INTERCALATION OF THE SEAM ANTERIOR DAUGHTER CELLS WITH THE P CELLS DURING L1.
At hatching, the P cells (pink) form the majority of the ventral hypodermis, whereas the dorsal hypodermis is made up entirely from the hyp7 syncytium (yellow). Black lines indicate apical junctions between cells. Seam cells (green) lie in a lateral row between the dorsal hyp7 and the ventral P cells, but at hatching exhibit a ventral projection between the P cells down to the ventral midline. In wild-type, this projection is always polarised to the anterior end of each seam cell. As the seam cells start to divide (second panel), the anterior, hypodermally-fated daughter cell inherits the widening projection, ensuring that the cytoplasm of the seam daughter cell moves ventrally. Simultaneously, the P cells start to remodel, drawing away from each other and towards the ventral midline (midline represented as the bottom of each panel). As the seam cell division completes cytokinesis, the anterior seam daughter loses its apical cell boundary with the dorsal hyp7 (dotted black line in the third panel) and the anterior daughter cell takes on hyp7 fate. The P cells now intercalate with their counterparts on the opposite side of the animal at the ventral midline, and the anterior seam daughters, now fused with the dorsal hyp7, complete the ventral hypodermis. The seam cells extend laterally and reconnect to form the new seam line, with no ventral projections to the midline (final panel). This process completes the ventral hypodermis to form the overall structure of the hyp7 that is present for the rest of the life of the animal.

P cells migrate independently of the L1 seam cell division

One of the questions posed in this mechanism of epidermal remodelling is whether the migration of the P cells or the division of the seam cells is the driving factor in this process of building the ventral hyp7 syncytium. One half of this question is answered by the results from the laser ablation of the seam cells. After ablating two adjacent seam cells which border either side of a ventrally-placed P cell, this P cell was still seen to migrate to the ventral midline in all cases, indicating that the division of the seam cell and the invasion of the projection between neighbouring P cells was not a driving factor of P cell migration to the ventral midline. In concurrence with this result, it was observed that in *lin-14(lf)* animals that underwent a symmetrical seam cell division as the first division in L1, although the seam cells divided, this did not trigger P cell migration down to the ventral midline. However, the P cells migrated only when a second, asymmetrical division occurred in these animals, raising the question of whether it could be the contact with a hyp7-fated cell or syncytium (in the case of the seam cell ablated animals) which triggers P cells to migrate. Signalling from the hyp7 is known to be able to trigger fate changes in other epidermal tissues which are not protected by intact apical junctions (Brabin, Appleford et al. 2011). A second hypothesis would be that the P cell migration is uncoupled entirely from seam cell development and the heterochronic pathway as perturbed by *lin-14*, and the P cell migration happened at the same time as the wild-type migration occurs in L1, regardless of seam cell development. This is yet to be tested.

The converse ablation experiment, that testing whether seam cell daughter migration is dependent on P cell migration to the ventral midline, was unfortunately unsuccessful, due to premature deaths of the animals involved. However, this is perhaps unsurprising; although seam cells play an important role in embryonic elongation and in contributing cells to the hypodermis as the animal grows post-embryonically, at the exact time of hatching they play a much smaller

role within the structural makeup of the hypodermis than the P cells, and are relatively easy to ablate without significantly altering the surface area of the epidermis. P cells, however, appear to play a much larger role in maintaining the structure of the hypodermis at hatching, as ablation of two or more adjacent cells either kills the animal, or results in a substantial rearrangement of the seam cells above to the ventral midline. This is unsurprising given only six P cells per side of the animal make up the majority of the ventral hypodermis at this stage, and the cells are relatively large. This in itself suggests that there is substantial pressure on the seam from both the dorsal hyp7 syncytium and the ventral P cells. By removing the P cells, the pressure becomes unbalanced and the seam cells are pushed ventrally. By adding this pressure into the mechanism during the wild-type seam cell division, it is perhaps more of an achievement that the seam-fated daughters of the L1 division remain in place on the lateral line during this process than that the seam hypodermal daughters move ventrally. Subsequent establishment of the ventral hyp7 would later ensure an equalisation of the dorsal and ventral forces upon the seam line. Together, this data suggests that maintaining equal dorsal and ventral pressures on the seam line during the swap over of the ventral hypodermis from the P cells to the seam hyp7 daughters requires this process to be a highly coordinated event.

P cell apical boundaries determine the final position of the seam daughter cells

In light of the presence of an intrinsic pressure, it makes some sense that the whole seam has the potential to move and the only mechanism of regulation regarding which seam cell daughter migrates is the position at which the ventral projection (forming a pathway between the P cells for migration) will form. From the mis-positioned projections formed in *pal-1(e2091)* mutants, it appears that the formation of the projection is dependent on the positioning of (and perhaps signals from) apical junctions between adjoining P cells which lie ventrally to the seam. The normally anteriorly-polarised projection on the seam cells seen in wild-type animals (which

therefore becomes associated to the anterior hyp7-fated seam daughter) is moved posteriorly in some cells in a *pal-1(e2091)* mutant, which corresponds to the perturbed relative positioning of the apical junctions between the ventrally-lying P cells. This results in the wrong, posterior seam-fated daughter moving to the ventral midline, presumably under the influence of dorsal pressure from the hyp7 syncytium. Although the wrong seam daughter moves, this does re-equilibrate the pressure on the seam line as the P cells retreat, just as the wild-type hyp7-fated daughter would normally do, and this pressure is perhaps the driving force for migration. Tension between cells is a common mechanism for driving morphogenesis during embryogenesis, so perhaps the P cells, through their own migration to the ventral midline, create tension that forces the formation of a ventral hypodermis through pressure exerted on the dividing seam. It may be interesting to measure the tension of the seam cell projections during this process by cutting through their attachment to the ventral midline with a laser. However, this would have to be executed with a laser with a wavelength outside that of GFP in order to prevent bleaching of the marker, and thus allow for measurement of the recoil of the projection. However, it appears that patterning by *pal-1*, driven during embryogenesis by the intronic enhancer, is essential for correctly establishing the relative positions of the seam/P cell boundaries, therefore allowing for correct morphogenesis of the seam during L1.

L1 epidermal remodelling is fast, requiring a rapid switch in the role of the P cells

Another remarkable feature of this process of ventral epidermal remodelling is the speed at which the switch from a mostly P cell-comprised ventral hypodermis to an entirely hyp7 hypodermis occurs. The process happens in approximately 30 minutes, and yet the cellular processes that must take place during this time are considerable. The P cells go from being large cells with an entirely hypodermal function, expressing the collagen *dpy-7* (Gilleard, Barry et al. 1997) and presumably synthesising and containing the components required to make up the

hemidesmosomes tethering the underlying muscle to the overlying cuticle (see Fig. 4.3.3), to small, neuroblast cells sitting along the ventral midline which no longer themselves fill a hypodermal cell role. At the same time, the daughters of the seam cells must take over the role of the P cells even before they have completed their division and differentiated fully into hyp7 cells. Given that there is no reported lethargic (or uncoordinated) phase in normal L1 division, the animals continue to move normally though this process, requiring a seamless transition of the hemidesmosomes from the P cells to the seam daughters. These substantial structures must be synthesised incredibly rapidly by the dividing seam cell hypodermal daughter during the L1 seam cell division.

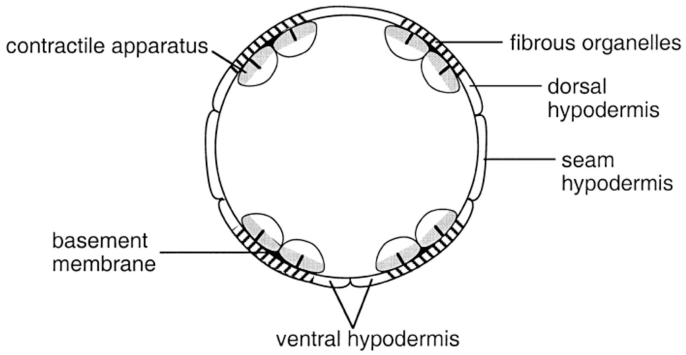

FIG. 4.3.3 – ILLUSTRATION OF THE CROSS-SECTION THROUGH A NEWLY HATCHED WORM SHOWING THE MUSCLE ATTACHMENTS THROUGH THE EPIDERMIS (ADAPTED FROM HRESKO, SCHRIEFER ET AL. 1999).
The ventral hypodermis is comprised of the P cells, and the dorsal hypodermis is made up of the syncytial hyp7.

Loss of hypodermal markers, such as *dpy-7* and *ajm-1*, and a transition in cell morphology have previously been used as some of the markers to indicate a transdifferentiation event between differentiated cell types in *C. elegans* (Jarriault, Schwab et al. 2008). It is interesting to observe that for the established case of natural transdifferentiation in *C. elegans* described in this work by Sophie Jarriault, the original fate of the cell is epidermal and the final cell fate is neuronal

(Jarriault, Schwab et al. 2008). Given that P cells are initially hypodermal in their role, and subsequently remodel to form neuroblasts before cell division (the L1 seam cell division occurs approximately 5 hours prior to the first P cell division in L1), this raises interesting questions about what constitutes a *bone fide* transdifferentiation event, whether hypodermal tissues are intrinsically more plastic than other tissues, and whether neuronal cell fates are more 'dominant' than other cell fates.

Another case of transdifferentiation in developmental biology is the epithelial-to-mesenchymal transition (EMT) in mammals. This describes an event in which cells previously epithelial in character, with cell-cell junctions and apical-basal polarity, down-regulate these characteristics to become migratory mesenchymal cells. EMT involves cytoskeleton rearrangements and a change in signalling programmes that define cell shape and gene expression, and results in cells that are no longer bound to an extracellular matrix (Lamouille, Xu et al. 2014). This is another example of epithelial plasticity, and bears striking characteristics to the P cell remodelling and fate transition in *C. elegans* at L1.

L1 seam lineages should not be considered entirely independent from one another

Seam cell projections from opposite sides of the animal meet each other at the ventral midline during the L1 seam cell division. At other stages of development, the separation of the seam cells to opposite lateral sides of the animal means that during development, cell lineages on different sides of the animal can be considered independent from one another. This is supported by the fact that the divisions on each side of the animal do not occur at identical times to one another. However, this may not be the case for L1 seam cell divisions, as not only do these cells directly contact one another for a short time, I have also observed that they divide at almost identical

times to one another, across opposite sides of the animal. This would suggest that for this division at least, the two sides of the animal should not be considered as separate lineages but may, at least in part, coordinate with one another. This may also be a source of the robustness against genetic manipulation observed for this division.

The unique nature of the L1 ventral hypodermis has been observed once before

It has been previously noted by John White and colleagues, in the Worm Breeder's Gazette 5(2): 43, published in 1980, that from reconstructions of electron micrographs it can be seen that the ventral hypodermis of the L1 animal 5 hours after hatching contains projections from the seam cells to the ventral midline (see drawing in Fig. 4.3.4). Interestingly, it was noted at the time that the anterior 'processes' of the seam cells take on distinctly hypodermal characteristics, even before completion of the L1 seam division, which would concur with observations made here of the speed with which the anterior cell takes over the role of the migrating P cell.

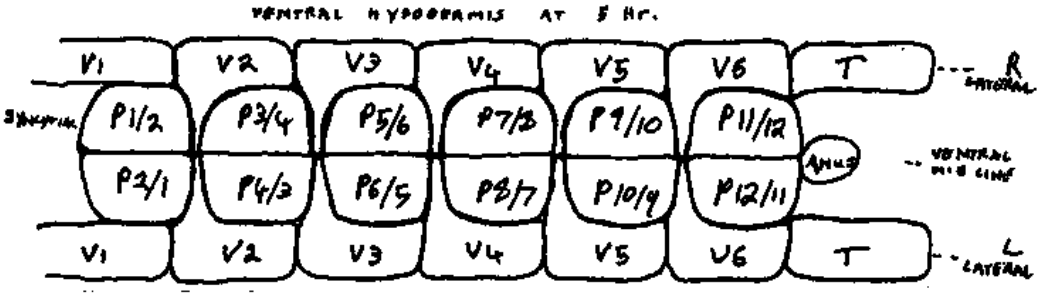

FIG. 4.3.4 – ACCURATE ANATOMICAL DRAWING OF THE VENTRAL HYPODERMIS BY JOHN WHITE AND COLLEAGUES, PUBLISHED IN THE WORM BREEDER'S GAZETTE 5(2): 43.

Addendum

After submission of this thesis, it was discovered by R. Poole (University College London), using the partially automated lineage analysis software SIMI°BioCell (developed by Ralph Schnabel and colleagues), that V3 and V4 in the *pal-1(e2091)* embryo swap positions along the anteroposterior axis so that V4 sits anteriorly to V3 by hatching. V3 and V4 are therefore labelled the wrong way around in the figures of this thesis. The rearrangement of V3 and V4 is due to a failure of V3 to intercalate into the single line of seam cells shortly after the seam cells are born, resulting in a later entry of V3 into the seam line that is now blocked by V4, which lies adjacent to V2. The anterior position of V4 leads to V3 entering the seam line posteriorly to V4. This delay in migration of V3 is the ultimate cause of the seam cell mis-positioning defect (overlap) in *pal-1(e2091)* L1 larvae. The preliminary results from this analysis are shown in figure 4.3.5.

Intriguingly, of all the V seam cell lineages, V3 and V5 are unique in that they originate from the ABpl/rap lineages as sisters of the P cells. The other V lineage cells originate from the ABarpp lineage, along with the H lineage seam cells. V5 has a unique lineage compared to other seam cells, whereas the V3 lineage is apparently the same as V1, V2 and V6 in hermaphrodite animals. It is tempting to speculate that this difference in the lineage origin for V3 compared to other V cells could account for its unique *pal-1*-dependent intercalation into the seam line in the embryo. This is yet another example of *pal-1* being required for cell movement (see Chapter 7 for further discussion).

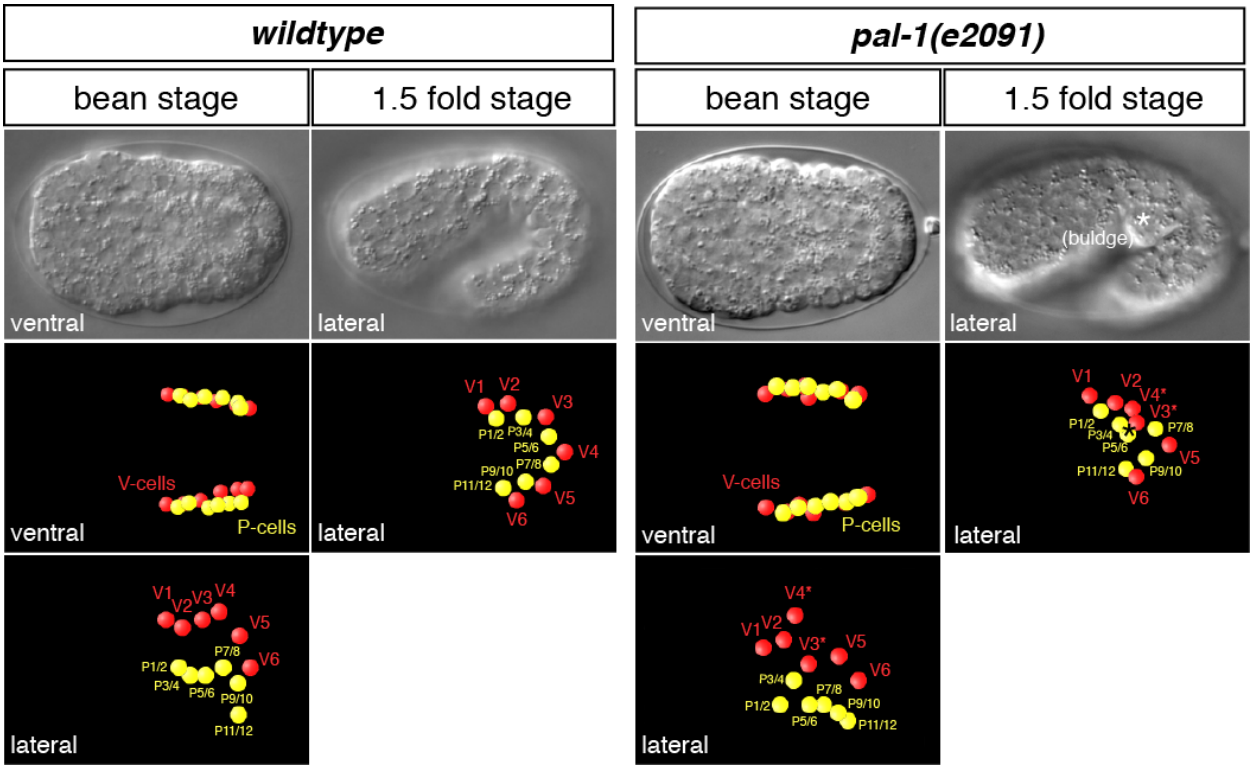

FIG. 4.3.5 – LINEAGED WILD-TYPE AND *PAL-1(E2091)* EMBRYOS SHOWING THE FAILURE OF V3 TO SUCCESSFULLY INTERCALATE INTO THE LATERAL SEAM CELL LINE DURING EMBRYOGENESIS.
Shortly after being born, the seam cells (red) and P cells (yellow) organise themselves into two parallel lateral lines on either side of the animal, with the P cells positioned ventrally to the seam cells. The lateral arrangement of seam cells involves an intercalation event during which the V seam cells move between each other to form a single line. Subsequently, during elongation, the two lines of seam and P cells remain parallel to each other, with P cell nuclei lying ventrally to the gaps between the seam cell nuclei. However, in a *pal-1(e2091)* animal, V3 fails to intercalate into the single line (asterisk) and therefore V4 lies adjacent to V2. As V3 later tries to enter the seam cell line, V4 blocks its entry, forcing V3 to enter the seam line more posteriorly. This causes V3 and V4 to switch positions along the anteroposterior axis, and is the cause of the overlapping seam cells in the *pal-1(e2091)* animal.

CHAPTER 5

Ventral hypodermal migration in L1: *pal-1* works with netrin to regulate posterior patterning

5.1 Introduction

In the previous chapter I described the cellular mechanism by which hypodermal daughters of the L1 asymmetric seam cell division move ventrally in order to complete the hyp7 sheath, which remains intact throughout the life of the animal. We have also determined that polarisation of this ventral movement is dependent on a strict arrangement of the P cells with respect to the seam cells, and that this arrangement is perturbed in *pal-1(e2091)* animals due to the abnormal positioning of seam cells which often overlap in the mid-body regions of these animals. However, up until now we have not had any insight into the molecular basis of this ventral cell movement, although factors regulating the simultaneous complementary movement of the P cells to the ventral midline have been investigated elsewhere and are discussed in the introduction

(Zipkin, Kindt et al. 1997, Spencer, Orita et al. 2001, Starr, Hermann et al. 2001, McGee, Rillo et al. 2006, Meyerzon, Fridolfsson et al. 2009, Fridolfsson, Ly et al. 2010, Bone, Tapley et al. 2014). We therefore used the abnormal migration of the posterior daughters of the L1 seam division in *pal-1(e2091)* mutants as the basis of an RNAi screen for suppressors and enhancers. The screen aimed to identify new regulators of seam cell development in L1, particularly factors that work with *pal-1* to influence the ventral migration of seam daughters to complete the ventral hypodermis.

5.2 Results

RNAi suppressor/enhancer screen for *pal-1(e2091)* L1 ventral seam movement

In order to probe for regulators of the seam anterior daughter cell movement after the L1 division, we performed an RNAi screen (knocking down genes from embryogenesis onwards) against known regulators of cell migration in *C. elegans* in the *pal-1(e2091)* background. Genes which were known to regulate any cell migratory process in *C. elegans* were selected for the screen, which was then performed using clone names rather than gene names to reduce bias. From this screen we isolated genes that had either a suppressing or an enhancing effect on the *pal-1(e2091)* branched seam phenotype, scored for in young larvae, using the Student's T-Test to determine significance.

Strikingly, the screen mostly pulled out members of two well-characterised migratory pathways in development, Wnt and netrin. Although netrin (*unc-6*) itself was not identified, this was likely due to the inefficiency of RNAi against this gene (R. Pocock, pers. comm.). We have previously investigated Wnt as a potential regulator of *pal-1* through an enhancer present in the 5th intron of *pal-1*, perturbed in *e2091* (see Chapter 3), whereas the involvement of netrin in either seam cell development or any process regulated by *pal-1* is completely novel. The only gene identified as a modulator of the *pal-1(e2091)* phenotype that was not a member of either the Wnt or netrin pathways was the *C. elegans* Ras protein, *let-60*.

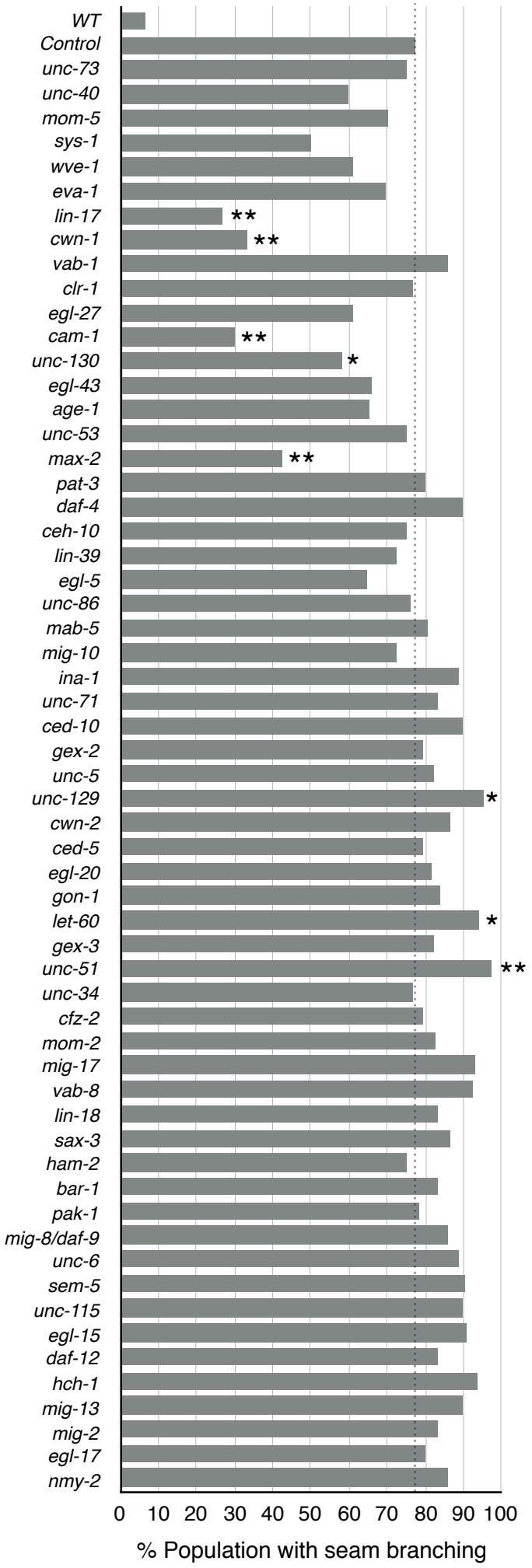

FIG. 5.2.1 – RNAi SCREEN TO IDENTIFY SUPPRESSORS AND ENHANCERS OF THE *PAL-1(E2091)* BRANCHED SEAM.
In order to identify genes which contribute to the control of the seam cell daughter movement after the L1 seam cell division, we performed a candidate RNAi screen and scored for incidences of seam branching in the *pal-1(e2091)* mutant background. Those genes when knocked out with RNAi that caused a significant decrease or increase in the number of animals with the branched phenotype, as determined by the Student's T-Test (* $P < 0.05$, ** $P < 0.01$), were recorded as suppressors or enhancers of *pal-1(e2091)* respectively. The control bar represents *pal-1(e2091)* animals grown on RNAi-competent bacteria transformed with an empty RNAi vector. Clones for all genes tested were obtained from the Ahringer RNAi library (Kamath and Ahringer 2003) except for the *nmy-2* clone, which was generated by S. S. Ding (D. Phil. thesis, 2015). $18 \leq n \leq 53$ per experiment, apart from *sys-1* ($n = 12$) and *pat-3* ($n = 10$). This was due to high levels of embryonic lethality.

Post-embryonic RNAi screen of embryonically lethal candidates

Many of the Wnt pathway genes and some other interesting candidates were embryonically lethal when knocked down with RNAi. We were therefore unable to score these genes for L1 phenotypes using the 'embryonic' RNAi protocol used for the main screen. For this small number of genes I performed a 'post-embryonic' RNAi screen: instead of subjecting L4 worms to RNAi and scoring their progeny, I bleached gravid hermaphrodites onto RNAi plates and scored seam cell movement in the hatched eggs after the L1 division. These results are shown in figure 5.2.2.

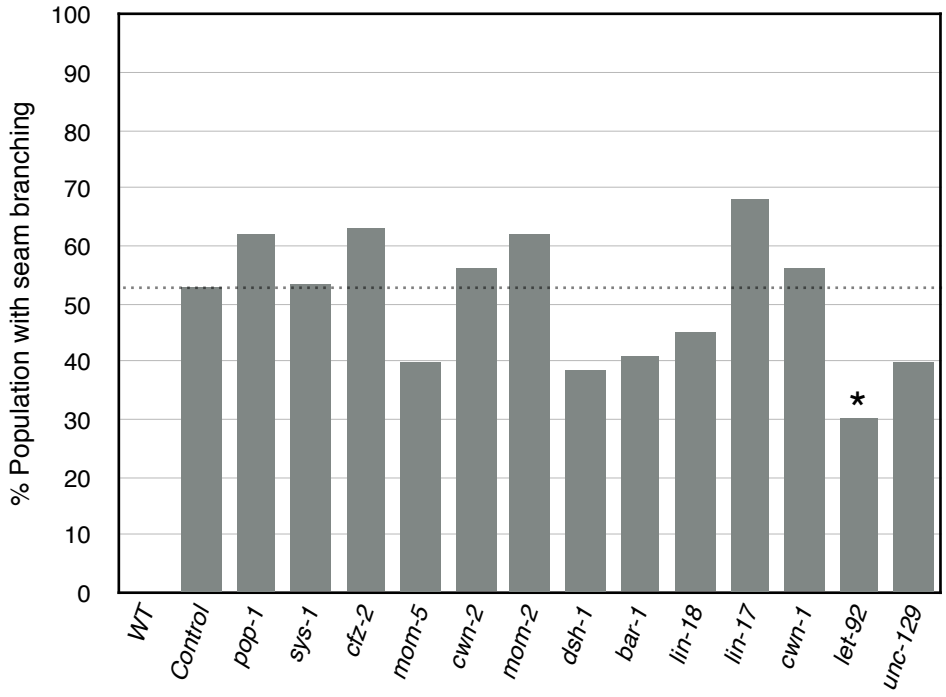

FIG. 5.2.2 – POST-EMBRYONIC RNAi SCREEN FOR GENES LETHAL WHEN KNOCKED OUT DURING EMBRYOGENESIS.
A smaller candidate post-embrypnic RNAi screen was performed against genes which were embryonically lethal when knocked down during embryogenesis. These were mainly members of the Wnt pathway, although others were included. Of the genes tested, only *let-92* had a significant enhancing or suppressing effect according to the Student's T-Test (*P < 0.05). The control bar represents *pal-1(e2091)* animals grown on RNAi-competent bacteria transformed with an empty RNAi vector. Clones for all genes tested were obtained from the Ahringer RNAi library (Kamath and Ahringer 2003) with the exception of the *pop-1* clone, which was generated by P. J. Appleford. 28 ≤ n ≤ 62 per experiment, except for *cwn-1* (n=16).

Summary of results from the RNAi suppressor/enhancer screen

Table 5.2.1 below summarises the results obtained from both RNAi screens. Notably, despite members of many different signalling pathways being screened, nearly all the genes identified as enhancers or suppressors of *pal-1* are members of the Wnt or netrin pathways. Convincingly, two of the genes isolated have opposing functions and opposite effects on the *pal-1* phenotype: *unc-51* and *let-92*. UNC-51 is a kinase for targets dephosphorylated by the LET-92 phosphatase during neuronal migration (Ogura, Okada et al. 2010). *unc-51* was found to be an enhancer of *pal-1*, whereas *let-92* is a suppressor. Upon repeating *let-60* RNAi for any effect on *pal-1(e2091)* seam cell phenotypes, we found that we could not reproduce the result from the screen, leading us to conclude that *let-60* RNAi has no real effect on *pal-1* phenotypes (data not shown). This gene was not therefore pursued.

	Gene	Effect	Description
Wnt	*lin-17*	suppressor	Wnt frizzled receptor
Wnt	*cwn-1*	suppressor	Wnt ligand - functions downstream of *pal-1*.
Wnt	*cam-1*	suppressor	Wnt pathway component - co-localises with *lin-17*.
netrin	*unc-130*	suppressor	Forkhead transcription factor required for expression of *unc-129* (TGF-β).
netrin	*max-2*	suppressor	p21-activated kinase required for P cell migration. Functions downstream of UNC-5.
netrin	*let-92*	suppressor	Dephosphorylates proteins phosphorylated by UNC-51 during neuron migration. Physically interacts with UNC-51.
netrin	*unc-129*	enhancer	TGF-β - promotes UNC-5/UNC-40 netrin pathway.
netrin	*unc-51*	enhancer	Kinase - regulates subcellular location of UNC-5.
netrin	*let-60*	enhancer	Ras

TABLE 5.2.1 – GENES IDENTIFIED AS EITHER SUPPRESSORS OR ENHANCERS OF THE *PAL-1(E2091)* BRANCHED SEAM PHENOTYPE.
An RNAi screen for enhancers or suppressors of the *pal-1(e2091)* branched seam phenotype was carried out for over 60 genes known to be involved in cell migration in *C. elegans*. From these, the 9 genes above were identified as either suppressors or enhancers of the phenotype. 8 of these genes were members of two known migration pathways in *C. elegans*: the Wnt and netrin pathways (indicated by the purple and blue bars respectively). The only gene identified not belonging to either of these pathways was *let-60*, encoding the *C. elegans* Ras protein.

A null mutant of *unc-6* enhances *pal-1* seam cell ventral movement during L1

In order to test the potential interaction of the netrin pathway with *pal-1*, we firstly investigated the effect of knocking out *unc-6*, the sole netrin ligand in *C. elegans* to which all other members of the netrin pathway must respond. We chose *ev400*, a null mutant of *unc-6* (Hedgecock, Culotti et al. 1990), and determined that this allele has no seam patterning phenotypes at L1 (Fig. 5.2.3 A). However, in combination with *pal-1(e2091)*, it acts to significantly increase the incidence of abnormal seam cell movement during the L1 seam division, and therefore acts as an enhancer of *pal-1*. In addition to the increase in the number of worms affected, the *unc-6* allele also increases the severity of the phenotype in each individual, with many more cells moving ventrally than in single *pal-1(e2091)* mutants alone. These effects are shown in figure 5.2.3.

unc-6 is synthetically lethal with *pal-1(e2091)*, both during larval and post-embryonic development

unc-6(ev400); pal-1(e2091) animals are very sick, with a very slow population growth compared to either single mutant. I therefore quantified the embryonic and larval lethalities in both the single and the double mutants (Fig. 5.2.4), and showed that there is a large increase in lethality in the double mutants compared to the single mutants at both stages of development. These results suggest that *pal-1* and *unc-6* act together to regulate other essential processes during both early and later development, in addition to cell movement after the L1 seam division.

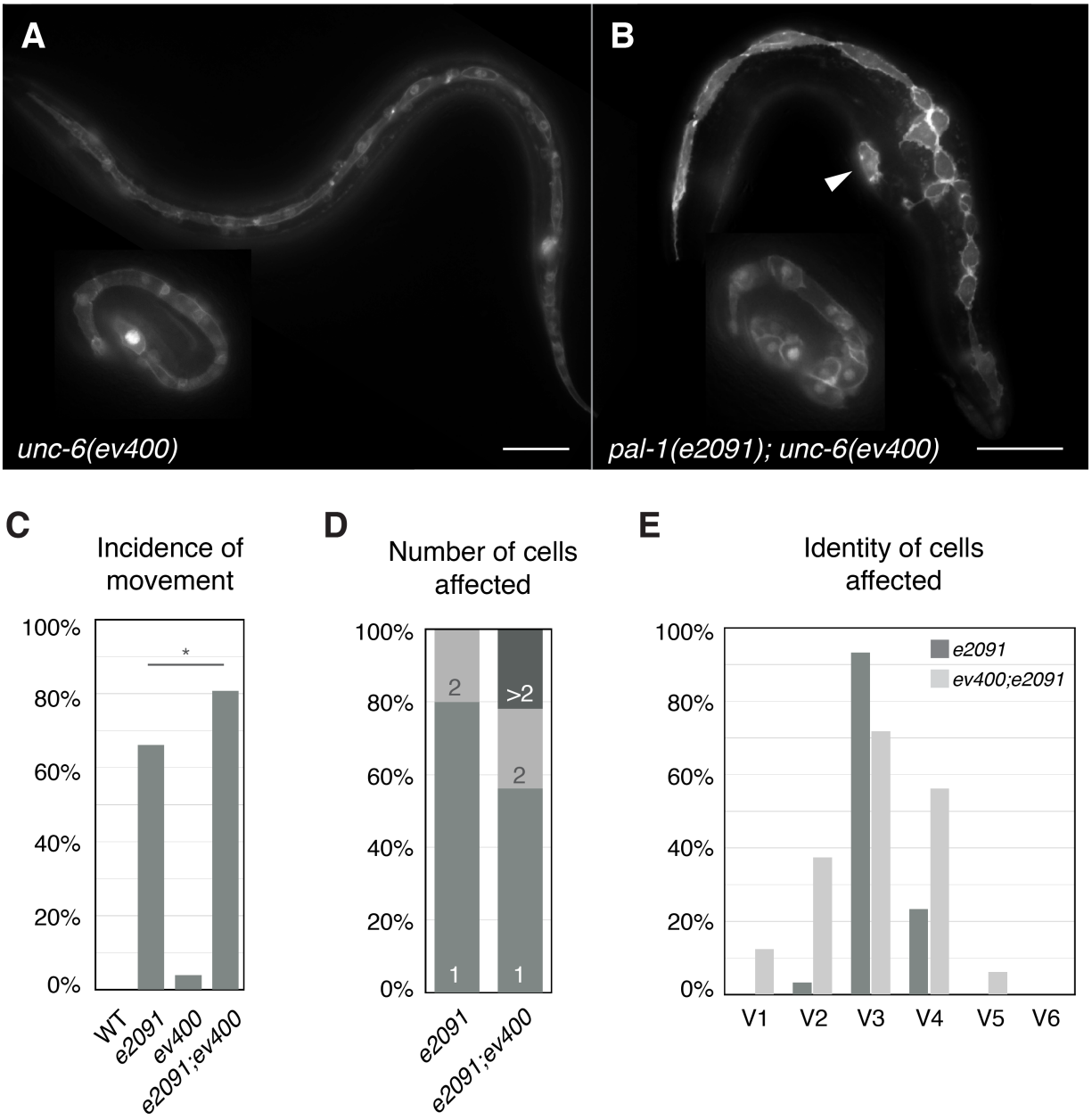

FIG. 5.2.3 – *UNC-6* IS AN ENHANCER OF THE *PAL-1(E2091)* VENTRAL SEAM MIGRATION AT L1.
A. *unc-6(ev400)* mutants do not have seam defects at any time during L1, or in embryonic development (inset). **B.** The *unc-6(ev400); pal-1(e2091)* double mutant displays an increased severity of seam cell movement defects associated with the *pal-1(e2091)* single mutant, with one seam cell embedded in the ventral midline completely, and no longer attached to the seam line (arrowhead). Scale bars = 10 μm. **C.** The incidence of ventral seam cell movement is increased in *unc-6(ev400); pal-1(e2091)* double mutants compared to *pal-1(e2091)* single mutants ($50 \leq n \leq 239$, Student's T-Test *$P < 0.01$). **D.** In *pal-1(e2091)* single mutants, only 20% of animals that display the seam movement phenotype have positional abnormalities in more than one cell. However, in the double *unc-6(ev400); pal-1(e2091)* mutants over 40% of animals display abnormal movements of more than one cell, with half of these having more than two cells displaced. $32 \leq n \leq 60$ per strain. **E.** Graph showing the identities of the misplaced cells in *pal-1(e2091)* and *unc-6(ev400); pal-1(e2091)* animals. The double mutants show a greater spread of cell identities are affected than in *pal-1(e2091)* single mutants (*pal-1(e2091)* data reproduced from figure 4.2.2 D). $32 \leq n \leq 60$ per strain.

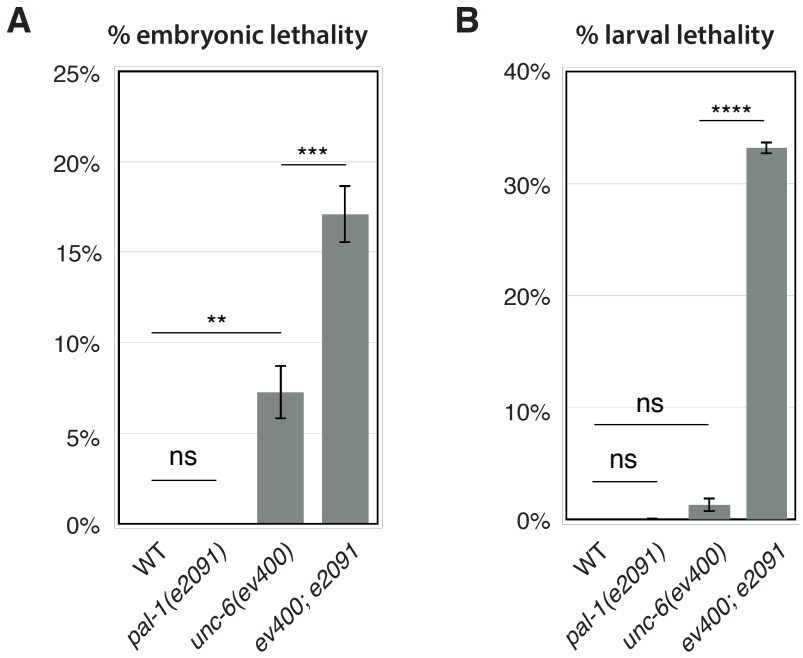

FIG. 5.2.4 – SYNTHETIC LETHALITY BETWEEN *PAL-1* AND *UNC-6* AT 20ºC.
pal-1(e2091) animals have no associated embryonic or larval lethality, whereas populations of *unc-6(ev400)* animals display over 5% embryonic and approximately 2% larval lethality (**A** and **B**). However, populations of double mutants display an increased level of lethality during both embryonic and larval development, showing that there is a synthetic genetic interaction between these two alleles. Error bars = S.E.M., $1119 \leq n \leq 1811$ individuals per population from a total of $6 \leq n \leq 8$ broods. Student's T-test *P < 0.05, **P < 0.01, ***P < 0.001, ****P < 0.0001.

unc-6 has a role in regulating posterior embryonic development

Whilst conducting the lethality assay upon *unc-6(ev400);pal-1(e2091)* mutants, I noticed that many of the L1s that later died before reaching adulthood had a severe Nob phenotype. This is a phenotype associated with *pal-1* null alleles (an alternative name for *pal-1* is *nob-2*) but the penetrance of this phenotype in *pal-1(e2091)* animals is very low (Fig. 5.2.5). A Nob phenotype has never been associated with any *unc-6* allele. However, over 20% of the double *unc-6(ev400); pal-1(e2091)* mutants hatch with a strong *pal-1* Nob phenotype (Fig. 5.2.5) suggesting that *unc-6* acts with *pal-1* to control posterior embryonic development.

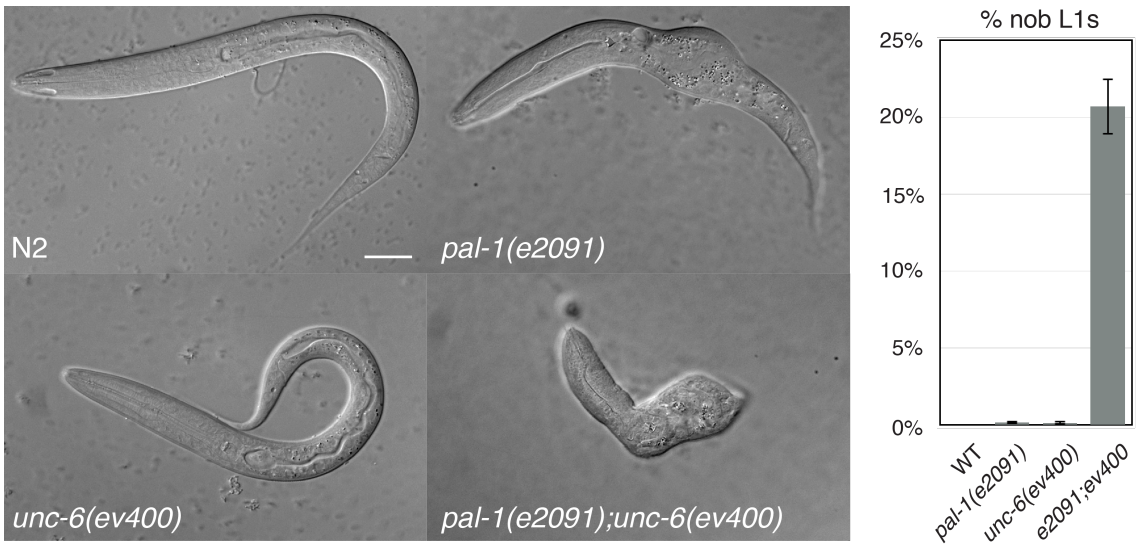

FIG. 5.2.5 – DIC IMAGES AND QUANTIFICATION OF THE *UNC-6(EV400); PAL-1(E2091)* SYNTHETIC NOB PHENOTYPE.
Whilst *pal-1(e2091)* or *unc-6(ev400)* single mutants have no associated Nob phenotype, over 20% of double mutants hatch with severe Nob phenotypes. This phenotype is associated with complete loss-of-function alleles of *pal-1*, suggesting that in the weaker *e2091*, a wild-type copy of *unc-6* is able to compensate for or work without *pal-1* to pattern posterior development in the embryo. Error bars = S.E.M, $1119 \leq n \leq 1811$ individuals per population from a total of $6 \leq n \leq 8$ broods. Scale bar = 10 μm.

unc-6(ev400); pal-1(e2091) adults show a synthetic increase in 'bagging'

In order to assess the health of single mutant *pal-1(e2091)* and *unc-6(ev400)* animals in comparison to surviving adult double mutant animals, I conducted a brood size assay. These results (Fig. 5.2.7) show that the double mutants do not have a significantly reduced brood size compared to that of the *unc-6(ev400)* single mutant. However, whilst conducting this assay, I realised that many of the L4s picked to study often failed to lay eggs and exhibited a 'bagged' phenotype, whereby eggs hatch inside the mother, for both the *unc-6(ev400)* and the *unc-6(ev400); pal-1-(e2091)* strains. Quantification of this bagging phenotype showed that there is a synthetic increase in the incidence of bagging in the double mutant compared to the single mutant (Fig. 5.2.6).

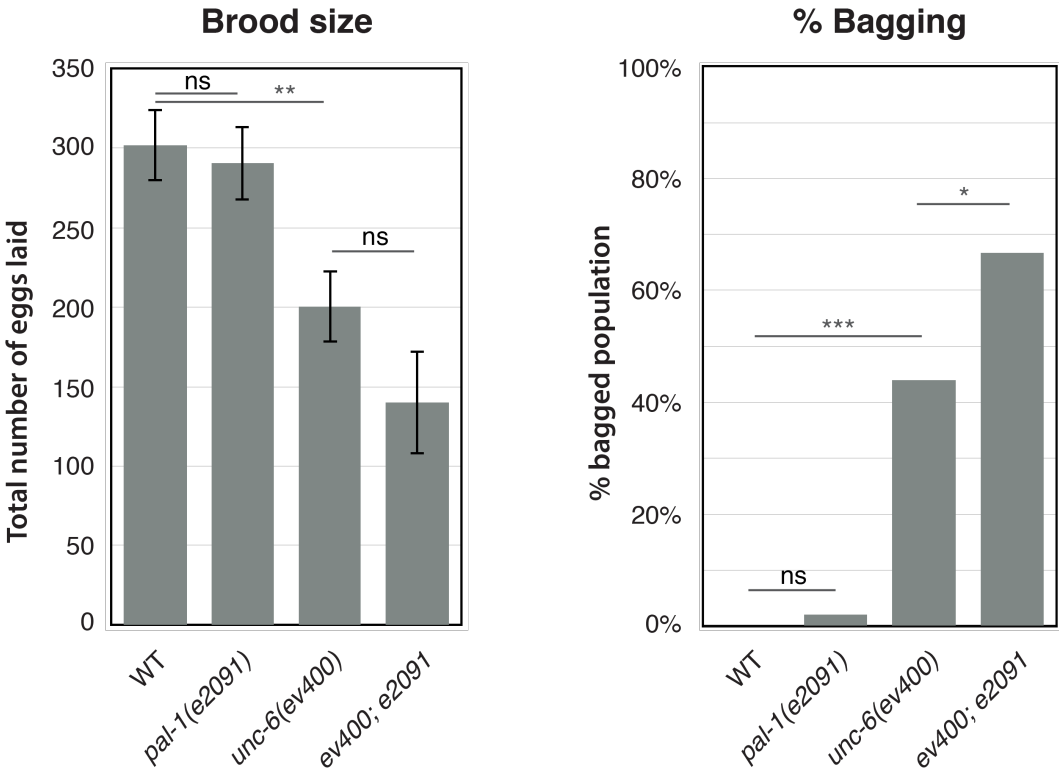

FIG. 5.2.6 – *UNC-6(EV400); PAL-1(E2091)* DOUBLE MUTANTS SHOW A SYNTHETIC INCREASE IN BAGGING BUT NO SIGNIFICANT BROOD SIZE REDUCTION.
A. Quantification of the brood size (total eggs laid) for 6-8 individuals per strain shows that although there is a significant reduction in the number of eggs laid for the *unc-6* mutant alone, this is not significantly increased in the double mutants. Error bars = S. E. M., Student's T-test **P < 0.01. **B.** Quantification of the number of L4 animals that bag before laying eggs (50 ≤ n ≤ 54 individuals per strain). There is a significant increase in the incidence of bagging in the double mutant compared to the single *unc-6* mutant (Student's T-test *P < 0.05 ***P < 0.001).

Abnormal gonad migration in *unc-6(ev400)* is not exacerbated by *pal-1(e2091)*

unc-6(ev400) is a known regulator of distal tip cell (DTC) migration during *C. elegans* development, with a common defect being that of a failure in the dorsal turn (Hedgecock, Culotti et al. 1990, Levy-Strumpf and Culotti 2014). In contrast, *pal-1* is not known for it's role in post-embryonic gonad development, although given the role of *pal-1* in regulating epidermal rearrangements during L1 and that *unc-6* and *pal-1* synthetically regulate posterior development, I looked to see whether *pal-1(e2091)* has a synthetic effect on DTC migration in double mutants.

There does not appear to be any synthetic effect of *pal-1(e2091)* on *unc-6(ev400)* DTC migration defects using this allele (Fig. 5.2.7). Although the wild-type N2 strain has no migration defects, the strain containing the background *heIs63* fluorescent seam cell reporter has a mild background effect on DTC migration (Fig. 5.2.7 B and C). Unfortunately this marker was present in all strains analysed for DTC migration defects, and so although *pal-1(e2091)* alone appears to have mild DTC migration defects, these are not significantly increased from the background *heIs63* reporter strain so are unlikely to be real effects of *pal-1(e2091)*.

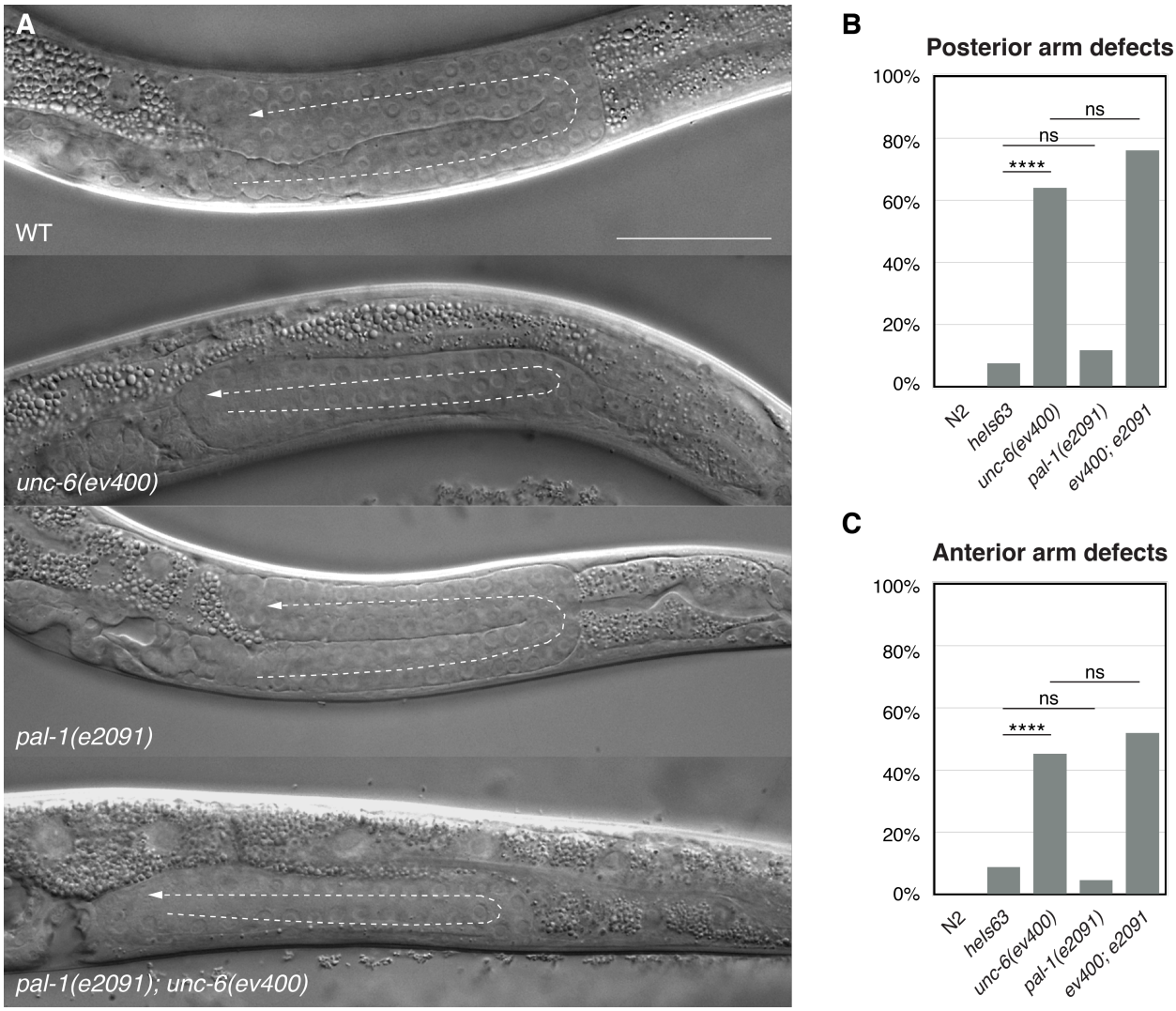

FIG. 5.2.7 – GONAD MIGRATION DEFECTS IN *UNC-6(EV400)* AND *PAL-1(E2091)* SINGLE AND DOUBLE MUTANTS.

The posterior arm of the L4 gonad of the wild-type, *pal-1(e2091)*, *unc-6(ev400)* and double mutant are shown in **A**. The migratory routes of the DTCs are indicated with a dotted white line and arrow. Wild-type DTCs migrate first out from the centre of the worm along the ventral side of the animal, before turning dorsalward and again to face in the opposite direction to the original migration. This allows them to migrate down the dorsal side of the animal until the middle of the worm is reached. In contrast, *unc-6(ev400)* animals often exhibit failures in the dorsal turn, migrating back into the middle of the worm on the ventral side, the way they migrated outwards originally. *pal-1(e2091)* gonad DTC migrations appear normal. Neither the anterior gonad arm (**C**) or the posterior gonad arm (**B**) exhibit any increase in the incidence of defects in the double *pal-1(e2091); unc-6(ev400)* compared to the single *unc-6(ev400)* mutant. There is a background level of DTC migration defects in the fluorescent marker parent strain (*hels63*) which is present in all of the mutant animals analysed. Student's T-test P**** < 0.00001, 57 ≤ n ≤ 75 animals per strain. Scale bar = 50μm.

Severity of male tail defects are synthetically increased in *unc-6(ev400); pal-1(e2091)* animals

pal-1 has been previously characterised for its role in mail tail development (Zhang and Emmons 2000). Given that *unc-6* synergises strongly with *pal-1* phenotypes in hermaphrodites, we asked whether the loss of rays in the male tail in *pal-1(e2091)* single mutants was made worse in *unc-6(ev400); pal-1(e2091)* double mutants. The results are shown in figure 5.2.8. We found that there is a small but significant decrease (0.3) in the average number of rays in the single *unc-6(ev400)* mutant compared to the wild-type average. However, the double mutants showed a further reduction of 1.2 rays from the average of 3 rays per side in *pal-1(e2091)* single mutants, bringing the average number of rays to 1.8 per side in the male tail ($38 \leq n \leq 57$).

In *pal-1(e2091)* single mutants, the rays of the T lineage (rays 7-9) are more likely to be present than the rays of the V5 or V6 lineages, although some rays are present from these V lineages (see Fig. 3.2.2 in Chapter 3). However, in the *unc-6(ev400); pal-1(e2091)* double mutants, the presence of rays from either of the V lineages is almost non-existent, with only two out of 38 tails observed having any V-derived rays. This would indicate that *unc-6* also has a role in the development of the male tail lineages of V5 and V6, working together with *pal-1*.

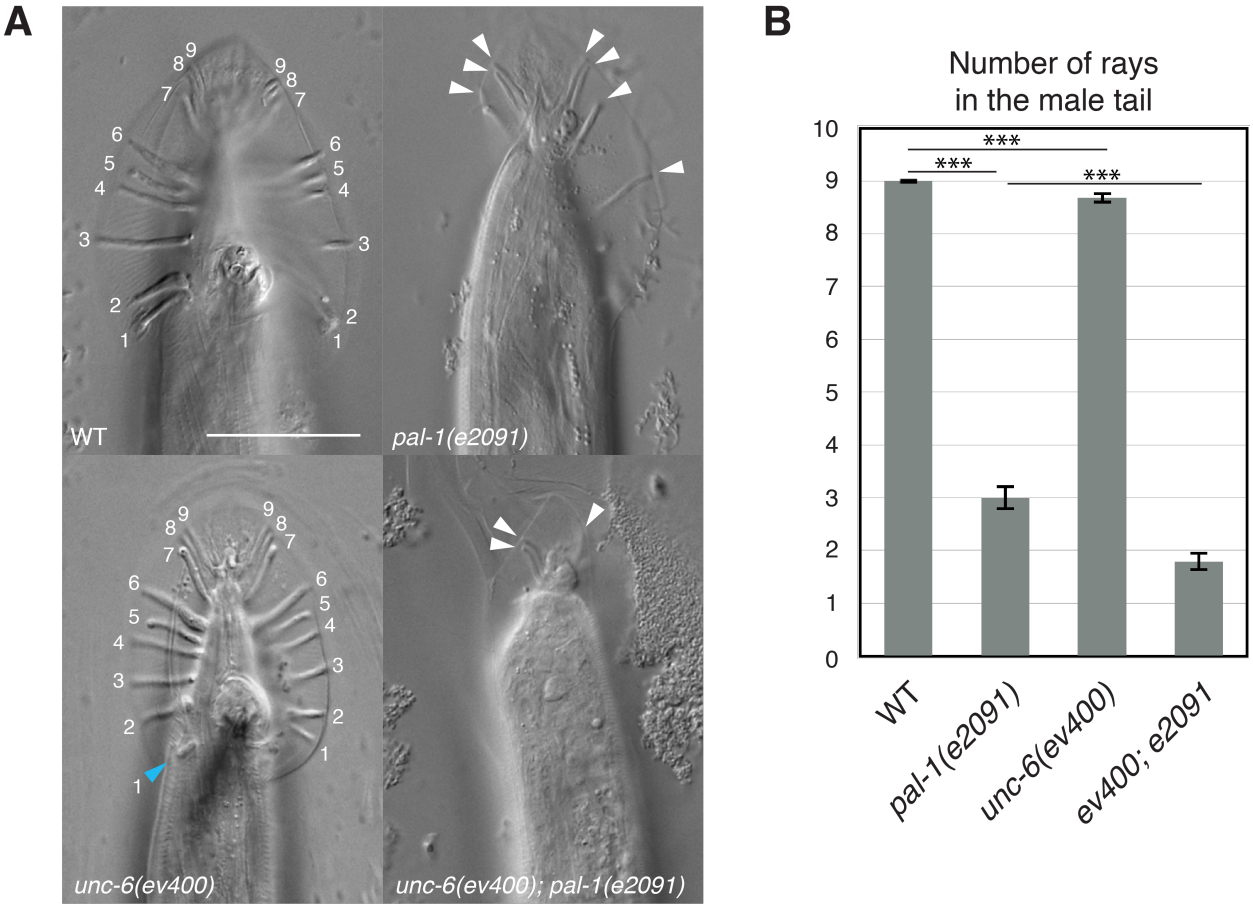

FIG. 5.2.8 – MALE TAIL DEFECTS SYNERGISE IN *UNC-6(EV400);PAL-1(E2091)* ANIMALS.
A. *pal-1(e2091)* and *unc-6(ev400)* single and double mutant male tails at L4. *pal-1(e2091)* animals have fewer rays and surprisingly *unc-6(ev400)* also display subtle ray phenotypes, such as a short ray 1 (blue arrow). In some *unc-6(ev400)* animals this ray does not form at all. The double mutant displays a synthetic effect on male tail development with an average of only two rays per side of the tail. Scale bar = 50 μm. **B.** Quantification of rays in the male tail of *pal-1(e2091)* and *unc-6(ev400)* single and double mutants. Wild-type animals have 9 rays per side of the animal, and *pal-1(e2091)* animals have on average 3. *unc-6(ev400)* single mutants have a small but significant reduction of 0.3 rays compared to wild-type, but the *unc-6(ev400); pal-1(e2091)* double mutant reduces the 3 rays per side of the *pal-1* single mutant to 1.7, a synthetic effect of *unc-6* with *pal-1* on male tail development. $38 \leq n \leq 57$ per strain, significance determined by the Student's T-test ***$P < 0.001$. Error bars = S. E. M.

An *unc-6* allele which affects ventral but not dorsal migration shows synthetic lethality and Nob phenotypes with *pal-1(e2091)*

The *unc-6(e78)* allele causes a substitution of cysteine to tyrosine that affects the binding of the *unc-6* ligand with the receptor responsible for ventral movement, *unc-40*, but does not affect binding of the ligand to *unc-5*, the predominant receptor responsible for dorsal migration (Hedgecock, Culotti et al. 1990, Lim and Wadsworth 2002). By making a double mutant of this allele with *pal-1(e2091)*, we could determine whether the genetic interaction between *pal-1* and *unc-6* is dependent on the netrin receptor *unc-40* or *unc-5*, thereby narrowing down the mode of interaction between *pal-1* and netrin.

A third, weak allele of *unc-6* that causes very mild axon migration defects, *ju152* (gift of Yishi Jin), was also crossed into *pal-1(e2091)* and the synthetic interaction analysed in order to build an allelic series to better understand the interactions between *unc-6* and *pal-1(e2091)*. The embryonic and larval lethality data is shown alongside that of *e78* in figure 5.2.9, showing that this allele of *unc-6* also acts synthetically with *pal-1*.

pal-1(e2091); unc-6(e78) shows a significant increase in embryonic and larval lethality from either single mutant, with the most significant increase shown in the increase in the number of Nobs in the population (Fig.5.2.9). The fact that this is lower than that of the *unc-6* null mutant, *ev400*, with *pal-1(e2091)* would indicate either that the single point mutation in *e78* is unable to completely eliminate binding of *e78* to *unc-40*, and therefore the Nob phenotype and synthetic lethality phenotypes of the *pal-1(e2091); unc-6* double mutants is *unc-40* dependent, or that the phenotype is both *unc-5* and *unc-40* dependent and knocking out binding to one receptor is not enough to fully recapitulate the phenotype of the null mutant.

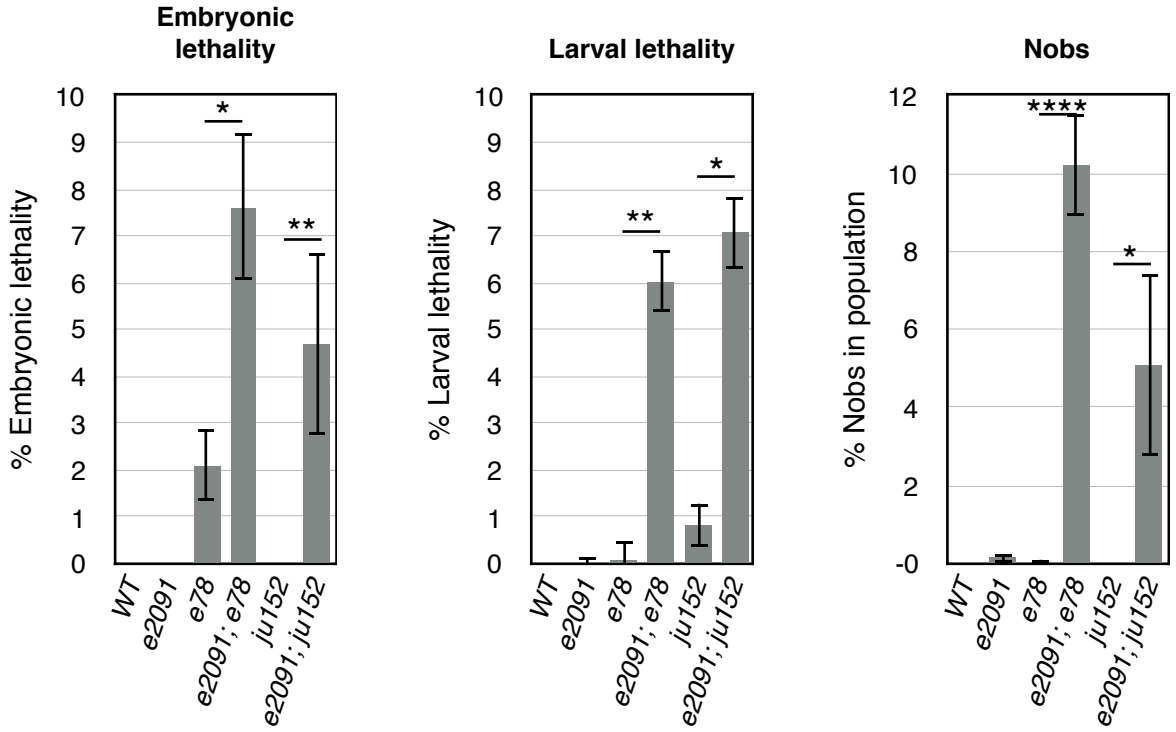

FIG. 5.2.9 – EMBRYONIC AND LARVAL LETHALITY DATA WITH THE INCIDENCE OF NOB L1S FOR *PAL-1(E2091); UNC-6(E78)* AND *PAL-1(E2091); UNC-6(JU152)* DOUBLE MUTANTS.
Both *unc-6* alleles *e78* and *ju152* display synthetic embryonic and larval lethality with *pal-1(e2091)* (Student's T-test P* < 0.05, P** < 0.01), although both alleles display much weaker phenotypes than those shown by the *unc-6* null allele (c.f. Fig. 5.2.4). Both *e78* and *ju152* double mutants display a percentage of Nob phenotype L1s in the hatched population, with this phenotype being absent in the population of either single mutant (Students T-test P* < 0.05, P**** < 0.0001) although again neither mutant displays the increase in Nobs to the same extent that the *unc-6* null mutant exhibits (c.f. Fig. 5.2.5). For all graphs, 1282 ≤ n ≤ 1811 individuals from 6 broods per strain, error bars = S.E.M.

unc-5 and *unc-40* display a synthetic interaction with *pal-1*

In order to more fully understand the nature of the *pal-1*-netrin interaction, we crossed strong mutant alleles for each netrin receptor, *unc-5(e53)* and *unc-40(e271)*, into the *pal-1(e2091)* strain. Consistent with the weaker interaction of *pal-1* with the *e78* allele of *unc-6*, both *unc-5* and *unc-40* alleles display synthetic lethality and occurrence of the Nob phenotype in their respective double mutant strains (Fig. 5.2.10). The incidence of Nob animals in either of the *unc-5* or *unc-40* double mutant populations is approximately half of the incidence of Nob animals in the *unc-6* null double mutant population. This would suggest that the requirement for netrin in posterior patterning in the absence of *pal-1* is dependent on both netrin receptors, *unc-5* and *unc-40*. From these results, it would also appear that the role of each receptor in posterior patterning functions independently of the other, as the total number of Nob animals from adding those in both receptor;*pal-1* double mutant populations gives a figure close to the number of Nob animals in the *pal-1(e2091);unc-6(0)* population. This would suggest there is no synthetic effect between *unc-5* and *unc-40* for this phenotype, although a triple mutant would confirm this hypothesis.

Strikingly, almost all of the associated embryonic (but not larval) lethality in *pal-1(e2091); unc-6(ev400)* mutants appears to be solely due to the interaction of *unc-6* with the *unc-5* receptor; neither the *unc-6(e78)* or the *unc-40(e271)* alleles display a large, if any, increase in embryonic lethality compared to the single mutants. By contrast, the *unc-5(e53)* allele displays a much higher level of synthetic embryonic lethality with *pal-1* (over 20%), consistent with the level of embryonic lethality observed in the *pal-1(e2091); unc-6(ev400)* double mutant. Presumably, therefore, the earliest function of netrin in *pal-1(e2091)* embryos is *unc-5*-dependent.

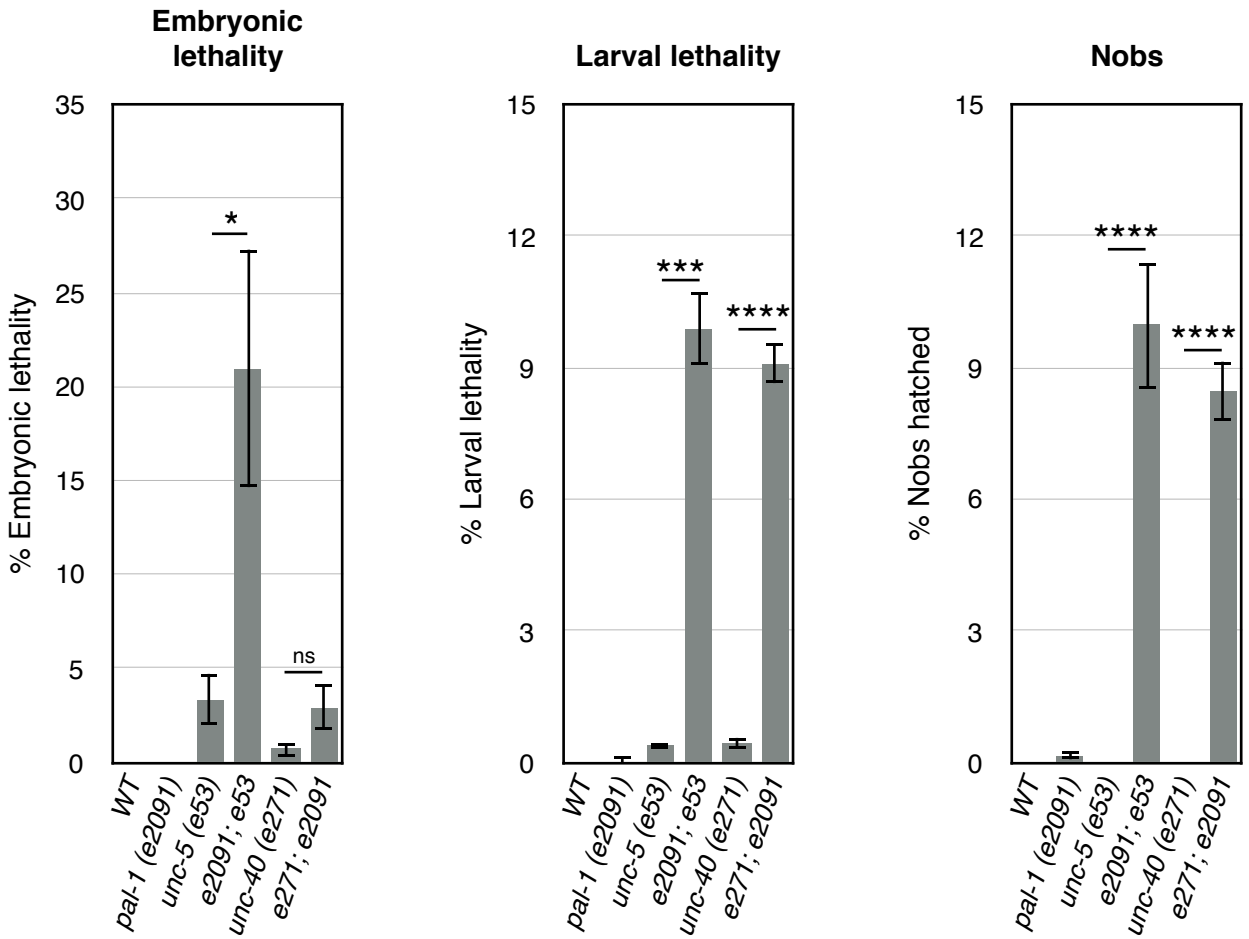

FIG. 5.2.10 – BOTH *UNC-5(E53)* AND *UNC-40(E271)* MUTANTS DISPLAY SYNTHETIC LETHALITY AND NOB PHENOTYPES WITH *PAL-1(E2091)*.
unc-5(e53) and *unc-40(e271)* single mutants have a low level of associated embryonic lethality; whereas this is significantly increased in the *pal-1(e2091); unc-5(e53)* double mutant, it is not increased in *unc-40(e271); pal-1(e2091)*. Both netrin receptors display a significant increase in larval lethality in the *pal-1(e2091)* double mutant compared to the single mutants, as well as a corresponding incidence of animals hatching with a Nob phenotype. For all graphs, $1282 \leq n \leq 1811$ individuals from $6 \leq n \leq 7$ broods, error bars = S. E. M., Student's T-test P* < 0.05, P*** < 0.001, ****P < 0.0001.

Axon migration defects in weak netrin mutants are increased by *pal-1(e2091)*

In an *unc-6* null mutant such as *ev400*, there is almost 100% failure of commissure migration from the VD and DD neurones of the ventral nerve cord (VNC) to the dorsal nerve cord (DNC). It is therefore difficult to use strong alleles to investigate any potential synthetic interaction of *pal-1(e2091)* with netrin in the context of neuronal development. Therefore, for this analysis, we used three netrin alleles with mild axon migration defects: *unc-6(ju152)*, *unc-5(ju181)* and *unc-40(e1430)*, kindly given to us by Yishi Jin of the University of California San Diego. Axons were visualised using an integrated *unc-25p::gfp* reporter (Jin, Jorgensen et al. 1999) also a gift of Yishi Jin. *unc-6(ju152)* and *unc-5(ju181)* have mild axon migration defects such that 15% and 20% of circumferential commissures exhibit guidance defects respectively (Huang, Huang et al. 2003). *unc-40(e1430)* changes the R157 codon to a UGA stop and is not thought to make a functional product (Colon-Ramos, Margeta et al. 2007).

By itself, *pal-1(e2091)* does not cause any failures in axon migration (Figs. 5.2.11 and 5.2.12). However, axon migration defects were increased significantly by *pal-1(e2091)* in all three netrin mutants, with the greatest increase seen in the *unc-40(e1430); pal-1(e2091)* double mutant (Fig. 5.2.12). A second unexpected phenotype was also observed in *pal-1(e2091); unc-6(ju152)* double mutants, whereby neuronal cell bodies were observed in abnormal lateral positions in the mid-body of the worm (Fig. 5.2.11). Presumably these are a result of the higher level of mid-body disorganisation in the L1 epidermis seen in *unc-6; pal-1(e2091)* double mutants, causing a perturbation of normal P cell migration and resulting in neurones being born in lateral positions. This misplaced cell phenotype was observed only very rarely in *pal-1(e2091); unc-5(ju181)* double mutants, but was found in *unc-40(e1430)* single mutant animals. By only counting the incidence of this misplacement in *unc-40(e1430); pal-1(e2091)* double mutants, it would appear that there is no increase in cell body misplacement in the double mutant compared to the single

mutant. However, upon closer inspection, the incidences of misplaced neuronal cell bodies in the single *unc-40(e1430)* mutant appeared mainly in the head region of the animal. This was in contrast to the cell body misplacement I observed in the *pal-1(e2091); unc-6(ju152)* double mutant. I therefore counted the incidences of either anterior or mid-body cell misplacements in the population of *unc-40(e1430)* single and double mutants, and found that although the incidence of misplacement in the head did not change upon addition of *pal-1(e2091)*, the incidence of cells displaced in the mid-body increased significantly (Fig. 5.2.12 C). This would suggest that the mechanism whereby cells get displaced in the mid-body in *pal-1(e2091)* animals is synthetically regulated by *unc-40* and *unc-6*, but not *unc-5*.

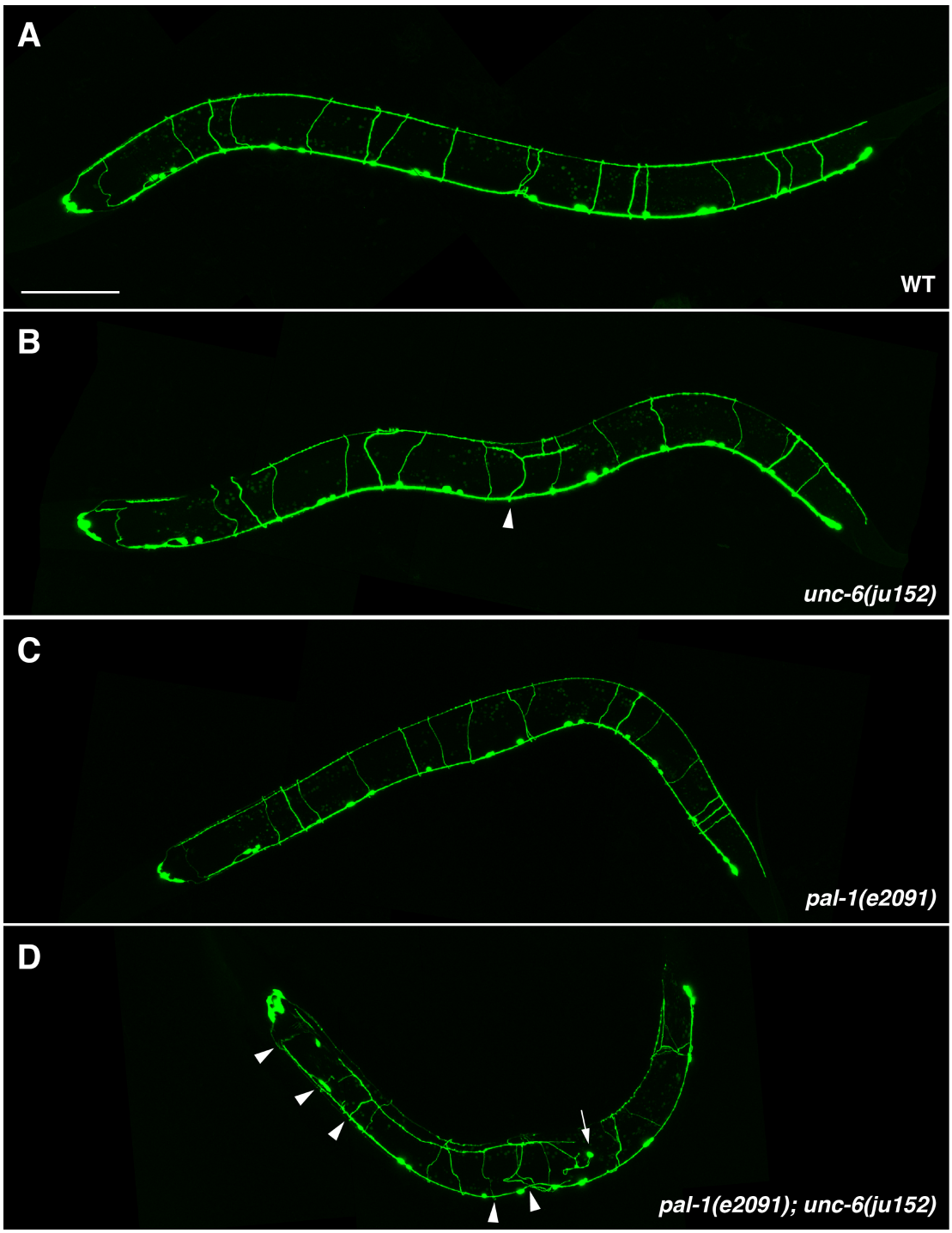

FIG. 5.2.11 – AXON MIGRATION DEFECTS IN THE WEAK *UNC-6(JU152)* ALLELE ARE INCREASED BY *PAL-1(E2091)*.
A. A compressed z stack of a set of confocal images taken of a wild-type L4 worm carrying the integrated VD motor-neurone marker *unc-25p::gfp*. Ventral is downwards and anterior is on the left. The cell bodies of the neurones can be seen as foci of gfp on the ventral midline, and the commissures extend from the ventral side of the worm to the dorsal side. Here they extend laterally to contribute to the dorsal nerve cord. **B.** An L4 *unc-6(ju152)* animal, displaying an axon migration defect whereby one of the commissures (arrowhead) does not extend fully to the dorsal midline before branching along the anteroposterior axis. **C.** A *pal-1(e2091)* L4 animal does not display any axon migration defects. **D.** A *pal-1(e2091); unc-6(ju152)* double mutant with an increased number of commissures that fail to reach the dorsal midline (arrowheads). In addition, the animal displays a misplaced lateral cell body (arrow) which does not lie on the ventral midline. Scale bar = 50 μm.

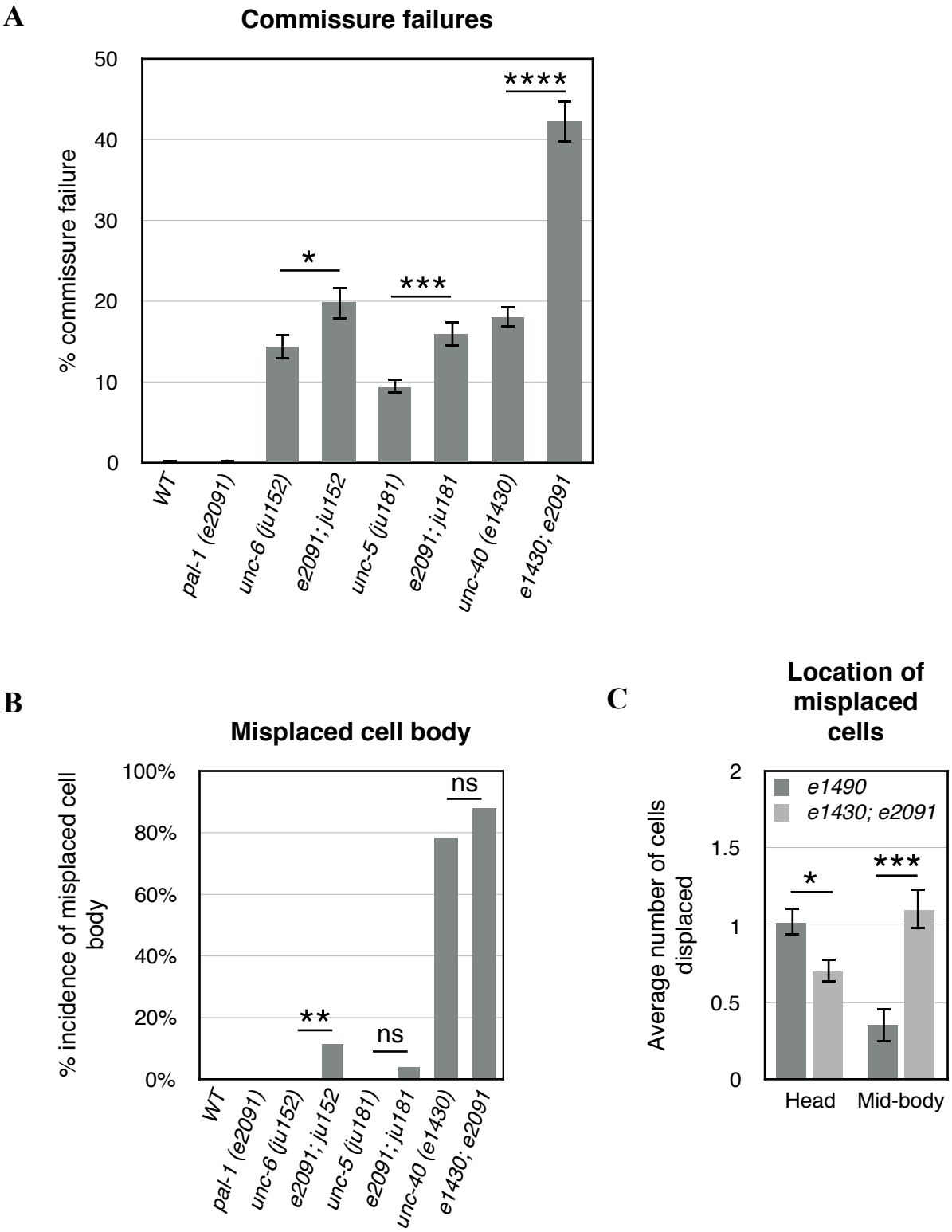

FIG. 5.2.12 – QUANTIFICATION OF VENTRAL NERVE CORD DEFECTS IN WEAK NETRIN ALLELES WITH AND WITHOUT *PAL-1(E2091).*

A. Percentage failure of commissures to reach the dorsal nerve cord. No failures were observed in the *pal-1(e2091)* single mutants, but failures significantly increased in all netrin mutants in a *pal-1(e2091)* genetic background. **B.** Incidence of abnormally laterally placed neuronal cell bodies. A small but significant percentage of animals in the *pal-1(e2091); unc-6(ju152)* population exhibited this phenotype, but this was not the case for *pal-1(e2091); unc-5(ju181)* animals. *unc-40(e1430)* single mutants exhibited a high incidence of misplaced cells, but these were mainly confined to the head region (**C**). **C.** Mid-body, but not anterior, cell misplacements were increased in *unc-40(e1430); pal-1(e2091)*. Student's standard T-test, P* < 0.05, P** < 0.01, P*** < 0.001, P**** < 0.0001. 50 ≤ n ≤ 61 . Error bars = S. E. M.

A mutant of the p21-activated kinase *max-2* suppresses the *pal-1(e2091)* seam branching phenotypes but not the seam cell overlap or mid-body bulge

max-2, isolated as a *pal-1* suppressor, is one of three p21-activated kinases (PAKs) in *C. elegans* (Lucanic, Kiley et al. 2006). PAKs are known for their role in cytoskeleton reorganisation, and have been implicated in processes of cell migration (Bokoch 2003). *max-2* is thought to be downstream of the *unc-5*-mediated netrin pathway as mutations in *max-2* are able to suppress ectopically active *unc-5*, although *unc-6* and *max-2* can act synergistically, suggesting that the pathway is not completely linear (Lucanic, Kiley et al. 2006). A deletion allele of *max-2*, *nv162*, removes the start codon as well as exons 1 to 4, and as such is likely a null allele (Lucanic, Kiley et al. 2006, Fujiki, Mizuno et al. 2010). As knockdown of *max-2* by RNAi acted to suppress the *pal-1(e2091)* seam migration phenotype, we tested this loss-of-function mutant with *e2091* for the same effect. We found that *max-2(nv162)* was able to suppress the migration of the seam after the L1 division from a 66% incidence in the *pal-1(e2091)* single mutant to a 44% incidence rate in the *max-2(nv162); pal-1(e2091)* double mutants (Fig. 5.2.13).

The model described in the previous chapter explains how the mis-positioning of the embryonic seam cells contributes to the aberrant L1 seam cell migration to the ventral midline in *pal-1(e2091)* single mutants. *unc-6* mutants enhance this phenotype by causing further embryonic disorganisation of the epidermis. We therefore looked to see whether *max-2* suppressed the seam movement defect at the level of embryonic seam cell organisation. Surprisingly, we discovered that *max-2(nv162)* has no effect on the seam cell overlap or that of the mid-body bulge, with no significant difference in the incidence of either phenotype between the double or the single mutant strain (Fig. 5.2.13). This would suggest that suppression of the cell movement phenotype by *max-2* is happening at the level of the mechanism of cell movement itself, and not by suppressing the *pal-1* mid-body or posterior patterning phenotype.

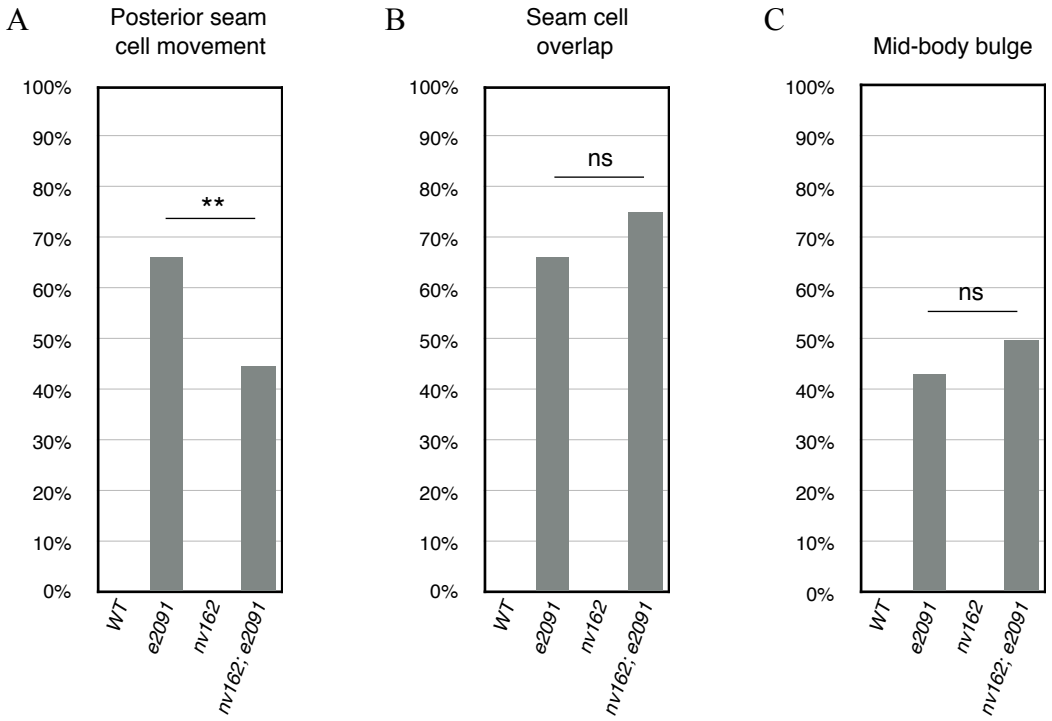

FIG. 5.2.13 – *MAX-2(NV162)* SUPPRESSES THE *PAL-1(E2091)* ABERRANT SEAM MOVEMENT DEFECT BUT NOT THE SEAM CELL OVERLAP DEFECT OR MID-BODY BULGE.
A. The *max-2(nv162)* loss-of-function mutant is able to suppress the incidence of seam cell migration after the L1 division down from 66% to 44% in *pal-1(e2091)* animals ($50 \geq n \geq 239$, $^{**}P < 0.001$ in Student's T-test). This concurs with the result from the screen that *max-2* RNAi knockdown can suppress the *pal-1(e2091)* seam branching phenotype. **B.** The incidence of seam cell overlap in *max-2(nv162); pal-1(e2091)* double mutants is not suppressed compared to that of *pal-1(e2091)* single mutants, and nor is the mid-body bulge associated with the *pal-1(e2091)* single mutant (**C**).

pak-1, another p21-activated kinase known to regulate P cell migration, is not able to suppress *pal-1(e2091)* seam movement after knockdown with RNAi

max-2 is a p21-activated kinase known to act redundantly with *pak-1*, another of three *C. elegans* p21-activated kinases, in the process of L1 P cell migration, but independently of *pak-1* during motoneuron axon guidance (Lucanic, Kiley et al. 2006). Since *max-2* is able to suppress the seam cell movement in *pal-1(e2091)* animals, we tested whether this suppression is stronger if *pak-1* is also knocked down by RNAi. However, we found in two separate experiments that *pak-1* RNAi has no effect on the incidence of seam cell ventral movement in *pal-1(e2091)* animals with or without *max-2(nv162)*, suggesting that in this capacity, *max-2* functions independently of *pak-1* (Fig. 5.2.14). However, since *pak-1* RNAi may simply have not have worked, this would need to be confirmed with a mutant phenotype.

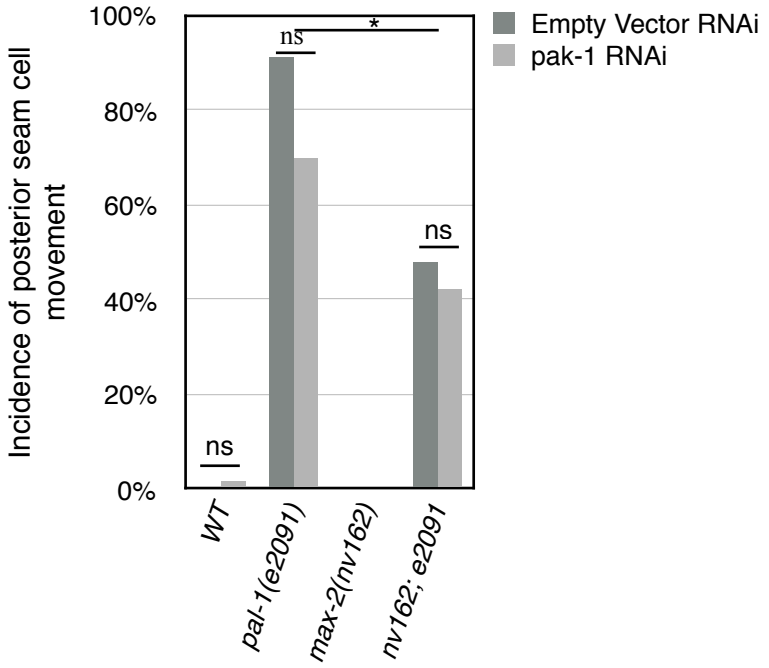

FIG. 5.2.14 – *PAK-1* RNAI IS UNABLE TO SUPPRESS ABERRANT *PAL-1(E2091)* SEAM MIGRATION. Graph showing the incidence of seam cell movement to the ventral midline after treatment with either control RNAi, involving the RNAi vector with no gene target insert, or *pak-1* RNAi. Although the p21-activated kinase *max-2(nv162)* can suppress the incidence of seam cell ventral movement, *pak-1* RNAi cannot, either on its own or in combination with the *max-2* mutant (Student's T-test *P < 0.01, 55 ≤ n ≤ 81 individuals per strain per RNAi).

max-2(nv162) is able to suppress the *unc-6(ev400); pal-1(e2091)* synthetic increase in seam cell migration

That *max-2(nv162)* is able to suppress the seam cell movement down to the ventral midline in *pal-1(e2091)* animals but not the seam cell disorganisation or bulge phenotype suggests that *max-2* functions at the mechanistic level of seam cell movement itself, rather than to suppress the patterning defects of *pal-1(e2091)*. Therefore, *max-2(nv162)* should also be able to suppress the exacerbated seam movement phenotype in *pal-1(e2091); unc-6(ev400)* double mutants, in which the seam cell disorganisation is increased, leading to an increase in the incidence of seam cell-fated daughter movement down to the ventral midline.

Upon analysis of the *max-2(nv162); pal-1(e2091); unc-6(ev400)* triple mutant, we found that there was indeed a significant reduction in the incidence of seam cell movement to the ventral midline, down to a level found not significantly different to the *pal-1(e2091)* single mutant alone (Fig. 5.2.15). This supports the idea of *max-2* as a mediator of ventral hypodermal cell movement during the L1 seam cell division.

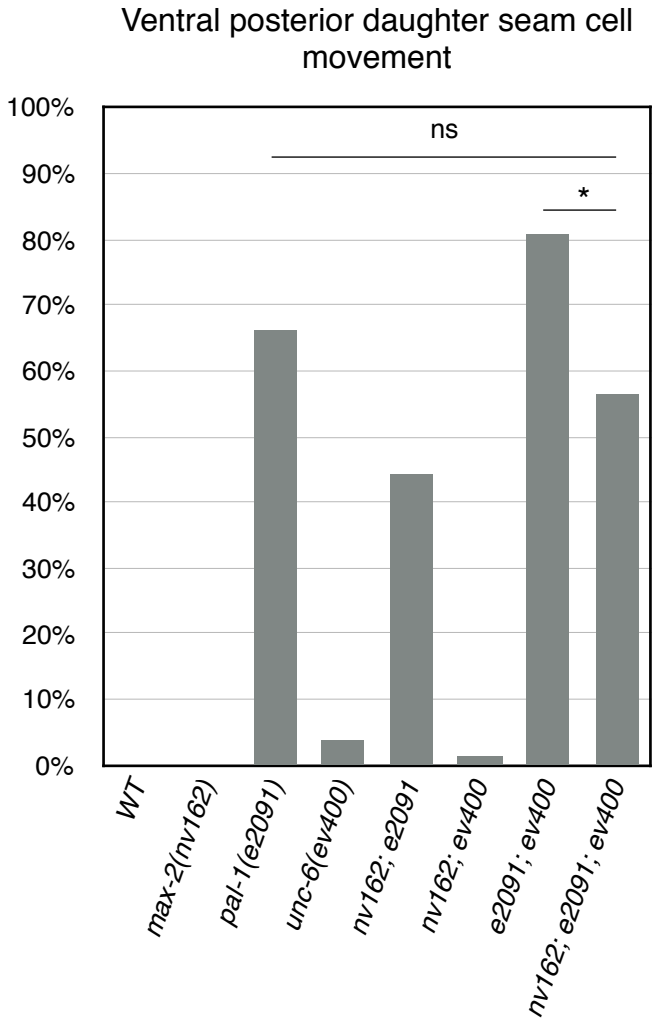

FIG. 5.2.15 – SUPPRESSION OF THE *UNC-6(EV400); PAL-1(E2091)* ENHANCEMENT OF SEAM CELL VENTRAL MOVEMENT BY *MAX-2(NV162)*.
Graph showing the incidence of the *pal-1* ventral seam cell movement defect after the L1 division in each of the single mutants *max-2(nv162)*, *pal-1(e2091)* and *unc-6(ev400)*, as well as each double mutant combination and the triple mutant. There is a significant decrease in the incidence of the seam cell movement in the triple mutant compared to the double *pal-1(e2091); unc-6(ev400)* mutant (which shows a synthetic increase in the phenotype compared to *pal-1(e2091)* alone). There is no significant change in the phenotype of the triple mutant compared to the *pal-1(e2091)* single mutant alone, suggesting that *max-2(nv162)* is able to suppress the synthetic increase shown in the *pal-1(e2091); unc-6(ev400)* double mutants (Student's T-test $P^* < 0.01$, $50 \leq n \leq 239$ individuals per strain).

5.3 Discussion

After discovery of the highly penetrant L1 seam branching phenotype caused by inappropriate ventral migration of posterior seam daughters in *pal-1(e2091)* animals, we were interested to discover the molecular mechanism of this event. We therefore took *pal-1(e2091)* animals and subjected them to RNAi knockdown of various genes known to be involved in migratory processes in *C. elegans*, in order to look for enhancers or suppressors of the branching phenotype after the L1 division. This screen, despite small numbers of animals being quantified, was surprisingly successful in isolating, out of the many different molecular migratory pathways screened for, only members of two signalling pathways: Wnt and netrin.

The relationship between Wnt and *pal-1* is likely to be complex

We have already explored a possible role for Wnt in regulating *pal-1* through the intronic enhancer element, discussed in Chapter 3, however it is interesting to note that all the members of the Wnt pathway isolated in this screen act as suppressors of the *pal-1* loss-of-function phenotype. If there was a simple direct linear relationship between Wnt and *pal-1*, with Wnt acting upstream, then mutating Wnt in a *pal-1* background should not have any effect on the *pal-1* phenotype, or, if Wnt has a separate, *pal-1*-independent function to regulate posterior development then this double knockout should enhance any *pal-1* phenotypes. The suppression of *pal-1* then would suggest that the relationship between Wnt and *pal-1* is more complex. In this arrangement, *pal-1* may also be able to work through Wnt mediators, placing Wnt downstream (as well as upstream) of *pal-1*. Interestingly, one of the members of the Wnt pathway isolated as a suppressor of *pal-1*, the Wnt ligand c*wn-1*, has already been suggested to work downstream of *pal-1* in specifying the C lineage during embryogenesis, mediating *pal-1* regulatory control of the *even-skipped* homologue *vab-7* (Baugh, Hill et al. 2005). It is tempting to speculate that,

since *cwn-1* was the only Wnt ligand isolated in the screen and the two other Wnt pathway genes isolated were either the Wnt receptor *lin-17* or the *lin-17* co-localisation component *cam-1*, that an interaction between CWN-1 and LIN-17 may lie in the *pal-1* regulatory pathway. *lin-17* is also known for its role in male tail development (Maloof, Whangbo et al. 1999).

A new role for netrin in posterior body patterning during embryogenesis

Five different members of the netrin pathway or known modulators of the netrin pathway were isolated as either suppressors or enhancers of the aberrant *pal-1* seam branching phenotype, making up the majority of the genes isolated in the screen. For the case of two of these genes, *let-92* and *unc-51*, their physiological roles oppose one another, and gratifyingly they were isolated as a suppressor and an enhancer of the *pal-1* phenotype respectively. *unc-51* is also a member of the autophagy pathway in *C. elegans*, a mechanism that degrades unwanted cellular components throughout development. However, RNAi knockdown of other members of the autophagy pathway in *C. elegans* had no effect on the *pal-1* cell migration phenotype, and therefore the role of *unc-51* with respect to *pal-1* appears to be specifically related to the netrin pathway (this data was not shown). In addition, another pair of genes isolated, *unc-129* and *unc-130* also have a direct relationship within the netrin pathway, as *unc-130* acts to regulate the expression of *unc-129*.

The sole netrin ligand, *unc-6*, was not isolated in the screen, but we have since been informed that *unc-6* RNAi is largely ineffective (R. Pocock, pers. comm.). The null mutant of this ligand, *unc-6(ev400)*, proved to be much more informative, as it displayed marked synthetic effects with *pal-1(e2091)* during the perturbed L1 morphogenic event of seam daughter migration. Not only was this larval phenotype made synthetically worse, but surprisingly, animals appeared in the hatched population that were severely ‘Nob’ in phenotype. As this is a characteristic *pal-1* null

phenotype, in which 80% of eggs hatch with this phenotype (Edgar, Carr et al. 2001), this suggests that *unc-6* and the netrin pathway have a novel role in patterning the posterior embryo in the absence of full native *pal-1* expression. This phenotype has never been associated with netrin mutants before this study.

Even in the *pal-1(e2091); unc-6(ev400)* double mutant population, there is still a discrepancy between the number of animals which hatch with a Nob phenotype (20%) and the amount of Nob animals observed in the *pal-1* null mutant populations (80%, with the remaining 20% dead before hatching). This would suggest that a third pathway regulates posterior patterning in the embryo, and that this pathway is normally regulated by fully-functional *pal-1*. Although a screen for either embryonic lethality or Nob phenotypes in a *pal-1(e2091); unc-6(ev400)* or *unc-6(ev400)* background would be informative, given the complex but intimate nature of the interaction of *pal-1* with the Wnt pathway, it may be interesting to observe the phenotypes of *pal-1; netrin; Wnt* animals as a starting point. Another potential candidate would be the *pal-1* Hox gene target *nob-1*, which from its name indicates a role in posterior development.

We have shown here that three separate alleles of *unc-6* all display some degree of synthetic phenotype with *pal-1(e2091)*, making it extremely unlikely that the synthetic effects seen are due to a second site mutation and not due to mutations in netrin. We have not been able to build an equivalent allelic series with null alleles of *pal-1* due to their lethal nature. However, there have been two other very weak alleles of *pal-1* isolated, *ns114* and *ns115*, of which *ns114* is thought to affect a rarely used alternative splice variant resulting in a null translated product (Maurer, Chiorazzi et al. 2007). It would be interesting, therefore, to cross these alleles into netrin mutants and see whether they are also able to produce synthetic effects. Alternatively, to be absolutely sure of the contribution of *pal-1(e2091)* to the synthetic phenotypes of the *pal-1; netrin* double

mutants, it would be best to show rescue of the double mutant phenotypes with a genomic *pal-1* transcript.

Dissecting the contributions of the netrin receptors *unc-5* and *unc-40* in posterior body patterning and embryonic development

In order to further dissect the role of netrin in posterior body patterning, we analysed null mutants of each of the known netrin receptors, *unc-5* and *unc-40*. It has previously been observed that if a cell or growth cone expresses both these receptors, they will be repulsed from high ventral concentrations of *unc-6*, whereas if the receptor *unc-40* is expressed alone, this stimulates an attraction to high concentrations of *unc-6*. Double mutants of each of the two receptors with *pal-1(e2091)* showed that both receptors were required in the netrin pathway for posterior patterning in the absence of *pal-1*, as indicated by both double mutants displaying a synthetic 'Nob' phenotype in the population of hatched animals. Furthermore, each *receptor; pal-1* double mutant displayed approximately half the percentage of Nob animals observed in the *pal-1(e2091); unc-6(ev400)* population, indicating that the contributions of each receptor to the pathway are independent. However, this would be confirmed with the creation of a triple *unc-40(e271); pal-1(e2091); unc-5(e53)* mutant.

pal-1(e2091); unc-6(ev400), as well as displaying a synthetic 'Nob' phenotype at hatching, also displays an increase in synthetic embryonic lethality that appears entirely dependent on the *unc-5* receptor. Interestingly, it has been shown previously that *pal-1* null alleles display 20% embryonic lethality due to failures in ventral intercalation, indicating that *pal-1* is essential for this event (Edgar, Carr et al. 2001). *pal-1(e2091)* displays no embryonic lethality in its population, suggesting that the loss of *pal-1* expression caused by the *e2091* allele is not enough to perturb ventral intercalation. However, since there is an approximately 20% synthetic

embryonic lethality in either of the *pal-1(e2091); unc-6(ev400)* or *pal-1(e2091); unc-5(e53)* populations, this suggests that *unc-6* and *unc-5* are required for an essential event during embryogenesis, separate from the role of netrin in posterior body patterning but also controlled by *pal-1*. It would be very interesting to see whether this requirement is during ventral enclosure, as with the *pal-1* null mutants.

Other experiments that would be useful to further dissect the roles of *unc-40* and *unc-5* in posterior patterning and embryonic development would be to analyse differences in the localisation of the full genomic translational reporters for these receptors. In light of the emerging importance of intronic enhancer elements described both in this work and elsewhere (C. Brabin, D. Phil. thesis, 2011), it is interesting to note that previous expression studies of these two reporters have not included the full genomic sequence of either gene.

The role of *pal-1* in neuronal development: a post-embryonic effect?

We have described how netrin has a previously uncovered role in regulating posterior patterning in embryos. However, we have also discovered that motor neurone axon migration, an event entirely dependent on the netrin pathway, is also partially dependent on *pal-1*. Axon migration defects in weak netrin alleles were found to synergise with *pal-1(e2091)* for both *unc-6* and its two receptors *unc-5* and *unc-40*. However, it is interesting to observe that proven roles of *pal-1* in post-embryonic development, as discovered so far, are limited to the activation of expression of Hox genes in the posterior seam cell V6 during male tail development. Otherwise, it has been shown that *pal-1* does not synergise with *unc-6* in the development and guidance of the gonad, and although there is a synthetic increase in the number of bagged mothers in the double mutant population, this could be accounted for by the general disorganisation of the epidermis at hatching and subsequently during the migration of P cells to form the vulval precursor cells.

Therefore, since the synthetic phenotype of *pal-1* with netrin in the migration of the axons is not 100% penetrant, it is conceivable that *pal-1* may have a role only in the migration of the DD motor neurones, those that migrate during embryogenesis, rather than the post-embryonic migration of the VD neurones descended from the P cells. Unfortunately I have only had time to score these strains for migration at the L4 stage prior to this report.

An unexpected synthetic phenotype of *pal-1(e2091); unc-6(ju152)* was observed when imaging the commissures of the motor neurones, which involved the abnormal positioning of mid-body neuronal cell bodies. However, defects in P cell migration lead to neurones being born in lateral positions along the worm (Spencer, Orita et al. 2001), and therefore this is likely to occur due to the severe patterning defects in the mid-body epidermis associated with *pal-1(e2091); unc-6* double mutants. The mis-positioning of the cell was much weaker in *pal-1(e2091); unc-5(ju181)* double mutants, although the *unc-5* allele appears weaker than the *unc-6* allele in terms of commissure guidance defects. The number of cell bodies misplaced in the mid-body of *unc-40(e1430); pal-1(e2091)* animals was increased from the number in the *unc-40(e1430)* single mutant, but the anterior cells misplaced in the single mutant appeared unaffected by *pal-1(e2091)*. These anterior cell body placement defects therefore appear to be independent of *pal-1*.

One phenotype observed (but not quantified) in *unc-40(e271); pal-1(e2091)* double mutants but not in *unc-40(e271)* single mutants or in any other netrin or *pal-1* single or double mutant strain is that worms appear to be compromised in their ability to find and stay with food. This behavioural defect may reflect a synthetic role for *unc-40* and *pal-1* in the development of neurones other than the motor neurones, for example in the sensory neurones.

pal-1 works with netrin to specify the development of the male tail

The post-embryonic phenotypes of *pal-1* appear to be restricted to the formation of the male tail. This is a process that requires the activation of expression of Hox genes in V6. However, the abnormally small number of rays seen on a *pal-1(e2091)* male tail is decreased further in a *unc-6* mutant background, suggesting that *unc-6* works with *pal-1* in the specification of the lineages which contribute to the male tail. However, without lineaging these mutants it is impossible to tell whether *unc-6* is required for fate specification or whether it is required for the morphological events which take place to form the sensory rays embedded in the cuticular fan that makes up the male tail.

max-2, a suppressor of *pal-1*, is a p21-activated kinase (PAK)

p21-activated kinases are well-known for their role in regulating cytoskeletal dynamics, particularly in the cell reshaping required for development of the nervous system (Bokoch 2003), and the role of *max-2* in suppressing *pal-1* migratory phenotypes therefore begins to shed some light on the cellular mechanics of the epidermal migration during L1. *max-2* is able to suppress the abnormal migration of seam cells in the *pal-1(e2091)* mutant not by correcting the abnormal arrangement of the seam cells to the ventral P cells, but by reducing the number of seam cells that physically move to the ventral midline. This would suggest that *max-2* is not in a regulatory pathway with *pal-1* in terms of epidermal patterning, but is rather one of the components required by the epidermis to remodel during L1. It would be interesting to observe the differences in wild-type anterior L1 seam daughter migration in a *max-2* mutant, and to analyse whether the protrusions grown by the dividing seam cells show any differences in their characteristics or display retarded growth.

max-2 has previously been identified as having a role in several migratory events during *C. elegans* development, including during netrin-mediated axon migration of the motor neurones (Lucanic, Kiley et al. 2006), gonadal distal tip cell migration (Lucanic and Cheng 2008, Peters, Gossett et al. 2013) and also P cell migration during L1 (Lucanic, Kiley et al. 2006). The single mutant effect on P cell migration cannot account for the failures in the seam cells to migrate during suppression of the *pal-1(e2091)* mutant phenotype, however, due to its complete redundancy in this process with a second *C. elegans* PAK, *pak-1* (Lucanic, Kiley et al. 2006). Although *max-2* acts redundantly with *pak-1* during both P cell migration and distal tip cell migration, it functions separately from other PAKs in the regulation of axon migration and is also regulated differently to *pak-1* (Lucanic, Kiley et al. 2006, Lucanic and Cheng 2008, Peters, Gossett et al. 2013). From this study it would also appear that *max-2* acts independently to and in a separate function from *pak-1* during seam daughter migration in L1.

It would be interesting to analyse whether the other enhancers and suppressors of *pal-1(e2091)* isolated in the initial RNAi screen suppress or enhance the *pal-1* phenotype at the level of mid-body cellular organisation, as with *unc-6*, or whether they repress or enhance *pal-1* phenotypes at the mechanistic level of cell movement, as with *max-2*.

CHAPTER 6

A *C. elegans* Hedgehog? The role of *wrt-2* in the hypodermis

6.1 Introduction

In their 2011 Development paper (Wildwater, Sander et al. 2011), the authors first described the use of a new *wrt-2* promotor-driven GFP strain to specifically mark the seam cells of *C. elegans*. The GFP driven by this promoter was so highly expressed that the construct could be used for automated video-lineaging of the seam (Wildwater, Sander et al. 2011). Throughout this project, I have been able to use this marker to both outline seam cell shapes, using the integrated *wrt-2p::gfp::PH* construct, and also to visualise the nuclei of the seam cells with the co-integrated *wrt-2p::gfp::H2B* construct. *wrt-2*, however, has not been characterised in terms of seam cell development or function. As this gene is so highly expressed in the seam cells throughout larval and adult development, therefore making a dramatic début on the scene of

seam cell development as a marker of seam fate within this lineage, it would be beneficial to further characterise this gene in able to more fully interpret the readout of this expression pattern.

The *wrt-2* promoter was selected as a suitable candidate for strong seam cell-specific expression of GFP on the advice of Thomas Bürglin, in a personal communication to Sander van den Heuvel (Sander van den Heuvel, pers. comm.). This chapter focuses on the expression pattern and function of *wrt-2*, with the aim of further understanding both the nature of the gene itself and also to gauge how the expression of the *wrt-2* promoter construct used throughout this study may be interpreted with regard to seam cell development.

Hedgehog (Hh) signalling in development

Hedgehog (Hh) was first identified during genetic screens for embryonic lethal patterning defects in *Drosophila*, and named due to the characteristic disorganised bristles on embryos null for Hh (Nusslein-Volhard and Wieschaus 1980). Subsequent cloning and molecular analysis of the gene found that the product was secreted and acts on adjacent cells to promote pattern formation (Lee, von Kessler et al. 1992, Mohler and Vani 1992, Tabata, Eaton et al. 1992, Tashiro, Michiue et al. 1993). Hedgehog signalling and function has been found to be conserved in many other species including mammals (Echelard, Epstein et al. 1993, Krauss, Concordet et al. 1993, Riddle, Johnson et al. 1993, Chang, Lopez et al. 1994, Roelink, Augsburger et al. 1994, Shimeld 1999); a malfunctioning Hedgehog pathway in humans is the cause of congenital diseases such as holoprosencephaly (Belloni, Muenke et al. 1996, Roessler, Belloni et al. 1996, Maity, Fuse et al. 2005). Hedgehog signalling has also been implicated in the development of various cancers (Beachy, Karhadkar et al. 2004).

Hedgehog processing and secretion

Hedgehog proteins are known to be auto-cleaved in the endoplasmic reticulum by their enzymatic carboxyl 'Hog' domain, before release of the active, signalling amino 'Hedge' domain (Lee, Ekker et al. 1994, Fan, Porter et al. 1995, Lopez-Martinez, Chang et al. 1995, Porter, von Kessler et al. 1995, Chen, Tukachinsky et al. 2011). At the same time, cholesterol is added to the signalling domain at its carboxyl terminus and palmitic acid near its amino terminus (Porter, Young et al. 1996, Pepinsky, Zeng et al. 1998). Both cleavage and subsequent post-translational modification have proven important for Hedgehog function, with lipidation particularly necessary for oligomerisation of the molecule with subsequent effects on the motility of Hedgehog (Roessler, Belloni et al. 1997, Pepinsky, Zeng et al. 1998, Chamoun, Mann et al. 2001, Lewis, Dunn et al. 2001, Taylor, Wen et al. 2001, Zeng, Goetz et al. 2001, Gallet, Rodriguez et al. 2003, Chen, Li et al. 2004, Feng, White et al. 2004, Callejo, Torroja et al. 2006, Gallet, Ruel et al. 2006, Li, Zhang et al. 2006, Huang, Litingtung et al. 2007, Dennis, Kurosaka et al. 2012, Ducuing, Mollereau et al. 2013, Petrova, Rios-Esteves et al. 2013, Callier, Calvel et al. 2014).

Release of the modified Hedgehog from the cell (Fig. 6.1.1) is dependent on the transmembrane protein Dispatched (DISP) which binds the cholesterol moiety (Burke, Nellen et al. 1999, Ma, Erkner et al. 2002, Tian, Jeong et al. 2005). In vertebrates, DISP acts synergistically with SCUBE2, a glycoprotein that also binds cholesterol at a different location to promote release of Hedgehog from the surface of the cell (Creanga, Glenn et al. 2012, Tukachinsky, Kuzmickas et al. 2012). Investigations into how the membrane-tethered Hedgehog is transported to target cells has lead to the discovery that cytonemes from cells active for Hedgehog signalling carry exosomes in order to direct the restricted distribution of the lipidated Hedgehog signalling protein (Bischoff, Gradilla et al. 2013, Gradilla, Gonzalez et al. 2014).

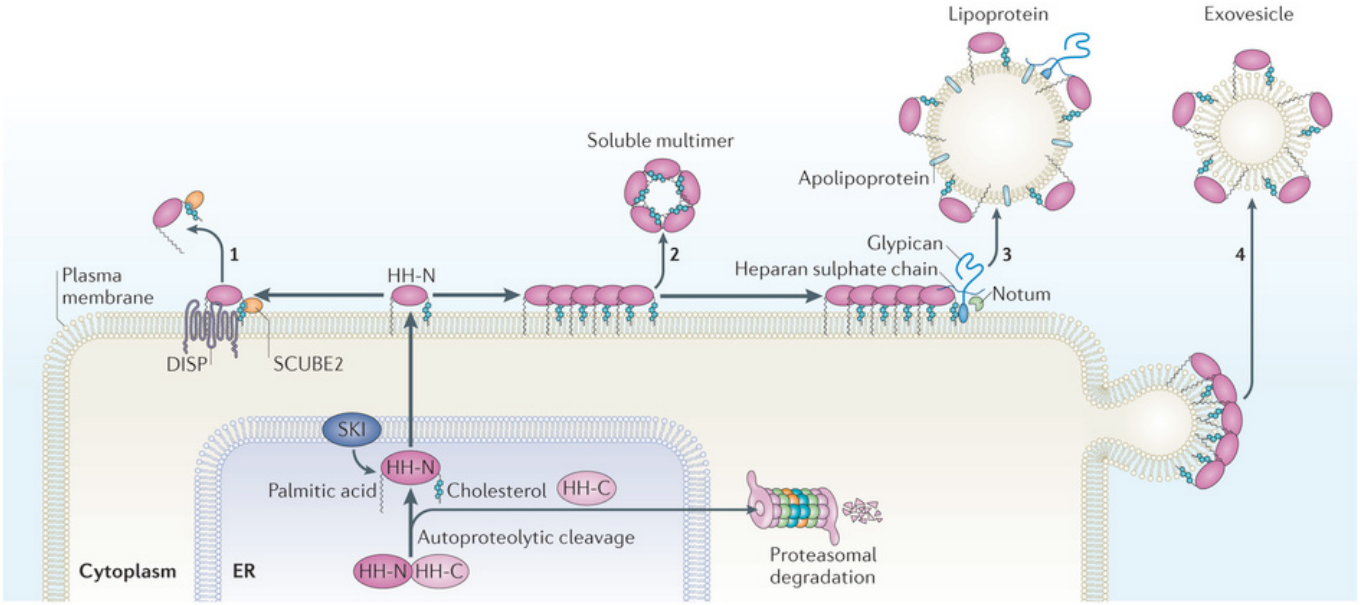

FIG. 6.1.1 – A SUMMARY OF HEDGEHOG PROCESSING AND SECRETION (FIGURE FROM BRISCOE AND THEROND 2013).
The Hedgehog pro-peptide contains an amino 'Hedge' signalling domain and a carboxyl 'Hog' domain, which catalyses the auto-proteolytic cleavage between the two domains in the endoplasmic reticulum (ER). The carboxyl 'Hog' domain is targeted for proteasomal degradation. During the auto-cleavage reaction, a cholesterol is added to the carboxyl terminus of the 'Hedge' domain and the enzyme Skinny Hedgehog (SKI) catalyses the addition of palmitic acid near the amino terminus. After these lipid modifications, the signalling domain of Hedgehog is transported out of the cell by Dispatched (DISP), or may form various multimeric complexes or exovesicles in order to leave the cell.

The Hedgehog signalling pathway

Core components of the Hedgehog signalling pathway (Fig. 6.1.2) were identified using genetic screens in *Drosophila (Forbes, Nakano et al. 1993)*. The first component in the pathway is the Hedgehog receptor, Patched, which constitutively represses Hedgehog signalling through inhibition of a second transmembrane protein, Smoothened (Smo) (Hooper and Scott 1989, Nakano, Guerrero et al. 1989, Alcedo, Ayzenzon et al. 1996, Chen and Struhl 1996, van den Heuvel and Ingham 1996). Upon Hedgehog binding to Patched, the inhibition of Smoothened is repressed, leading to the activation of the GLI family of transcription factors, targets of the Hedgehog pathway (Alexandre, Jacinto et al. 1996, Dominguez, Brunner et al. 1996, Marigo, Johnson et al. 1996, Lee, Platt et al. 1997, Von Ohlen, Lessing et al. 1997).

Hedgehog signalling in *C. elegans*

Thomas Bürglin has previously identified many Hedgehog-related genes in *C. elegans*: 22-32% homology was detected between protein sequences of the carboxyl terminus of a group of *C. elegans* proteins to the carboxyl-terminal 'Hog' domain of Hedgehog molecules in flies and vertebrates (Burglin 1996). Surprisingly, the active signalling domain of Hedgehog, the 'Hedge' domain, contained in the amino terminus of the protein, was not found to share homology with the *C. elegans* family of Hog-containing proteins (Burglin 1996). This lead to the classification of novel amino-terminal domains associated with Hog in *C. elegans*, initially Warthog (WRT) and Groundhog (GRD) (Burglin 1996), followed by Groundhog like (GRL) and Quahog (QUA) (Aspock, Kagoshima et al. 1999). Further to their identification, the group of Hedgehog-related genes in *C. elegans* - a total of 61 of which 10 are associated with a Hog domain (Aspock, Kagoshima et al. 1999) - were analysed for expression patterns from their predicted promotors, or from the promotor and predicted first exon (Aspock, Kagoshima et al. 1999, Hao, Johnsen et

al. 2006). Many of these genes were found to be expressed in the ectoderm, including the seam cells; genes expressed in but not limited to the seam include *wrt-2*, *wrt-9*, *wrt-5*, *wrt-10*, *grd-5*, *grd-10*, *grd-14*, *grl-4*, *grl-5*, *grl-7*, *grl-15*, *grl-17* and *grl-21* (Aspock, Kagoshima et al. 1999, Hao, Johnsen et al. 2006).

Despite having no Hh homologues, the *C. elegans* genome does contain Patched and Patched-related genes (Kuwabara, Lee et al. 2000, Zugasti, Rajan et al. 2005), as well as a homologue of Dispatched, CHE-14 (Michaux, Gansmuller et al. 2000). However, *C. elegans* has no *bone fide* Hedgehog signalling pathway, in part due to the lack of a homologous 'Hedge' domain, but vitally, the *C. elegans* genome lacks an orthologue of Smoothened (Smo).

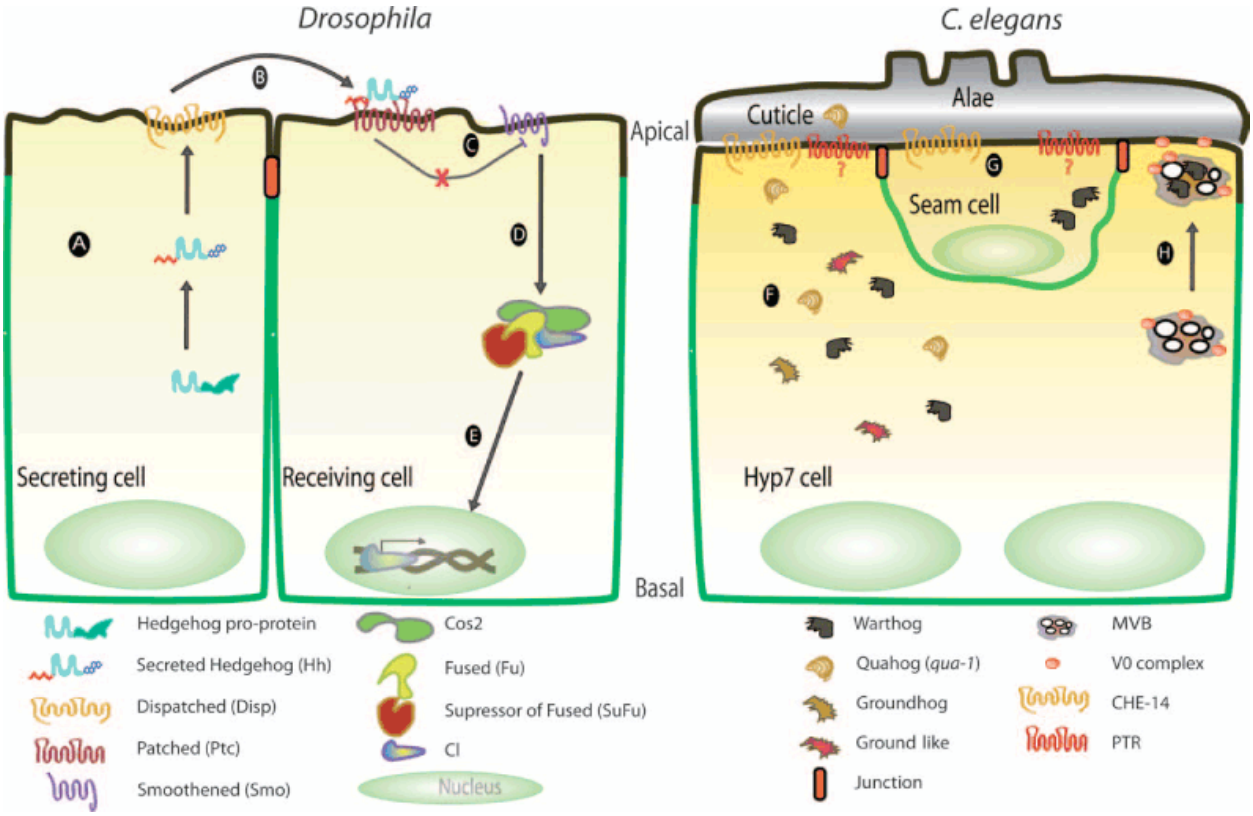

FIG. 6.1.2 – A COMPARISON OF HEDGEHOG SIGNALLING IN *DROSOPHILA* AND *C. ELEGANS* (FROM *KOLOTUEV, APAYDIN ET AL. 2009*).
A. In *Drosophila*, the signal-secreting cell expresses a pro-protein version of Hedgehog. The carboxyl terminal domain possesses auto-catalytic activity and cleaves the protein in two; after subsequent post-translational modification (see fig. 6.1.1) the amino-terminal signalling peptide is secreted and the carboxyl terminal is sequestered to the endoplasmic reticulum and proteolytically degraded. The membrane protein Dispatched is responsible for transporting Hedgehog out of the cell. **B.** The signal-receiving cell expresses the Patched receptor on its apical surface. **C.** Upon binding Hedgehog, Patched ceases its inhibitory effect upon a second transmembrane protein, Smoothened. **D, E.** The loss of the Patched interaction allows Smoothened to signal, through multi-protein complex intermediates, to the nucleus of the cell and activate transcription of target genes. **F.** In *C. elegans*, the hypodermis is known to express most Hedgehog-related genes, including Warthogs, Quahogs and Groundhogs. The transporter CHE-14, a homologue of Dispatched, mediates secretion of these proteins apically, along with the V0 subunit of the V0-ATPase which secretes multi-vesicular bodies (MVBs), which then shed exosomes containing Hedgehog-related proteins (**H**). **G.** The seam cells of the hypodermis may express Patched, along with known expression of Hedgehog-related genes, although association of a Hedgehog-like ligand with a receptor in *C. elegans* has not been identified. Notably, *C. elegans* does not possess a homologue of Smoothened.

wrt-2: a *C. elegans* Warthog

wrt-2 was identified in the initial genomic screen by Thomas Bürglin (Burglin 1996). Interestingly, it was not identified through homology of a 'Hog' domain (which it is not predicted to contain) but rather in a secondary analysis, subsequent to the characterisation of the novel *C. elegans* 'Wart' domain (Burglin 1996, Aspock, Kagoshima et al. 1999). The only hog-containing *wrt* genes, out of *wrt-1* to *-10*, are *wrt-1*, *wrt-4*, *wrt-6*, *wrt-7* and *wrt-8* (Fig. 6.1.3 A, Aspock, Kagoshima et al. 1999). A summary of the relationships between the Wart-containing genes in *C. elegans*, *C. briggsae* and *B. malayi* (a pathogenic nematode closely related to the *Caenorhabditis* genus) is shown in figure 6.1.3 B.

To date, the only *wrt* gene in *C. elegans* that has undergone extensive analysis is *wrt-5*, which does not contain a 'Hog' domain (Hao, Aspock et al. 2006). In this study, the expression pattern of *wrt-5* was investigated using a carboxyl-terminal full-length GFP fusion: GFP expression shows that WRT-5 is a secreted protein. As the carboxyl-terminal GFP tag is not cleaved or degraded, this expression pattern is consistent with the predicted absence of an auto-catalytic carboxyl 'Hog' domain; furthermore, rescue studies of a strong deletion mutant of *wrt-5* causing a hypodermal patterning phenotype establishes that there is no need for a 'Hog' domain for the 'Wart' domain to have a functional role in *C. elegans* (Hao, Aspock et al. 2006). However, it has been shown *in vitro* that the *C. elegans* 'Hog' domain of WRT-1 acts as an auto-catalytic subunit to cleave between the two protein domains (Porter, Ekker et al. 1996), although no phenotypic or functional analysis of WRT-1 or its amino-terminal signalling component has been performed *in vivo*.

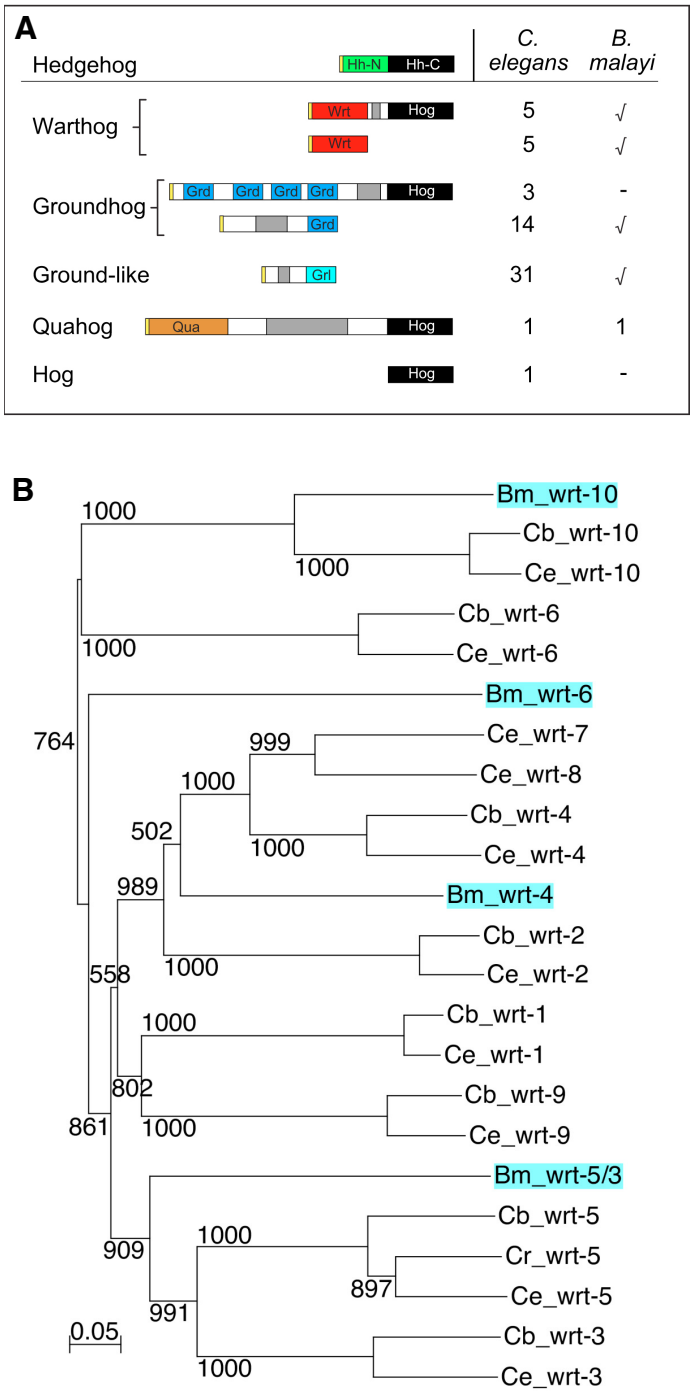

FIG. 6.1.3 – HEDGEHOG RELATED GENES IN *C. ELEGANS*.
A. Structural features of the Hedgehog related genes in *C. elegans* (adapted from Burglin and Kuwabara 2006). Numbers indicate the number of genes in each gene class in *C. elegans* and the tick represents whether or not the gene class is represented in the *B. malayi* genome. **B.** Phylogenetic tree of Wart domains of Warthog Hedgehog-related genes in *C. elegans* (Ce), *C. briggsae* (Cb) and *B. malayi* (BM) (Burglin 2008). *B. malayi* genes are highlighted in light blue. The numbers represent the results of 100 bootstrap trials used to generate the tree.

The expression pattern of *wrt-2* has been analysed previously in a global *C. elegans* Warthog expression pattern study using a construct containing the entire upstream intergenic region and only the first few exons of the coding region (Aspock, Kagoshima et al. 1999). This construct was found to express in the seam cells from the 1.8-fold stage in the embryo to adulthood. Using a full-length amino-terminal GFP fusion construct of *wrt-2*, Michael Labouesse and colleagues determined that *wrt-2* was exported from the seam cells apically by the V0 domain of the V0-ATPase: mutations in this transporter lead to a build up of GFP inside the cells (Liegeois, Benedetto et al. 2006).

In a genome-wide study that measured with high temporal resolution the levels of mRNA transcripts in developing larvae, *wrt-2* was found to have one of the most highly cyclical gene expression profiles of any gene in *C. elegans* (Hendriks, Gaidatzis et al. 2014). Indeed, many Hedgehog-related genes were found to be highly oscillatory, including the Patched genes, the putative *C. elegans* Hedgehog receptors (Hendriks, Gaidatzis et al. 2014). Consistent with its strongly cyclical expression, *wrt-2* has been implicated in moulting and cuticle formation: RNAi experiments showed that knockdown of *wrt-2* resulted in a low penetrance of moulting defects between the L4 and adult moult, as well as growth and unc (uncoordinated) defects (Zugasti, Rajan et al. 2005). However, no analysis yet of *wrt-2* has been performed on a mutant allele.

6.2 Results

heIs63, containing *wrt-2p::gfp::PH* and *wrt-2::gfp::H2B*, is expressed in the seam and remodelling P cells

heIs63, driven by the *wrt-2* promoter and kindly given to us by M. Wildwater from Sander van den Heuvel's laboratory in Utrecht, is expressed in the seam cells from the start of embryonic elongation throughout post-embryonic development and continues to express during adulthood in the fused seam (not shown). In addition to the seam cell expression, we observed that ventral cells start to show high expression of the reporter midway through L1 although expression is gone again by L2. Closer analysis revealed that these additional expressing cells were the remodelling P cells during their L1 migration down to the ventral midline (Fig. 6.2.1, third and fourth panels).

The *heIs63* reporter (which is visible in the nucleus as well as on the membrane of expressing cells) is not visible in P cells upon hatching (Fig. 6.2.1, first panel). Midway though L1, the seam cells start to divide. During this time, expression of the *wrt-2* reporter remains high in the posterior daughters of the seam cells, the Vn.ps, but begins to fade in the hypodermally-fated anterior seam daughters (Vn.as, see Fig. 6.2.1 second panel). Until this point, the seam cell lineages are the only cells to express from the *wrt-2* promoter.

However, as the anterior daughters fuse to the hypodermal syncytium, the P cells start to reduce their cytoplasmic volume and retreat down to the ventral midline, where they intercalate with their corresponding partner from the opposite side of the animal to form a single line of cells. It is during this migration that the *wrt-2* promoter is strongly expressed in these cells (Fig. 6.2.1, third panel). P cells continue to express from *wrt-2* during the intercalation process, but appear to lose GFP as they begin to rapidly divide to produce the Pn.p cells, hypodermal and neuronal

tissue. This can be seen in the fifth panel of figure 6.2.1, which shows a projection of a z stack though one lateral half of the animal at the end of the L1 seam cell division. A single z frame has been isolated from the stack and shown adjacent to the panel in order to observe the P cell descendants at the ventral midline in more detail. The P cell descendants show very weak expression of the *heIs63* reporter at the membrane of the cells, but no nuclear expression indicating that this expression is perhaps a result of perdurance of the GFP protein inherited from the ancestral P cells and the *wrt-2* promoter is no longer being actively turned on.

By the L2 stage of development, the *heIs63* construct is completely turned off in any ventral cell. No other cells have been observed which express *wrt-2p::GFP* from this construct.

Expression analysis of the upstream intergenic region of *wrt-2*

In order to further dissect expression of *wrt-2* in the seam cells and P cells, I cloned the entire upstream intergenic region of *wrt-2* into the GFP expression vector pPD107.94, which contains the GFP ORF with an NLS, and a minimal *C. elegans* promoter, *pes-10*. This construct was able to recapitulate expression of the *heIs63* construct in the seam and P cells during L1 (Fig. 6.2.2).

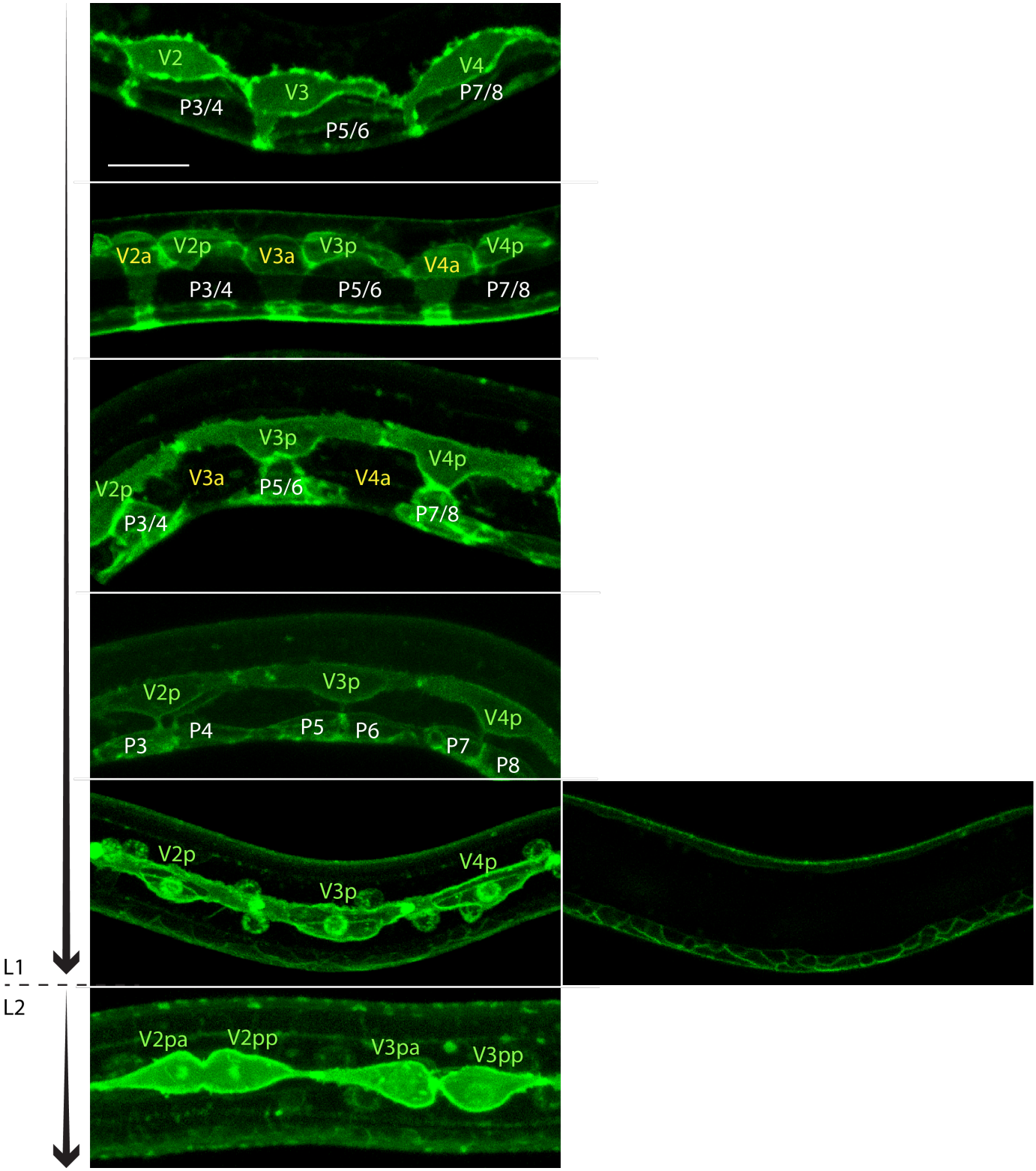

FIG. 6.2.1 – DYNAMIC EXPRESSION OF *HEIS63* IN THE P CELLS DURING THE FIRST TWO SEAM CELL DIVISIONS.
In addition to all of the seam cells (V cells indicated), *heIs63* is also expressed in the migrating P cells during L1, and is gone again by the time of the first L2 seam cell division. Arrows represent time, with the L1/L2 moult indicated. There is no P cell expression in newly hatched animals (first panel) but expression is turned on as the cells start to migrate to the ventral midline (third and fourth panels). Expression in the P cells is almost completely gone by the end of L1, when the P cells have undergone several divisions in order to contribute to hypodermal and neuronal tissues (fifth panel). A single z plane has been isolated from the stacked image adjacent to the fifth panel to display with better resolution the P cell descendants at the ventral midline. P cell expression is completely gone by the time of the L2 symmetrical division. Scale bar = 10 μm.

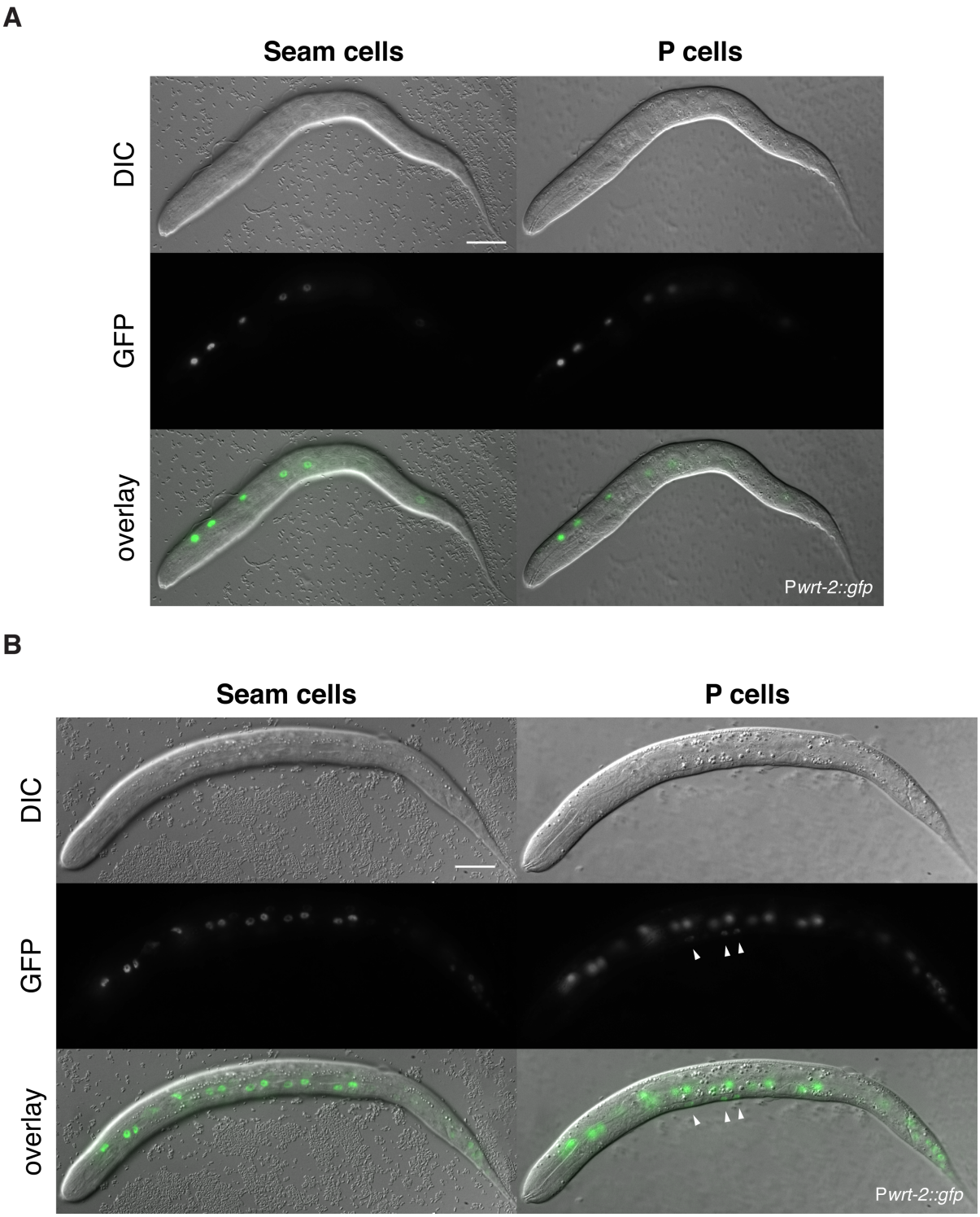

FIG. 6.2.2 – EXPRESSION OF A TRANSCRIPTIONAL REPORTER FOR THE *WRT-2* UPSTREAM INTERGENIC REGION DURING L1.
The entire upstream intergenic region of *wrt-2* was cloned into the GFP expression vector pPD107.94 and transgenic animals carrying this reporter were analysed. **A.** A newly hatched transgenic worm containing the P*wrt-2::gfp* reporter. Two planes of focus are shown: the reporter can be seen in the nuclei of the seam cells in one plane (not all seam cells can be seen due to the mosaicism of the reporter line) but no green nuclei are seen at the ventral midline (second plane of focus). **B.** The same transgene in a worm undergoing the first seam cell division in L1. Again, two planes of focus are shown. The first image shows the GFP-positive dividing seam cells, with the anterior daughters losing GFP as they differentiate. The second plane of focus shows the ventral midline, at which there are several green nuclei corresponding to the intercalating P cells (arrowheads). Scale bars = 10 μm.

Bioinformatic analysis of the *wrt-2* promotor region reveals three highly conserved TF target sequences

From an alignment of the upstream *wrt-2* intergenic promoter region in *C. elegans* with other *Caenorhabditis* species (Supplementary Fig. S1), we discovered that the region closest to the start codon of *wrt-2* is more highly conserved between species than the distal portion (see figure 6.2.3 B). This conservation suggests that this region is likely to contain important enhancer elements for *wrt-2* expression. Subsequently, this intergenic sequence was also found to contain a predicted but uncharacterised non-coding RNA (ncRNA) in a region of strong sequence conservation (Gerstein, Lu et al. 2010). The position of this ncRNA, F52E4.12, is shown in figure 6.2.3.

We entered the conserved sequence into the vertebrate JASPAR transcription factor binding site database (Mathelier, Zhao et al. 2014), with a relative profile score threshold of 90%, and cross-referenced any hits with the alignment in Fig. S1. Only those hits that were conserved between all three *Caenorhabditis* species were noted. This method narrowed potential transcription factor binding sites down to those of three candidate transcription factors (TFs): *egl-13*. *ets-4* and *blmp-1*, *egl-13* and *ets-4* were identified as potential candidates by Vitan Blagotinsek during his summer studentship in the laboratory. Of these candidates, *ets-4* and *blmp-1* are known to be expressed in the seam cells, with *ets-4* also expressed in the P cells during their remodelling down to the ventral midline in L1. The SOX transcription factor *egl-13* is not known to be expressed in the seam cells. The only predicted transcription factor binding site also within the ncRNA sequence is the *blmp-1* binding site.

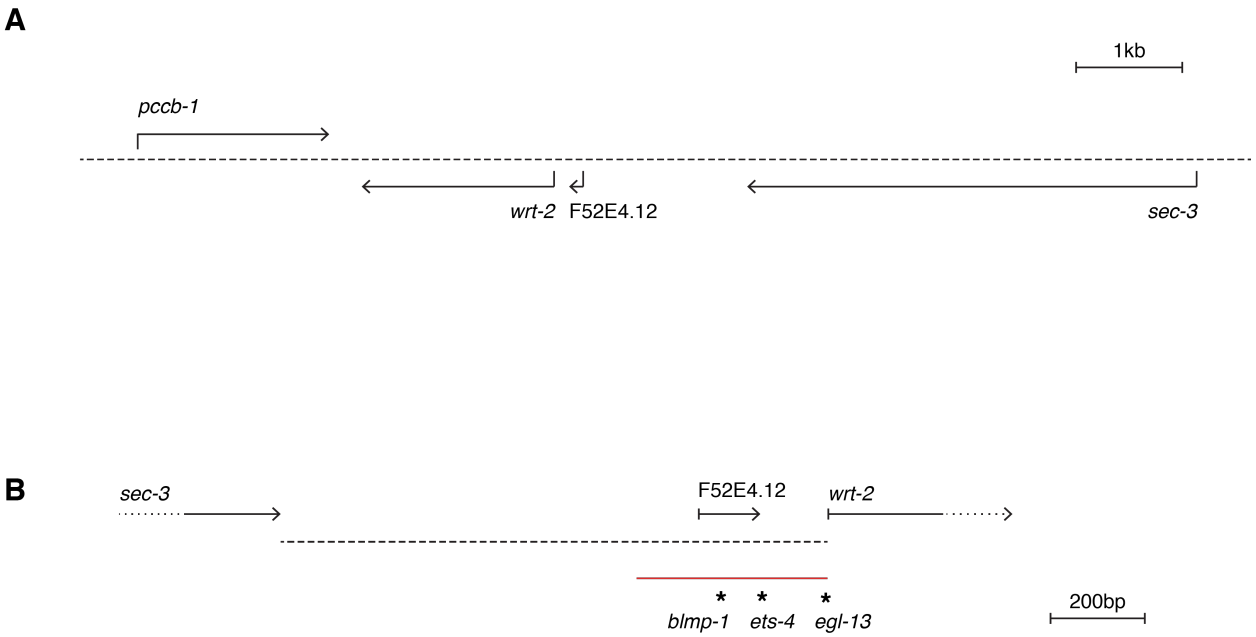

FIG. 6.2.3 – BIOINFORMATIC ANALYSIS OF THE INTERGENIC REGION UPSTREAM OF *WRT-2* REVEALS *BLMP-1, ETS-4* AND *EGL-13* AS POTENTIAL ACTIVATORS OF *WRT-2* TRANSCRIPTION.
A. *wrt-2 in situ* on chromosome X, to scale. Open reading frames of *wrt-2* and surrounding genes are indicated with arrows corresponding to gene length and direction (scale bar indicates length). The intergenic region between *sec-3* and *wrt-2* contains the promoter for *wrt-2*, as determined in figure 6.2.2. However, this region also contains an uncharacterised predicted ncRNA, F52E4.12. **B.** Intergenic region between the end of *sec-3* and the start of *wrt-2* (to scale). The region of high sequence conservation is indicated with a red bar, and the predicted sites of transcription factor binding are shown with asterisks. Scale bar indicates length.

Full-length WRT-2 localisation *in vivo*

Given that *wrt-2* is not predicted to encode an auto-catalytic carboxyl 'Hog' domain, I first constructed a carboxyl-terminus GFP reporter containing the entire open reading frame of *wrt-2* and the same upstream intergenic region used to drive GFP expression in figure 6.2.2. However, I found that I could not observe any GFP expression in any lines of the transgenic animals carrying this *wrt-2* construct (image not shown). wrt-2 has a particularly long coding sequence compared to the other C. elegans Warthog genes lacking predicted 'Hog' domains. As we know that the promoter for wrt-2 expresses well (Fig. 6.2.2) then the likely reasons for the lack of GFP expression in the carboxyl-GFP construct are either that the protein is degraded shortly after expression, or that the unusually long (but previously thought not 'Hog'-containing) carboxyl domain of wrt-2 is nevertheless post-translationally cleaved from the amino 'Wart' domain. The amino end of the 'Wart' domain of wrt-2 encodes a high number of leucine residues typical of signal peptides (Labaj, Leparc et al. 2010), and Michelle Labouesse and colleagues have shown that an amino-terminal GFP construct for WRT-2 is visible and is exported from expressing cells (Liegeois, Benedetto et al. 2006).

On obtaining this previously generated GFP reporter for *wrt-2*, with the fluorophore positioned within the amino-terminal portion of the gene after the predicted signal peptide, we found it contained a frame-shift, causing a premature stop codon shortly after the GFP insert. I therefore made my own amino-tagged construct by adding an mCherry fluorophore to the amino 'Wart' domain of *wrt-2::gfp*. In order to avoid the signal peptide, I used a naturally occurring *PacI* restriction site in the third intron of *wrt-2* into which I introduced the mCherry exons without a stop codon and including additional splice sites. The schematic for this final construct can been seen in figure 6.2.4.

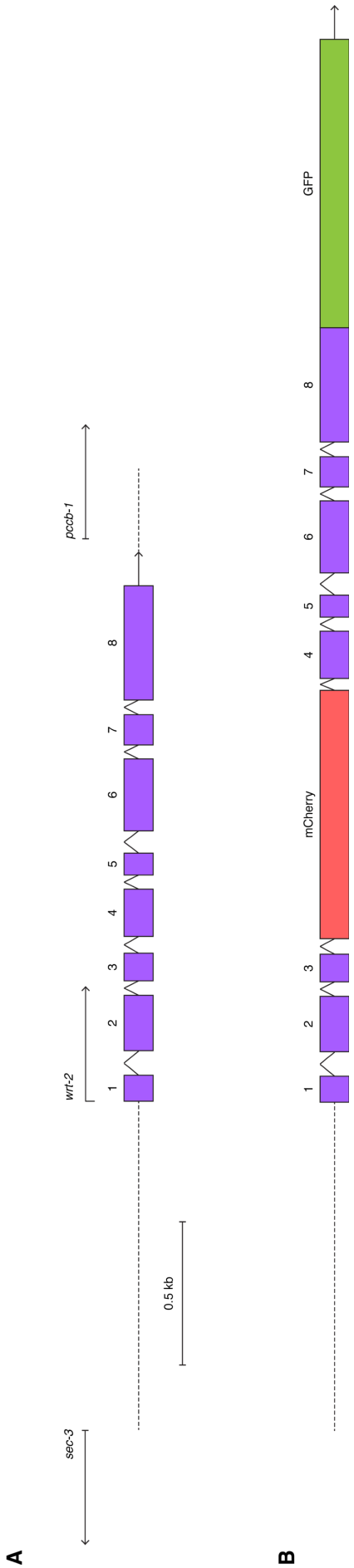

FIG. 6.2.4 – SCALED SCHEMATIC OF THE *MCHERRY::WRT-2::GFP* TRANSGENIC REPORTER.
A. Genomic structure of *wrt-2* (to scale). Exons are shown in purple and introns are shown as pointed lines. The intergenic sequences are shown with dotted lines and the 3' UTR is shown as a solid line with an arrowhead. Genes upstream and downstream are indicated. **B.** A reporter construct containing two separate fluorophores was generated. GFP (green, introns not shown) was tagged to the carboxyl-terminus and mCherry was cloned, without its stop codon, as additional exons into a naturally occurring *PacI* site in intron 3 in order to avoid perturbing the predicted signal peptide encoded at the amino-terminus of the gene.

WRT-2 is cleaved before export of the amino-terminal fragment into the hypodermis

Animals carrying the *mCherry::wrt-2::gfp* extrachromosomal array display mCherry but not GFP expression in the hypodermis surrounding the seam cells (Fig. 6.2.5 A). This shows that WRT-2 is cleaved at a site somewhere between the two fluorophores before export of the amino-terminal, presumably signalling fragment from the seam cells to the hypodermis. Some seam cells show mCherry expression, which is likely due to aggregation of the over-expressed transgene product trapped in these cells.

Intriguingly, the expression of *wrt-2* is not uniform throughout the hyp7 syncytium; mCherry expression does not extend past a lateral stripe on both sides of the hypodermis, and is not present ventrally or dorsally at this stage, despite the hyp7 extending around the entire circumference of the animal. The non-fluorescent hypodermis corresponds to that which overlies the body wall muscles and hence would contain hemidesmosomes, among other unique features.

A low level of GFP but not mCherry expression can be detected in a cell beside the pharynx (Fig. 6.2.5 B); comparison to the expression pattern of an excretory cell GFP marker suggests that the GFP carboxyl-terminal fragment is transported here for processing (Fig. 6.2.5 C).

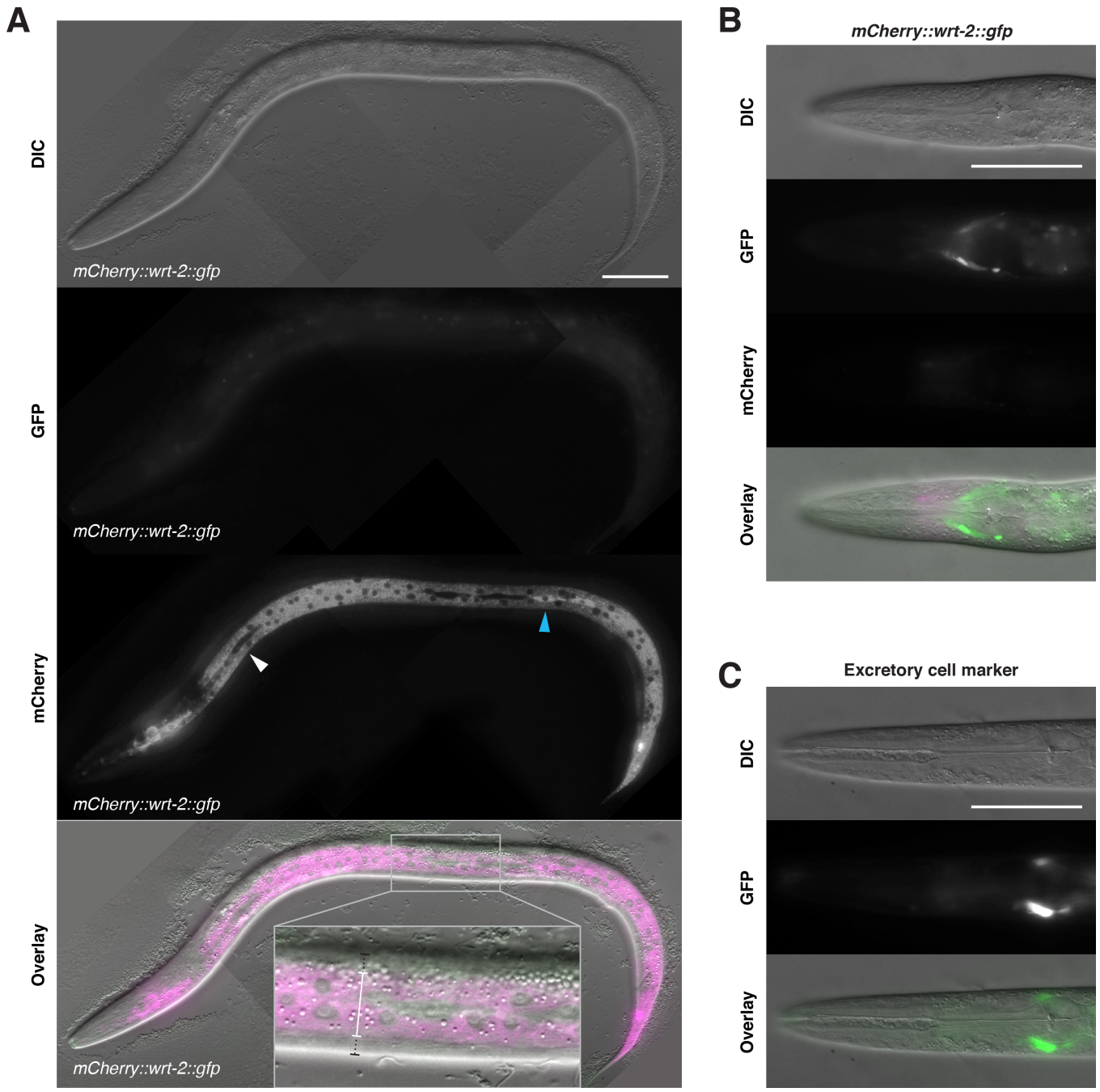

FIG. 6.2.5 – TRANSGENIC REPORTER LINE EXPRESSING *MCHERRY::WRT-2::GFP*.
A. An L2 worm transformed with the doubly-labelled *mCherry::wrt-2::gfp* reporter. There is no GFP expression in the hypodermis of this animal, showing *in vivo* that WRT-2 is cleaved before export of the amino terminus to the hypodermis (mCherry). Seam cells can be seen as either dark areas in the hypodermis, with no mCherry fluorescence (white arrowhead) or as brightly mCherry expressing cells (blue arrowhead) in which the transgene product is possibly aggregated and unable to leave the cell. The expression of *wrt-2* is not uniform throughout the hyp7 syncytium; as indicated in the inset of the overlayed image, the mCherry expression does not extend past a lateral stripe in the hypodermis (white bar), and is not present ventrally or dorsally at this stage (black dotted extensions to the bar). **B.** GFP expression from the *mCherry::wrt-2::gfp* reporter can be seen in one cell beside the pharynx (mCherry expression is absent in this cell). **C.** Expression of *bgIs312[vha-8p::GFP]*, expressed in the excretory cell, focused on the cell body. The similarity in expression between GFP from the *wrt-2* reporter and that of the excretory cell reporter indicates that the carboxyl terminus of WRT-2 (GFP) is sequestered to the excretory system. Scale bars = 25μm.

An in-frame *wrt-2* deletion mutant removes a large section of the carboxyl domain

ok2810 is a deletion allele for *wrt-2* which, unusually, is in-frame (Fig. 6.2.6). In order to understand how this mutation may affect the function of WRT-2, we first predicted where the site of cleavage between the amino 'Wart' and carboxyl domains was likely to occur. For Hedgehogs in other systems, the conserved cleavage site is comprised of the residues GCF, with cleavage occurring between G and C (Porter, von Kessler et al. 1995, see Fig. 6.2.6 B). This full motif is absent in *C. elegans* Warthog protein sequences. However, there is a strongly conserved CF motif at the same position in all the Warthog proteins containing a 'Hog' domain, absent in WRT-2, which would be the most likely site of auto-cleavage if the mechanism is the same as that for Hedgehog proteins. Notably, the side-chain of glycine is not directly involved in the Hedgehog reaction (Fig. 6.2.6 B). If CF is the conserved cleavage site in *C. elegans* proteins, as alignments would suggest, and the carboxyl terminus of WRT-2 encodes a divergent 'Hog' domain, then WRT-2 has a cleavage site a few residues upstream of that contained in other Warthogs (Fig. 6.2.6 A). The alignments and protein sequences for 'Hog'-containing Warthog proteins with WRT-2 is shown in Supplementary Fig. S2.

Although the *ok2810* mutation does not cover the predicted cleavage site in WRT-2, it does remove a large portion of the carboxyl-terminal domain. If this domain were a 'Hog' domain, then I would predict it to auto-cleave the protein to release the active amino-terminal 'Wart' domain. We do know that WRT-2 does undergo cleavage (Fig. 6.2.5); without this reaction it is conceivable that post-translational processing, such as the cholesterol modification of Hedgehogs in other organisms, would not be achieved and the signalling peptide could remain inefficient or retained or degraded by the cell.

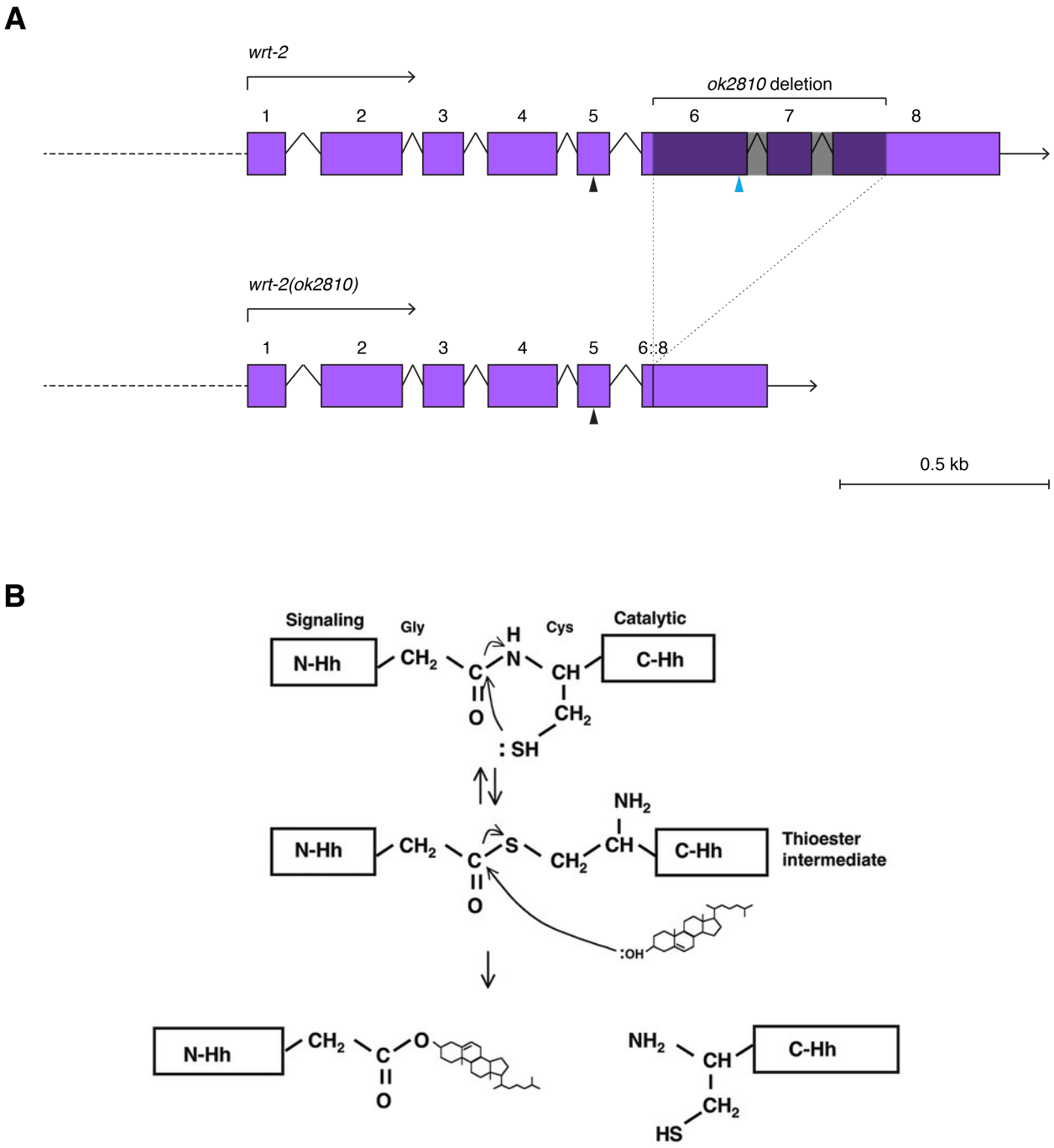

FIG. 6.2.6 – *OK2810*, AN IN-FRAME DELETION ALLELE OF *WRT-2*, REMOVES MUCH OF THE 'HOG' DOMAIN OF WRT-2 BUT IS DOWNSTREAM OF THE PREDICTED PROTEIN CLEAVAGE SITE.
A. Schematic of the *ok2810* deletion allele of *wrt-2*. The deletion removes all of exon 7, as well as much of exon 6 and a portion of exon 8. As *ok2810* is in frame, the remainder of exons 6 and 8 fuse to form one exon and the native stop codon is preserved. The blue arrowhead corresponds to the location in all other *C. elegans* WRT proteins at which cleavage between the 'Wart' and 'Hog' domains is likely to occur; *wrt-2* is unique in not encoding a 'CF' motif at this location, but instead encodes a 'CF' at the location indicated with the black arrowhead (see supplementary Fig. S2 for sequences of Warthog proteins). **B.** *Drosophila melanogaster* mechanism of Hedgehog auto-cleavage and simultaneous cholesterol modification (adapted from Jeong and McMahon 2002). The conserved cleavage peptide motif in known Hedgehogs is 'GCF'. During cleavage, the thiol group of the cystine residue attacks the carboxyl group of the glycine and generates a thioester intermediate before cholesterol attacks to form a covalent bond with the amino-terminal 'Hedge' domain. In *C. elegans* WRT protein sequences, there is a strongly conserved 'CF' motif between the 'Wart' and 'Hog' domains (see Fig. S2). Given that the side-chain of glycine is not involved in the proposed cleavage reaction, it is likely that this 'CF' is the cleavage site in *C. elegans*.

wrt-2(ok2810) does not cause abnormal hermaphrodite seam cell development

The *wrt-2(ok2810)* strain obtained from the CGC was not outcrossed. After outcrossing this strain four times with N2 males ('*wrt-2(ok2810)* x4' in the strain list), we looked, using various seam cell markers, for mutant phenotypes (these reporter strains were created by Elizabeth Liao during her undergraduate project in the laboratory). Due to the high level of expression of *wrt*-2 in the seam, we first analysed seam cell development in *wrt-2(ok2810)* animals by looking at terminal seam cell number at the end of L4 as well as male tail development. Seam cell number was analysed using an integrated *scm::gfp* seam fate marker expressed throughout seam cell development.

ok2810 animals do not exhibit defects in terminal seam cell number, although there is a small but significant decrease in the number of rays in the male tail (Fig. 6.2.7). It may therefore be interesting to analyse sex-specific roles for *wrt-2* further.

wrt-2(ok2810) mutants do not display embryonic lethality at 15ºC or 25ºC

Due to the cold-sensitive embryonic lethal hypodermal phenotypes previously reported for *wrt-5* mutants (Hao, Aspock et al. 2006), we quantified the embryonic lethality in *wrt-2(ok2810)* mutants at 15ºC and 25ºC. However, we did not find any significant embryonic lethality associated with *wrt-2(ok2810)* at either temperature (2% at 15ºC, n = 1406 individuals from 6 broods; 0% at 25ºC, n = 1246 individuals from 6 broods), suggesting that in these conditions *wrt-2* is not an essential gene.

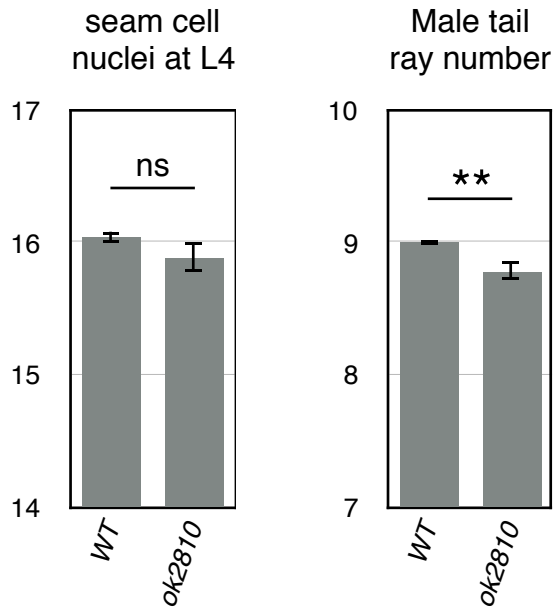

FIG. 6.2.7 – *WRT-2(OK2810)* SEAM CELL PHENOTYPES.
wrt-2(ok2810) L4 hermaphrodites expressing the *scm::gfp* marker for seam cell fate do not display any significant difference in terminal seam cell number ($55 \leq n \leq 59$, error bars = S. E. M., significance determined by the Student's T-test with a threshold of $P < 0.05$). However, there is a small but significant decrease in the number of rays in the tails of young adult males, suggesting *wrt-2* may have a sex-specific role in seam cell development ($51 \leq n \leq 57$, error bars = S. E. M., Student's T-test $^{**}P < 0.01$).

wrt-2(ok2810) animals exhibit a low penetrant Muv phenotype

Whilst using *ajm-1::gfp* to analyse seam cell development in *wrt-2(ok2810)* animals, I observed L4 animals with more than one developing vulva, as outlined by the *ajm-1::gfp* marker (Fig. 6.2.8). The penetrance of this phenotype in the L4 population is low: 6% (n = 69). Because I ran out of time to attempt to rescue this phenotype with the wild-type *mCherry::wrt-2::gfp* construct, I performed RNAi of *wrt-2* (see materials and methods for plasmid construction) on the wild-type *ajm-1::gfp; scm::gfp* marker strain, but was unable to replicate the phenotype. Simultaneous *wrt-2* RNAi on the strain expressing *mCherry::wrt-2::gfp* indicated that this RNAi clone of *wrt-2* is unable to completely knock down *wrt-2* expression, as worms subjected to *wrt-2* RNAi did not show strong knockdown of *mCherry::wrt-2::gfp* expression compared to the empty vector control (data not shown). However, it has been shown previously that the Warthog genes *wrt-4* and *wrt-7*, when knocked down with RNAi, exhibit a low penetrant Muv phenotype (Table 2 of Zugasti, Rajan et al. 2005), so it is conceivable that this is a real phenotype of *wrt-2(ok2810)* and not due to an off-site mutation. Interestingly, of all the Hedgehog-related genes analysed, only *wrt-4* and *wrt-8*, and in this study *wrt-2*, are reported to express in the P blast cells at L1; no expression for *wrt-7* was detected in any tissue (Aspock, Kagoshima et al. 1999).

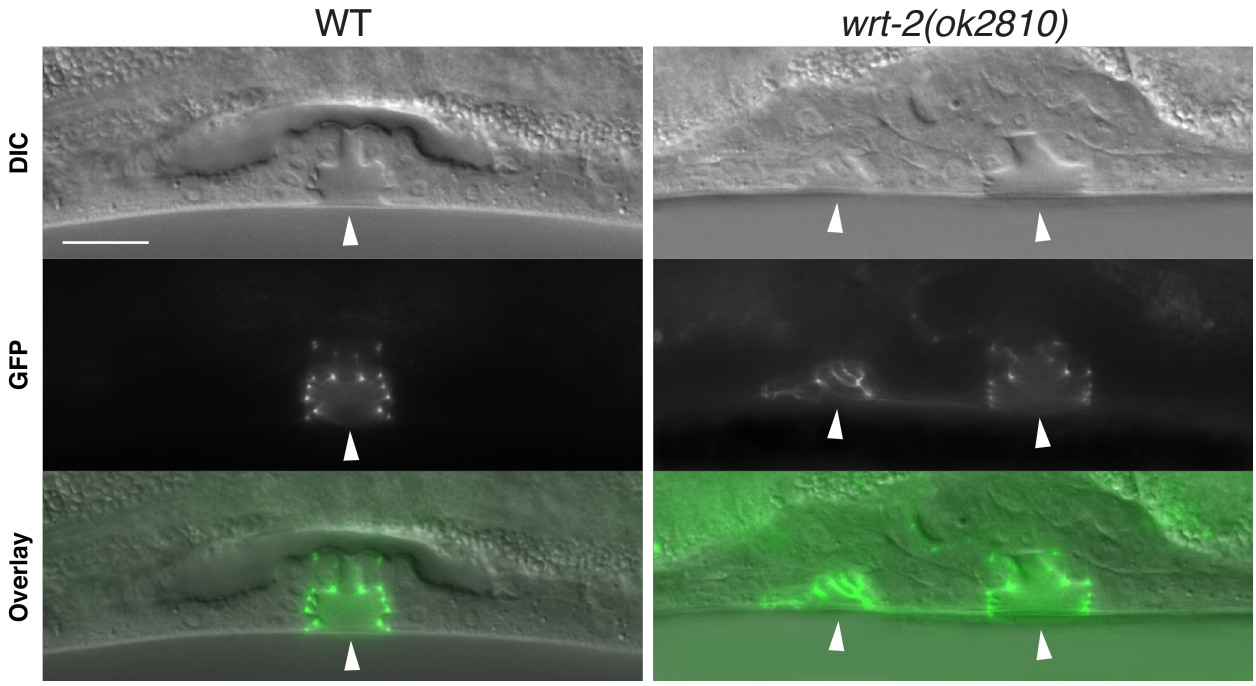

FIG. 6.2.8 – *WRT-2(OK2810)* MUTANTS DISPLAY A LOW PENETRANT MUV PHENOTYPE.
Wild-type L4 animals develop one vulva on the ventral side of the animal, indicated by the single arrowhead. *wrt-2(ok2810)* L4 animals display a Muv phenotype where more than one ventral site undergoes vulval induction; in this example two developing vulvas are indicated with arrowheads. 6% of *wrt-2(ok2810)* animals observed (n = 69) exhibited more than one developing vulva (Muv phenotype); this was never observed in wild-type animals carrying the same marker (n = 66). Scale bar = 20 μm.

The *wrt-2(ok2810)* mutant has defects in gonad arm left-right positioning

One of the key roles of Hh signalling in other organisms is in specification of the left-right axis of the animal. Although *C. elegans* is largely symmetrical along this axis, there are some key examples where this symmetry is broken, for example in Q neuroblast migration and gonad arm positioning. In wild-type animals (with no fluorescent transgene or integrated marker), the gonad arms are strictly polarised so that the anterior arm migrates along the righthand side of the animal and the posterior arm migrates along the lefthand side (see Fig. 6.2.9 A and B). To see whether this polarisation is perturbed in *wrt-2(ok2810)* animals, I compared the outcrossed strain to the parent N2 strain. I found that although the majority of the gonad arm often adhered to the wild-type pattern of left-right polarisation, parts of the arm (for both the posterior and the anterior) often crossed over to the opposite side of the animal (Fig. 6.2.9 C and D). As this was never seen in the N2 animals, this indicates that *wrt-2(ok2810)* animals do display defects in left-right polarisation, whether through patterning or adhesion defects, of the hermaphrodite gonad.


A
Posterior lefthand arm
WT
B
Anterior righthand arm
WT
C
Righthand plane
wrt-2(ok2810)
D
% Gonad left/right defects in each arm
50%
40%
30%
20%
10%
0%
Wild-type
wrt-2(ok2810)
ns
****
****
Anterior
Posterior

wrt-2 over-expressing strain displays abnormal body morphologies

Whilst studying the expression pattern of *mCherry::wrt-2::gfp*, I noticed that there was a low percentage (10%, n = 51) of L4s in the transformed population that exhibited morphological defects along their bodies. These manifested as bulges at various positions along the length of the body (Fig. 6.2.10). This phenotype was never observed in *unc-119(ed3)* mutants rescued with just the *unc-119* rescuing plasmid (n = 54), and is therefore likely to be due to the over-expression of *mCherry::wrt-2::gfp* in the transforming array. However, it is interesting to note that neither this phenotype nor any other morphological abnormality in body shape was observed in the *wrt-2(ok2810)* mutant (n = 50).

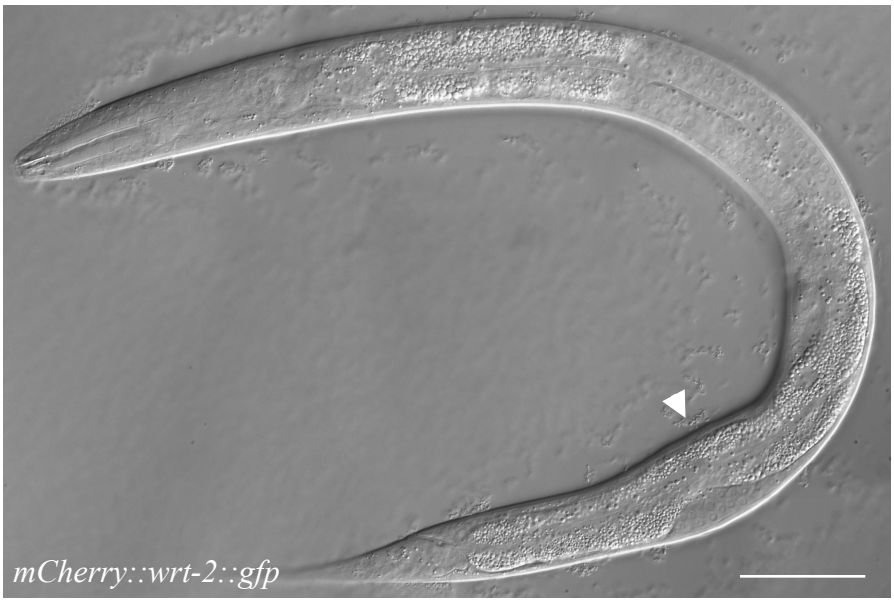

FIG. 6.2.10 – DIC IMAGE OF ABNORMAL BODY MORPHOLOGY IN THE *MCHERRY::WRT-2::GFP* OVER-EXPRESSING STRAIN.
The over-expressing strain of *mCherry::wrt-2::gfp* in a wild-type *wrt-2* background exhibits 10% of transformed worms (n = 51) with body morphology defects (arrowhead). These phenotypes were not observed in worms transformed with the selection marker only (*unc-119*$^{+}$) suggesting that these effects are due to the over-expression of *wrt-2* in the *mCherry::wrt-2::gfp* array. Scale bar = 50 μm.

6.3 Discussion

Because of its role as a new seam cell reporter, it is of particular interest to the study of seam cell development to analyse the exact expression pattern driven by the promoter of *wrt-2*. Since protein expression is intrinsically linked to protein function, I have also attempted to analyse the function of WRT-2 with respect to the reason for it being so highly expressed in the seam cells continuously from embryonic elongation.

Possible function of *wrt-2* expression in the P cells

Using the *heIs63* reporter containing *wrt-2p::gfp::PH* and *wrt-2::gfp::H2B*, I observed that although in later development *wrt-2* expression is confined to the seam cells, during L1 the migrating P cells express the reporter. As no cell divisions have taken place in these cells after the activation of the reporter, the *wrt-2::gfp::H2B* reporter cannot be observed, but for the short time that it takes for the P cells to intercalate with each other at the ventral midline, *wrt-2::gfp::PH* is expressed. It is then turned off in the P cells when they undergo their cell divisions during L1. This expression pattern was reconstituted by a second *wrt-2* promoter construct driving GFP with a nuclear localisation signal only. An uncharacterised deletion mutant of *wrt-2*, *ok2810*, has shown after outcrossing to have a low penetrance multi-vulva (Muv) phenotype. The *C. elegans* vulva is formed from vulval precursor cells, born during the first division of the P cells once they have reached the ventral midline during L1. As this is very close to the time when *wrt-2* is being expressed in these cells, it is tempting to think that *wrt-2* may act in these cells to somehow modulate later vulval development. The *C. elegans* genome contains 10 Warthogs, and of these two others, *wrt-4* and *wrt-7* have been reported to induce a Muv phenotype upon RNAi knockdown (Zugasti, Rajan et al. 2005). Since many of these 10 Warthog genes have overlapping expression patterns , it is likely that there is some degree of redundancy

between Warthog functions, and therefore knocking out *wrt-4* and *wrt-7* in a *wrt-2(ok2810)* mutant background may result in a more penetrant phenotype. An essential experiment left to do is to rescue the *wrt-2(ok2810)* Muv phenotype with a wild-type genomic version of *wrt-2*, to ensure that the *ok2810* mutation is responsible for this phenotype.

Bioinformatics on the *wrt-2* promoter has highlighted potential regulatory interactions

Comparative genomics of promoter regions between *C. elegans*, *C. remanei*, and *C. briggsae* has previously proven very useful in the laboratory for identifying conserved enhancer elements (Brabin, Appleford et al. 2011). Upon aligning *wrt-2* promoter sequences, we have identified a highly conserved region upstream of *wrt-2* which contains three putative transcription factor binding sites for *blmp-1*, *ets-4* and *egl-13*. It is unlikely that all of these sites will be real, for example *egl-13* is not known to be expressed in either the seam cells or the P cells. Although *ets-4* is expressed in the seam cells as well as the P cells, in a genome-wide search for genes which were up-regulated or down-regulated in *ets-4* mutants *wrt-2* was not identified, and Hedgehog-related genes in general were not found to be enriched (Thyagarajan, Blaszczak et al. 2010). However, the regulatory interaction with *blmp-1* is much more interesting. *blmp-1* is expressed in the seam cells and ventral nerve cord among other tissues, and in a search for genes which changed expression in a *blmp-1* mutant background, *wrt-2* was identified as one of seven. The only other Hedgehog-related gene in this set was the putative receptor *ptr-8*, also expressed in the hypodermis (Horn, Geisen et al. 2014). *blmp-1* has been found to be a heterochronic gene that controls epidermal and gonad maturation, with effects on dauer formation, moulting and life-span (Horn, Geisen et al. 2014). Effects on seam terminal fusion at L4 only appear as synthetic effects with other members of the heterochronic pathway. In light of this role for *blmp-1*, it may be the case that *ets-4*, a gene also implicated in longevity and expressed in the

same tissues, works redundantly with *blmp-1* to regulate *wrt-2* expression, but this remains to be tested.

Interestingly, previous findings from *wrt-2* expression data suggests that *wrt-2* expression oscillates considerably during development, consistent with a role downstream of the heterochronic pathway (Hendriks, Gaidatzis et al. 2014). *wrt-2*, along with *ptr-5*, has also been isolated as a target for dynamic regulation by miRNAs, and this might be the cause of more rapid oscillations in expression than could be accounted for by changes in transcription factor binding alone (Zhang, Hammell et al. 2009).

One final consideration when analysing the *wrt-2* upstream promoter sequence is the prediction of an uncharacterised non-coding RNA (ncRNA) sequence just upstream from the *wrt-2* transcription start site. ncRNAs have diverse functions in *C. elegans* so it is hard to predict how this may affect *wrt-2* expression, however, part of this upstream sequence may be devoted to the regulation of ncRNA expression, rather than that of *wrt-2*.

Expression of the translational reporter indicates *wrt-2* encodes a divergent Hog

The *wrt-2* gene was identified in the *C. elegans* genome because of its 'Wart' domain, and not because it was predicted to contain a homologous auto-catalytic 'Hog' domain. Although some *wrt* genes are short and do not contain a carboxylic 'Hog' domain (such as *wrt-5*), *wrt-2* was unusual in that its sequence was comparable to the length of those *wrt* genes which do contain a predicted 'Hog' domain and only the amino portion of the sequence aligned with the 'Wart' domain, leaving half the sequence uncharacterised. However, given that we now know that the carboxyl terminus of the protein is cleaved from the final protein product, and that this carboxyl domain is exported to the excretory cell and degraded (or the other way around), the most likely

scenario would be that *wrt-2* encodes a highly divergent 'Hog' domain that was not predicted by protein sequence alone. Homologues in *C. elegans* characterised by functional but not sequence homology have been identified previously (Kidd, Miskowski et al. 2005). However, to be sure of this homology, the auto-catalytic potential of WRT-2 must be tested, an experiment performed previously for WRT-1 *in vitro* in which the protein was purified from *Drosophila* cell culture cells (Porter, Ekker et al. 1996). However, if *wrt-2* does encode a functional 'Hog' domain, then this work would be the first demonstration that the 'Hog' domain of *C. elegans* is able to cleave *in vivo*.

The second question raised by this reporter construct is where the site of cleavage would be between the two domains. In other WRT proteins this is easy to predict due to the conserved CF motif between the domains, very similar to the conserved Hedgehog cleavage site of GCF. However, as this is not preserved in WRT-2, either the Hog domain recognises a different cleavage site, or a secondary, non-WRT protein performs the cleavage, or loss of the first CF site in WRT-2 coincided with the gain of it in another location. This appears to be a valid prediction, given that a CF motif further upstream yet still between the two protein domains has been identified, which is not present in other WRT sequences. By mutating these residues out of the reporter construct, it would be interesting to see whether expression is changed. However, since it is likely that an un-cleaved product would be degraded in the same way the GFP-tagged 'Hog' domain is, the expression may not be able to distinguish an un-cleaved product from one which is just mis-folded and therefore aggregates and is also targeted for degradation. Perhaps, therefore, this would also be a good experiment to perform *in vitro*, as well as *in vivo*.

A notable feature of the carboxyl terminal protein sequence of WRT-2 is that it contains many glutamine residues (Q). Q-rich protein sequences are associated with protein aggregation, often

leading to neurodegenerative disorders in humans (Stott, Blackburn et al. 1995, Fiumara, Fioriti et al. 2010), and in *C. elegans* this aggregation is a mechanism employed by the linker cell to initiate cell death (Blum, Abraham et al. 2012). Given that Q-rich part of the protein appears to be degraded, perhaps this degradation is mediated by protein aggregation pathways.

The hyp7 syncytium is not uniform

One of the striking things about the *mCherry::wrt-2::gfp* expression pattern is that although the amino terminal portion of the WRT-2 protein appears to be exported from the seam cells into the hypodermis, which should run as a single syncytium, basal to the seam cells and surrounding the entire animal from late L1 onwards, the expression of the *mCherry* appears localised to two lateral strips within the syncytium. It would seem that the *mCherry* construct cannot either be transported or freely diffuse through the regions of the hypodermal syncytium which cover the muscle quadrants, although it has not been determined whether the molecule is cytoplasmic or fixed to the basal membrane of the hypodermis.

The sections of the syncytium overlying the muscle quadrants must be different from lateral sections if only because they contain hemidesmosome structures linking the muscle to the cuticle. However, even beyond this it is known that the basement hypodermal membrane over the muscle quadrants has unique characteristics: one example is the lack of collagen type IV, which is present in all other *C. elegans* basement membranes including the lateral hypodermal membrane (Graham, Johnson et al. 1997). Extracellular matrices are full of signalling molecules and cell-cell contacts with means of communicating via signalling pathways into the interior of the adjacent cells. Therefore it is perhaps not so surprising that the local environments within a large syncytium such as the hyp7 are different from one another due to different cell contacts, but the implications are interesting when one considers transcription from individual nuclei. It would

be interesting to see if transcription too is not uniform within the syncytium, and whether transcription in one nucleus can trigger an event in another, or whether they maintain separate identities. The syncytial embryo of *Drosophila*, for example, is certainly not uniform and relies on the strict patterning of mRNAs. Perhaps there is a similar mechanism employed in the syncytial hypodermis in order to preserve local characteristics even when cell boundaries are lost.

There has been one previous report of hyp7 syncytial nuclei displaying differential spacial expression, where during an enhancer trap Ian Hope and colleagues identified a section of the genome mapped to chromosome IV that drove LacZ expression in some but not all of the hyp7 syncytial nuclei (Young and Hope 1993). The plasmid pUL#64A1 was found to express in the lateral nuclei of the hyp7 adjacent to the anterior and posterior branches of the excretory cell, as well as in the excretory cell itself. It would therefore be interesting to investigate whether the full-length expression pattern of *wrt-2*, also laterally restricted in the hyp7, is due to the position of the excretory cell as the expression of pUL#64A1 appears to be.

Analysis of the previously uncharacterised *wrt-2(ok2810)* deletion mutant

The only available deletion mutant of *wrt-2* is the allele *ok2810*. Given that the *ok2810* deletion mutant is an in frame deletion of most of the carboxyl putative 'Hog' domain, it would be very nice to have an *ok2810* version of the *mCherry::wrt-2::gfp* translational reporter construct to really see how this deletion affects *wrt-2* expression and function. This would not only answer the question of whether this mutant is likely to be a null, but would also give us information on how important the auto-catalytic cleavage event of the protein is to its function, since the mutant leaves the amino signalling domain intact. For *bone fide* Hedgehogs, the post-translational modifications mediated by the auto-processing of the ligand are essential for the behaviour of the

ligand once it leaves the cell (see the introduction to this chapter). However, it is not known whether the same is true for *C. elegans*, or even if such lipidation events that are undergone by Hhs are carried out by *C. elegans*. Since the role of cholesterol is integral to the auto-cleavage mechanism in Hh processing, and if the cleavage motif is 'CF' in *C. elegans*, then it would make sense that the catalytic mechanism has been conserved and also requires a covalent cholesterol modification of the protein in *C. elegans*.

From studies of the outcrossed *wrt-2(ok2810)* strain, it would appear that *wrt-2* has only very subtle phenotypes, perhaps due to redundancy with other members of the *wrt* gene family, and no effect as a single mutant on hermaphrodite seam cell development. One phenotype of *wrt-2(ok2810)*, the Muv phenotype, has already been discussed, but another phenotype described here is a gonad migration phenotype. This is very subtle, but is perhaps linked to the lateral restriction of WRT-2 within the hyp7 syncytium, as gonad arms that would normally remain in contact with the hypodermal basement membrane during longitudinal migrations were found to move off this strictly lateral trajectory and onto the basement membrane under the muscles. At least one of the *C. elegans* Patched genes, the putative receptors of the *C. elegans* Hedgehog-like ligands, is known to be expressed in the gonad and so an interaction between the gonad and the hypodermis would not be inconceivable (Kuwabara, Lee et al. 2000). In the course of the studies presented here, the alae of *wrt-2* young adult animals were observed to be normal, consistent with observations in other studies that *wrt-2* RNAi does not perturb alae development, as is the case for knockdown of other *wrt* genes (Zugasti, Rajan et al. 2005). We have also noticed a possible over-expression phenotype of the *mCherry::wrt-2::gfp* reporter strain, in which body morphology at L4 appears to be perturbed in some animals. This could reflect a role for *wrt-2* in regulating body size or shape.

CHAPTER 7

General Discussion

7.1 Development as an integration of signalling pathways

One of the important aspects of development that this work highlights is that no signalling pathway can be investigated in isolation, without any consideration for the many other cellular processes that are taking place inside the cell or organism, either at the same time or during its lifetime. Given the limited number of signalling pathways discovered so far, and yet the vast array of physiological processes that these pathways are able to regulate, it is inevitable that more fine-tuned developmental processes rely on complex interaction networks between the different signalling pathways. In this respect, genetic techniques are still the most powerful way to study development of a whole organism *in vivo*, and to discover the links and interactions between the many different pathways that contribute to the making of an animal. The rise of the

systems biology field, whereby interactions are modelled mathematically, reflects this growing emphasis on the importance of whole-organism global signalling networks.

7.2 Expression driven from an intron

Cis regulatory elements are discrete modules of around 6 - 200 bp motifs that regulate the spatial and temporal dynamics of gene expression. Often each motif can be studied in isolation from the rest of the gene in order to explore its effect on gene function. The precise combination of motifs that controls a gene specifies the complete native expression of that gene. As each regulatory component of gene expression is relatively independent from the other regulatory modules, the loss or inheritance of motifs in the genome is a driving force in evolution. An example of this is the freshwater stickleback fish, which, through loss of a single enhancer for gene expression, has lost its pelvic fin (Shapiro, Marks et al. 2004).

Cis regulatory elements contained in introns of genes are not unique to the seam cells, or to *C. elegans*, as examples of gene regulation through intronic binding sites can be found in mammals (Hiroki, Liebhaber et al. 2007, Khandekar, Brandt et al. 2007, Paul, Li et al. 2007, Feng, Huang et al. 2008, Huang, Chiribau et al. 2009, Abbasi, Paparidis et al. 2010, Rojas, Schachterle et al. 2010, Nicoll, Davidson et al. 2012, Hoffmann, Zimmermann et al. 2013, Huong le, Kobayashi et al. 2013, Sauter, Bouhlel et al. 2013, Altonsy, Sasse et al. 2014, Imamichi, Mizutani et al. 2014, O'Hara, Alvarez de la Rosa et al. 2014, Sanalkumar, Johnson et al. 2014, Takahashi, Yamaguchi et al. 2014, Visser, Palstra et al. 2015), *Drosophila* (Kalay and Wittkopp 2010), zebrafish (Prasad, Reed et al. 2011), ascidians (Yoshida and Saiga 2008) and plants (Schauer, Schluter et al. 2009, Khan and Ali 2013).

However, why some intronic enhancers should be present in intronic sequences whereas others are located in the upstream 'promoter' sequence remains a mystery. Studies that have analysed the chromatin architecture of intronic enhancers have detected peaks in enhancer-related chromatin features (Hiroki, Liebhaber et al. 2007, Ott, Suszko et al. 2009, Sanalkumar, Johnson et al. 2014), with some hints of a mechanism for epigenetic memory in intronic but not upstream elements (Sanalkumar, Johnson et al. 2014), and that factors that bind to the intronic sequences often form a loop back to the promoter sequence (Ott, Blackledge et al. 2009, Ott, Suszko et al. 2009, Deshane, Kim et al. 2010, Sanalkumar, Johnson et al. 2014, Visser, Palstra et al. 2015). This is perhaps unsurprising since RNA polymerase loading sites for gene transcription must be located near the coding start site. However, this does suggest a possible functional difference between intronic *versus* upstream cis-acting elements; perhaps the complex looping at the site of transcriptional activation allows for a more composite and tightly controlled means of regulating developmental gene expression in a precise spatial and temporal manner. It is also interesting to consider that the RNA polymerases will be passing through the site of transcription factor binding to the intronic enhancer during active transcription. Could this disrupt the 3D transcriptional activation complex at the promoter to limit gene expression? It could be interesting to look at the precise dynamics of transcription in real time to compare transcription driven by upstream enhancers to that driven by intronic elements.

7.3 Migration is a theme of *pal-1* expression

An intense investigation into the exact requirements for maternal and zygotic expression of *pal-1* from the 5' upstream promotor during embryogenesis has been carried out by Lois Edgar and colleagues (Edgar, Carr et al. 2001). In this study, maternal transcripts were found to be required

for early C and D blastomere expression of *pal-1* until the the 26 cell stage, after which expression in the descendants of C and D, as well as later embryonic expression in other lineages including the AB, MS and E lineages, was dependent on zygotic transcripts.

The additional expression of *pal-1* in lineages other than C or D was found to be consistent with null mutant phenotypes affecting these lineages and data from mosaic analyses. For example, it was found that MS descendants mu intR and the mesoblast M, whilst usually completing substantial posterior migrations along the ventral midline during morphogenesis, did not migrate at all in *pal-1* mutants. In addition, mosaic loss of *pal-1* from the AB lineage resulted in ventral cleft enclosure defects and embryonic lethality. No role for *pal-1* was observed in E, although the two cells that express *pal-1* are unusual in that they intercalate during gut formation.

Although most of the functions of *pal-1* were found to be cell autonomous, some inconsistencies between the *pal-1* expression pattern and the mutant phenotypes remained. The majority of these relate to seam cell phenotypes of *pal-1* null mutants; mosaic loss of *pal-1* from the seam cells resulted in 'lumpy' animals with bulges along their lengths, yet expression of *pal-1* was only observed in V6. In addition, in completely null embryos, seam cells failed to migrate to lateral positions and frequently fused with the hyp7 syncytium, resulting in a loss of seam cells upon hatching (Edgar, Carr et al. 2001). In other null animals, seam cells bunched up around V4, rather than lying in a single straight line along the lateral side of the worm (Edgar, Carr et al. 2001). Although it is possible that *pal-1* functions non-autonomously in these cells, given that there are no other known examples of *pal-1* functioning cell non-autonomously, it was noted even during this study that not all *pal-1* regulatory elements appeared to be encapsulated by the reporter construct used. This extra regulation is most likely that contained in the last intron of *pal-1*, not present in the reporter gene used previously. It would be interesting to use the rescue

construct without the last intron to rescue a null mutant of *pal-1*. The resulting animals could be used to assess whether the phenotype of removing the entire intron is comparable to animals of the *e2091* genotype, or whether, since this intron contains elements that can drive expression in the body wall muscle in addition to the seam cells (not perturbed in the *e2091* mutant) these phenotypes are worse.

One central theme when analysing the expression of *pal-1* is that many of the cells which normally express *pal-1* do so whilst undergoing morphogenic movements, processes which fail in a *pal-1* mutant. Migration therefore, as well as fate specification, appears to be a central theme for those cells which express *pal-1*. As well as the processes described above, *pal-1* has been shown to be required during dorsal intercalation, and in *pal-1* null animals the nuclei of C-derived hyp7 cells fail to migrate (Edgar, Carr et al. 2001). This is even more striking given the results presented here that the netrin pathway, known for its essential role in other migratory processes, acts synthetically with *pal-1* during embryonic development. However, that *pal-1* expression is associated with cell migration raises interesting questions about the role of the transient *pal-1* expression in the seam cells V2-T during L1. Perhaps, as these are the seam cells which undergo ventral movements during their first division, *pal-1* is permissive for cell migration, although not required since the *e2091* mutant still undergoes seam daughter migration, just of the wrong daughter.

7.4 When is the end of embryogenesis?

Once animals hatch, the L1 larvae do not progress through post-embryonic development until they encounter food. Both hatching and the initiation of post-embryonic events can be thought of as a temporal closure on the developmental events described as ‘embryogenesis’. However, it is

curious to observe that during epidermal development, the dorsal hypodermis forms first during embryogenesis, fusing to become the start of the hyp7 syncytium shortly after dorsal intercalation, and yet the ventral epidermis remains cellular until after hatching, made up of P cells which fulfil only a transient structural role until the daughters of the seam cells can take over in L1.

The event of seam cell hypodermal daughters taking over from P cells in the ventral hypodermis during L1 looks remarkably similar to the dorsal intercalation event of embryonic hypodermal development. Hypodermal cells make processes to the ventral midline (in the case of embryonic dorsal intercalation, this is the dorsal midline) and then, as the cells get into position having remodelled along this projection, they fuse to form a hyp7 syncytium. This event, therefore, could be described as a ventral intercalation event, essential for the formation of the ventral hyp7 syncytium, just as the dorsal intercalation event forms the dorsal hyp7 syncytium.

Although this process of ventral intercalation does not take place during embryogenesis, perhaps it should still be perceived as an 'embryonic' morphological event: before this process, the hypodermal syncytium is not complete, and the process of this event defines the overall structure of the hypodermis for the remaining life of the animal. By extension of this theory, it could be argued that the seam cells present in the animal upon hatching are 'blast seam cells' that have yet to divide to produce a 'post-embryonic' seam cell of the lineage that we can perturb with mutations in the Wnt and Runx signalling pathways. It appears that even heterochronic mutants cannot perturb the event of hypodermal daughter cells from the seam intercalating with P cells as they move down to the ventral midline, supporting this idea of L1 epidermal development being 'embryonic' in nature.

7.5 An edit of Wormbook and WormAtlas

The findings presented here on the importance of the relative positions of cells and junctional complexes in the development of an organism demonstrate the importance of accuracy when it comes to representing these cells in anatomical drawings. There are two distinct categories of *C. elegans* anatomical representation shown in the *C. elegans* community resources Wormbook and WormAtlas: those diagrams copied from original anatomical drawings by John White and colleagues, which are accurate in their depiction of cell boundaries in the late embryo and L1 larva, and diagrams which have been drawn later, which are wrong. If these later diagrams were to progress though development, the L1 epidermis would be in a lot of trouble! An example of this from each resource is shown in figure 7.1, where the P cell apical boundaries are mismatched with respect to the lateral seam cell positions. The accurate boundaries are shown in the diagram below the Wormbook and WormAtlas scheme. One of John White's accurate anatomical drawings of the embryonic epidermis prior to elongation was reproduced in Fig. 1.3.7 A, in the introductory chapter of this thesis, and is included in Fig 7.1 for comparison.

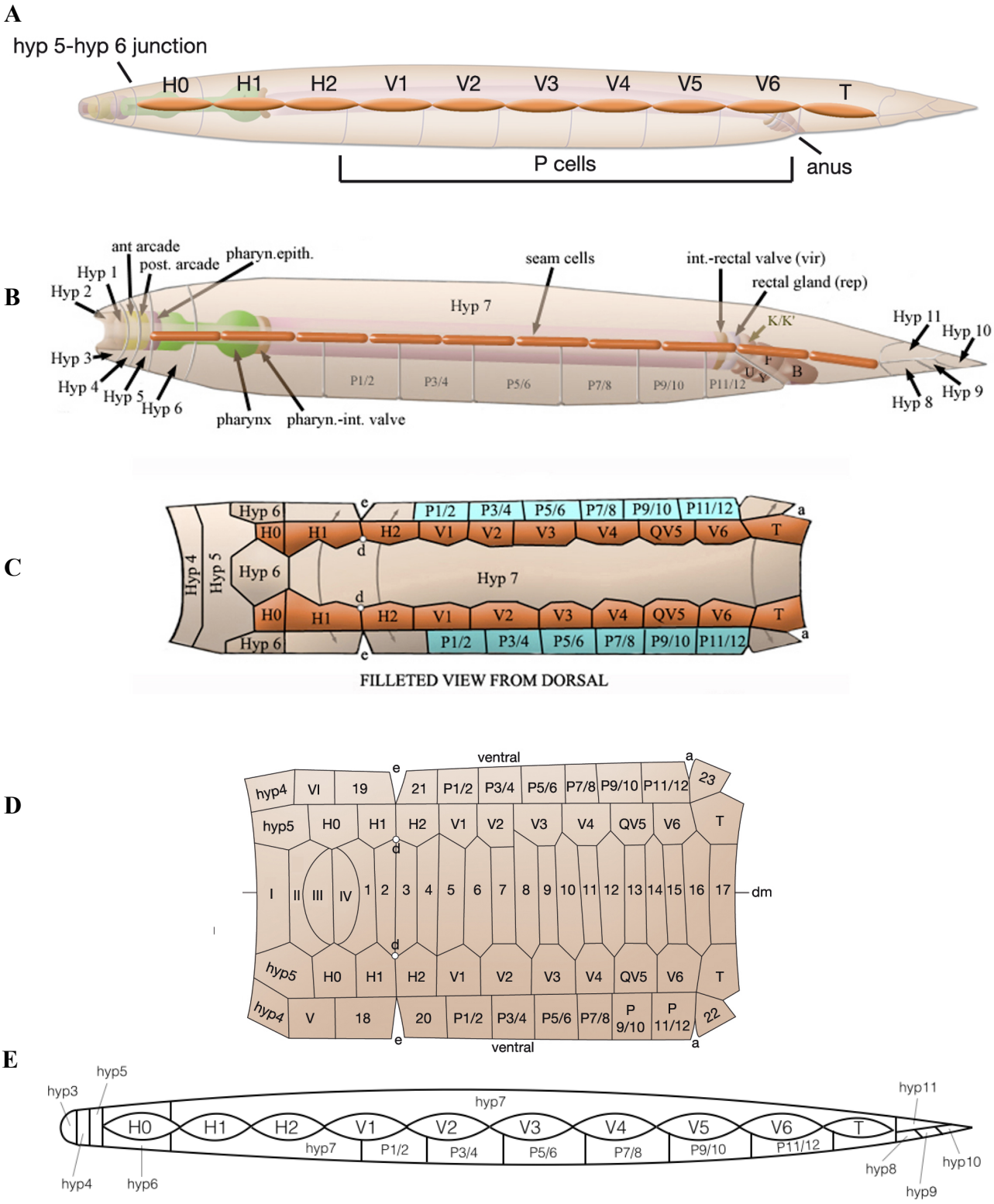

FIG. 7.1 – DIAGRAMS OF THE L1 EPIDERMIS IN WORMATLAS AND WORMBOOK WITH INACCURATE EPIDERMAL PATTERNING.

A. An inaccurate diagram taken from Altun, Z.F. and Hall, D.H. 2009. Epithelial system, seam cells, in WormAtlas. P cells extend anteriorly to V1, and the P cell apical junction boundaries are not aligned to the anterior end of the seam cells. **B and C.** Inaccurate drawings taken from Wormbook (Herman 2006). **D.** Accurate representation of the ventrally enclosed epidermis in Wormbook, copied directly from a drawing by John White. **E.** An accurate depiction of the boundaries between the P and the seam cells at L1.

Appendix I

Interaction of PAL-1 with RNT-1

I.i Introduction

The interest in *pal-1* within the context of seam cell development was first conceived with respect to the synthetic effect of *pal-1* RNAi on *rnt-1(tm388)* mutants. Previous work in the laboratory has identified that the single *C. elegans* Runx transcription factor homologue, *rnt-1*, together with its co-factor *bro-1*, has a role in promoting proliferative seam cell divisions (Nimmo, Antebi et al. 2005, Kagoshima, Nimmo et al. 2007, Brabin, Appleford et al. 2011). In the *rnt-1* deletion mutant *tm388*, the number of seam cells at adulthood is reduced from 16 to around 13 due to failures of the symmetrical division at the beginning of L2, as well as other seam division failures (Nimmo, Antebi et al. 2005). However, RNT-1 is unlikely to function alone in controlling seam cell divisions; this is supported by the fact that 100% of symmetrical seam divisions do not fail in a *rnt-1(tm388)* animal. However, no protein other than BRO-1 has

been implicated in a transcription factor complex with RNT-1. In an attempt to identify interactors with the RNT-1/BRO-1 complex, a small scale candidate RNAi screen was carried out for genes which display synthetic lethality with *rnt-1(tm388)* (C. Brabin, D. Phil. thesis 2011). One such gene is *pal-1* (*p*osterior *al*ae), the *C. elegans* homologue of the *caudal* homeobox transcription factor, well characterised in *C. elegans* for its role in posterior embryonic patterning (Hunter and Kenyon 1996, Ahringer 1997, Edgar, Carr et al. 2001, Baugh, Hill et al. 2005, Maduro, Kasmir et al. 2005, Maurer, Chiorazzi et al. 2007, Lei, Liu et al. 2009). Due to the essential role of *pal-1* in embryogenesis, RNAi against *pal-1* in wild-type worms resulted in 79% lethality, although this is increased to 98% using a *rnt-1(tm388)* mutant, proving to be a statistically significant change (Fig. I.i.i, reproduced from C. Brabin, D. Phil. thesis, 2011).

In an attempt to further characterise the interaction of *pal-1* with *rnt-1*, I used a bimolecular fluorescent complementation (BiFC) technique (Hiatt, Shyu et al. 2008, Shyu, Hiatt et al. 2008) to directly visualise the interaction between the RNT-1 and PAL-1 proteins *in vivo*. Although the results from this experiment support the existence of an interaction between the two proteins, I have been unable to further identify a significant biological relevance to the development of the seam cells associated with the interaction using *rnt-1;pal-1* double mutants. I therefore decided to pursue other aspects of *pal-1* seam biology during the main part of this study, although the RNT-1/PAL-1 interaction data is described below and may prove to be more exciting when viewed through the interest of, for example, muscle development.

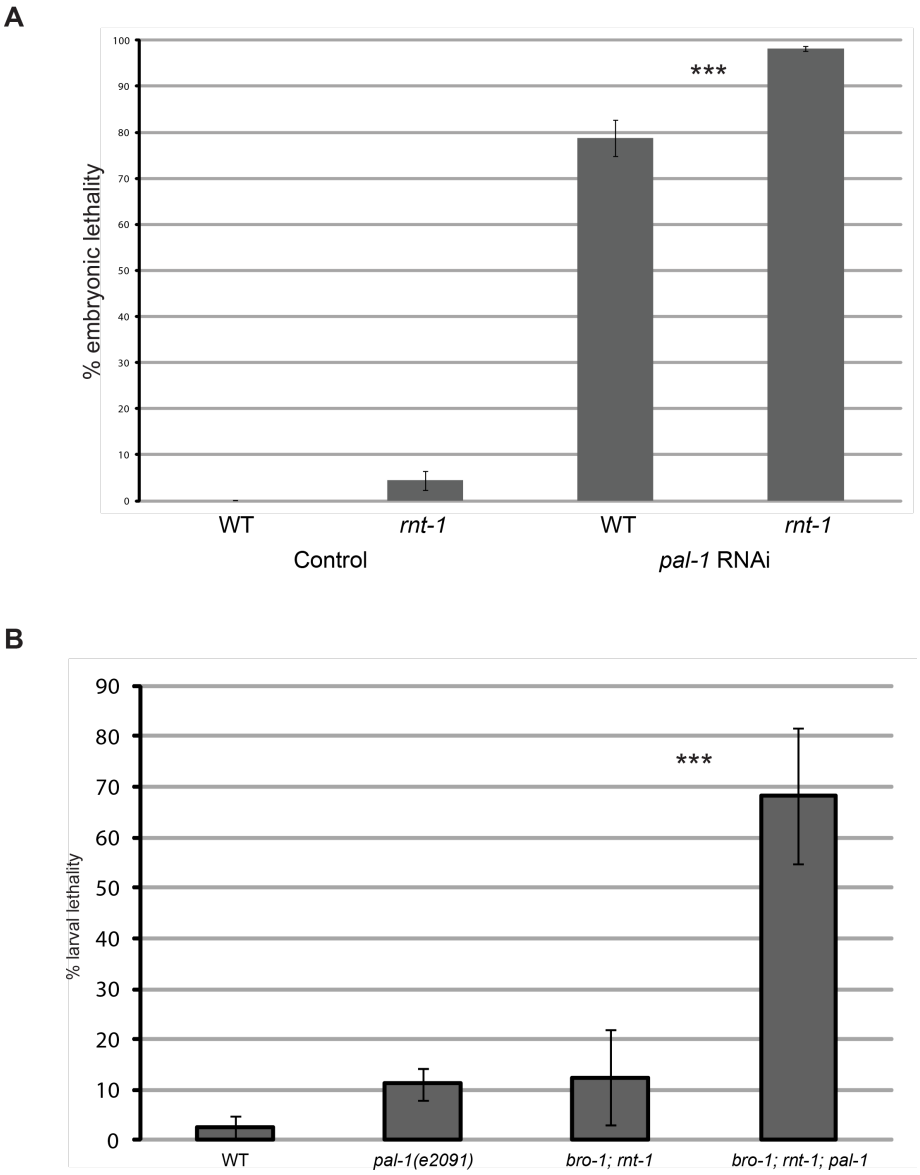

FIG. I.I.I – SYNTHETIC LETHALITY BETWEEN *RNT-1* AND *PAL-1* (ADAPTED FROM C. BRABIN, D. PHIL. THESIS, 2011).
A. Synthetic embryonic lethality observed after *pal-1* RNAi on *rnt-1* mutant animals. Although *pal-1* RNAi results in a high level of embryonic lethality, this is significantly increased in a *rnt-1* mutant background. There is little embryonic lethality associated with the *rnt-1* mutant alone. **B.** Synthetic larval lethality between the *pal-1(e2091)* mutant and the linked *rnt-1 bro-1* double mutant.

I.ii Results

rnt-1; pal-1 double mutants exhibit a synthetic decrease in seam cell number

Previous experiments investigating a synthetic interaction between *pal-1* and *rnt-1* have used a *rnt-1* deletion allele, *tm388*, and *pal-1* RNAi. As it would be beneficial to be able to use a mutant of *pal-1* to investigate this interaction, I decided to cross the viable *pal-1(e2091)* allele into the *rnt-1(tm388)* and *rnt-1(e1241)* backgrounds. The product of the *e1241* allele is unable to bind to the BRO-1 co-factor (Kagoshima, Nimmo et al. 2007). By using *pal-1(e2091); rnt-1(tm388)* and *pal-1(e2091); rnt-1(e1241)* double mutants, I established that there is no apparent synthetic lethality for either allele of *rnt-1* with *pal-1(e2091)*, although there is a small synthetic decrease in seam cell number (Fig. i.ii.i). As *pal-1* RNAi in a *rnt-1; bro-1* background results in an over 40% increase in larval lethality compared to the predicted additive effect (C. Brabin, D. Phil. thesis, 2011), we can conclude that the processes in post-embryonic development regulated by both *rnt-1* and *pal-1* are not perturbed in the *e2091* mutant.

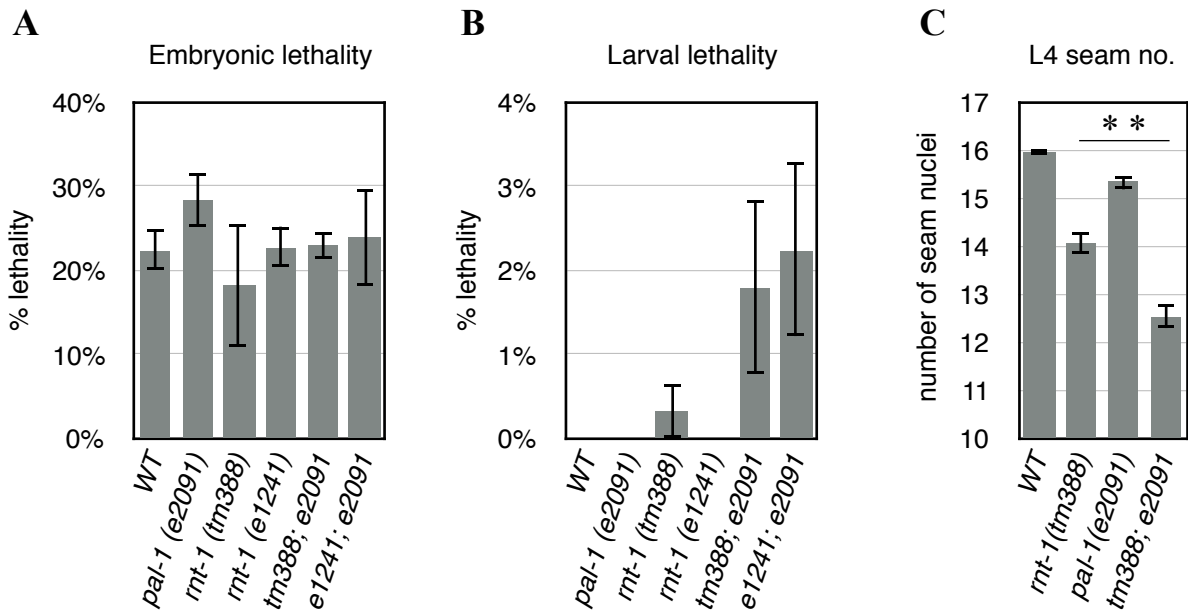

FIG. I.II.I – *PAL-1(E2091); RNT-1* DOUBLE MUTANTS DO NOT SHOW SYNTHETIC LETHALITY BUT DO DISPLAY A SMALL SYNTHETIC DECREASE IN TERMINAL SEAM CELL NUMBER.

A. Embryonic lethality in *pal-1* and *rnt-1* single and double mutants. The experiment was carried out in a *him-5(e1490)* background which accounts for the high level of baseline lethality, although this remains significantly unchanged for any strain ($4 \leq n \leq 8$ total broods). B. There is no significant increase in larval lethality in the double mutants compared to the single mutants ($4 \leq n \leq 8$ total broods). C. There is a small decrease in the number of seam cells in the double mutant compared to the sum of the single mutants alone, with a significant decrease in seam cell number between the *rnt-1* single mutant and the *rnt-1; pal-1* double mutant. For all graphs, error bars = S. E. M. and significance has been calculated using the Student's T-Test (***$P < 0.0001$).

Using BiFC to visualise the RNT-1/BRO-1 interaction *in vivo*

For the BiFC assay of *in vivo* protein-protein visualisation, two stable, non-fluorescent fragments of a fluorophore ('VN173', Venus 1-172 and 'VC155', Venus 155-238) are tethered to two potentially interacting proteins. If the proteins of interest interact, they bring into close proximity the two halves of the fluorophore, resulting in reconstitution of the Venus protein and restoring fluorescence (Fig. i.ii.ii, Hiatt, Shyu et al. 2008, Shyu, Hiatt et al. 2008).

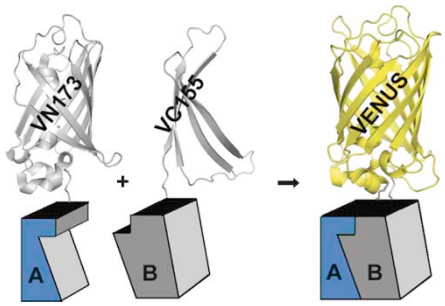

FIG. I.II.II – SCHEMATIC REPRESENTATION OF THE BIFC TECHNIQUE (ADAPTED FROM SHYU, HIATT ET AL. 2008).
Two halves of the Venus fluorescent protein, VN173 and VC155, are tethered to two potentially interacting protein partners, A and B. If A and B interact, the two halves of the Venus protein are brought into close proximity and an intact fluorescent protein is restored.

In order to establish whether I could use the Venus-based protein fragmentation complementation BiFC system to investigate the PAL-1 interaction with RNT-1, I first chose to visualise the well characterised interaction between RNT-1 and BRO-1. By choosing this interaction, I was able to make use of the mutant allele *rnt-1(e1241)*, encoding the substitution $I_{112}K$, which has been shown to perturb binding of RNT-1 to BRO-1 (Kagoshima, Nimmo et al. 2007). This interaction therefore provided optimal positive and negative controls. The two cDNA-Venus fragment constructs were injected simultaneously to generate a single array, and both expressed under the heat shock promoter *hsp-16.41*. The results of these experiments are shown in figure i.ii.iii, and support BiFC as a method of visualising protein-protein interactions *in vivo*.

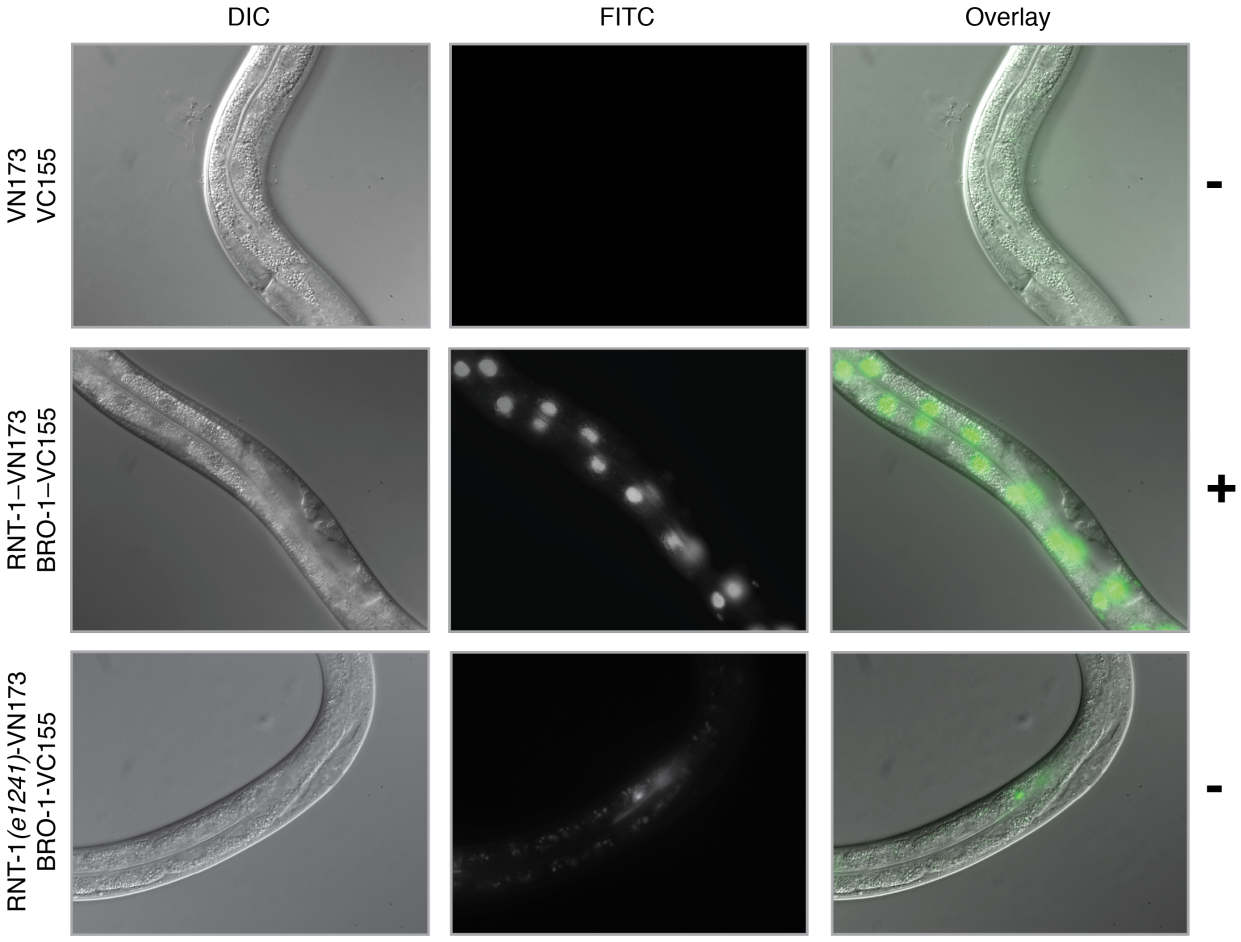

FIG. I.II.III – BIFC VISUALISATION OF THE RNT-1/BRO-1 INTERACTION *IN VIVO*.
DIC and fluorescent images using an FITC filter are shown of transgenic worms containing the constructs indicated. Heat shocking was carried out at 33ºC for 2hrs with a 30min 20ºC recovery period before imaging. Empty BiFC constructs expressing only the Venus fragments under control of the heat shock promoter were used as an additional negative control. Wild-type RNT-1 expressed from the BiFC transgene appears to interact with the BRO-1 construct using this assay, shown by the bright reconstitution of fluorescence in the second panel. As expected, there is a great reduction in fluorescence upon introduction of the *e1241* mutation (third panel).

BiFC analysis supports a RNT-1 and PAL-1 interaction

Using the same constructs for RNT-1 and BRO-1 BiFC analysis, I tested each of these proteins for an interaction with a PAL-1 BiFC construct. I was able to reconstitute fluorescence in both RNT-1/PAL-1 lines as well as lines containing BRO-1 and PAL-1, supporting the genetic evidence of an interaction between the Runx complex and *pal-1* (Fig. i.ii.iv panels 1 and 2).

In order to probe further into this interaction and to find out whether BRO-1 binds PAL-1 independently of RNT-1 or only within the context of a complex containing RNT-1, I injected the PAL-1 and BRO-1 constructs into animals of the *rnt-1(tm388)* genotype, containing no native RNT-1 protein. *rnt-1* is also expressed in the gut, where the heat shock promoter expresses strongly, and so the presence of a three-way complex was a distinct possibility. The *rnt-1(tm388)* worms containing BRO-1 and PAL-1 constructs were unable to reconstitute fluorescence after heat shock, suggesting that BRO-1 does not bind PAL-1 directly, but is present in the same transcription factor complex (Fig. i.ii.iv panel 3).

Conversely, by using the *e1241* version of the RNT-1 BiFC clone with PAL-1, I was able to test whether RNT-1 was able to bind PAL-1 independently of BRO-1, as this RNT-1 construct is unable to bind BRO-1. These worms were able to reconstitute fluorescence after heat shock suggesting that RNT-1 is still able to bind PAL-1 in a complex without BRO-1 (Fig. i.ii.iv panel 4).

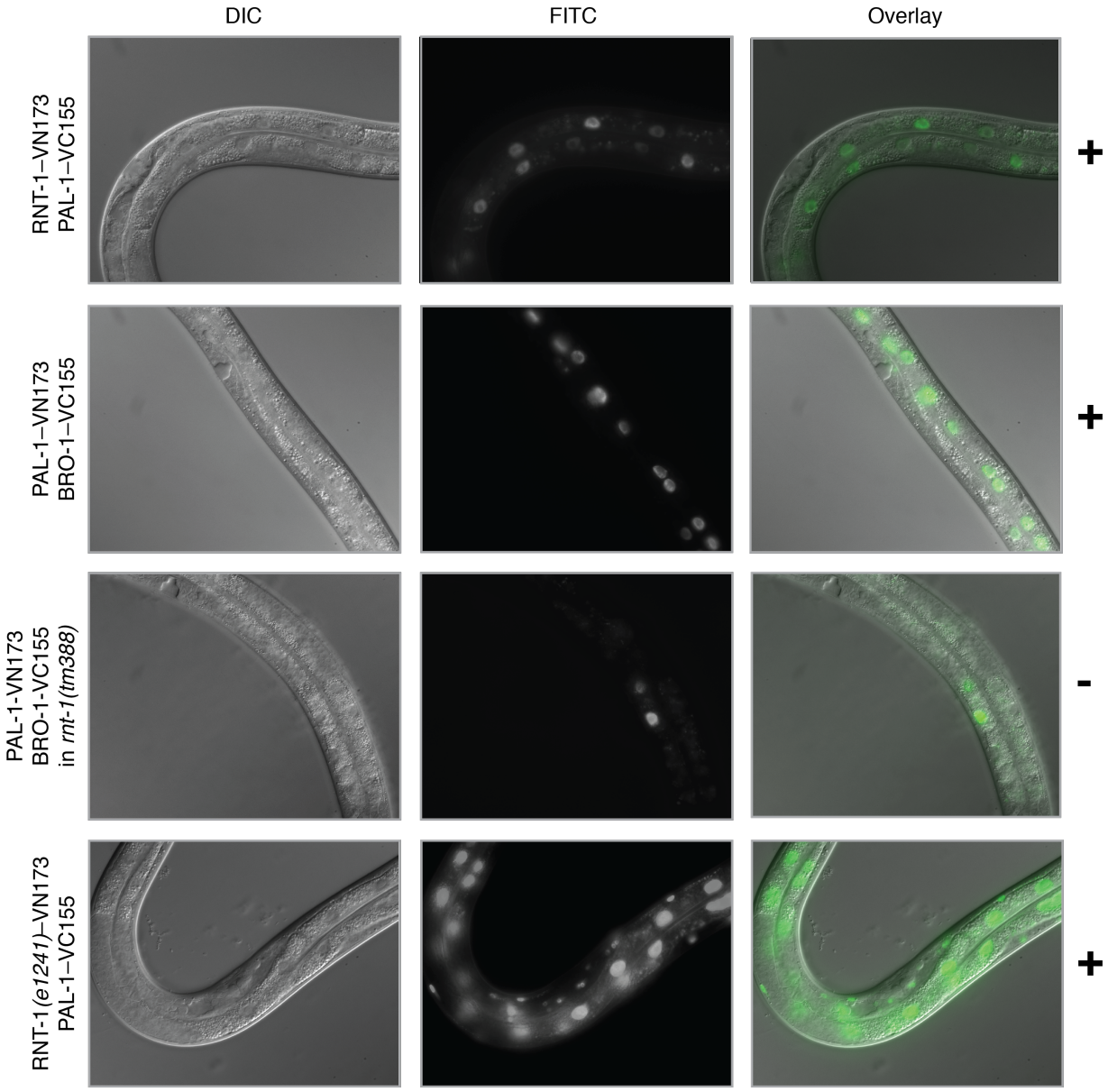

FIG. I.II.IV – BIFC ANALYSIS OF THE INTERACTION BETWEEN PAL-1 AND MEMBERS OF THE RUNX COMPLEX.

DIC and FITC images of BiFC transgenic worms after heat shock. The PAL-1 BiFC construct is able to reconstitute fluorescence after co-injection with either of the RNT-1 or BRO-1 BiFC constructs. However, in a *rnt-1(tm388)* background where there is no native RNT-1 protein expressed in the gut, BRO-1 is unable to bind PAL-1 (panel 3). RNT-1*(e1241)* is still able to bind PAL-1 however (panel 4), despite not being able to bind to BRO-1, suggesting that a direct interaction between RNT-1 and PAL-1 mediates the close proximity between PAL-1 and BRO-1 in order to reconstitute fluorescence in the animal shown in panel 2.

I.III Discussion

Although *pal-1* was identified in an RNAi screen for synthetic lethality with *rnt-1*, we found that the viable mutant *pal-1(e2091)* was unable to reproduce this phenotype in a *rnt-1(tm388)* or *rnt-1(e1241)* mutant background. However, given the evidence of a synthetic interaction between *rnt-1* and *pal-1* from the full knockdown of *pal-1* by RNAi in a *rnt-1* null background (shown in figure I.i.i of the introduction to this section), this may be due to *pal-1* function remaining unperturbed in *pal-1(e2091)* in the relevant tissues that co-express *rnt-1* and *pal-1*. It is important to note that *pal-1* and *rnt-1* are both expressed in the body wall muscle as well as in the seam cells, and that this expression remains unperturbed in a *pal-1(e2091)* mutant (Nimmo, Antebi et al. 2005, C. Brabin, D. Phil. thesis, 2011). Thus, the synthetic lethal interaction between *rnt-1* and *pal-1* RNAi could relate to the role of these genes in body wall muscle; in contrast to the *e2091* mutation, which affects seam expression, RNAi knockdown will affect *pal-1* function in both seam and muscle, therefore causing synthetic lethality in *rnt-1* mutants. Intriguingly, both seam cells and muscle provide the driving forces behind elongation, and *rnt-1* expression is first detected at the 1.5-fold stage (Nimmo, Antebi et al. 2005); it is plausible that embryonic development may stop at the two-fold stage in *rnt-1* mutants subjected to *pal-1* RNAi, contributing to the additional embryonic lethality compared to *pal-1* RNAi alone.

The detection of synthetic interactions with *rnt-1* is of particular interest since so much of the Runx regulatory interaction network is unknown. In addition to *pal-1*, several other genes have been identified as interacting synthetically with *rnt-1*. These include *eat-3* and *pha-2* (Morck and Pilon 2006) and *sop-1* (T. Braun, D. Phil thesis, 2009). Interestingly, parts of the *rnt-1* promoter are able to drive expression in the intestine (C. Brabin, D. Phil. thesis, 2011), and *rnt-1* mutants exhibit starvation defects (R. Nimmo, pers. comm., T. Braun D. Phil. thesis, 2009), which may explain the synthetic larval lethality effect with *pha-2*, a transcription factor required for fate

specification of the pharynx and which is required for normal feeding (Avery 1993, Morck, Rauthan et al. 2004). *eat-3* encodes a mitochondrial protein which, when mutated, causes the animals to be highly sensitive to conditions of elevated stress (Avery 1993, Kanazawa, Zappaterra et al. 2008): again synthetic larval lethality with *rnt-1* may also be linked to the starvation phenotype of *rnt-1* mutants. That *sop-1* was identified as a synthetic interactor with *rnt-1* is very interesting given that *sop-1* is also known to be a suppressor of *pal-1* (Zhang and Emmons 2000). The work shown in Chapter 3 of this thesis shows that *sop-1* is unable to suppress all of the *pal-1(e2091)* phenotypes, however, and *sop-1* has also not been shown to suppress the embryonic lethality of *pal-1* null alleles. This suggests that *pal-1* functions only partially through *sop-1*; as both *pal-1* and *sop-1* act synthetically with *rnt-1*, this partial role of *pal-1* function may be the cause of the synthetic interaction with *rnt-1*.

That *pal-1* does interact physically as well as genetically with *rnt-1* is supported by the BiFC experiments described in this appendix. BiFC has the advantage of being an *in vivo* assay for protein-protein interaction, ideal for the detection of transcription factor interactions that are often transient and supported by other components of large complexes. However, the primary drawback with this technique is that it is not quantitative; the detection of an interaction in transgenic, often mosaic, lines is subject to the eye of the beholder rather than determined by any rigorous statistical threshold. Thus, this technique may be more suited to screening a small number of candidate proteins for possible interactions, rather than being used to validate an interaction. Thus, along with the fact that pinpointing the PAL-1/RNT-1 interaction with respect to a tissue-specific mechanism has been particularly difficult, we decided to pursue other lines of investigation with respect to *pal-1* in the epidermis, as described in Chapters 3, 4 and 5.

Appendix II

Strain List

Name	Genotype	Fig. no.
AW060	*wsIs51 [scm::gfp + unc-119⁺] him-5(e1490)* V	
AW1169	*pal-1(e2091) unc-119(ed3)* III	
AW1170	*pal-1(e2091) unc-119(ed3)* III; *him-5 (e1490) heIs63 [wrt-2p::gfp::PH + wrt-2p::gfp::H2B + lin-48p::mCherry]* V; *ouEx866[pAW634(pal-1::gfp) + unc-119⁺]*	3.2.4
AW1171	*pal-1(e2091) unc-119(ed3)* III; *him-5 (e1490) heIs63 [wrt-2p::gfp::PH + wrt-2p::gfp::H2B + lin-48p::mCherry]* V; *ouEx867[pAW857(pal-1A2110G::gfp) + unc-119⁺]*	3.2.4
AW1172	*wrm-1(ne1982)ts* III; *heIs63 [wrt-2p::gfp::PH + wrt-2p::gfp::H2B + lin-48p::mCherry]* V	
AW1173	*lin-39(n1880)* III; *him-5(e1490)*	
AW1174	*pal-1(e2091) unc-32(e189)* III; *him-5 (e1490) heIs63 [wrt-2p::gfp::PH + wrt-2p::gfp::H2B + lin-48p::mCherry]* V	
AW1175	*pal-1(e2091) lin-39(n1880)* III; *him-5 (e1490) heIs63 [wrt-2p::gfp::PH + wrt-2p::gfp::H2B + lin-48p::mCherry]* V	
AW1176	*stIs10166 [dpy-7p::his-24::mCherry + unc-119⁺] ?; heIs63 [wrt-2p::gfp::PH + wrt-2p::gfp::H2B + lin-48p::mCherry]* V	
AW1177	*heIs63 [wrt-2p::gfp::PH + wrt-2p::gfp::H2B + lin-48p::mCherry]* V; *lin-14(n179)ts* X	
AW1178	*him-5(e1490) heIs63 [wrt-2p::gfp::PH + wrt-2p::gfp::H2B + lin-48p::mCherry]* V; *lin-14(n179)ts* X	
AW1179	*heIs63 [wrt-2p::gfp::PH + wrt-2p::gfp::H2B + lin-48p::mCherry]* V; *unc-6(ev400)* X	
AW1180	*pal-1(e2091)* III; *heIs63 [wrt-2p::gfp::PH + wrt-2p::gfp::H2B + lin-48p::mCherry]* V*; unc-6(ev400)* X	
AW1181	*him-5(e1490) heIs63 [wrt-2p::gfp::PH + wrt-2p::gfp::H2B + lin-48p::mCherry]* V*; unc-6(ev400)* X	
AW1182	*pal-1(e2091)* III; *him-5(e1490) heIs63 [wrt-2p::gfp::PH + wrt-2p::gfp::H2B + lin-48p::mCherry]* V*; unc-6(ev400)* X	
AW1183	*heIs63 [wrt-2p::gfp::PH + wrt-2p::gfp::H2B + lin-48p::mCherry]* V*; unc-6(e78)* X	
AW1184	*punc-25::gfp(juIs76)* II	
AW1185	*punc-25::gfp(juIs76)* II; *him-5(e1490)* V	
AW1186	*heIs63 [wrt-2p::gfp::PH + wrt-2p::gfp::H2B + lin-48p::mCherry]* V; *unc-6(ju152)* X	
AW1187	*pal-1(e2091)* III; *heIs63 [wrt-2p::gfp::PH + wrt-2p::gfp::H2B + lin-48p::mCherry]* V; *unc-6(ju152)* X	
AW1188	*pal-1(e2091)* III; *heIs63 [wrt-2p::gfp::PH + wrt-2p::gfp::H2B + lin-48p::mCherry]* V; *unc-6(e78)* X	
AW1189	*unc-5(e53)* IV; *heIs63 [wrt-2p::gfp::PH + wrt-2p::gfp::H2B + lin-48p::mCherry]* V	
AW1190	*unc-40(e271)* I; *heIs63 [wrt-2p::gfp::PH + wrt-2p::gfp::H2B + lin-48p::mCherry]* V	
AW1191	*pal-1(e2091)* III; *unc-5(e53)* IV; *heIs63 [wrt-2p::gfp::PH + wrt-2p::gfp::H2B + lin-48p::mCherry]* V	
AW1192	*unc-40(e271)* I; *pal-1(e2091)* III; *heIs63 [wrt-2p::gfp::PH + wrt-2p::gfp::H2B + lin-48p::mCherry]* V	
AW1193	*punc-25::gfp(juIs76)* II; *pal-1(e2091)* III; *unc-6(ju152)* X	
AW1194	*punc-25::gfp(juIs76)* II; *pal-1(e2091)* III	

Name	Genotype	Fig. no.
AW1195	*punc-25::gfp(juIs76)* II; *pal-1(e2091)* III; *unc-5(ju181)* IV	
AW1196	*unc-40(e1430)* I; *punc-25::gfp(juIs76)* II; *pal-1(e2091)* III	
AW1197	*max-2(nv162)* II	
AW1198	*max-2(nv162)* II; *him-5(e1490)* V	
AW1199	*max-2(nv162)* II; *heIs63 [wrt-2p::gfp::PH + wrt-2p::gfp::H2B + lin-48p::mCherry]* V	
AW1200	*max-2(nv162)* II; *pal-1(e2091)* III; *heIs63 [wrt-2p::gfp::PH + wrt-2p::gfp::H2B + lin-48p::mCherry]* V	
AW1201	*max-2(nv162)* II; *heIs63 [wrt-2p::gfp::PH + wrt-2p::gfp::H2B + lin-48p::mCherry]* V; *unc-6(ev400)* X	
AW1202	*max-2(nv162)* II; *pal-1(e2091)* III; *heIs63 [wrt-2p::gfp::PH + wrt-2p::gfp::H2B + lin-48p::mCherry]* V; *unc-6(ev400)* X	
AW1203	*unc-119(ed3) III; ouEx868[pAW864(wrt-2p::gfp) + unc-119^{+}]*	6.2.2
AW1204	*unc-119(ed3) III; ouEx869[pAW865(mCherry::wrt-2p::gfp) + unc-119^{+}]*	6.2.5
AW1205	*wrt-2(ok2810)* X (outcrossed x4)	
AW1206	*him-5(e1490)* V; *wrt-2(ok2810)* X (outcrossed x4)	
AW1207	*wIs78 [scm::gfp + ajm-1::gfp + F58E10(cosmid) + unc-119^{+}]* IV; *wrt-2(ok2810)* X (outcrossed x4)	
AW1208	*rnt-1(tm388)* I; *pal-1(e2091)* III; *him-5(e1490)* V	
AW1209	*rnt-1(e1241)* I; *pal-1(e2091)* III; *him-5(e1490)* V	
AW1210	*rnt-1(tm388)* I; *unc-119(ed3)* III	
AW1211	*unc-119(ed3)* III; *ouEx870[pCE-BiFC-VN173 + pCE-BiFC-VC155 + unc-119^{+}]*	
AW1212	*unc-119(ed3)* III; *ouEx871[pAW854(pCE-RNT-1(e1241)-VN173) + pAW726(pCE-BRO-1-VC155) + unc-119^{+}]*	
AW1213	*unc-119(ed3)* III; *ouEx872[pAW724(pCE-RNT-1-VN173) + pAW878(pCE-PAL-1-VC155) + unc-119^{+}]*	
AW1214	*unc-119(ed3)* III; *ouEx873[pAW877(pCE-PAL-1-VN173) + pAW726(pCE-BRO-1-VC155) + unc-119^{+}]*	
AW1215	*rnt-1(tm388)* I; *unc-119(ed3)* III; *ouEx874[pAW877(pCE-PAL-1-VN173) + pAW726(pCE-BRO-1-VC155) + unc-119^{+}]*	
AW1216	*unc-119(ed3)* III; *ouEx875[pAW854(pCE-RNT-1(e1241)-VN173) + pAW878(pCE-PAL-1-VC155) + unc-119^{+}]*	
AW1217	*lin-39 (n1880)* III; *him-5 (e1490) heIs63 [wrt-2p::gfp::PH + wrt-2p::gfp::H2B + lin-48p::mCherry]* V	
AW177	*rnt-1(tm388)* I; *him-5(e1490)* V	
AW298	*wIs78 [ajm-1::gfp + scm::gfp + F58E10(cosmid) + unc-119^{+}]* IV ; *him-5(e1490)* V	
AW707	*unc-119 (ed3)* III*; him-8 (e1489) IV; ouEx642 [pAW638+unc-119^{+}]*	3.1.2
AW708	*unc-119 (ed3)* III*; him-8 (e1489) IV; ouEx643 [pAW640+unc-119^{+}]*	3.1.2
AW710	*pal-1(e2091)* III; *him-5(e1490) wIs51 [scm::gfp + unc-119^{+}]* V	
AW712	*pal-1(e2091)* III; *him-5(e1490)* V; *wIs78 [scm::gfp + ajm-1::gfp + F58E10(cosmid) + unc-119^{+}]* IV	

Name	Genotype	Fig. no.
AW825	*unc-119(ed3)* III; *ouEx689[pAW724(pCE-RNT-1-VN173) + pAW726(pCE-BRO-1-VC155) + unc-119⁺]*	i.ii.iii
AW827	*him-5(e1490) heIs63 [wrt-2p::gfp::PH + wrt-2p::gfp::H2B + lin-48p::mCherry]* V	
AW828	*pal-1(e2091)* III; *heIs63 [wrt-2p::gfp::PH + wrt-2p::gfp::H2B + lin-48p::mCherry]* V	
AW829	*pal-1(e2091)* III; *him-5 (e1490) heIs63 [wrt-2p::gfp::PH + wrt-2p::gfp::H2B + lin-48p::mCherry]* V	
CB271	*unc-40(e271)* I	
CB3924	*pal-1(e2091)* III; *him-5(e1490)* V	
CB4088	*him-5(e1490)* V	
CB4320	*rnt-1(e1241)* I; *him-5(e1490)* V	
CB53	*unc-5(e53)* IV	
CB78	*unc-6(e78)* X	
CZ1919	*punc-25::gfp(juIs76)* II; *unc-6(ju152)* X	
CZ1984	*punc-25::gfp(juIs76)* II; *unc-5(ju181)* X	
CZ2139	*unc-40(e1430)* I; *punc-25::gfp(juIs76)* II	
EW95	*wrm-1(ne1982)ts* III; *wsIs51 [scm::gfp + unc-119⁺]*	
HJ154	*max-2(nv162)* II; *oxIs12[unc-47p::gfp]* X	
HT1593	*unc-119(ed3)* III	
JR667	*wsIs51 [scm::gfp + unc-119⁺]* V	
MT4498	*lin-39(n1880)* III	
N2	Bristol wild-type	
NW434	*unc-6(ev400)* X	
PS4657	*syIs78 [ajm-1::gfp + unc-119⁺] ?*; *him-5(e1490)* V	
RB2125	*wrt-2(ok2810)* X (not outcrossed)	
RG733	*wIs78 [ajm-1::gfp + scm::gfp + F58E10(cosmid) + unc-119⁺]* IV	
SD1546	*ccIs4251 [myo-3p::gfp(NLS)::LacZ + myo-3p::gfp* (mitochondrially targeted) + *dyp-20⁺]; stIs10166 [dpy-7p::his-24::mCherry + unc-119⁺]*	
SP471	*dpy-17(e164) unc-32(e189)* III	
SV1009	*heIs63 [wrt-2p::gfp::PH + wrt-2p::gfp::H2B + lin-48p::mCherry]* V	
Unknown	*bgIs312[vha-8p::gfp]* (Excretory cell marker)	
WM74	*wrm-1(ne1982)ts* III	
YK101	*rnt-1(tm388)* I	

Plasmid List

Name	Description
L4440	Empty RNAi vector
pAW634	TOPO XL with *pal-1::gfp* (rev) translational fusion (made by Charles Brabin)
pAW638	pPD107.94 with *pal-1* last intron (fwd) (made by Charles Brabin)
pAW640	pPD107.94 with *pal-1(e2091)* last intron (fwd) (made by Charles Brabin)
pAW723	*rnt-1* cDNA no stop in TOPO XL fwd with frame shift for BiFC cloning
pAW724	pCE-RNT-1-VN173 vector
pAW725	*bro-1* cDNA no stop in TOPO XL fwd with frame shift for BiFC cloning
pAW726	pCE-BRO-1-VC155 vector
pAW852	*rnt-1(e1241)* cDNA no stop in TOPO XL fwd with frame shift for BiFC cloning
pAW853	pCE-RNT-1(e1241)-VC155 vector
pAW854	pCE-RNT-1(e1241)-VN173 vector
pAW855	pCE-RNT-1-VC155 vector
pAW856	pCE-BRO-1-VN173 vector
pAW857	Same as pAW634 but with A2110G of *e2091*
pAW858	Three tandem repeats of *pal-1* bit of last intron with A2110G of *e2091* in TOPO XL rev
pAW859	Three tandem repeats of pal-1 bit of last intron WT in TOPO XL fwd
pAW860	*pal-1* cDNA (full length) in TOPO XL fwd
pAW862	*wrt-2* 5' 'promoter' in TOPO XL fwd
pAW864	*wrt-2* 5' 'promoter' in pPD107.94
pAW865	*wrt-2p::wrt-2(genomic)::gfp* in TOPO XL rev
pAW867	mCherry in TOPO XL no stop with flanking splice sites and PacI sites fwd
pAW868	*pwrt-2::wrt-2(exons 1-3)::mCherry::wrt-2(exons 4-end no stop)::gfp* in TOPO XL rev
pAW869	pLacZi with three tandem repeats of the enhancer portion of the *pal-1* intron with A2110G from *e2091*
pAW870	pLacZi with three tandem repeats of the enhancer portion of the *pal-1* intron (WT)
pAW871	pHisi-1 with three tandem repeats of the enhancer portion of the *pal-1* intron with A2110G from *e2091*
pAW872	pHisi-1 with three tandem repeats of the enhancer portion of the *pal-1* intron (WT)
pAW873	pAW871 with a yeast KanR cassette cloned from pAW875
pAW874	pAW872 with a yeast KanR cassette cloned from pAW875
pAW875	Yeast KanR cassette from PFA6a-kanMX6 in TOPO XL rev with BamHI and SalI sites for cloning into pHisi-1.
pAW876	*pal-1* cDNA no stop in TOPO XL fwd in frame for BiFC cloning

Name	Description
pAW877	pCE-PAL-1-VN173
pAW878	pCE-PAL-1-VC155
pAW879	*wrt-2* RNAi clone
pCE-BiFC-VC155	BiFC vector containing the carboxyl terminus of Venus for *C. elegans* expression (Hiatt, Shyu et al. 2008, Shyu, Hiatt et al. 2008)
pCE-BiFC-VN173	BiFC vector containing the amino terminus of Venus for *C. elegans* expression (Hiatt, Shyu et al. 2008, Shyu, Hiatt et al. 2008)
pcFJ104	*myo-3p::mCherry::unc-54* 3' UTR
pDP#MM016ß	*unc-119* rescuing plasmid (Maduro and Pilgrim 1995)
PFA6a-kanMX6	Yeast resistance to Kanamycin cassette (Longtine, McKenzie et al. 1998)
pHisi-1	Yeast integration vector (Clontech)
pLacZi	Yeast integration vector (Clontech)
pPD107.94	Fire lab vector with *pes-10* minimal promoter and GFP(NLS) for transcriptional reporter construction
pPD95.75	Fire lab vector containing GFP with no NLS

Primer List

Name	Sequence
oSG3	ctacagaaatgataaagcaaggGtttctgaccagctcgcagag
oSG4	ctctgcgagctggtcagaaaCccttgctttatcatttctgtag
oSG9	agatcttaatgaccaacgtcttccatcacg
oSG10	ggtaccaaaaggcctccaaatagtcggag
oSG11	agatcttaatgaaaagaacgacaacggaccag
oSG12	ggtaccaatgggaagaccatcgcgtc
oSG26	agatctTAATGTCGGTCGATGTCAAGTCGG
oSG27	ggtaccTAGCCGAATCTTCTGTTTGTCACG
oSG76	PHO-atgatggtggccaccgtc
oSG77	PHO-cggcgccgaatgtTtaacg
oSG84	CATGCGAAGAAGTTCGAAATG
oSG85	ccgattactaggctttctgaaaac
oSG101	TCTAGAGTCGACCTGCAGGCATGCAAGC
oSG102	cccaattgtcgacgatgttaagcttgac
oSG107	CCGAAAATTCCATTTGACAATCGTCAT
oSG108	CCACCATCATCGGCGCCGAATATT
oSG109	TCCAATAAACTGATGATTCCACCTGAGTAGTCTG
oSG110	TGTATTATTCATTTGCGAGTTGTAGCAGCC
oSG132	ggtggcaaattgggatACGATGTTAAGCTTGACAGAACGAC
oSG133	GTCAAGCTTAACATCGTatcccaatttgccacctctcatc
oSG165	cacggaactgacttcttggttacac
oSG166	ccgagaaacaattggcaggttg
oSG167	CGACCTGCAGGCATGCAAGCtGAGGACTCCGAAAAATTTGGCAAC
oSG168	GCTTGCATGCCTGCAGGTCG
oSG169	AACAGTTATGTTTGGTATATTGGG
oSG170	AAGGGCCCGTACGGCCGACTAGTAGG
oSG181	CATTCGCTGACCAACTGGAGgtatg
oSG185	GATGAAGCTGACACTGATGTAGATGG
oSG186	cgtatgacccgtcatctttatgtcc
oSG187	CACGAATAGCGATGACGATGATGTG
oSG191	AGCTgtcgacGCTTGGGCTCTTGATGAATTGATC

Name	Sequence
oSG192	AGCTgagctcATGCATACGCCGATCATATTCC
oSG195	AATTAAttatctaatttttcagATGGTCTCAAAGGGTGAAGAAG
oSG196	AATTAAatgttaaaacttacCTTATACAATTCATCCATGCCACC
oSG198	CAACGGTGGCAGCAGATCTAAC
oSG199	GTGATGTCGGCGATATAGGCG

Supplementary Figures

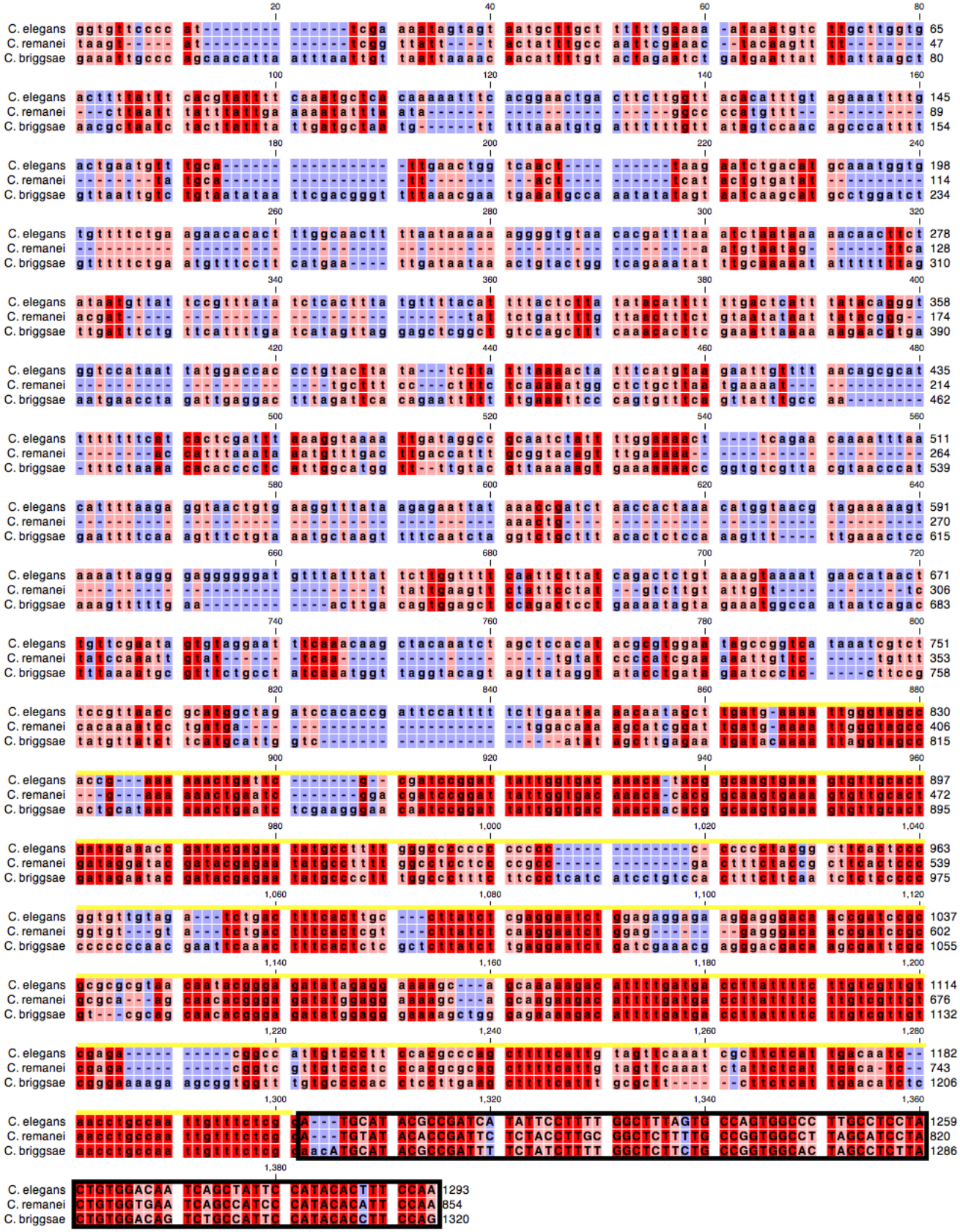

FIG. S1 – ALIGNMENT OF THE *WRT-2* UPSTREAM INTERGENIC REGION BETWEEN DIFFERENT *CAENORHABDITIS* SPECIES.
The black outline highlights the first exon of *wrt-2* (sequence in capitals). Regions of high conservation are indicated in red; low conservation is shown in blue. The conserved region closest to the start codon of *wrt-2* is highlighted in yellow.

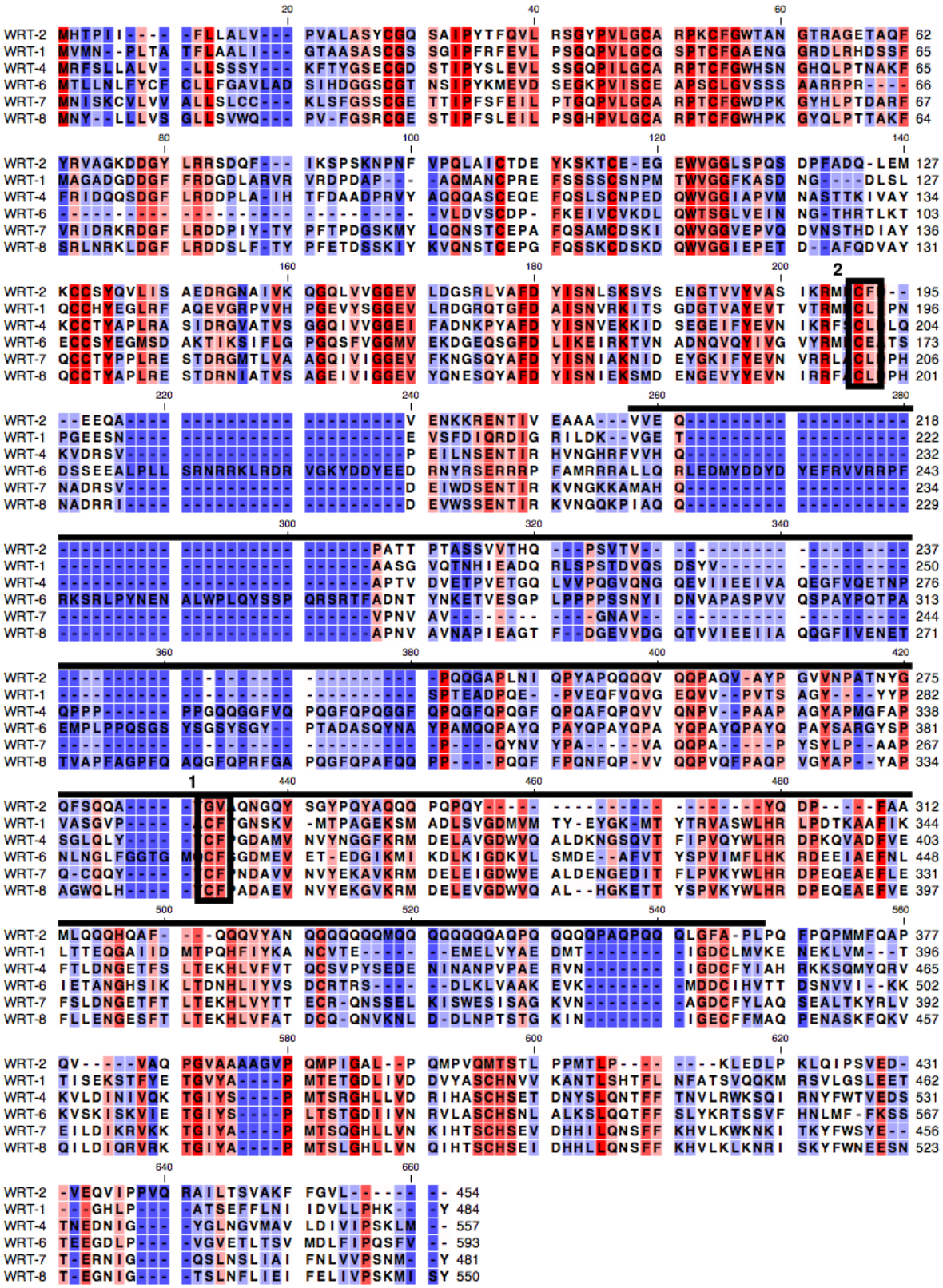

FIG. S2 – ALIGNMENT OF *C. ELEGANS* WRT-2 WITH PREDICTED 'HOG'-CONTAINING WARTHOGS. Those sequences with the highest similarity to WRT-2 have been aligned, incidentally corresponding to the only 'Hog'-containing *C. elegans* Warthog sequences. Red indicates good conservation whereas blue indicates regions that are not conserved. The black line above the alignment highlights the residues deleted in the *wrt-2(ok2810)* mutant. Predicted Warthog cleavage sites are shown with black boxes: box 1 shows the conserved Hedgehog-like cleavage 'CF' motif present in all Warthogs shown apart from WRT-2. However, an upstream CF motif is present in WRT-2 that does not occur in other Warthog protein sequences, shown in box 2, and may be the site of WRT-2 cleavage.

References

Abbasi, A. A., Z. Paparidis, S. Malik, F. Bangs, A. Schmidt, S. Koch, J. Lopez-Rios and K. H. Grzeschik (2010). "Human intronic enhancers control distinct sub-domains of Gli3 expression during mouse CNS and limb development." BMC Dev Biol **10**: 44.

Ackerman, S. L., L. P. Kozak, S. A. Przyborski, L. A. Rund, B. B. Boyer and B. B. Knowles (1997). "The mouse rostral cerebellar malformation gene encodes an UNC-5-like protein." Nature **386**(6627): 838-842.

Adya, N., L. H. Castilla and P. P. Liu (2000). "Function of CBFbeta/Bro proteins." Semin Cell Dev Biol **11**(5): 361-368.

Ahringer, J. (1996). "Posterior patterning by the Caenorhabditis elegans even-skipped homolog vab-7." Genes Dev **10**(9): 1120-1130.

Ahringer, J. (1997). "Maternal control of a zygotic patterning gene in Caenorhabditis elegans." Development **124**(19): 3865-3869.

Albertson, D. G. and J. N. Thomson (1982). "The kinetochores of Caenorhabditis elegans." Chromosoma **86**(3): 409-428.

Alcedo, J., M. Ayzenzon, T. Von Ohlen, M. Noll and J. E. Hooper (1996). "The Drosophila smoothened gene encodes a seven-pass membrane protein, a putative receptor for the hedgehog signal." Cell **86**(2): 221-232.

Alexandre, C., A. Jacinto and P. W. Ingham (1996). "Transcriptional activation of hedgehog target genes in Drosophila is mediated directly by the cubitus interruptus protein, a member of the GLI family of zinc finger DNA-binding proteins." Genes Dev **10**(16): 2003-2013.

Alper, S. and C. Kenyon (2001). "REF-1, a protein with two bHLH domains, alters the pattern of cell fusion in C. elegans by regulating Hox protein activity." Development **128**(10): 1793-1804.

Alper, S. and C. Kenyon (2002). "The zinc finger protein REF-2 functions with the Hox genes to inhibit cell fusion in the ventral epidermis of C. elegans." Development **129**(14): 3335-3348.

Altonsy, M. O., S. K. Sasse, T. L. Phang and A. N. Gerber (2014). "Context-dependent cooperation between nuclear factor kappaB (NF-kappaB) and the glucocorticoid receptor at a TNFAIP3 intronic enhancer: a mechanism to maintain negative feedback control of inflammation." J Biol Chem **289**(12): 8231-8239.

Ambros, V. (2011). "MicroRNAs and developmental timing." Curr Opin Genet Dev **21**(4): 511-517.

Ambros, V. and H. R. Horvitz (1984). "Heterochronic mutants of the nematode Caenorhabditis elegans." Science **226**(4673): 409-416.

Ambros, V. and H. R. Horvitz (1987). "The lin-14 locus of Caenorhabditis elegans controls the time of expression of specific postembryonic developmental events." Genes Dev **1**(4): 398-414.

Andachi, Y. (2004). "Caenorhabditis elegans T-box genes tbx-9 and tbx-8 are required for formation of hypodermis and body-wall muscle in embryogenesis." Genes Cells **9**(4): 331-344.

Angers, S. and R. T. Moon (2009). "Proximal events in Wnt signal transduction." Nat Rev Mol Cell Biol **10**(7): 468-477.

Antoshechkin, I. and M. Han (2002). "The C. elegans evl-20 gene is a homolog of the small GTPase ARL2 and regulates cytoskeleton dynamics during cytokinesis and morphogenesis." Dev Cell **2**(5): 579-591.

Aoki, K., Y. Tamai, S. Horiike, M. Oshima and M. M. Taketo (2003). "Colonic polyposis caused by mTOR-mediated chromosomal instability in Apc+/Delta716 Cdx2+/- compound mutant mice." Nat Genet **35**(4): 323-330.

Asakura, T., N. Waga, K. Ogura and Y. Goshima (2010). "Genes required for cellular UNC-6/netrin localization in Caenorhabditis elegans." Genetics **185**(2): 573-585.

Aspock, G., H. Kagoshima, G. Niklaus and T. R. Burglin (1999). "Caenorhabditis elegans has scores of hedgehog-related genes: sequence and expression analysis." Genome Res **9**(10): 909-923.

Austin, J. and C. Kenyon (1994). "Cell contact regulates neuroblast formation in the Caenorhabditis elegans lateral epidermis." Development **120**(2): 313-323.

Avery, L. (1993). "The genetics of feeding in Caenorhabditis elegans." Genetics **133**(4): 897-917.

Baldwin, A. T. and B. T. Phillips (2014). "The tumor suppressor APC differentially regulates multiple beta-catenins through the function of axin and CKIalpha during C. elegans asymmetric stem cell divisions." J Cell Sci **127**(Pt 12): 2771-2781.

Baroux, C., P. Fransz and U. Grossniklaus (2004). "Nuclear fusions contribute to polyploidization of the gigantic nuclei in the chalazal endosperm of Arabidopsis." Planta **220**(1): 38-46.

Baugh, L. R., A. A. Hill, J. M. Claggett, K. Hill-Harfe, J. C. Wen, D. K. Slonim, E. L. Brown and C. P. Hunter (2005). "The homeodomain protein PAL-1 specifies a lineage-specific regulatory network in the C. elegans embryo." Development **132**(8): 1843-1854.

Beachy, P. A., S. S. Karhadkar and D. M. Berman (2004). "Tissue repair and stem cell renewal in carcinogenesis." Nature **432**(7015): 324-331.

Beck, F., K. Chawengsaksophak, P. Waring, R. J. Playford and J. B. Furness (1999). "Reprogramming of intestinal differentiation and intercalary regeneration in Cdx2 mutant mice." Proc Natl Acad Sci U S A **96**(13): 7318-7323.

Bel-Vialar, S., N. Itasaki and R. Krumlauf (2002). "Initiating Hox gene expression: in the early chick neural tube differential sensitivity to FGF and RA signaling subdivides the HoxB genes in two distinct groups." Development **129**(22): 5103-5115.

Beland, M., N. Pilon, M. Houle, K. Oh, J. R. Sylvestre, P. Prinos and D. Lohnes (2004). "Cdx1 autoregulation is governed by a novel Cdx1-LEF1 transcription complex." Mol Cell Biol **24**(11): 5028-5038.

Belloni, E., M. Muenke, E. Roessler, G. Traverso, J. Siegel-Bartelt, A. Frumkin, H. F. Mitchell, H. Donis-Keller, C. Helms, A. V. Hing, H. H. Heng, B. Koop, D. Martindale, J. M. Rommens, L. C. Tsui and S. W. Scherer (1996). "Identification of Sonic hedgehog as a candidate gene responsible for holoprosencephaly." Nat Genet **14**(3): 353-356.

Bienkowska, D. and C. R. Cowan (2012). "Centrosomes can initiate a polarity axis from any position within one-cell C. elegans embryos." Curr Biol **22**(7): 583-589.

Bischoff, M., A. C. Gradilla, I. Seijo, G. Andres, C. Rodriguez-Navas, L. Gonzalez-Mendez and I. Guerrero (2013). "Cytonemes are required for the establishment of a normal Hedgehog morphogen gradient in Drosophila epithelia." Nat Cell Biol **15**(11): 1269-1281.

Blelloch, R. and J. Kimble (1999). "Control of organ shape by a secreted metalloprotease in the nematode Caenorhabditis elegans." Nature **399**(6736): 586-590.

Blum, E. S., M. C. Abraham, S. Yoshimura, Y. Lu and S. Shaham (2012). "Control of nonapoptotic developmental cell death in Caenorhabditis elegans by a polyglutamine-repeat protein." Science **335**(6071): 970-973.

Blumenthal, T., D. Evans, C. D. Link, A. Guffanti, D. Lawson, J. Thierry-Mieg, D. Thierry-Mieg, W. L. Chiu, K. Duke, M. Kiraly and S. K. Kim (2002). "A global analysis of Caenorhabditis elegans operons." Nature **417**(6891): 851-854.

Bokoch, G. M. (2003). "Biology of the p21-activated kinases." Annu Rev Biochem **72**: 743-781.

Bone, C. R., E. C. Tapley, M. Gorjanacz and D. A. Starr (2014). "The Caenorhabditis elegans SUN protein UNC-84 interacts with lamin to transfer forces from the cytoplasm to the nucleoskeleton during nuclear migration." Mol Biol Cell **25**(18): 2853-2865.

Bonhomme, C., I. Duluc, E. Martin, K. Chawengsaksophak, M. P. Chenard, M. Kedinger, F. Beck, J. N. Freund and C. Domon-Dell (2003). "The Cdx2 homeobox gene has a tumour suppressor function in the distal colon in addition to a homeotic role during gut development." Gut **52**(10): 1465-1471.

Bosher, J. M., B. S. Hahn, R. Legouis, S. Sookhareea, R. M. Weimer, A. Gansmuller, A. D. Chisholm, A. M. Rose, J. L. Bessereau and M. Labouesse (2003). "The Caenorhabditis elegans vab-10 spectraplakin isoforms protect the epidermis against internal and external forces." J Cell Biol **161**(4): 757-768.

Brabin, C., P. J. Appleford and A. Woollard (2011). "The Caenorhabditis elegans GATA factor ELT-1 works through the cell proliferation regulator BRO-1 and the Fusogen EFF-1 to maintain the seam stem-like fate." PLoS Genet **7**(8): e1002200.

Brenner, S. (1973). "The genetics of behaviour." Br Med Bull **29**(3): 269-271.

Brenner, S. (1974). "The genetics of Caenorhabditis elegans." Genetics **77**(1): 71-94.

Briscoe, J. and P. P. Therond (2013). "The mechanisms of Hedgehog signalling and its roles in development and disease." Nat Rev Mol Cell Biol **14**(7): 416-429.

Brooke, N. M., J. Garcia-Fernandez and P. W. Holland (1998). "The ParaHox gene cluster is an evolutionary sister of the Hox gene cluster." Nature **392**(6679): 920-922.

Brunschwig, K., C. Wittmann, R. Schnabel, T. R. Burglin, H. Tobler and F. Muller (1999). "Anterior organization of the Caenorhabditis elegans embryo by the labial-like Hox gene ceh-13." Development **126**(7): 1537-1546.

Buchon, N., D. Osman, F. P. David, H. Y. Fang, J. P. Boquete, B. Deplancke and B. Lemaitre (2013). "Morphological and molecular characterization of adult midgut compartmentalization in Drosophila." Cell Rep **3**(5): 1725-1738.

Burglin, T. R. (1996). "Warthog and groundhog, novel families related to hedgehog." Curr Biol **6**(9): 1047-1050.

Burglin, T. R. (2008). "Evolution of hedgehog and hedgehog-related genes, their origin from Hog proteins in ancestral eukaryotes and discovery of a novel Hint motif." BMC Genomics **9**: 127.

Burglin, T. R. and P. E. Kuwabara (2006). "Homologs of the Hh signalling network in C. elegans." WormBook: 1-14.

Burke, R., D. Nellen, M. Bellotto, E. Hafen, K. A. Senti, B. J. Dickson and K. Basler (1999). "Dispatched, a novel sterol-sensing domain protein dedicated to the release of cholesterol-modified hedgehog from signaling cells." Cell **99**(7): 803-815.

Byerly, L., R. C. Cassada and R. L. Russell (1976). "The life cycle of the nematode Caenorhabditis elegans. I. Wild-type growth and reproduction." Dev Biol **51**(1): 23-33.

C. elegans Sequencing Consortium (1998). "Genome sequence of the nematode C. elegans: a platform for investigating biology." Science **282**(5396): 2012-2018.

Cadigan, K. M. and R. Nusse (1997). "Wnt signaling: a common theme in animal development." Genes Dev **11**(24): 3286-3305.

Callejo, A., C. Torroja, L. Quijada and I. Guerrero (2006). "Hedgehog lipid modifications are required for Hedgehog stabilization in the extracellular matrix." Development **133**(3): 471-483.

Callier, P., P. Calvel, A. Matevossian, P. Makrythanasis, P. Bernard, H. Kurosaka, A. Vannier, C. Thauvin-Robinet, C. Borel, S. Mazaud-Guittot, A. Rolland, C. Desdoits-Lethimonier, M. Guipponi, C. Zimmermann, I. Stevant, F. Kuhne, B. Conne, F. Santoni, S. Lambert, F. Huet, F. Mugneret, J. Jaruzelska, L. Faivre, D. Wilhelm, B. Jegou, P. A. Trainor, M. D. Resh, S. E. Antonarakis and S. Nef (2014). "Loss of function mutation in the palmitoyl-transferase HHAT leads to syndromic 46,XY disorder of sex development by impeding Hedgehog protein palmitoylation and signaling." PLoS Genet **10**(5): e1004340.

Cassada, R. C. and R. L. Russell (1975). "The dauerlarva, a post-embryonic developmental variant of the nematode Caenorhabditis elegans." Dev Biol **46**(2): 326-342.

Cassata, G., G. Shemer, P. Morandi, R. Donhauser, B. Podbilewicz and R. Baumeister (2005). "ceh-16/engrailed patterns the embryonic epidermis of Caenorhabditis elegans." Development **132**(4): 739-749.

Cau, J. and A. Hall (2005). "Cdc42 controls the polarity of the actin and microtubule cytoskeletons through two distinct signal transduction pathways." J Cell Sci **118**(Pt 12): 2579-2587.

Ch'ng, Q. and C. Kenyon (1999). "egl-27 generates anteroposterior patterns of cell fusion in C. elegans by regulating Hox gene expression and Hox protein function." Development **126**(15): 3303-3312.

Chalfie, M., Y. Tu, G. Euskirchen, W. W. Ward and D. C. Prasher (1994). "Green fluorescent protein as a marker for gene expression." Science **263**(5148): 802-805.

Chamoun, Z., R. K. Mann, D. Nellen, D. P. von Kessler, M. Bellotto, P. A. Beachy and K. Basler (2001). "Skinny hedgehog, an acyltransferase required for palmitoylation and activity of the hedgehog signal." Science **293**(5537): 2080-2084.

Chan, S. S., H. Zheng, M. W. Su, R. Wilk, M. T. Killeen, E. M. Hedgecock and J. G. Culotti (1996). "UNC-40, a C. elegans homolog of DCC (Deleted in Colorectal Cancer), is required in motile cells responding to UNC-6 netrin cues." Cell **87**(2): 187-195.

Chang, D. T., A. Lopez, D. P. von Kessler, C. Chiang, B. K. Simandl, R. Zhao, M. F. Seldin, J. F. Fallon and P. A. Beachy (1994). "Products, genetic linkage and limb patterning activity of a murine hedgehog gene." Development **120**(11): 3339-3353.

Charite, J., W. de Graaff, D. Consten, M. J. Reijnen, J. Korving and J. Deschamps (1998). "Transducing positional information to the Hox genes: critical interaction of cdx gene products with position-sensitive regulatory elements." Development **125**(22): 4349-4358.

Chawengsaksophak, K., W. de Graaff, J. Rossant, J. Deschamps and F. Beck (2004). "Cdx2 is essential for axial elongation in mouse development." Proc Natl Acad Sci U S A **101**(20): 7641-7645.

Chawengsaksophak, K., R. James, V. E. Hammond, F. Kontgen and F. Beck (1997). "Homeosis and intestinal tumours in Cdx2 mutant mice." Nature **386**(6620): 84-87.

Cheeks, R. J., J. C. Canman, W. N. Gabriel, N. Meyer, S. Strome and B. Goldstein (2004). "C. elegans PAR proteins function by mobilizing and stabilizing asymmetrically localized protein complexes." Curr Biol **14**(10): 851-862.

Chen, E. H. and E. N. Olson (2004). "Towards a molecular pathway for myoblast fusion in Drosophila." Trends Cell Biol **14**(8): 452-460.

Chen, M. H., Y. J. Li, T. Kawakami, S. M. Xu and P. T. Chuang (2004). "Palmitoylation is required for the production of a soluble multimeric Hedgehog protein complex and long-range signaling in vertebrates." Genes Dev **18**(6): 641-659.

Chen, M. J., T. Yokomizo, B. M. Zeigler, E. Dzierzak and N. A. Speck (2009). "Runx1 is required for the endothelial to haematopoietic cell transition but not thereafter." Nature **457**(7231): 887-891.

Chen, W., S. Chen, S. F. Yap and L. Lim (1996). "The Caenorhabditis elegans p21-activated kinase (CePAK) colocalizes with CeRac1 and CDC42Ce at hypodermal cell boundaries during embryo elongation." J Biol Chem **271**(42): 26362-26368.

Chen, X., H. Tukachinsky, C. H. Huang, C. Jao, Y. R. Chu, H. Y. Tang, B. Mueller, S. Schulman, T. A. Rapoport and A. Salic (2011). "Processing and turnover of the Hedgehog protein in the endoplasmic reticulum." J Cell Biol **192**(5): 825-838.

Chen, Y. and G. Struhl (1996). "Dual roles for patched in sequestering and transducing Hedgehog." Cell **87**(3): 553-563.

Chen, Z., D. J. Eastburn and M. Han (2004). "The Caenorhabditis elegans nuclear receptor gene nhr-25 regulates epidermal cell development." Mol Cell Biol **24**(17): 7345-7358.

Chen, Z. and M. Han (2001). "C. elegans Rb, NuRD, and Ras regulate lin-39-mediated cell fusion during vulval fate specification." Curr Biol **11**(23): 1874-1879.

Chinnaiyan, A. M., K. O'Rourke, B. R. Lane and V. M. Dixit (1997). "Interaction of CED-4 with CED-3 and CED-9: a molecular framework for cell death." Science **275**(5303): 1122-1126.

Chisholm, A. (1991). "Control of cell fate in the tail region of C. elegans by the gene egl-5." Development **111**(4): 921-932.

Chisholm, A. D. and J. Hardin (2005). "Epidermal morphogenesis." WormBook: 1-22.

Chourrout, D., F. Delsuc, P. Chourrout, R. B. Edvardsen, F. Rentzsch, E. Renfer, M. F. Jensen, B. Zhu, P. de Jong, R. E. Steele and U. Technau (2006). "Minimal ProtoHox cluster inferred from bilaterian and cnidarian Hox complements." Nature **442**(7103): 684-687.

Clark, S. G., A. D. Chisholm and H. R. Horvitz (1993). "Control of cell fates in the central body region of C. elegans by the homeobox gene lin-39." Cell **74**(1): 43-55.

Clevers, H. and R. Nusse (2012). "Wnt/beta-catenin signaling and disease." Cell **149**(6): 1192-1205.

Colavita, A. and J. G. Culotti (1998). "Suppressors of ectopic UNC-5 growth cone steering identify eight genes involved in axon guidance in Caenorhabditis elegans." Dev Biol **194**(1): 72-85.

Colavita, A., S. Krishna, H. Zheng, R. W. Padgett and J. G. Culotti (1998). "Pioneer axon guidance by UNC-129, a C. elegans TGF-beta." Science **281**(5377): 706-709.

Colon-Ramos, D. A., M. A. Margeta and K. Shen (2007). "Glia promote local synaptogenesis through UNC-6 (netrin) signaling in C. elegans." Science **318**(5847): 103-106.

Copf, T., R. Schroder and M. Averof (2004). "Ancestral role of caudal genes in axis elongation and segmentation." Proc Natl Acad Sci U S A **101**(51): 17711-17715.

Costa, M., B. W. Draper and J. R. Priess (1997). "The role of actin filaments in patterning the Caenorhabditis elegans cuticle." Dev Biol **184**(2): 373-384.

Costa, M., W. Raich, C. Agbunag, B. Leung, J. Hardin and J. R. Priess (1998). "A putative catenin-cadherin system mediates morphogenesis of the Caenorhabditis elegans embryo." J Cell Biol **141**(1): 297-308.

Cowan, C. R. and A. A. Hyman (2004). "Centrosomes direct cell polarity independently of microtubule assembly in C. elegans embryos." Nature **431**(7004): 92-96.

Cowing, D. and C. Kenyon (1996). "Correct Hox gene expression established independently of position in Caenorhabditis elegans." Nature **382**(6589): 353-356.

Cowing, D. W. and C. Kenyon (1992). "Expression of the homeotic gene mab-5 during Caenorhabditis elegans embryogenesis." Development **116**(2): 481-490.

Cox, G. N., S. Staprans and R. S. Edgar (1981). "The cuticle of Caenorhabditis elegans. II. Stage-specific changes in ultrastructure and protein composition during postembryonic development." Dev Biol **86**(2): 456-470.

Cram, E. J., H. Shang and J. E. Schwarzbauer (2006). "A systematic RNA interference screen reveals a cell migration gene network in C. elegans." J Cell Sci **119**(Pt 23): 4811-4818.

Creanga, A., T. D. Glenn, R. K. Mann, A. M. Saunders, W. S. Talbot and P. A. Beachy (2012). "Scube/You activity mediates release of dually lipid-modified Hedgehog signal in soluble form." Genes Dev **26**(12): 1312-1325.

Cross, J. C., Z. Werb and S. J. Fisher (1994). "Implantation and the placenta: key pieces of the development puzzle." Science **266**(5190): 1508-1518.

Cuenca, A. A., A. Schetter, D. Aceto, K. Kemphues and G. Seydoux (2003). "Polarization of the C. elegans zygote proceeds via distinct establishment and maintenance phases." Development **130**(7): 1255-1265.

Dang, L. H., F. Chen, C. Ying, S. Y. Chun, S. A. Knock, H. D. Appelman and D. T. Dang (2006). "CDX2 has tumorigenic potential in the human colon cancer cell lines LOVO and SW48." Oncogene **25**(15): 2264-2272.

de la Torre, J. R., V. H. Hopker, G. L. Ming, M. M. Poo, M. Tessier-Lavigne, A. Hemmati-Brivanlou and C. E. Holt (1997). "Turning of retinal growth cones in a netrin-1 gradient mediated by the netrin receptor DCC." Neuron **19**(6): 1211-1224.

del Campo, J. J., E. Opoku-Serebuoh, A. B. Isaacson, V. L. Scranton, M. Tucker, M. Han and W. A. Mohler (2005). "Fusogenic activity of EFF-1 is regulated via dynamic localization in fusing somatic cells of C. elegans." Curr Biol **15**(5): 413-423.

Dennis, J. F., H. Kurosaka, A. Iulianella, J. Pace, N. Thomas, S. Beckham, T. Williams and P. A. Trainor (2012). "Mutations in Hedgehog acyltransferase (Hhat) perturb Hedgehog signaling, resulting in severe acrania-holoprosencephaly-agnathia craniofacial defects." PLoS Genet **8**(10): e1002927.

Deppe, U., E. Schierenberg, T. Cole, C. Krieg, D. Schmitt, B. Yoder and G. von Ehrenstein (1978). "Cell lineages of the embryo of the nematode Caenorhabditis elegans." Proc Natl Acad Sci U S A **75**(1): 376-380.

Deshane, J., J. Kim, S. Bolisetty, T. D. Hock, N. Hill-Kapturczak and A. Agarwal (2010). "Sp1 regulates chromatin looping between an intronic enhancer and distal promoter of the human heme oxygenase-1 gene in renal cells." J Biol Chem **285**(22): 16476-16486.

Ding, M., A. Goncharov, Y. Jin and A. D. Chisholm (2003). "C. elegans ankyrin repeat protein VAB-19 is a component of epidermal attachment structures and is essential for epidermal morphogenesis." Development **130**(23): 5791-5801.

Doench, J. G., C. P. Petersen and P. A. Sharp (2003). "siRNAs can function as miRNAs." Genes Dev **17**(4): 438-442.

Dominguez, M., M. Brunner, E. Hafen and K. Basler (1996). "Sending and receiving the hedgehog signal: control by the Drosophila Gli protein Cubitus interruptus." Science **272**(5268): 1621-1625.

Draper, B. W., C. C. Mello, B. Bowerman, J. Hardin and J. R. Priess (1996). "MEX-3 is a KH domain protein that regulates blastomere identity in early C. elegans embryos." Cell **87**(2): 205-216.

Driscoll, M. (1992). "Molecular genetics of cell death in the nematode Caenorhabditis elegans." J Neurobiol **23**(9): 1327-1351.

Driscoll, M. (1995). "Methods for the study of cell death in the nematode Caenorhabditis elegans." Methods Cell Biol **46**: 323-353.

Ducuing, A., B. Mollereau, J. D. Axelrod and S. Vincent (2013). "Absolute requirement of cholesterol binding for Hedgehog gradient formation in Drosophila." Biol Open **2**(6): 596-604.

Duprey, P., K. Chowdhury, G. R. Dressler, R. Balling, D. Simon, J. L. Guenet and P. Gruss (1988). "A mouse gene homologous to the Drosophila gene caudal is expressed in epithelial cells from the embryonic intestine." Genes Dev **2**(12A): 1647-1654.

Echelard, Y., D. J. Epstein, B. St-Jacques, L. Shen, J. Mohler, J. A. McMahon and A. P. McMahon (1993). "Sonic hedgehog, a member of a family of putative signaling molecules, is implicated in the regulation of CNS polarity." Cell **75**(7): 1417-1430.

Edgar, L. G., S. Carr, H. Wang and W. B. Wood (2001). "Zygotic expression of the caudal homolog pal-1 is required for posterior patterning in Caenorhabditis elegans embryogenesis." Dev Biol **229**(1): 71-88.

Ehrman, L. A. and K. E. Yutzey (2001). "Anterior expression of the caudal homologue cCdx-B activates a posterior genetic program in avian embryos." Dev Dyn **221**(4): 412-421.

Eisenmann, D. M., J. N. Maloof, J. S. Simske, C. Kenyon and S. K. Kim (1998). "The beta-catenin homolog BAR-1 and LET-60 Ras coordinately regulate the Hox gene lin-39 during Caenorhabditis elegans vulval development." Development **125**(18): 3667-3680.

Erickson, P., J. Gao, K. S. Chang, T. Look, E. Whisenant, S. Raimondi, R. Lasher, J. Trujillo, J. Rowley and H. Drabkin (1992). "Identification of breakpoints in t(8;21) acute myelogenous leukemia and isolation of a fusion transcript, AML1/ETO, with similarity to Drosophila segmentation gene, runt." Blood **80**(7): 1825-1831.

Evans, T. C., S. L. Crittenden, V. Kodoyianni and J. Kimble (1994). "Translational control of maternal glp-1 mRNA establishes an asymmetry in the C. elegans embryo." Cell **77**(2): 183-194.

Fainsod, A., L. D. Bogarad, T. Ruusala, M. Lubin, D. M. Crothers and F. H. Ruddle (1986). "The homeo domain of a murine protein binds 5' to its own homeo box." Proc Natl Acad Sci U S A **83**(24): 9532-9536.

Fan, C. M., J. A. Porter, C. Chiang, D. T. Chang, P. A. Beachy and M. Tessier-Lavigne (1995). "Long-range sclerotome induction by sonic hedgehog: direct role of the amino-terminal cleavage product and modulation by the cyclic AMP signaling pathway." Cell **81**(3): 457-465.

Feng, J., B. White, O. V. Tyurina, B. Guner, T. Larson, H. Y. Lee, R. O. Karlstrom and J. D. Kohtz (2004). "Synergistic and antagonistic roles of the Sonic hedgehog N- and C-terminal lipids." Development **131**(17): 4357-4370.

Feng, W., J. Huang, J. Zhang and T. Williams (2008). "Identification and analysis of a conserved Tcfap2a intronic enhancer element required for expression in facial and limb bud mesenchyme." Mol Cell Biol **28**(1): 315-325.

Ferreira, H. B., Y. Zhang, C. Zhao and S. W. Emmons (1999). "Patterning of Caenorhabditis elegans posterior structures by the Abdominal-B homolog, egl-5." Dev Biol **207**(1): 215-228.

Fiedler, M., M. Graeb, J. Mieszczanek, T. J. Rutherford, C. M. Johnson and M. Bienz (2015). "An ancient Pygo-dependent Wnt enhanceosome integrated by Chip/LDB-SSDP." Elife **4**.

Fiumara, F., L. Fioriti, E. R. Kandel and W. A. Hendrickson (2010). "Essential role of coiled coils for aggregation and activity of Q/N-rich prions and PolyQ proteins." Cell **143**(7): 1121-1135.

Forbes, A. J., Y. Nakano, A. M. Taylor and P. W. Ingham (1993). "Genetic analysis of hedgehog signalling in the Drosophila embryo." Dev Suppl: 115-124.

Forrester, W. C., M. Dell, E. Perens and G. Garriga (1999). "A C. elegans Ror receptor tyrosine kinase regulates cell motility and asymmetric cell division." Nature **400**(6747): 881-885.

Frand, A. R., S. Russel and G. Ruvkun (2005). "Functional genomic analysis of C. elegans molting." PLoS Biol **3**(10): e312.

Fridolfsson, H. N., N. Ly, M. Meyerzon and D. A. Starr (2010). "UNC-83 coordinates kinesin-1 and dynein activities at the nuclear envelope during nuclear migration." Dev Biol **338**(2): 237-250.

Fujiki, K., T. Mizuno, N. Hisamoto and K. Matsumoto (2010). "The Caenorhabditis elegans Ste20-related kinase and Rac-type small GTPase regulate the c-Jun N-terminal kinase signaling pathway mediating the stress response." Mol Cell Biol **30**(4): 995-1003.

Gallet, A., R. Rodriguez, L. Ruel and P. P. Therond (2003). "Cholesterol modification of hedgehog is required for trafficking and movement, revealing an asymmetric cellular response to hedgehog." Dev Cell **4**(2): 191-204.

Gallet, A., L. Ruel, L. Staccini-Lavenant and P. P. Therond (2006). "Cholesterol modification is necessary for controlled planar long-range activity of Hedgehog in Drosophila epithelia." Development **133**(3): 407-418.

Gamer, L. W. and C. V. Wright (1993). "Murine Cdx-4 bears striking similarities to the Drosophila caudal gene in its homeodomain sequence and early expression pattern." Mech Dev **43**(1): 71-81.

Gao, N. and K. H. Kaestner (2010). "Cdx2 regulates endo-lysosomal function and epithelial cell polarity." Genes Dev **24**(12): 1295-1305.

Gao, N., P. White and K. H. Kaestner (2009). "Establishment of intestinal identity and epithelial-mesenchymal signaling by Cdx2." Dev Cell **16**(4): 588-599.

Gattegno, T., A. Mittal, C. Valansi, K. C. Nguyen, D. H. Hall, L. V. Chernomordik and B. Podbilewicz (2007). "Genetic control of fusion pore expansion in the epidermis of Caenorhabditis elegans." Mol Biol Cell **18**(4): 1153-1166.

George, S. E., K. Simokat, J. Hardin and A. D. Chisholm (1998). "The VAB-1 Eph receptor tyrosine kinase functions in neural and epithelial morphogenesis in C. elegans." Cell **92**(5): 633-643.

Gergen, J. P. and B. A. Butler (1988). "Isolation of the Drosophila segmentation gene runt and analysis of its expression during embryogenesis." Genes Dev **2**(9): 1179-1193.

Gerstein, M. B., Z. J. Lu, E. L. Van Nostrand, C. Cheng, B. I. Arshinoff, T. Liu, K. Y. Yip, R. Robilotto, A. Rechtsteiner, K. Ikegami, P. Alves, A. Chateigner, M. Perry, M. Morris, R. K. Auerbach, X. Feng, J. Leng, A. Vielle, W. Niu, K. Rhrissorrakrai, A. Agarwal, R. P. Alexander, G. Barber, C. M. Brdlik, J. Brennan, J. J. Brouillet, A. Carr, M. S. Cheung, H. Clawson, S. Contrino, L. O. Dannenberg, A. F. Dernburg, A. Desai, L. Dick, A. C. Dose, J. Du, T. Egelhofer, S. Ercan, G. Euskirchen, B. Ewing, E. A. Feingold, R. Gassmann, P. J. Good, P. Green, F. Gullier, M. Gutwein, M. S. Guyer, L. Habegger, T. Han, J. G. Henikoff, S. R. Henz, A. Hinrichs, H. Holster, T. Hyman, A. L. Iniguez, J. Janette, M. Jensen, M. Kato, W. J. Kent, E. Kephart, V. Khivansara, E. Khurana, J. K. Kim, P. Kolasinska-Zwierz, E. C. Lai, I. Latorre, A. Leahey, S. Lewis, P. Lloyd, L. Lochovsky, R. F. Lowdon, Y. Lubling, R. Lyne, M. MacCoss, S. D. Mackowiak, M. Mangone, S. McKay, D. Mecenas, G. Merrihew, D. M. Miller, 3rd, A. Muroyama, J. I. Murray, S. L. Ooi, H. Pham, T. Phippen, E. A. Preston, N. Rajewsky, G. Ratsch, H. Rosenbaum, J. Rozowsky, K. Rutherford, P. Ruzanov, M. Sarov, R. Sasidharan, A. Sboner, P. Scheid, E. Segal, H. Shin, C. Shou, F. J. Slack, C. Slightam, R. Smith, W. C. Spencer, E. O. Stinson, S. Taing, T. Takasaki, D. Vafeados, K. Voronina, G. Wang, N. L. Washington, C. M. Whittle, B. Wu, K. K. Yan, G. Zeller, Z. Zha, M. Zhong, X. Zhou, E. C. mod, J. Ahringer, S. Strome, K. C. Gunsalus, G. Micklem, X. S. Liu, V. Reinke, S. K. Kim, L. W. Hillier, S. Henikoff, F. Piano, M. Snyder, L. Stein, J. D. Lieb and R. H. Waterston (2010). "Integrative analysis of the Caenorhabditis elegans genome by the modENCODE project." Science **330**(6012): 1775-1787.

Gilleard, J. S., J. D. Barry and I. L. Johnstone (1997). "cis regulatory requirements for hypodermal cell-specific expression of the Caenorhabditis elegans cuticle collagen gene dpy-7." Mol Cell Biol **17**(4): 2301-2311.

Gleason, J. E. and D. M. Eisenmann (2010). "Wnt signaling controls the stem cell-like asymmetric division of the epithelial seam cells during C. elegans larval development." Dev Biol **348**(1): 58-66.

Gleason, J. E., H. C. Korswagen and D. M. Eisenmann (2002). "Activation of Wnt signaling bypasses the requirement for RTK/Ras signaling during C. elegans vulval induction." Genes Dev **16**(10): 1281-1290.

Goldstein, B. and S. N. Hird (1996). "Specification of the anteroposterior axis in Caenorhabditis elegans." Development **122**(5): 1467-1474.

Goldstein, B., H. Takeshita, K. Mizumoto and H. Sawa (2006). "Wnt signals can function as positional cues in establishing cell polarity." Dev Cell **10**(3): 391-396.

Gradilla, A. C., E. Gonzalez, I. Seijo, G. Andres, M. Bischoff, L. Gonzalez-Mendez, V. Sanchez, A. Callejo, C. Ibanez, M. Guerra, J. R. Ortigao-Farias, J. D. Sutherland, M. Gonzalez, R. Barrio, J. M. Falcon-Perez and I. Guerrero (2014). "Exosomes as Hedgehog carriers in cytoneme-mediated transport and secretion." Nat Commun **5**: 5649.

Graham, P. L., J. J. Johnson, S. Wang, M. H. Sibley, M. C. Gupta and J. M. Kramer (1997). "Type IV collagen is detectable in most, but not all, basement membranes of Caenorhabditis elegans and assembles on tissues that do not express it." J Cell Biol **137**(5): 1171-1183.

Grainger, S., J. G. Savory and D. Lohnes (2010). "Cdx2 regulates patterning of the intestinal epithelium." Dev Biol **339**(1): 155-165.

Green, J. L., T. Inoue and P. W. Sternberg (2008). "Opposing Wnt pathways orient cell polarity during organogenesis." Cell **134**(4): 646-656.

Grill, S. W., P. Gonczy, E. H. Stelzer and A. A. Hyman (2001). "Polarity controls forces governing asymmetric spindle positioning in the Caenorhabditis elegans embryo." Nature **409**(6820): 630-633.

Grill, S. W., J. Howard, E. Schaffer, E. H. Stelzer and A. A. Hyman (2003). "The distribution of active force generators controls mitotic spindle position." Science **301**(5632): 518-521.

Hajduskova, M., M. Jindra, M. A. Herman and M. Asahina (2009). "The nuclear receptor NHR-25 cooperates with the Wnt/beta-catenin asymmetry pathway to control differentiation of the T seam cell in C. elegans." J Cell Sci **122**(Pt 17): 3051-3060.

Hall, D. H., V. P. Winfrey, G. Blaeuer, L. H. Hoffman, T. Furuta, K. L. Rose, O. Hobert and D. Greenstein (1999). "Ultrastructural features of the adult hermaphrodite gonad of Caenorhabditis elegans: relations between the germ line and soma." Dev Biol **212**(1): 101-123.

Hall, M. N. and A. D. Johnson (1987). "Homeo domain of the yeast repressor alpha 2 is a sequence-specific DNA-binding domain but is not sufficient for repression." Science **237**(4818): 1007-1012.

Hamill, D. R., A. F. Severson, J. C. Carter and B. Bowerman (2002). "Centrosome maturation and mitotic spindle assembly in C. elegans require SPD-5, a protein with multiple coiled-coil domains." Dev Cell **3**(5): 673-684.

Hammell, C. M., X. Karp and V. Ambros (2009). "A feedback circuit involving let-7-family miRNAs and DAF-12 integrates environmental signals and developmental timing in Caenorhabditis elegans." Proc Natl Acad Sci U S A **106**(44): 18668-18673.

Hao, L., G. Aspock and T. R. Burglin (2006). "The hedgehog-related gene wrt-5 is essential for hypodermal development in Caenorhabditis elegans." Dev Biol **290**(2): 323-336.

Hao, L., R. Johnsen, G. Lauter, D. Baillie and T. R. Burglin (2006). "Comprehensive analysis of gene expression patterns of hedgehog-related genes." BMC Genomics **7**: 280.

Haremaki, T., Y. Tanaka, I. Hongo, M. Yuge and H. Okamoto (2003). "Integration of multiple signal transducing pathways on Fgf response elements of the Xenopus caudal homologue Xcad3." Development **130**(20): 4907-4917.

Harris, J., L. Honigberg, N. Robinson and C. Kenyon (1996). "Neuronal cell migration in C. elegans: regulation of Hox gene expression and cell position." Development **122**(10): 3117-3131.

Harris, R., L. M. Sabatelli and M. A. Seeger (1996). "Guidance cues at the Drosophila CNS midline: identification and characterization of two Drosophila Netrin/UNC-6 homologs." Neuron **17**(2): 217-228.

Harrison, P. M., N. Echols and M. B. Gerstein (2001). "Digging for dead genes: an analysis of the characteristics of the pseudogene population in the Caenorhabditis elegans genome." Nucleic Acids Res **29**(3): 818-830.

Hassan, M. Q., J. A. Gordon, M. M. Beloti, C. M. Croce, A. J. van Wijnen, J. L. Stein, G. S. Stein and J. B. Lian (2010). "A network connecting Runx2, SATB2, and the miR-23a~27a~24-2 cluster regulates the osteoblast differentiation program." Proc Natl Acad Sci U S A **107**(46): 19879-19884.

Hedgecock, E. M., J. G. Culotti and D. H. Hall (1990). "The unc-5, unc-6, and unc-40 genes guide circumferential migrations of pioneer axons and mesodermal cells on the epidermis in C. elegans." Neuron **4**(1): 61-85.

Hedgecock, E. M. and J. G. White (1985). "Polyploid tissues in the nematode Caenorhabditis elegans." Dev Biol **107**(1): 128-133.

Heid, P. J., W. B. Raich, R. Smith, W. A. Mohler, K. Simokat, S. B. Gendreau, J. H. Rothman and J. Hardin (2001). "The zinc finger protein DIE-1 is required for late events during epithelial cell rearrangement in C. elegans." Dev Biol **236**(1): 165-180.

Hendriks, G. J., D. Gaidatzis, F. Aeschimann and H. Grosshans (2014). "Extensive oscillatory gene expression during C. elegans larval development." Mol Cell **53**(3): 380-392.

Hengartner, M. O. and H. R. Horvitz (1994). "Activation of C. elegans cell death protein CED-9 by an amino-acid substitution in a domain conserved in Bcl-2." Nature **369**(6478): 318-320.

Hengartner, M. O. and H. R. Horvitz (1994). "C. elegans cell survival gene ced-9 encodes a functional homolog of the mammalian proto-oncogene bcl-2." Cell **76**(4): 665-676.

Herman, M. A. (2006). "Hermaphrodite cell-fate specification." WormBook: 1-16.

Herman, M. A., L. L. Vassilieva, H. R. Horvitz, J. E. Shaw and R. K. Herman (1995). "The C. elegans gene lin-44, which controls the polarity of certain asymmetric cell divisions, encodes a Wnt protein and acts cell nonautonomously." Cell **83**(1): 101-110.

Hiatt, S. M., Y. J. Shyu, H. M. Duren and C. D. Hu (2008). "Bimolecular fluorescence complementation (BiFC) analysis of protein interactions in Caenorhabditis elegans." Methods **45**(3): 185-191.

Hickey, P. C., D. Jacobson, N. D. Read and N. L. Glass (2002). "Live-cell imaging of vegetative hyphal fusion in Neurospora crassa." Fungal Genet Biol **37**(1): 109-119.

Hinoi, T., M. Loda and E. R. Fearon (2003). "Silencing of CDX2 expression in colon cancer via a dominant repression pathway." J Biol Chem **278**(45): 44608-44616.

Hird, S. N., J. E. Paulsen and S. Strome (1996). "Segregation of germ granules in living Caenorhabditis elegans embryos: cell-type-specific mechanisms for cytoplasmic localisation." Development **122**(4): 1303-1312.

Hird, S. N. and J. G. White (1993). "Cortical and cytoplasmic flow polarity in early embryonic cells of Caenorhabditis elegans." J Cell Biol **121**(6): 1343-1355.

Hiroki, T., S. A. Liebhaber and N. E. Cooke (2007). "An intronic locus control region plays an essential role in the establishment of an autonomous hepatic chromatin domain for the human vitamin D-binding protein gene." Mol Cell Biol **27**(21): 7365-7380.

Hirsh, D., D. Oppenheim and M. Klass (1976). "Development of the reproductive system of Caenorhabditis elegans." Dev Biol **49**(1): 200-219.

Hodgkin, J. (1983). "Male Phenotypes and Mating Efficiency in CAENORHABDITIS ELEGANS." Genetics **103**(1): 43-64.

Hoffmann, C., A. Zimmermann, A. Hinney, A. L. Volckmar, H. W. Jarrett, T. Fromme and M. Klingenspor (2013). "A novel SP1/SP3 dependent intronic enhancer governing transcription of the UCP3 gene in brown adipocytes." PLoS One **8**(12): e83426.

Holland, P. W. (2013). "Evolution of homeobox genes." Wiley Interdiscip Rev Dev Biol **2**(1): 31-45.

Honigberg, L. and C. Kenyon (2000). "Establishment of left/right asymmetry in neuroblast migration by UNC-40/DCC, UNC-73/Trio and DPY-19 proteins in C. elegans." Development **127**(21): 4655-4668.

Hooper, J. E. and M. P. Scott (1989). "The Drosophila patched gene encodes a putative membrane protein required for segmental patterning." Cell **59**(4): 751-765.

Horn, M., C. Geisen, L. Cermak, B. Becker, S. Nakamura, C. Klein, M. Pagano and A. Antebi (2014). "DRE-1/FBXO11-dependent degradation of BLMP-1/BLIMP-1 governs C. elegans developmental timing and maturation." Dev Cell **28**(6): 697-710.

Hresko, M. C., L. A. Schriefer, P. Shrimankar and R. H. Waterston (1999). "Myotactin, a novel hypodermal protein involved in muscle-cell adhesion in Caenorhabditis elegans." J Cell Biol **146**(3): 659-672.

Hryniuk, A., S. Grainger, J. G. Savory and D. Lohnes (2012). "Cdx function is required for maintenance of intestinal identity in the adult." Dev Biol **363**(2): 426-437.

Hryniuk, A., S. Grainger, J. G. Savory and D. Lohnes (2014). "Cdx1 and Cdx2 function as tumor suppressors." J Biol Chem **289**(48): 33343-33354.

Hu, Y., J. Kazenwadel and R. James (1993). "Isolation and characterization of the murine homeobox gene Cdx-1. Regulation of expression in intestinal epithelial cells." J Biol Chem **268**(36): 27214-27225.

Huang, C. C., C. B. Chiribau, M. Majumder, C. M. Chiang, R. C. Wek, R. J. Kelm, Jr., K. Khalili, M. D. Snider and M. Hatzoglou (2009). "A bifunctional intronic element regulates the expression of the arginine/lysine transporter Cat-1 via mechanisms involving the purine-rich element binding protein A (Pur alpha)." J Biol Chem **284**(47): 32312-32320.

Huang, C. C., D. H. Hall, E. M. Hedgecock, G. Kao, V. Karantza, B. E. Vogel, H. Hutter, A. D. Chisholm, P. D. Yurchenco and W. G. Wadsworth (2003). "Laminin alpha subunits and their role in C. elegans development." Development **130**(14): 3343-3358.

Huang, S., P. Shetty, S. M. Robertson and R. Lin (2007). "Binary cell fate specification during C. elegans embryogenesis driven by reiterated reciprocal asymmetry of TCF POP-1 and its coactivator beta-catenin SYS-1." Development **134**(14): 2685-2695.

Huang, X., P. Huang, M. K. Robinson, M. J. Stern and Y. Jin (2003). "UNC-71, a disintegrin and metalloprotease (ADAM) protein, regulates motor axon guidance and sex myoblast migration in C. elegans." Development **130**(14): 3147-3161.

Huang, X., Y. Litingtung and C. Chiang (2007). "Region-specific requirement for cholesterol modification of sonic hedgehog in patterning the telencephalon and spinal cord." Development **134**(11): 2095-2105.

Huang, X., E. Tian, Y. Xu and H. Zhang (2009). "The C. elegans engrailed homolog ceh-16 regulates the self-renewal expansion division of stem cell-like seam cells." Dev Biol **333**(2): 337-347.

Hughes, S., C. Brabin, P. J. Appleford and A. Woollard (2013). "CEH-20/Pbx and UNC-62/Meis function upstream of rnt-1/Runx to regulate asymmetric divisions of the C. elegans stem-like seam cells." Biol Open **2**(7): 718-727.

Hui, J. H., P. W. Holland and D. E. Ferrier (2008). "Do cnidarians have a ParaHox cluster? Analysis of synteny around a Nematostella homeobox gene cluster." Evol Dev **10**(6): 725-730.

Hunter, C. P., J. M. Harris, J. N. Maloof and C. Kenyon (1999). "Hox gene expression in a single Caenorhabditis elegans cell is regulated by a caudal homolog and intercellular signals that inhibit wnt signaling." Development **126**(4): 805-814.

Hunter, C. P. and C. Kenyon (1996). "Spatial and temporal controls target pal-1 blastomere-specification activity to a single blastomere lineage in C. elegans embryos." Cell **87**(2): 217-226.

Huong le, T., M. Kobayashi, M. Nakata, G. Shioi, H. Miyachi, T. Honjo and H. Nagaoka (2013). "In vivo analysis of Aicda gene regulation: a critical balance between upstream enhancers and intronic silencers governs appropriate expression." PLoS One **8**(4): e61433.

Hutter, H. and R. Schnabel (1994). "glp-1 and inductions establishing embryonic axes in C. elegans." Development **120**(7): 2051-2064.

Hutter, H. and R. Schnabel (1995). "Establishment of left-right asymmetry in the Caenorhabditis elegans embryo: a multistep process involving a series of inductive events." Development **121**(10): 3417-3424.

Hutvagner, G. and P. D. Zamore (2002). "A microRNA in a multiple-turnover RNAi enzyme complex." Science **297**(5589): 2056-2060.

Ikeya, M. and S. Takada (2001). "Wnt-3a is required for somite specification along the anteroposterior axis of the mouse embryo and for regulation of cdx-1 expression." Mech Dev **103**(1-2): 27-33.

Imamichi, Y., T. Mizutani, Y. Ju, T. Matsumura, S. Kawabe, M. Kanno, T. Yazawa and K. Miyamoto (2014). "Transcriptional regulation of human ferredoxin reductase through an intronic enhancer in steroidogenic cells." Biochim Biophys Acta **1839**(1): 33-42.

Inoue, K., S. Ozaki, T. Shiga, K. Ito, T. Masuda, N. Okado, T. Iseda, S. Kawaguchi, M. Ogawa, S. C. Bae, N. Yamashita, S. Itohara, N. Kudo and Y. Ito (2002). "Runx3 controls the axonal projection of proprioceptive dorsal root ganglion neurons." Nature neuroscience **5**(10): 946-954.

Inoue, T., H. S. Oz, D. Wiland, S. Gharib, R. Deshpande, R. J. Hill, W. S. Katz and P. W. Sternberg (2004). "C. elegans LIN-18 is a Ryk ortholog and functions in parallel to LIN-17/Frizzled in Wnt signaling." Cell **118**(6): 795-806.

Isaacs, H. V., M. E. Pownall and J. M. Slack (1998). "Regulation of Hox gene expression and posterior development by the Xenopus caudal homologue Xcad3." EMBO J **17**(12): 3413-3427.

Ishii, N., W. G. Wadsworth, B. D. Stern, J. G. Culotti and E. M. Hedgecock (1992). "UNC-6, a laminin-related protein, guides cell and pioneer axon migrations in C. elegans." Neuron **9**(5): 873-881.

Jarriault, S., Y. Schwab and I. Greenwald (2008). "A Caenorhabditis elegans model for epithelial-neuronal transdifferentiation." Proc Natl Acad Sci U S A **105**(10): 3790-3795.

Jee, W. S. and P. D. Nolan (1963). "Origin of Osteoclasts from the Fusion of Phagocytes." Nature **200**: 225-226.

Jeong, J. and A. P. McMahon (2002). "Cholesterol modification of Hedgehog family proteins." J Clin Invest **110**(5): 591-596.

Jin, Y., E. Jorgensen, E. Hartwieg and H. R. Horvitz (1999). "The Caenorhabditis elegans gene unc-25 encodes glutamic acid decarboxylase and is required for synaptic transmission but not synaptic development." J Neurosci **19**(2): 539-548.

Johnson, T. E., D. H. Mitchell, S. Kline, R. Kemal and J. Foy (1984). "Arresting development arrests aging in the nematode Caenorhabditis elegans." Mech Ageing Dev **28**(1): 23-40.

Kagoshima, H., R. Nimmo, N. Saad, J. Tanaka, Y. Miwa, S. Mitani, Y. Kohara and A. Woollard (2007). "The C. elegans CBFbeta homologue BRO-1 interacts with the Runx factor, RNT-1, to promote stem cell proliferation and self-renewal." Development **134**(21): 3905-3915.

Kalay, G. and P. J. Wittkopp (2010). "Nomadic enhancers: tissue-specific cis-regulatory elements of yellow have divergent genomic positions among Drosophila species." PLoS Genet **6**(11): e1001222.

Kamachi, Y., E. Ogawa, M. Asano, S. Ishida, Y. Murakami, M. Satake, Y. Ito and K. Shigesada (1990). "Purification of a mouse nuclear factor that binds to both the A and B cores of the polyomavirus enhancer." J Virol **64**(10): 4808-4819.

Kamath, R. S. and J. Ahringer (2003). "Genome-wide RNAi screening in Caenorhabditis elegans." Methods **30**(4): 313-321.

Kanazawa, T., M. D. Zappaterra, A. Hasegawa, A. P. Wright, E. D. Newman-Smith, K. F. Buttle, K. McDonald, C. A. Mannella and A. M. van der Bliek (2008). "The C. elegans Opa1 homologue EAT-3 is essential for resistance to free radicals." PLoS Genet **4**(2): e1000022.

Katsuyama, Y., Y. Sato, S. Wada and H. Saiga (1999). "Ascidian tail formation requires caudal function." Dev Biol **213**(2): 257-268.

Kawano, T., H. Zheng, D. C. Merz, Y. Kohara, K. K. Tamai, K. Nishiwaki and J. G. Culotti (2009). "C. elegans mig-6 encodes papilin isoforms that affect distinct aspects of DTC migration, and interacts genetically with mig-17 and collagen IV." Development **136**(9): 1433-1442.

Keating, H. H. and J. G. White (1998). "Centrosome dynamics in early embryos of Caenorhabditis elegans." J Cell Sci **111 (Pt 20)**: 3027-3033.

Keino-Masu, K., M. Masu, L. Hinck, E. D. Leonardo, S. S. Chan, J. G. Culotti and M. Tessier-Lavigne (1996). "Deleted in Colorectal Cancer (DCC) encodes a netrin receptor." Cell **87**(2): 175-185.

Kemphues, K. J., J. R. Priess, D. G. Morton and N. S. Cheng (1988). "Identification of genes required for cytoplasmic localization in early C. elegans embryos." Cell **52**(3): 311-320.

Kennedy, T. E., T. Serafini, J. R. de la Torre and M. Tessier-Lavigne (1994). "Netrins are diffusible chemotropic factors for commissural axons in the embryonic spinal cord." Cell **78**(3): 425-435.

Kenyon, C. (1986). "A gene involved in the development of the posterior body region of C. elegans." Cell **46**(3): 477-487.

Khan, M. R. and G. M. Ali (2013). "Functional evolution of cis-regulatory modules of STMADS11 superclade MADS-box genes." Plant Mol Biol **83**(4-5): 489-506.

Khandekar, M., W. Brandt, Y. Zhou, S. Dagenais, T. W. Glover, N. Suzuki, R. Shimizu, M. Yamamoto, K. C. Lim and J. D. Engel (2007). "A Gata2 intronic enhancer confers its pan-endothelia-specific regulation." Development **134**(9): 1703-1712.

Kidd, A. R., 3rd, J. A. Miskowski, K. R. Siegfried, H. Sawa and J. Kimble (2005). "A beta-catenin identified by functional rather than sequence criteria and its role in Wnt/MAPK signaling." Cell **121**(5): 761-772.

Kikuchi, T., Y. Shibata, H. S. Kim, Y. Kubota, S. Yoshina, S. Mitani and K. Nishiwaki (2015). "The BED finger domain protein MIG-39 halts migration of distal tip cells in Caenorhabditis elegans." Dev Biol **397**(2): 151-161.

Kimble, J. and D. Hirsh (1979). "The postembryonic cell lineages of the hermaphrodite and male gonads in Caenorhabditis elegans." Dev Biol **70**(2): 396-417.

Kimble, J. E. and J. G. White (1981). "On the control of germ cell development in Caenorhabditis elegans." Dev Biol **81**(2): 208-219.

Kiontke, K. C., M. A. Felix, M. Ailion, M. V. Rockman, C. Braendle, J. B. Penigault and D. H. Fitch (2011). "A phylogeny and molecular barcodes for Caenorhabditis, with numerous new species from rotting fruits." BMC Evol Biol **11**: 339.

Kiosses, W. B., R. H. Daniels, C. Otey, G. M. Bokoch and M. A. Schwartz (1999). "A role for p21-activated kinase in endothelial cell migration." J Cell Biol **147**(4): 831-844.

Kirby, C., M. Kusch and K. Kemphues (1990). "Mutations in the par genes of Caenorhabditis elegans affect cytoplasmic reorganization during the first cell cycle." Dev Biol **142**(1): 203-215.

Koh, K., Y. Bernstein and M. V. Sundaram (2004). "The nT1 translocation separates vulval regulatory elements from the egl-18 and elt-6 GATA factor genes." Dev Biol **267**(1): 252-263.

Koh, K., S. M. Peyrot, C. G. Wood, J. A. Wagmaister, M. F. Maduro, D. M. Eisenmann and J. H. Rothman (2002). "Cell fates and fusion in the C. elegans vulval primordium are regulated by the EGL-18 and ELT-6 GATA factors -- apparent direct targets of the LIN-39 Hox protein." Development **129**(22): 5171-5180.

Koh, K. and J. H. Rothman (2001). "ELT-5 and ELT-6 are required continuously to regulate epidermal seam cell differentiation and cell fusion in C. elegans." Development **128**(15): 2867-2880.

Kolodziej, P. A., L. C. Timpe, K. J. Mitchell, S. R. Fried, C. S. Goodman, L. Y. Jan and Y. N. Jan (1996). "frazzled encodes a Drosophila member of the DCC immunoglobulin subfamily and is required for CNS and motor axon guidance." Cell **87**(2): 197-204.

Kolotuev, I., A. Apaydin and M. Labouesse (2009). "Secretion of Hedgehog-related peptides and WNT during Caenorhabditis elegans development." Traffic **10**(7): 803-810.

Komori, T., H. Yagi, S. Nomura, A. Yamaguchi, K. Sasaki, K. Deguchi, Y. Shimizu, R. T. Bronson, Y. H. Gao, M. Inada, M. Sato, R. Okamoto, Y. Kitamura, S. Yoshiki and T. Kishimoto (1997). "Targeted disruption of Cbfa1 results in a complete lack of bone formation owing to maturational arrest of osteoblasts." Cell **89**(5): 755-764.

Korswagen, H. C., D. Y. Coudreuse, M. C. Betist, S. van de Water, D. Zivkovic and H. C. Clevers (2002). "The Axin-like protein PRY-1 is a negative regulator of a canonical Wnt pathway in C. elegans." Genes Dev **16**(10): 1291-1302.

Korswagen, H. C., M. A. Herman and H. C. Clevers (2000). "Distinct beta-catenins mediate adhesion and signalling functions in C. elegans." Nature **406**(6795): 527-532.

Kramerova, I. A., N. Kawaguchi, L. I. Fessler, R. E. Nelson, Y. Chen, A. A. Kramerov, M. Kusche-Gullberg, J. M. Kramer, B. D. Ackley, A. L. Sieron, D. J. Prockop and J. H. Fessler (2000). "Papilin in development; a pericellular protein with a homology to the ADAMTS metalloproteinases." Development **127**(24): 5475-5485.

Krauss, S., J. P. Concordet and P. W. Ingham (1993). "A functionally conserved homolog of the Drosophila segment polarity gene hh is expressed in tissues with polarizing activity in zebrafish embryos." Cell **75**(7): 1431-1444.

Kubota, Y., R. Kuroki and K. Nishiwaki (2004). "A fibulin-1 homolog interacts with an ADAM protease that controls cell migration in C. elegans." Curr Biol **14**(22): 2011-2018.

Kuszak, J. R., M. S. Macsai, K. J. Bloom, J. L. Rae and R. S. Weinstein (1985). "Cell-to-cell fusion of lens fiber cells in situ: correlative light, scanning electron microscopic, and freeze-fracture studies." J Ultrastruct Res **93**(3): 144-160.

Kuwabara, P. E., M. H. Lee, T. Schedl and G. S. Jefferis (2000). "A C. elegans patched gene, ptc-1, functions in germ-line cytokinesis." Genes Dev **14**(15): 1933-1944.

Labaj, P. P., G. G. Leparc, A. F. Bardet, G. Kreil and D. P. Kreil (2010). "Single amino acid repeats in signal peptides." FEBS J **277**(15): 3147-3157.

Labbe, J. C., E. K. McCarthy and B. Goldstein (2004). "The forces that position a mitotic spindle asymmetrically are tethered until after the time of spindle assembly." J Cell Biol **167**(2): 245-256.

Lafontaine, C. A., S. Grainger, B. L. Hess, M. Beland and D. Lohnes (2012). "Cdx1 Interacts Physically with a Subset of Hox Proteins." Biochemistry.

Lamouille, S., J. Xu and R. Derynck (2014). "Molecular mechanisms of epithelial-mesenchymal transition." Nat Rev Mol Cell Biol **15**(3): 178-196.

Larroux, C., B. Fahey, S. M. Degnan, M. Adamski, D. S. Rokhsar and Bernard M. Degnan (2007). "The NK Homeobox Gene Cluster Predates the Origin of Hox Genes." Current Biology **17**(8): 706-710.

Lauderdale, J. D., N. M. Davis and J. Y. Kuwada (1997). "Axon tracts correlate with netrin-1a expression in the zebrafish embryo." Mol Cell Neurosci **9**(4): 293-313.

Laughon, A., W. Howell and M. P. Scott (1988). "The interaction of proteins encoded by Drosophila homeotic and segmentation genes with specific DNA sequences." Development **104 Suppl**: 75-83.

Lawrence, P. A., G. Struhl and J. Casal (2007). "Planar cell polarity: one or two pathways?" Nat Rev Genet **8**(7): 555-563.

Lee, J., J. Ahnn and S. C. Bae (2004). "Homologs of RUNX and CBF beta/PEBP2 beta in C. elegans." Oncogene **23**(24): 4346-4352.

Lee, J., K. A. Platt, P. Censullo and A. Ruiz i Altaba (1997). "Gli1 is a target of Sonic hedgehog that induces ventral neural tube development." Development **124**(13): 2537-2552.

Lee, J. J., S. C. Ekker, D. P. von Kessler, J. A. Porter, B. I. Sun and P. A. Beachy (1994). "Autoproteolysis in hedgehog protein biogenesis." Science **266**(5190): 1528-1537.

Lee, J. J., D. P. von Kessler, S. Parks and P. A. Beachy (1992). "Secretion and localized transcription suggest a role in positional signaling for products of the segmentation gene hedgehog." Cell **71**(1): 33-50.

Lee, R. C., R. L. Feinbaum and V. Ambros (1993). "The C. elegans heterochronic gene lin-4 encodes small RNAs with antisense complementarity to lin-14." Cell **75**(5): 843-854.

Lei, H., J. Liu, T. Fukushige, A. Fire and M. Krause (2009). "Caudal-like PAL-1 directly activates the bodywall muscle module regulator hlh-1 in C. elegans to initiate the embryonic muscle gene regulatory network." Development **136**(8): 1241-1249.

Lengerke, C., S. Schmitt, T. V. Bowman, I. H. Jang, L. Maouche-Chretien, S. McKinney-Freeman, A. J. Davidson, M. Hammerschmidt, F. Rentzsch, J. B. Green, L. I. Zon and G. Q. Daley (2008). "BMP and Wnt specify hematopoietic fate by activation of the Cdx-Hox pathway." Cell Stem Cell **2**(1): 72-82.

Leonardo, E. D., L. Hinck, M. Masu, K. Keino-Masu, S. L. Ackerman and M. Tessier-Lavigne (1997). "Vertebrate homologues of C. elegans UNC-5 are candidate netrin receptors." Nature **386**(6627): 833-838.

Leung-Hagesteijn, C., A. M. Spence, B. D. Stern, Y. Zhou, M. W. Su, E. M. Hedgecock and J. G. Culotti (1992). "UNC-5, a transmembrane protein with immunoglobulin and thrombospondin type 1 domains, guides cell and pioneer axon migrations in C. elegans." Cell **71**(2): 289-299.

Levanon, D., D. Bettoun, C. Harris-Cerruti, E. Woolf, V. Negreanu, R. Eilam, Y. Bernstein, D. Goldenberg, C. Xiao, M. Fliegauf, E. Kremer, F. Otto, O. Brenner, A. Lev-Tov and Y. Groner (2002). "The Runx3 transcription factor regulates development and survival of TrkC dorsal root ganglia neurons." The EMBO journal **21**(13): 3454-3463.

Levy-Strumpf, N. and J. G. Culotti (2014). "Netrins and Wnts function redundantly to regulate antero-posterior and dorso-ventral guidance in C. elegans." PLoS Genet **10**(6): e1004381.

Lewis, E. B. (1978). "A gene complex controlling segmentation in Drosophila." Nature **276**(5688): 565-570.

Lewis, P. M., M. P. Dunn, J. A. McMahon, M. Logan, J. F. Martin, B. St-Jacques and A. P. McMahon (2001). "Cholesterol modification of sonic hedgehog is required for long-range signaling activity and effective modulation of signaling by Ptc1." Cell **105**(5): 599-612.

Li, Q. L., K. Ito, C. Sakakura, H. Fukamachi, K. Inoue, X. Z. Chi, K. Y. Lee, S. Nomura, C. W. Lee, S. B. Han, H. M. Kim, W. J. Kim, H. Yamamoto, N. Yamashita, T. Yano, T. Ikeda, S. Itohara, J. Inazawa, T. Abe, A. Hagiwara, H. Yamagishi, A. Ooe, A. Kaneda, T. Sugimura, T. Ushijima, S. C. Bae and Y. Ito (2002). "Causal relationship between the loss of RUNX3 expression and gastric cancer." Cell **109**(1): 113-124.

Li, X., R. P. Kulkarni, R. J. Hill and H. M. Chamberlin (2009). "HOM-C genes, Wnt signaling and axial patterning in the C. elegans posterior ventral epidermis." Dev Biol **332**(1): 156-165.

Li, Y., H. Zhang, Y. Litingtung and C. Chiang (2006). "Cholesterol modification restricts the spread of Shh gradient in the limb bud." Proc Natl Acad Sci U S A **103**(17): 6548-6553.

Liegeois, S., A. Benedetto, J. M. Garnier, Y. Schwab and M. Labouesse (2006). "The V0-ATPase mediates apical secretion of exosomes containing Hedgehog-related proteins in Caenorhabditis elegans." J Cell Biol **173**(6): 949-961.

Lim, Y. S. and W. G. Wadsworth (2002). "Identification of domains of netrin UNC-6 that mediate attractive and repulsive guidance and responses from cells and growth cones." J Neurosci **22**(16): 7080-7087.

Lin, R., R. J. Hill and J. R. Priess (1998). "POP-1 and anterior-posterior fate decisions in C. elegans embryos." Cell **92**(2): 229-239.

Lin, R., S. Thompson and J. R. Priess (1995). "pop-1 encodes an HMG box protein required for the specification of a mesoderm precursor in early C. elegans embryos." Cell **83**(4): 599-609.

Liu, J. and A. Fire (2000). "Overlapping roles of two Hox genes and the exd ortholog ceh-20 in diversification of the C. elegans postembryonic mesoderm." Development **127**(23): 5179-5190.

Lo, M. C., F. Gay, R. Odom, Y. Shi and R. Lin (2004). "Phosphorylation by the beta-catenin/MAPK complex promotes 14-3-3-mediated nuclear export of TCF/POP-1 in signal-responsive cells in C. elegans." Cell **117**(1): 95-106.

Longtine, M. S., A. McKenzie, 3rd, D. J. Demarini, N. G. Shah, A. Wach, A. Brachat, P. Philippsen and J. R. Pringle (1998). "Additional modules for versatile and economical PCR-based gene deletion and modification in Saccharomyces cerevisiae." Yeast **14**(10): 953-961.

Lopez-Martinez, A., D. T. Chang, C. Chiang, J. A. Porter, M. A. Ros, B. K. Simandl, P. A. Beachy and J. F. Fallon (1995). "Limb-patterning activity and restricted posterior localization of the amino-terminal product of Sonic hedgehog cleavage." Curr Biol **5**(7): 791-796.

Lorentz, O., A. Cadoret, I. Duluc, J. Capeau, C. Gespach, G. Cherqui and J. N. Freund (1999). "Downregulation of the colon tumour-suppressor homeobox gene Cdx-2 by oncogenic ras." Oncogene **18**(1): 87-92.

Lu, W., V. Yamamoto, B. Ortega and D. Baltimore (2004). "Mammalian Ryk is a Wnt coreceptor required for stimulation of neurite outgrowth." Cell **119**(1): 97-108.

Lucanic, M. and H. J. Cheng (2008). "A RAC/CDC-42-independent GIT/PIX/PAK signaling pathway mediates cell migration in C. elegans." PLoS Genet **4**(11): e1000269.

Lucanic, M., M. Kiley, N. Ashcroft, N. L'Etoile and H. J. Cheng (2006). "The Caenorhabditis elegans P21-activated kinases are differentially required for UNC-6/netrin-mediated commissural motor axon guidance." Development **133**(22): 4549-4559.

Lundquist, E. A., P. W. Reddien, E. Hartwieg, H. R. Horvitz and C. I. Bargmann (2001). "Three C. elegans Rac proteins and several alternative Rac regulators control axon guidance, cell migration and apoptotic cell phagocytosis." Development **128**(22): 4475-4488.

Ma, Y., A. Erkner, R. Gong, S. Yao, J. Taipale, K. Basler and P. A. Beachy (2002). "Hedgehog-mediated patterning of the mammalian embryo requires transporter-like function of dispatched." Cell **111**(1): 63-75.

Macdonald, P. M. and G. Struhl (1986). "A molecular gradient in early Drosophila embryos and its role in specifying the body pattern." Nature **324**(6097): 537-545.

MacNeil, L. T., W. R. Hardy, T. Pawson, J. L. Wrana and J. G. Culotti (2009). "UNC-129 regulates the balance between UNC-40 dependent and independent UNC-5 signaling pathways." Nat Neurosci **12**(2): 150-155.

Maduro, M. and D. Pilgrim (1995). "Identification and cloning of unc-119, a gene expressed in the Caenorhabditis elegans nervous system." Genetics **141**(3): 977-988.

Maduro, M. F., J. J. Kasmir, J. Zhu and J. H. Rothman (2005). "The Wnt effector POP-1 and the PAL-1/Caudal homeoprotein collaborate with SKN-1 to activate C. elegans endoderm development." Dev Biol **285**(2): 510-523.

Maity, T., N. Fuse and P. A. Beachy (2005). "Molecular mechanisms of Sonic hedgehog mutant effects in holoprosencephaly." Proc Natl Acad Sci U S A **102**(47): 17026-17031.

Mallo, G. V., P. Soubeyran, J. C. Lissitzky, F. Andre, C. Farnarier, J. Marvaldi, J. C. Dagorn and J. L. Iovanna (1998). "Expression of the Cdx1 and Cdx2 homeotic genes leads to reduced malignancy in colon cancer-derived cells." J Biol Chem **273**(22): 14030-14036.

Malone, C. J., W. D. Fixsen, H. R. Horvitz and M. Han (1999). "UNC-84 localizes to the nuclear envelope and is required for nuclear migration and anchoring during C. elegans development." Development **126**(14): 3171-3181.

Maloof, J. N. and C. Kenyon (1998). "The Hox gene lin-39 is required during C. elegans vulval induction to select the outcome of Ras signaling." Development **125**(2): 181-190.

Maloof, J. N., J. Whangbo, J. M. Harris, G. D. Jongeward and C. Kenyon (1999). "A Wnt signaling pathway controls hox gene expression and neuroblast migration in C. elegans." Development **126**(1): 37-49.

Marigo, V., R. L. Johnson, A. Vortkamp and C. J. Tabin (1996). "Sonic hedgehog differentially regulates expression of GLI and GLI3 during limb development." Dev Biol **180**(1): 273-283.

Marom, K., E. Shapira and A. Fainsod (1997). "The chicken caudal genes establish an anterior-posterior gradient by partially overlapping temporal and spatial patterns of expression." Mech Dev **64**(1-2): 41-52.

Mathelier, A., X. Zhao, A. W. Zhang, F. Parcy, R. Worsley-Hunt, D. J. Arenillas, S. Buchman, C. Y. Chen, A. Chou, H. Ienasescu, J. Lim, C. Shyr, G. Tan, M. Zhou, B. Lenhard, A. Sandelin and W. W. Wasserman (2014). "JASPAR 2014: an extensively expanded and updated open-access database of transcription factor binding profiles." Nucleic Acids Res **42**(Database issue): D142-147.

Maurer, C. W., M. Chiorazzi and S. Shaham (2007). "Timing of the onset of a developmental cell death is controlled by transcriptional induction of the C. elegans ced-3 caspase-encoding gene." Development **134**(7): 1357-1368.

McGee, M. D., R. Rillo, A. S. Anderson and D. A. Starr (2006). "UNC-83 IS a KASH protein required for nuclear migration and is recruited to the outer nuclear membrane by a physical interaction with the SUN protein UNC-84." Mol Biol Cell **17**(4): 1790-1801.

Mello, C. and A. Fire (1995). "DNA transformation." Methods in cell biology **48**: 451-482.

Mello, C. C., J. M. Kramer, D. Stinchcomb and V. Ambros (1991). "Efficient gene transfer in C.elegans: extrachromosomal maintenance and integration of transforming sequences." EMBO J **10**(12): 3959-3970.

Meyers, S., N. Lenny and S. W. Hiebert (1995). "The t(8;21) fusion protein interferes with AML-1B-dependent transcriptional activation." Mol Cell Biol **15**(4): 1974-1982.

Meyerzon, M., H. N. Fridolfsson, N. Ly, F. J. McNally and D. A. Starr (2009). "UNC-83 is a nuclear-specific cargo adaptor for kinesin-1-mediated nuclear migration." Development **136**(16): 2725-2733.

Michaux, G., A. Gansmuller, C. Hindelang and M. Labouesse (2000). "CHE-14, a protein with a sterol-sensing domain, is required for apical sorting in C. elegans ectodermal epithelial cells." Curr Biol **10**(18): 1098-1107.

Mickey, K. M., C. C. Mello, M. K. Montgomery, A. Fire and J. R. Priess (1996). "An inductive interaction in 4-cell stage C. elegans embryos involves APX-1 expression in the signalling cell." Development **122**(6): 1791-1798.

Middelkoop, T. C., L. Williams, P. T. Yang, J. Luchtenberg, M. C. Betist, N. Ji, A. van Oudenaarden, C. Kenyon and H. C. Korswagen (2012). "The thrombospondin repeat containing protein MIG-21 controls a left-right asymmetric Wnt signaling response in migrating C. elegans neuroblasts." Dev Biol **361**(2): 338-348.

Mitchell, K. J., J. L. Doyle, T. Serafini, T. E. Kennedy, M. Tessier-Lavigne, C. S. Goodman and B. J. Dickson (1996). "Genetic analysis of Netrin genes in Drosophila: Netrins guide CNS commissural axons and peripheral motor axons." Neuron **17**(2): 203-215.

Miura, M., H. Zhu, R. Rotello, E. A. Hartwieg and J. Yuan (1993). "Induction of apoptosis in fibroblasts by IL-1 beta-converting enzyme, a mammalian homolog of the C. elegans cell death gene ced-3." Cell **75**(4): 653-660.

Miyoshi, H., K. Shimizu, T. Kozu, N. Maseki, Y. Kaneko and M. Ohki (1991). "t(8;21) breakpoints on chromosome 21 in acute myeloid leukemia are clustered within a limited region of a single gene, AML1." Proc Natl Acad Sci U S A **88**(23): 10431-10434.

Mizumoto, K. and H. Sawa (2007). "Cortical beta-catenin and APC regulate asymmetric nuclear beta-catenin localization during asymmetric cell division in C. elegans." Dev Cell **12**(2): 287-299.

Mlodzik, M., A. Fjose and W. J. Gehring (1985). "Isolation of caudal, a Drosophila homeo box-containing gene with maternal expression, whose transcripts form a concentration gradient at the pre-blastoderm stage." EMBO J **4**(11): 2961-2969.

Mohler, J. and K. Vani (1992). "Molecular organization and embryonic expression of the hedgehog gene involved in cell-cell communication in segmental patterning of Drosophila." Development **115**(4): 957-971.

Mohler, W. A., G. Shemer, J. J. del Campo, C. Valansi, E. Opoku-Serebuoh, V. Scranton, N. Assaf, J. G. White and B. Podbilewicz (2002). "The type I membrane protein EFF-1 is essential for developmental cell fusion." Dev Cell **2**(3): 355-362.

Morck, C. and M. Pilon (2006). "C. elegans feeding defective mutants have shorter body lengths and increased autophagy." BMC Dev Biol **6**: 39.

Morck, C., M. Rauthan, F. Wagberg and M. Pilon (2004). "pha-2 encodes the C. elegans ortholog of the homeodomain protein HEX and is required for the formation of the pharyngeal isthmus." Dev Biol **272**(2): 403-418.

Moreno, E. and G. Morata (1999). "Caudal is the Hox gene that specifies the most posterior Drosophile segment." Nature **400**(6747): 873-877.

Morton, D. G., J. M. Roos and K. J. Kemphues (1992). "par-4, a gene required for cytoplasmic localization and determination of specific cell types in Caenorhabditis elegans embryogenesis." Genetics **130**(4): 771-790.

Motola, D. L., C. L. Cummins, V. Rottiers, K. K. Sharma, T. Li, Y. Li, K. Suino-Powell, H. E. Xu, R. J. Auchus, A. Antebi and D. J. Mangelsdorf (2006). "Identification of ligands for DAF-12 that govern dauer formation and reproduction in C. elegans." Cell **124**(6): 1209-1223.

Muller-Tidow, C., B. Steffen, T. Cauvet, L. Tickenbrock, P. Ji, S. Diederichs, B. Sargin, G. Kohler, M. Stelljes, E. Puccetti, M. Ruthardt, S. deVos, S. W. Hiebert, H. P. Koeffler, W. E. Berdel and H. Serve (2004). "Translocation products in acute myeloid leukemia activate the Wnt signaling pathway in hematopoietic cells." Mol Cell Biol **24**(7): 2890-2904.

Munro, E., J. Nance and J. R. Priess (2004). "Cortical flows powered by asymmetrical contraction transport PAR proteins to establish and maintain anterior-posterior polarity in the early C. elegans embryo." Dev Cell **7**(3): 413-424.

Murgan, S., W. Kari, U. Rothbacher, M. Iche-Torres, P. Melenec, O. Hobert and V. Bertrand (2015). "Atypical Transcriptional Activation by TCF via a Zic Transcription Factor in C. elegans Neuronal Precursors." Dev Cell **33**(6): 737-745.

Mutoh, H., Y. Hakamata, K. Sato, A. Eda, I. Yanaka, S. Honda, H. Osawa, Y. Kaneko and K. Sugano (2002). "Conversion of gastric mucosa to intestinal metaplasia in Cdx2-expressing transgenic mice." Biochem Biophys Res Commun **294**(2): 470-479.

Mutoh, H., M. Sashikawa and K. Sugano (2011). "Sox2 expression is maintained while gastric phenotype is completely lost in Cdx2-induced intestinal metaplastic mucosa." Differentiation **81**(2): 92-98.

Nakano, Y., I. Guerrero, A. Hidalgo, A. Taylor, J. R. Whittle and P. W. Ingham (1989). "A protein with several possible membrane-spanning domains encoded by the Drosophila segment polarity gene patched." Nature **341**(6242): 508-513.

Nash, B., A. Colavita, H. Zheng, P. J. Roy and J. G. Culotti (2000). "The forkhead transcription factor UNC-130 is required for the graded spatial expression of the UNC-129 TGF-beta guidance factor in C. elegans." Genes Dev **14**(19): 2486-2500.

Natarajan, L., N. E. Witwer and D. M. Eisenmann (2001). "The divergent Caenorhabditis elegans beta-catenin proteins BAR-1, WRM-1 and HMP-2 make distinct protein interactions but retain functional redundancy in vivo." Genetics **159**(1): 159-172.

Nicoll, G., S. Davidson, L. Shanley, B. Hing, M. Lear, P. McGuffin, R. Ross and A. MacKenzie (2012). "Allele-specific differences in activity of a novel cannabinoid receptor 1 (CNR1) gene intronic enhancer in hypothalamus, dorsal root ganglia, and hippocampus." J Biol Chem **287**(16): 12828-12834.

Nimmo, R., A. Antebi and A. Woollard (2005). "mab-2 encodes RNT-1, a C. elegans Runx homologue essential for controlling cell proliferation in a stem cell-like developmental lineage." Development **132**(22): 5043-5054.

Nishiwaki, K. (1999). "Mutations affecting symmetrical migration of distal tip cells in Caenorhabditis elegans." Genetics **152**(3): 985-997.

Nordstrom, U., E. Maier, T. M. Jessell and T. Edlund (2006). "An early role for WNT signaling in specifying neural patterns of Cdx and Hox gene expression and motor neuron subtype identity." PLoS Biol **4**(8): e252.

Novelli, J., S. Ahmed and J. Hodgkin (2004). "Gene interactions in Caenorhabditis elegans define DPY-31 as a candidate procollagen C-proteinase and SQT-3/ROL-4 as its predicted major target." Genetics **168**(3): 1259-1273.

Nusslein-Volhard, C. and E. Wieschaus (1980). "Mutations affecting segment number and polarity in Drosophila." Nature **287**(5785): 795-801.

O'Connell, K. F., K. N. Maxwell and J. G. White (2000). "The spd-2 gene is required for polarization of the anteroposterior axis and formation of the sperm asters in the Caenorhabditis elegans zygote." Dev Biol **222**(1): 55-70.

O'Hara, B., D. Alvarez de la Rosa and V. M. Rajendran (2014). "Multiple mineralocorticoid response elements localized in different introns regulate intermediate conductance K+ (Kcnn4) channel expression in the rat distal colon." PLoS One **9**(6): e98695.

Oberhofer, G., D. Grossmann, J. L. Siemanowski, T. Beissbarth and G. Bucher (2014). "Wnt/beta-catenin signaling integrates patterning and metabolism of the insect growth zone." Development **141**(24): 4740-4750.

Ogura, K., T. Okada, S. Mitani, K. Gengyo-Ando, D. L. Baillie, Y. Kohara and Y. Goshima (2010). "Protein phosphatase 2A cooperates with the autophagy-related kinase UNC-51 to regulate axon guidance in Caenorhabditis elegans." Development **137**(10): 1657-1667.

Okuda, T., J. van Deursen, S. W. Hiebert, G. Grosveld and J. R. Downing (1996). "AML1, the target of multiple chromosomal translocations in human leukemia, is essential for normal fetal liver hematopoiesis." Cell **84**(2): 321-330.

Olsen, P. H. and V. Ambros (1999). "The lin-4 regulatory RNA controls developmental timing in Caenorhabditis elegans by blocking LIN-14 protein synthesis after the initiation of translation." Dev Biol **216**(2): 671-680.

Ott, C. J., N. P. Blackledge, J. L. Kerschner, S. H. Leir, G. E. Crawford, C. U. Cotton and A. Harris (2009). "Intronic enhancers coordinate epithelial-specific looping of the active CFTR locus." Proc Natl Acad Sci U S A **106**(47): 19934-19939.

Ott, C. J., M. Suszko, N. P. Blackledge, J. E. Wright, G. E. Crawford and A. Harris (2009). "A complex intronic enhancer regulates expression of the CFTR gene by direct interaction with the promoter." J Cell Mol Med **13**(4): 680-692.

Otto, F., A. P. Thornell, T. Crompton, A. Denzel, K. C. Gilmour, I. R. Rosewell, G. W. Stamp, R. S. Beddington, S. Mundlos, B. R. Olsen, P. B. Selby and M. J. Owen (1997). "Cbfa1, a candidate gene for cleidocranial dysplasia syndrome, is essential for osteoblast differentiation and bone development." Cell **89**(5): 765-771.

Pasquinelli, A. E., B. J. Reinhart, F. Slack, M. Q. Martindale, M. I. Kuroda, B. Maller, D. C. Hayward, E. E. Ball, B. Degnan, P. Muller, J. Spring, A. Srinivasan, M. Fishman, J. Finnerty, J. Corbo, M. Levine, P. Leahy, E. Davidson and G. Ruvkun (2000). "Conservation of the sequence and temporal expression of let-7 heterochronic regulatory RNA." Nature **408**(6808): 86-89.

Paul, T., S. Li, S. Khurana, N. S. Leleiko and M. J. Walsh (2007). "The epigenetic signature of CFTR expression is co-ordinated via chromatin acetylation through a complex intronic element." Biochem J **408**(3): 317-326.

Pepinsky, R. B., C. Zeng, D. Wen, P. Rayhorn, D. P. Baker, K. P. Williams, S. A. Bixler, C. M. Ambrose, E. A. Garber, K. Miatkowski, F. R. Taylor, E. A. Wang and A. Galdes (1998). "Identification of a palmitic acid-modified form of human Sonic hedgehog." J Biol Chem **273**(22): 14037-14045.

Petalcorin, M. I., T. Oka, M. Koga, K. Ogura, Y. Wada, Y. Ohshima and M. Futai (1999). "Disruption of clh-1, a chloride channel gene, results in a wider body of Caenorhabditis elegans." J Mol Biol **294**(2): 347-355.

Peters, E. C., A. J. Gossett, B. Goldstein, C. J. Der and D. J. Reiner (2013). "Redundant canonical and noncanonical Caenorhabditis elegans p21-activated kinase signaling governs distal tip cell migrations." G3 (Bethesda) **3**(2): 181-195.

Petrova, E., J. Rios-Esteves, O. Ouerfelli, J. F. Glickman and M. D. Resh (2013). "Inhibitors of Hedgehog acyltransferase block Sonic Hedgehog signaling." Nat Chem Biol **9**(4): 247-249.

Phillips, B. T., A. R. Kidd, 3rd, R. King, J. Hardin and J. Kimble (2007). "Reciprocal asymmetry of SYS-1/beta-catenin and POP-1/TCF controls asymmetric divisions in Caenorhabditis elegans." Proc Natl Acad Sci U S A **104**(9): 3231-3236.

Piekny, A. J., J. L. Johnson, G. D. Cham and P. E. Mains (2003). "The Caenorhabditis elegans nonmuscle myosin genes nmy-1 and nmy-2 function as redundant components of the let-502/Rho-binding kinase and mel-11/myosin phosphatase pathway during embryonic morphogenesis." Development **130**(23): 5695-5704.

Pilon, N., K. Oh, J. R. Sylvestre, N. Bouchard, J. Savory and D. Lohnes (2006). "Cdx4 is a direct target of the canonical Wnt pathway." Dev Biol **289**(1): 55-63.

Pocock, R., J. Ahringer, M. Mitsch, S. Maxwell and A. Woollard (2004). "A regulatory network of T-box genes and the even-skipped homologue vab-7 controls patterning and morphogenesis in C. elegans." Development **131**(10): 2373-2385.

Podbilewicz, B., E. Leikina, A. Sapir, C. Valansi, M. Suissa, G. Shemer and L. V. Chernomordik (2006). "The C. elegans developmental fusogen EFF-1 mediates homotypic fusion in heterologous cells and in vivo." Dev Cell **11**(4): 471-481.

Podbilewicz, B. and J. G. White (1994). "Cell fusions in the developing epithelial of C. elegans." Dev Biol **161**(2): 408-424.

Porter, J. A., S. C. Ekker, W. J. Park, D. P. von Kessler, K. E. Young, C. H. Chen, Y. Ma, A. S. Woods, R. J. Cotter, E. V. Koonin and P. A. Beachy (1996). "Hedgehog patterning activity: role of a lipophilic modification mediated by the carboxy-terminal autoprocessing domain." Cell **86**(1): 21-34.

Porter, J. A., D. P. von Kessler, S. C. Ekker, K. E. Young, J. J. Lee, K. Moses and P. A. Beachy (1995). "The product of hedgehog autoproteolytic cleavage active in local and long-range signalling." Nature **374**(6520): 363-366.

Porter, J. A., K. E. Young and P. A. Beachy (1996). "Cholesterol modification of hedgehog signaling proteins in animal development." Science **274**(5285): 255-259.

Porter, S., I. M. Clark, L. Kevorkian and D. R. Edwards (2005). "The ADAMTS metalloproteinases." Biochem J **386**(Pt 1): 15-27.

Prasad, M. K., X. Reed, D. U. Gorkin, J. C. Cronin, A. R. McAdow, K. Chain, C. J. Hodonsky, E. A. Jones, J. Svaren, A. Antonellis, S. L. Johnson, S. K. Loftus, W. J. Pavan and A. S. McCallion (2011). "SOX10 directly modulates ERBB3 transcription via an intronic neural crest enhancer." BMC Dev Biol **11**: 40.

Priess, J. R. and D. I. Hirsh (1986). "Caenorhabditis elegans morphogenesis: the role of the cytoskeleton in elongation of the embryo." Dev Biol **117**(1): 156-173.

Priess, J. R. and J. N. Thomson (1987). "Cellular interactions in early C. elegans embryos." Cell **48**(2): 241-250.

Prinos, P., S. Joseph, K. Oh, B. I. Meyer, P. Gruss and D. Lohnes (2001). "Multiple pathways governing Cdx1 expression during murine development." Dev Biol **239**(2): 257-269.

Raich, W. B., C. Agbunag and J. Hardin (1999). "Rapid epithelial-sheet sealing in the Caenorhabditis elegans embryo requires cadherin-dependent filopodial priming." Curr Biol **9**(20): 1139-1146.

Reece-Hoyes, J. S., I. D. Keenan and H. V. Isaacs (2002). "Cloning and expression of the Cdx family from the frog Xenopus tropicalis." Dev Dyn **223**(1): 134-140.

Reinhart, B. J., F. J. Slack, M. Basson, A. E. Pasquinelli, J. C. Bettinger, A. E. Rougvie, H. R. Horvitz and G. Ruvkun (2000). "The 21-nucleotide let-7 RNA regulates developmental timing in Caenorhabditis elegans." Nature **403**(6772): 901-906.

Reinhart, B. J., E. G. Weinstein, M. W. Rhoades, B. Bartel and D. P. Bartel (2002). "MicroRNAs in plants." Genes Dev **16**(13): 1616-1626.

Riddle, R. D., R. L. Johnson, E. Laufer and C. Tabin (1993). "Sonic hedgehog mediates the polarizing activity of the ZPA." Cell **75**(7): 1401-1416.

Ro, H. and I. B. Dawid (2011). "Modulation of Tcf3 repressor complex composition regulates cdx4 expression in zebrafish." EMBO J **30**(14): 2894-2907.

Roberts, B., C. Clucas and I. L. Johnstone (2003). "Loss of SEC-23 in Caenorhabditis elegans causes defects in oogenesis, morphogenesis, and extracellular matrix secretion." Mol Biol Cell **14**(11): 4414-4426.

Robertson, A. J., A. Coluccio, P. Knowlton, C. Dickey-Sims and J. A. Coffman (2008). "Runx expression is mitogenic and mutually linked to Wnt activity in blastula-stage sea urchin embryos." PLoS One **3**(11): e3770.

Roelink, H., A. Augsburger, J. Heemskerk, V. Korzh, S. Norlin, A. Ruiz i Altaba, Y. Tanabe, M. Placzek, T. Edlund, T. M. Jessell and et al. (1994). "Floor plate and motor neuron induction by vhh-1, a vertebrate homolog of hedgehog expressed by the notochord." Cell **76**(4): 761-775.

Roessler, E., E. Belloni, K. Gaudenz, P. Jay, P. Berta, S. W. Scherer, L. C. Tsui and M. Muenke (1996). "Mutations in the human Sonic Hedgehog gene cause holoprosencephaly." Nat Genet **14**(3): 357-360.

Roessler, E., E. Belloni, K. Gaudenz, F. Vargas, S. W. Scherer, L. C. Tsui and M. Muenke (1997). "Mutations in the C-terminal domain of Sonic Hedgehog cause holoprosencephaly." Hum Mol Genet **6**(11): 1847-1853.

Rojas, A., W. Schachterle, S. M. Xu, F. Martin and B. L. Black (2010). "Direct transcriptional regulation of Gata4 during early endoderm specification is controlled by FoxA2 binding to an intronic enhancer." Dev Biol **346**(2): 346-355.

Rose, L. and P. Gonczy (2014). "Polarity establishment, asymmetric division and segregation of fate determinants in early C. elegans embryos." WormBook: 1-43.

Ruddle, F. H., J. L. Bartels, K. L. Bentley, C. Kappen, M. T. Murtha and J. W. Pendleton (1994). "Evolution of Hox genes." Annu Rev Genet **28**: 423-442.

Sadler, P. L. and D. C. Shakes (2000). "Anucleate Caenorhabditis elegans sperm can crawl, fertilize oocytes and direct anterior-posterior polarization of the 1-cell embryo." Development **127**(2): 355-366.

Salari, K., M. E. Spulak, J. Cuff, A. D. Forster, C. P. Giacomini, S. Huang, M. E. Ko, A. Y. Lin, M. van de Rijn and J. R. Pollack (2012). "CDX2 is an amplified lineage-survival oncogene in colorectal cancer." Proc Natl Acad Sci U S A **109**(46): E3196-3205.

Salser, S. J. and C. Kenyon (1996). "A C. elegans Hox gene switches on, off, on and off again to regulate proliferation, differentiation and morphogenesis." Development **122**(5): 1651-1661.

Salser, S. J., C. M. Loer and C. Kenyon (1993). "Multiple HOM-C gene interactions specify cell fates in the nematode central nervous system." Genes Dev **7**(9): 1714-1724.

Sammut, M., S. J. Cook, K. C. Nguyen, T. Felton, D. H. Hall, S. W. Emmons, R. J. Poole and A. Barrios (2015). "Glia-derived neurons are required for sex-specific learning in C. elegans." Nature **526**(7573): 385-390.

Sanalkumar, R., K. D. Johnson, X. Gao, M. E. Boyer, Y. I. Chang, K. J. Hewitt, J. Zhang and E. H. Bresnick (2014). "Mechanism governing a stem cell-generating cis-regulatory element." Proc Natl Acad Sci U S A **111**(12): E1091-1100.

Sanchez-Ferras, O., B. Coutaud, T. Djavanbakht Samani, I. Tremblay, O. Souchkova and N. Pilon (2012). "Caudal-related homeobox (Cdx) protein-dependent integration of canonical Wnt signaling on paired-box 3 (Pax3) neural crest enhancer." J Biol Chem **287**(20): 16623-16635.

Sapir, A., J. Choi, E. Leikina, O. Avinoam, C. Valansi, L. V. Chernomordik, A. P. Newman and B. Podbilewicz (2007). "AFF-1, a FOS-1-regulated fusogen, mediates fusion of the anchor cell in C. elegans." Dev Cell **12**(5): 683-698.

Sauter, K. A., M. A. Bouhlel, J. O'Neal, D. P. Sester, H. Tagoh, R. M. Ingram, C. Pridans, C. Bonifer and D. A. Hume (2013). "The function of the conserved regulatory element within the second intron of the mammalian Csf1r locus." PLoS One **8**(1): e54935.

Savory, J. G., N. Pilon, S. Grainger, J. R. Sylvestre, M. Beland, M. Houle, K. Oh and D. Lohnes (2009). "Cdx1 and Cdx2 are functionally equivalent in vertebral patterning." Dev Biol **330**(1): 114-122.

Sawa, M., S. Suetsugu, A. Sugimoto, H. Miki, M. Yamamoto and T. Takenawa (2003). "Essential role of the C. elegans Arp2/3 complex in cell migration during ventral enclosure." J Cell Sci **116**(Pt 8): 1505-1518.

Schauer, S. E., P. M. Schluter, R. Baskar, J. Gheyselinck, A. Bolanos, M. D. Curtis and U. Grossniklaus (2009). "Intronic regulatory elements determine the divergent expression patterns of AGAMOUS-LIKE6 subfamily members in Arabidopsis." Plant J **59**(6): 987-1000.

Serafini, T., T. E. Kennedy, M. J. Galko, C. Mirzayan, T. M. Jessell and M. Tessier-Lavigne (1994). "The netrins define a family of axon outgrowth-promoting proteins homologous to C. elegans UNC-6." Cell **78**(3): 409-424.

Serinsoz, E., M. Neusch, G. Busche, R. Wasielewski, H. Kreipe and O. Bock (2004). "Aberrant expression of beta-catenin discriminates acute myeloid leukaemia from acute lymphoblastic leukaemia." Br J Haematol **126**(3): 313-319.

Severson, A. F., D. L. Baillie and B. Bowerman (2002). "A Formin Homology protein and a profilin are required for cytokinesis and Arp2/3-independent assembly of cortical microfilaments in C. elegans." Curr Biol **12**(24): 2066-2075.

Shapiro, M. D., M. E. Marks, C. L. Peichel, B. K. Blackman, K. S. Nereng, B. Jonsson, D. Schluter and D. M. Kingsley (2004). "Genetic and developmental basis of evolutionary pelvic reduction in threespine sticklebacks." Nature **428**(6984): 717-723.

Shemer, G., R. Kishore and B. Podbilewicz (2000). "Ring formation drives invagination of the vulva in Caenorhabditis elegans: Ras, cell fusion, and cell migration determine structural fates." Dev Biol **221**(1): 233-248.

Shemer, G. and B. Podbilewicz (2002). "LIN-39/Hox triggers cell division and represses EFF-1/fusogen-dependent vulval cell fusion." Genes Dev **16**(24): 3136-3141.

Shemer, G., M. Suissa, I. Kolotuev, K. C. Nguyen, D. H. Hall and B. Podbilewicz (2004). "EFF-1 is sufficient to initiate and execute tissue-specific cell fusion in C. elegans." Curr Biol **14**(17): 1587-1591.

Shimeld, S. M. (1999). "The evolution of the hedgehog gene family in chordates: insights from amphioxus hedgehog." Dev Genes Evol **209**(1): 40-47.

Shimizu, T., Y. K. Bae, O. Muraoka and M. Hibi (2005). "Interaction of Wnt and caudal-related genes in zebrafish posterior body formation." Dev Biol **279**(1): 125-141.

Shimomura, O., F. H. Johnson and Y. Saiga (1962). "Extraction, purification and properties of aequorin, a bioluminescent protein from the luminous hydromedusan, Aequorea." J Cell Comp Physiol **59**: 223-239.

Shyu, Y. J., S. M. Hiatt, H. M. Duren, R. E. Ellis, T. K. Kerppola and C. D. Hu (2008). "Visualization of protein interactions in living Caenorhabditis elegans using bimolecular fluorescence complementation analysis." Nat Protoc **3**(4): 588-596.

Silberg, D. G., J. Sullivan, E. Kang, G. P. Swain, J. Moffett, N. J. Sund, S. D. Sackett and K. H. Kaestner (2002). "Cdx2 ectopic expression induces gastric intestinal metaplasia in transgenic mice." Gastroenterology **122**(3): 689-696.

Silberg, D. G., G. P. Swain, E. R. Suh and P. G. Traber (2000). "Cdx1 and cdx2 expression during intestinal development." Gastroenterology **119**(4): 961-971.

Simon, M., V. L. Grandage, D. C. Linch and A. Khwaja (2005). "Constitutive activation of the Wnt/beta-catenin signalling pathway in acute myeloid leukaemia." Oncogene **24**(14): 2410-2420.

Singh, D. and C. Pohl (2014). "Coupling of rotational cortical flow, asymmetric midbody positioning, and spindle rotation mediates dorsoventral axis formation in C. elegans." Dev Cell **28**(3): 253-267.

Slack, F. J., M. Basson, Z. Liu, V. Ambros, H. R. Horvitz and G. Ruvkun (2000). "The lin-41 RBCC gene acts in the C. elegans heterochronic pathway between the let-7 regulatory RNA and the LIN-29 transcription factor." Mol Cell **5**(4): 659-669.

Smurova, K. and B. Podbilewicz (2016). "RAB-5- and DYNAMIN-1-Mediated Endocytosis of EFF-1 Fusogen Controls Cell-Cell Fusion." Cell Rep **14**(6): 1517-1527.

Soto, M. C., H. Qadota, K. Kasuya, M. Inoue, D. Tsuboi, C. C. Mello and K. Kaibuchi (2002). "The GEX-2 and GEX-3 proteins are required for tissue morphogenesis and cell migrations in C. elegans." Genes Dev **16**(5): 620-632.

Spencer, A. G., S. Orita, C. J. Malone and M. Han (2001). "A RHO GTPase-mediated pathway is required during P cell migration in Caenorhabditis elegans." Proc Natl Acad Sci U S A **98**(23): 13132-13137.

Starr, D. A., G. J. Hermann, C. J. Malone, W. Fixsen, J. R. Priess, H. R. Horvitz and M. Han (2001). "unc-83 encodes a novel component of the nuclear envelope and is essential for proper nuclear migration." Development **128**(24): 5039-5050.

Stott, K., J. M. Blackburn, P. J. Butler and M. Perutz (1995). "Incorporation of glutamine repeats makes protein oligomerize: implications for neurodegenerative diseases." Proc Natl Acad Sci U S A **92**(14): 6509-6513.

Strahle, U., N. Fischer and P. Blader (1997). "Expression and regulation of a netrin homologue in the zebrafish embryo." Mech Dev **62**(2): 147-160.

Streit, A., R. Kohler, T. Marty, M. Belfiore, K. Takacs-Vellai, M. A. Vigano, R. Schnabel, M. Affolter and F. Muller (2002). "Conserved regulation of the Caenorhabditis elegans labial/Hox1 gene ceh-13." Dev Biol **242**(2): 96-108.

Strumpf, D., C. A. Mao, Y. Yamanaka, A. Ralston, K. Chawengsaksophak, F. Beck and J. Rossant (2005). "Cdx2 is required for correct cell fate specification and differentiation of trophectoderm in the mouse blastocyst." Development **132**(9): 2093-2102.

Su, M., D. C. Merz, M. T. Killeen, Y. Zhou, H. Zheng, J. M. Kramer, E. M. Hedgecock and J. G. Culotti (2000). "Regulation of the UNC-5 netrin receptor initiates the first reorientation of migrating distal tip cells in Caenorhabditis elegans." Development **127**(3): 585-594.

Subramanian, V., B. Meyer and G. S. Evans (1998). "The murine Cdx1 gene product localises to the proliferative compartment in the developing and regenerating intestinal epithelium." Differentiation **64**(1): 11-18.

Subramanian, V., B. I. Meyer and P. Gruss (1995). "Disruption of the murine homeobox gene Cdx1 affects axial skeletal identities by altering the mesodermal expression domains of Hox genes." Cell **83**(4): 641-653.

Sugimoto, A., P. D. Friesen and J. H. Rothman (1994). "Baculovirus p35 prevents developmentally programmed cell death and rescues a ced-9 mutant in the nematode Caenorhabditis elegans." EMBO J **13**(9): 2023-2028.

Sugioka, K., K. Mizumoto and H. Sawa (2011). "Wnt regulates spindle asymmetry to generate asymmetric nuclear beta-catenin in C. elegans." Cell **146**(6): 942-954.

Suh, E. and P. G. Traber (1996). "An intestine-specific homeobox gene regulates proliferation and differentiation." Mol Cell Biol **16**(2): 619-625.

Sullivan, J. C., D. Sher, M. Eisenstein, K. Shigesada, A. M. Reitzel, H. Marlow, D. Levanon, Y. Groner, J. R. Finnerty and U. Gat (2008). "The evolutionary origin of the Runx/CBFbeta transcription factors--studies of the most basal metazoans." BMC Evol Biol **8**: 228.

Sulston, J. E. and H. R. Horvitz (1977). "Post-embryonic cell lineages of the nematode, Caenorhabditis elegans." Developmental biology **56**(1): 110-156.

Sulston, J. E., E. Schierenberg, J. G. White and J. N. Thomson (1983). "The embryonic cell lineage of the nematode Caenorhabditis elegans." Dev Biol **100**(1): 64-119.

Sundararajan, L. and E. A. Lundquist (2012). "Transmembrane proteins UNC-40/DCC, PTP-3/LAR, and MIG-21 control anterior-posterior neuroblast migration with left-right functional asymmetry in Caenorhabditis elegans." Genetics **192**(4): 1373-1388.

Tabaries, S., J. Lapointe, T. Besch, M. Carter, J. Woollard, C. K. Tuggle and L. Jeannotte (2005). "Cdx protein interaction with Hoxa5 regulatory sequences contributes to Hoxa5 regional expression along the axial skeleton." Mol Cell Biol **25**(4): 1389-1401.

Tabata, T., S. Eaton and T. B. Kornberg (1992). "The Drosophila hedgehog gene is expressed specifically in posterior compartment cells and is a target of engrailed regulation." Genes Dev **6**(12B): 2635-2645.

Takahashi, N., K. Yamaguchi, T. Ikenoue, T. Fujii and Y. Furukawa (2014). "Identification of two Wnt-responsive elements in the intron of RING finger protein 43 (RNF43) gene." PLoS One **9**(1): e86582.

Takeshita, H. and H. Sawa (2005). "Asymmetric cortical and nuclear localizations of WRM-1/beta-catenin during asymmetric cell division in C. elegans." Genes Dev **19**(15): 1743-1748.

Taniuchi, I., M. Osato, T. Egawa, M. J. Sunshine, S. C. Bae, T. Komori, Y. Ito and D. R. Littman (2002). "Differential requirements for Runx proteins in CD4 repression and epigenetic silencing during T lymphocyte development." Cell **111**(5): 621-633.

Tashiro, S., T. Michiue, S. Higashijima, S. Zenno, S. Ishimaru, F. Takahashi, M. Orihara, T. Kojima and K. Saigo (1993). "Structure and expression of hedgehog, a Drosophila segment-polarity gene required for cell-cell communication." Gene **124**(2): 183-189.

Taylor, F. R., D. Wen, E. A. Garber, A. N. Carmillo, D. P. Baker, R. M. Arduini, K. P. Williams, P. H. Weinreb, P. Rayhorn, X. Hronowski, A. Whitty, E. S. Day, A. Boriack-Sjodin, R. I. Shapiro, A. Galdes and R. B. Pepinsky (2001). "Enhanced potency of human Sonic hedgehog by hydrophobic modification." Biochemistry **40**(14): 4359-4371.

Terada, N., T. Hamazaki, M. Oka, M. Hoki, D. M. Mastalerz, Y. Nakano, E. M. Meyer, L. Morel, B. E. Petersen and E. W. Scott (2002). "Bone marrow cells adopt the phenotype of other cells by spontaneous cell fusion." Nature **416**(6880): 542-545.

Thomas-Virnig, C. L., P. A. Sims, J. S. Simske and J. Hardin (2004). "The inositol 1,4,5-trisphosphate receptor regulates epidermal cell migration in Caenorhabditis elegans." Curr Biol **14**(20): 1882-1887.

Thorsteinsdottir, U., E. Kroon, L. Jerome, F. Blasi and G. Sauvageau (2001). "Defining roles for HOX and MEIS1 genes in induction of acute myeloid leukemia." Mol Cell Biol **21**(1): 224-234.

Thyagarajan, B., A. G. Blaszczak, K. J. Chandler, J. L. Watts, W. E. Johnson and B. J. Graves (2010). "ETS-4 is a transcriptional regulator of life span in Caenorhabditis elegans." PLoS Genet **6**(9): e1001125.

Tian, H., J. Jeong, B. D. Harfe, C. J. Tabin and A. P. McMahon (2005). "Mouse Disp1 is required in sonic hedgehog-expressing cells for paracrine activity of the cholesterol-modified ligand." Development **132**(1): 133-142.

Timmons, L., D. L. Court and A. Fire (2001). "Ingestion of bacterially expressed dsRNAs can produce specific and potent genetic interference in Caenorhabditis elegans." Gene **263**(1-2): 103-112.

Tukachinsky, H., R. P. Kuzmickas, C. Y. Jao, J. Liu and A. Salic (2012). "Dispatched and scube mediate the efficient secretion of the cholesterol-modified hedgehog ligand." Cell Rep **2**(2): 308-320.

Vadlamudi, R. K., C. J. Barnes, S. Rayala, F. Li, S. Balasenthil, S. Marcus, H. V. Goodson, A. A. Sahin and R. Kumar (2005). "p21-activated kinase 1 regulates microtubule dynamics by phosphorylating tubulin cofactor B." Mol Cell Biol **25**(9): 3726-3736.

Van Auken, K., D. C. Weaver, L. G. Edgar and W. B. Wood (2000). "Caenorhabditis elegans embryonic axial patterning requires two recently discovered posterior-group Hox genes." Proc Natl Acad Sci U S A **97**(9): 4499-4503.

van de Ven, C., M. Bialecka, R. Neijts, T. Young, J. E. Rowland, E. J. Stringer, C. Van Rooijen, F. Meijlink, A. Novoa, J. N. Freund, M. Mallo, F. Beck and J. Deschamps (2011). "Concerted involvement of Cdx/Hox genes and Wnt signaling in morphogenesis of the caudal neural tube and cloacal derivatives from the posterior growth zone." Development **138**(16): 3451-3462.

van den Akker, E., S. Forlani, K. Chawengsaksophak, W. de Graaff, F. Beck, B. I. Meyer and J. Deschamps (2002). "Cdx1 and Cdx2 have overlapping functions in anteroposterior patterning and posterior axis elongation." Development **129**(9): 2181-2193.

van den Heuvel, M. and P. W. Ingham (1996). "smoothened encodes a receptor-like serpentine protein required for hedgehog signalling." Nature **382**(6591): 547-551.

van Nes, J., W. de Graaff, F. Lebrin, M. Gerhard, F. Beck and J. Deschamps (2006). "The Cdx4 mutation affects axial development and reveals an essential role of Cdx genes in the ontogenesis of the placental labyrinth in mice." Development **133**(3): 419-428.

Vella, M. C. and F. J. Slack (2005). "C. elegans microRNAs." WormBook: 1-9.

Visser, M., R. J. Palstra and M. Kayser (2015). "Allele-specific transcriptional regulation of IRF4 in melanocytes is mediated by chromatin looping of the intronic rs12203592 enhancer to the IRF4 promoter." Hum Mol Genet **24**(9): 2649-2661.

Von Ohlen, T., D. Lessing, R. Nusse and J. E. Hooper (1997). "Hedgehog signaling regulates transcription through cubitus interruptus, a sequence-specific DNA binding protein." Proc Natl Acad Sci U S A **94**(6): 2404-2409.

Wadsworth, W. G. (2002). "Moving around in a worm: netrin UNC-6 and circumferential axon guidance in C. elegans." Trends Neurosci **25**(8): 423-429.

Wadsworth, W. G., H. Bhatt and E. M. Hedgecock (1996). "Neuroglia and pioneer neurons express UNC-6 to provide global and local netrin cues for guiding migrations in C. elegans." Neuron **16**(1): 35-46.

Wallenfang, M. R. and G. Seydoux (2000). "Polarization of the anterior-posterior axis of C. elegans is a microtubule-directed process." Nature **408**(6808): 89-92.

Wallingford, J. B. (2012). "Planar cell polarity and the developmental control of cell behavior in vertebrate embryos." Annu Rev Cell Dev Biol **28**: 627-653.

Wang, B. B., M. M. Muller-Immergluck, J. Austin, N. T. Robinson, A. Chisholm and C. Kenyon (1993). "A homeotic gene cluster patterns the anteroposterior body axis of C. elegans." Cell **74**(1): 29-42.

Wang, Q., T. Stacy, M. Binder, M. Marin-Padilla, A. H. Sharpe and N. A. Speck (1996). "Disruption of the Cbfa2 gene causes necrosis and hemorrhaging in the central nervous system and blocks definitive hematopoiesis." Proc Natl Acad Sci U S A **93**(8): 3444-3449.

Wang, Y., A. V. Krivtsov, A. U. Sinha, T. E. North, W. Goessling, Z. Feng, L. I. Zon and S. A. Armstrong (2010). "The Wnt/beta-catenin pathway is required for the development of leukemia stem cells in AML." Science **327**(5973): 1650-1653.

Waring, D. A. and C. Kenyon (1990). "Selective silencing of cell communication influences anteroposterior pattern formation in C. elegans." Cell **60**(1): 123-131.

Waring, D. A. and C. Kenyon (1991). "Regulation of cellular responsiveness to inductive signals in the developing C. elegans nervous system." Nature **350**(6320): 712-715.

Watts, J. L., B. Etemad-Moghadam, S. Guo, L. Boyd, B. W. Draper, C. C. Mello, J. R. Priess and K. J. Kemphues (1996). "par-6, a gene involved in the establishment of asymmetry in early C. elegans embryos, mediates the asymmetric localization of PAR-3." Development **122**(10): 3133-3140.

Whangbo, J., J. Harris and C. Kenyon (2000). "Multiple levels of regulation specify the polarity of an asymmetric cell division in C. elegans." Development **127**(21): 4587-4598.

Whangbo, J. and C. Kenyon (1999). "A Wnt signaling system that specifies two patterns of cell migration in C. elegans." Mol Cell **4**(5): 851-858.

Wightman, B., I. Ha and G. Ruvkun (1993). "Posttranscriptional regulation of the heterochronic gene lin-14 by lin-4 mediates temporal pattern formation in C. elegans." Cell **75**(5): 855-862.

Wildwater, M., N. Sander, G. de Vreede and S. van den Heuvel (2011). "Cell shape and Wnt signaling redundantly control the division axis of C. elegans epithelial stem cells." Development **138**(20): 4375-4385.

Williams, B. D., B. Schrank, C. Huynh, R. Shownkeen and R. H. Waterston (1992). "A genetic mapping system in Caenorhabditis elegans based on polymorphic sequence-tagged sites." Genetics **131**(3): 609-624.

Williams, B. D. and R. H. Waterston (1994). "Genes critical for muscle development and function in Caenorhabditis elegans identified through lethal mutations." J Cell Biol **124**(4): 475-490.

Williams-Masson, E. M., P. J. Heid, C. A. Lavin and J. Hardin (1998). "The cellular mechanism of epithelial rearrangement during morphogenesis of the Caenorhabditis elegans dorsal hypodermis." Dev Biol **204**(1): 263-276.

Williams-Masson, E. M., A. N. Malik and J. Hardin (1997). "An actin-mediated two-step mechanism is required for ventral enclosure of the C. elegans hypodermis." Development **124**(15): 2889-2901.

Withee, J., B. Galligan, N. Hawkins and G. Garriga (2004). "Caenorhabditis elegans WASP and Ena/VASP proteins play compensatory roles in morphogenesis and neuronal cell migration." Genetics **167**(3): 1165-1176.

Wong, H. C., A. Bourdelas, A. Krauss, H. J. Lee, Y. Shao, D. Wu, M. Mlodzik, D. L. Shi and J. Zheng (2003). "Direct binding of the PDZ domain of Dishevelled to a conserved internal sequence in the C-terminal region of Frizzled." Mol Cell **12**(5): 1251-1260.

Woo, W. M., A. Goncharov, Y. Jin and A. D. Chisholm (2004). "Intermediate filaments are required for C. elegans epidermal elongation." Dev Biol **267**(1): 216-229.

Wood, W. B. (1988). The Nematode Caenorhabditis Elegans, Cold Spring Harbor Laboratory.

Wood, W. B. (1991). "Evidence from reversal of handedness in C. elegans embryos for early cell interactions determining cell fates." Nature **349**(6309): 536-538.

Wu, L. H. and J. A. Lengyel (1998). "Role of caudal in hindgut specification and gastrulation suggests homology between Drosophila amnioproctodeal invagination and vertebrate blastopore." Development **125**(13): 2433-2442.

Wu, M. and M. A. Herman (2006). "A novel noncanonical Wnt pathway is involved in the regulation of the asymmetric B cell division in C. elegans." Dev Biol **293**(2): 316-329.

Xiang, Q., C. Rasmussen and N. L. Glass (2002). "The ham-2 locus, encoding a putative transmembrane protein, is required for hyphal fusion in Neurospora crassa." Genetics **160**(1): 169-180.

Xu, Y. K. and R. Nusse (1998). "The Frizzled CRD domain is conserved in diverse proteins including several receptor tyrosine kinases." Curr Biol **8**(12): R405-406.

Xue, D. and H. R. Horvitz (1997). "Caenorhabditis elegans CED-9 protein is a bifunctional cell-death inhibitor." Nature **390**(6657): 305-308.

Yamamoto, Y., H. Takeshita and H. Sawa (2011). "Multiple Wnts redundantly control polarity orientation in Caenorhabditis elegans epithelial stem cells." PLoS Genet **7**(10): e1002308.

Yang, X. D., S. Huang, M. C. Lo, K. Mizumoto, H. Sawa, W. Xu, S. Robertson and R. Lin (2011). "Distinct and mutually inhibitory binding by two divergent beta-catenins coordinates TCF levels and activity in C. elegans." Development **138**(19): 4255-4265.

Ye, S., S. Dhillon, X. Ke, A. R. Collins and I. N. Day (2001). "An efficient procedure for genotyping single nucleotide polymorphisms." Nucleic Acids Res **29**(17): E88-88.

Ying, Q. L., J. Nichols, E. P. Evans and A. G. Smith (2002). "Changing potency by spontaneous fusion." Nature **416**(6880): 545-548.

Yoshida, K. and H. Saiga (2008). "Left-right asymmetric expression of Pitx is regulated by the asymmetric Nodal signaling through an intronic enhancer in Ciona intestinalis." Dev Genes Evol **218**(7): 353-360.

Yoshikawa, S., R. D. McKinnon, M. Kokel and J. B. Thomas (2003). "Wnt-mediated axon guidance via the Drosophila Derailed receptor." Nature **422**(6932): 583-588.

Young, J. M. and I. A. Hope (1993). "Molecular markers of differentiation in Caenorhabditis elegans obtained by promoter trapping." Dev Dyn **196**(2): 124-132.

Ysebaert, L., G. Chicanne, C. Demur, F. De Toni, N. Prade-Houdellier, J. B. Ruidavets, V. Mansat-De Mas, F. Rigal-Huguet, G. Laurent, B. Payrastre, S. Manenti and C. Racaud-Sultan (2006). "Expression of beta-catenin by acute myeloid leukemia cells predicts enhanced clonogenic capacities and poor prognosis." Leukemia **20**(7): 1211-1216.

Yu, T. W. and C. I. Bargmann (2001). "Dynamic regulation of axon guidance." Nat Neurosci **4 Suppl**: 1169-1176.

Zarkower, D. (2006). "Somatic sex determination." WormBook: 1-12.

Zecca, M., K. Basler and G. Struhl (1996). "Direct and long-range action of a wingless morphogen gradient." Cell **87**(5): 833-844.

Zeng, X., J. A. Goetz, L. M. Suber, W. J. Scott, Jr., C. M. Schreiner and D. J. Robbins (2001). "A freely diffusible form of Sonic hedgehog mediates long-range signalling." Nature **411**(6838): 716-720.

Zeng, Y., E. J. Wagner and B. R. Cullen (2002). "Both natural and designed micro RNAs can inhibit the expression of cognate mRNAs when expressed in human cells." Mol Cell **9**(6): 1327-1333.

Zeng, Y., R. Yi and B. R. Cullen (2003). "MicroRNAs and small interfering RNAs can inhibit mRNA expression by similar mechanisms." Proc Natl Acad Sci U S A **100**(17): 9779-9784.

Zhang, H. and S. W. Emmons (2000). "A C. elegans mediator protein confers regulatory selectivity on lineage-specific expression of a transcription factor gene." Genes Dev **14**(17): 2161-2172.

Zhang, H. and S. W. Emmons (2001). "The novel C. elegans gene sop-3 modulates Wnt signaling to regulate Hox gene expression." Development **128**(5): 767-777.

Zhang, H., F. Landmann, H. Zahreddine, D. Rodriguez, M. Koch and M. Labouesse (2011). "A tension-induced mechanotransduction pathway promotes epithelial morphogenesis." Nature **471**(7336): 99-103.

Zhang, L., M. Hammell, B. A. Kudlow, V. Ambros and M. Han (2009). "Systematic analysis of dynamic miRNA-target interactions during C. elegans development." Development **136**(18): 3043-3055.

Zhao, T., Q. Gan, A. Stokes, R. N. Lassiter, Y. Wang, J. Chan, J. X. Han, D. E. Pleasure, J. A. Epstein and C. J. Zhou (2014). "beta-catenin regulates Pax3 and Cdx2 for caudal neural tube closure and elongation." Development **141**(1): 148-157.

Zinovyeva, A. Y., Y. Yamamoto, H. Sawa and W. C. Forrester (2008). "Complex network of Wnt signaling regulates neuronal migrations during Caenorhabditis elegans development." Genetics **179**(3): 1357-1371.

Zipkin, I. D., R. M. Kindt and C. J. Kenyon (1997). "Role of a new Rho family member in cell migration and axon guidance in C. elegans." Cell **90**(5): 883-894.

Zugasti, O., J. Rajan and P. E. Kuwabara (2005). "The function and expansion of the Patched- and Hedgehog-related homologs in C. elegans." Genome Res **15**(10): 1402-1410.